MANCHESTER 1824

The University of Manchester

AEROSOLS IN AND ABOVE THE BORNEAN RAINFOREST

A THESIS
SUBMITTED TO THE UNIVERSITY OF MANCHESTER
FOR THE DEGREE OF
DOCTOR OF PHILOSOPHY (PHD)
IN THE FACULTY OF ENGINEERING AND PHYSICAL SCIENCES

NIALL HAMILTON ROBINSON

SCHOOL OF EARTH, ATMOSPHERIC AND ENVIRONMENTAL SCIENCES
2011

CONTENTS

Final word count: 53634

LIST OF FIGURES

LIST OF TABLES

ABSTRACT

Atmospheric aerosols affect climate directly by scattering and absorbing solar radiation, and indirectly by affecting the albedo and lifetime of clouds through their role as cloud condensation nuclei. Aerosol sources, and the processes that govern their evolution in the atmosphere are not well understood, making the aerosol effects a significant source of uncertainty in future climate predictions. The tropics experience a large solar flux meaning that any radiative forcing in this region is particularly important. Despite this, there is a paucity of data from the tropics, with the majority of previous studies performed in the northern mid-latitudes. The few in-situ studies of aerosol composition that have been performed are all in the continental settings of Amazonia or Africa. Until now the "maritime continent" region of South East Asia has remained unstudied. Presented here are Aerosol Mass Spectrometer composition measurements from the Oxidant and Particulate Processes Above a South East Asian Rainforest project, performed from ground and airborne measurement platforms in and around the rainforest of Borneo, South-East Asia. Unlike the previous tropical studies, this allows for the characterisation of a region of mixed terrestrial and marine biogenic emissions. The region is also undergoing rapid land use change, with forest being converted for agriculture, particularly the cultivation of oil palms. This study also allows for the characterisation of a region that is beginning to undergo land use change, providing insight into emissions from different land use types, and providing a benchmark to measure the effects of land use change against in the future.

Total sub-micron aerosol loadings were found to be lower than studies in the northern mid-latitudes, similar to previous tropical studies. However, aerosol composition was different to that observed in Amazonia, with much greater sulphate loadings in Borneo. A regional background of sulphate and highly oxidised organic aerosol was identified, with organic aerosol that is less oxidised originating inland. Aerosol confined to a shallow marine boundary layer upwind of Borneo is lofted higher into the troposphere as it advects across the island, with regional aerosol being removed and biogenic terrestrial aerosol added. The lofting of this aerosol is expected to extend its atmospheric lifetime and change its role in the Earth's radiative budget.

A novel organic aerosol signal was identified which correlated with gas phase isoprene oxidation products, strongly suggesting that it was significant of isoprene SOA. Aerosol associated with this signal made up a substantial fraction of the organic aerosol loading. This opens up the opportunity for future studies to make isoprene SOA measurements using the Aerosol Mass Spectrometer in other studies. A substantial amount of the organic aerosol in Borneo was attributed to isoprene oxidation.

LAY ABSTRACT

Aerosols (microscopic particles suspended in the air) play an important role in the climate of the Earth. They can absorb or reflect sunlight, changing the amount of radiation that goes into heating the Earth. They also play an important role in cloud formation, acting as "nuclei" for cloud droplets to form upon. They tend to make clouds whiter and longer lasting, acting to reflect more sunlight back into space. Their role in cloud formation and heating of the atmosphere can also affect rainfall, potentially even affecting systems as large as the Indian Monsoon. Despite the important influence aerosol can have on climate, their affects are still not precisely understood, in fact the Intergovernmental Panel for Climate Change state that they are one of the biggest unknowns in predicting future climate change.

To predict the effect man-made aerosols have on climate, we first need to understand the role of natural aerosols. This is particularly important as these natural systems are being rapidly changed thanks to deforestation for timber, crops and to build new settlements. We can only predict what effects this land use change will have on the environment if we have a good understanding of the natural systems. Many studies of atmospheric aerosol have been conducted around the more developed parts of the Northern Hemisphere (e.g. Europe, North America, Japan) however there have been very few studies in the tropics, in fact only a handful in South America and Africa. It is particularly important to understand aerosol climate effects in the tropics as the large amount of sun the region experiences means it can make a bigger difference than in other, less sunny parts of the World.

One region of the tropics that has received particularly little attention in recent studies is the "maritime continent" — South East Asia. This region is made up of a network of tropical islands, so it is likely to be very different from the other continental regions that have previously been studied in the tropics. The measurements presented in this thesis are from Borneo, a very large island in South East Asia and home to one of the largest rainforests in the World. The forest is being rapidly cut down to make way for plantations to manufacture palm oil — a ubiquitous ingredient as "vegetable oil" in very many high street products.

This work found that aerosols in Borneo are indeed very different from those measured in the Amazon Rainforest — it seems that emissions from the sea are a large source

of aerosol. The project found that palm oil produces a very different mixture of gases from the rainforest and the work presented here shows that these gases react in an unexpected way to condense and make aerosol. It could even be the case that the sea emissions are the reason that so much of this unexpected aerosol is formed, although more work needs to be done to figure out the precise chemistry. When air is transported across Borneo, it tends to get lifted higher into the atmosphere, meaning it is above a lot of the rain (which can remove the aerosol though wash-out) and is likely to have a longer atmospheric lifetime. Results from other studies show that man-made pollution can increase the amount of natural gases that go into making aerosol. This means that if Borneo becomes more polluted in the future there could be a lot of aerosol produced, not just from the pollution itself, but from natural gases from the rainforest and crops which are not currently converted to aerosol.

DECLARATION

The University of Manchester
PhD by Alternate Submission Declaration

Candidate Name: Niall Hamilton Robinson

Faculty: Engineering and Physical Sciences

Thesis Title: Aerosols in and above the Bornean rainforest

I declare that no portion of this work referred to in this thesis has been submitted in support of an application for another degree or qualification of this or any other university or other institute of learning.

COPYRIGHT

[1] This excludes material already printed in academic journals, for which the copyright belongs to said journal and publisher. Pages for which the author does not own the copyright are numbered differently from the rest of the thesis.

ACKNOWLEDGEMENTS

Firstly I would like to thank James, who, in all the countless times I tapped him on the shoulder never told me he was too busy and was never grumpy to see me. And thanks for telling me it was not so bad every time I thought all was lost. Thanks also to Hugh who, despite being overworked, always provided a sage hand at the tiller and food for thought. Thanks to Gordon the Sisyphean task master — it was worth pushing that rock up the hill 40 times. A special thanks to Julia, who reminded me there was more to life than my PhD. Thanks also to all the people at Manchester who started off as colleagues and have ended up as friends. From putting up flat-pack sheds deep in the rainforest to racing bag samples along dirt tracks and singing karaoke in Malaysian bars, its been a lot of fun.

NOMENCLATURE

Instruments

AMS Aerosol Mass Spectrometer, 47

C-AMS Compact Aerosol Mass Spectrometer, 47

DMA Differential Mobility Analyser, 53

HR-AMS High Resolution Time of Flight Mass Spectrometer, 47

IToF Ion Time of Flight, 47

LIDAR Light Detection and Ranging, 75

PALMS Particle Analysis by Laser Mass Spectrometry, 40

Q-AMS Quadrupole Aerosol Mass Spectrometer, 47

WIBS Wide Interest Biological Sampler, 75

Other

ADC Analogue-to-Digital Converter, 51

AR4 IPCC Fourth Assessment Report, 23

BFSP Brute Force Single Particle, 51

CCN Cloud Condensation Nuclei, 26

CE Collection Efficiency, 54

EI Electron Impact, 49

FAAM Facility for Airborne Atmospheric Measurement BAe-146 research aircraft, 59

IE Ionisation Efficiency, 51

IR Infra-red, 26

IVOC Intermediate Volatile Organic Compounds, 38

LLGHG Long Lived Greenhouse Gases, 26

MACR Methacrolein, 78

MCP Micro-Channel Plate, 50

MVK Methylvinylketone, 78

NEP Net Ecosystem Production, 31

NR Non-refractory, 49

PBAP Primary Biological Aerosol Particles, 75

PMF Positive Matrix Factorisation, 57

PSLs Polystyrene Latex (spheres), 54

PToF Particle Time of Flight, 49

RAM Random Access Memory, 51

RF Radiative Forcing, 26

RIE Relative Ionisation Efficiency, 53

SVOC Semi-Volatile Organic Compounds, 38

VBS Volatility Basis Set, 41

VOC Volatile Organic Compounds, 38

Projects/Organisations

ACES Atmospheric Coupling in the Earth's System, 79

AMAZE-08 Amazonian Aerosol Characterization Experiment, 60

IPCC Inter-governmental Panel for Climate Change, 23

LBA Large Scale Biosphere-Atmosphere Experiment in Amazonia, 60

MILAGRO Megacity Initiative: Local and

Global Re- search Observations, 45

NIST National Institute of Standards and Technology, 50

Symbols

χ Shape factor, 34

ρ Density, 34

ρ_0 Unit density, 34

A, B and C Constants of the Clausius-Clapeyron equation, 72

b Particle ToF calibration param., 54

C Ambient concentration, 52

C^* Effective saturation concentration, 38

C_{aer} Condensed phase concentration, 38

C_{OA} Total organic aerosol concentration, 38

C_{vap} Vapour concentration, 38

D^* Particle ToF calibration param., 54

D_a Aerodynamic diameter, 33

D_v Volume equivalent diameter, 33

D_{va} Vacuum aerodynamic diameter, 34

f_i Mass fraction of species i, 42

f_x Fractional mass loadings of m/z x, 70

I Ion rate, 52

IE Ionisation efficiency, 52

L Distance, 50

MW Molecular weight, 52

N_A Avagadro's number, 52

p Static pressure, 72

$p(X)$ Partial pressure of X, 72

$p*$ Saturation vapour pressure, 72

q Dynamic pressure, 72

RIE Relative ionisation efficiency, 53

t Time of flight, 50

V Voltage, 50

v_a Gas velocity after aerodynamic lens, 54

v_l Gas velocity in the aerodynamic lens, 54

X_p Particle fraction, 42

CHAPTER

ONE

INTRODUCTION

"...the only feasible explanation of the Earth's highly improbable atmosphere was that it was being manipulated on a day-to-day basis from the surface, and that the manipulator was life itself. The significant decrease in entropy...was on its own clear proof of life's activity."

Gaia: a new look at life on Earth, James Lovelock 1979

Aerosols are present throughout the Earth's atmosphere; they can be found in vast numbers from the largest mega-cities to pristine wildernesses. Aerosols are defined as "a suspension of fine solid or liquid particles in a gas" (Seinfeld and Pandis, 2006). These particles cover a large range of sizes, from newly nucleated particles that have a diameter of a few nanometres, to biogenic particles that have diameters approaching 100 μm (Hinds, 1999). They have many impacts on our environment. Amongst other things they absorb and scatter solar radiation and drive the formation of clouds, which affects our weather and climate (Forster et al., 2007); they can cause respiratory and cardiovascular diseases (Mauderly and Chow, 2008); they degrade buildings (Grossi and Brimblecombe, 2002); and can affect visibility (Park et al., 2003). However, their beneficial effects have also been harnessed: they are widely used in the delivery of drugs and it has been proposed that they could ameliorate climate change through geo-engineering (Latham and Smith, 1990). Their effects on climate in particular are complex, and understanding the mechanisms of formation, processing and deposition of atmospheric aerosols is important for the accurate modelling of climate change.

Aerosols can be emitted directly into the atmosphere (primary aerosols) or formed by the condensation of atmospheric gases (secondary aerosols), either onto existing particles or to nucleate entirely new particles. Once formed, an aerosol is processed by condensation of vapours, evaporation, coagulation, chemical reaction or activation as a cloud droplet. The mechanisms by which aerosols affect climate are not currently well understood or quantified; in fact the Intergovernmental Panel for Climate Change (IPCC) Fourth Assessment Report (AR4) gave most aerosol effects on climate a "low" or "medium-low" level of scientific understanding. Rockström et al. (2009) also highlighted atmospheric aerosol concentrations as one of the "planetary boundaries" that must not be transgressed for mankind to achieve long term socio-economic development, but stated that we do not

currently have sufficient knowledge to define where that boundary lies.

The work presented here investigates the role of tropical biogenic aerosol in the previously unstudied region of South East Asia. This Chapter will present a background of aerosol science and their influence on the atmosphere, with Chapter 2 detailing the Aerodyne Aerosol Mass Spectrometer which was used for the majority of aerosol measurements reported herein. Chapter 3 reviews previous aerosol measurements to highlight the need for further characterisation of tropical aerosol. Chapter 4 presents results from the OP3 project in Borneo, with Chapter 5 setting these results in the wider context.

1.1 The Influence of Aerosol

Climate Change

Since the industrial revolution, man has been affecting the Earth through land use change, increased mechanisation and power generation, which have come as the global population has grown and living standards have increased. Historical temperature records show that there has been a rapid net warming of the Earth since the mid 19th Century (Brohan et al., 2006; Le Treut et al., 2007). This has mainly been attributed to greenhouse gases, which are shown to have increased since the beginning of the industrial revolution in 1750 (Le Treut et al., 2007). This rapid change in greenhouse gas concentrations is largely due to anthropogenic land use change and the combustion of fossil fuels. However, mankind is affecting the global climate balance in many other, often less well understood, ways. This section will give an overview of the main drivers of climate change. It will also show the role of aerosols in the climate debate and why more needs to be known about their influence.

Radiative Forcing

Radiative forcing (RF) is a useful metric in the discussion of contributions to climate change. It is defined by the IPCC as

> the change in net (down minus up) irradiance (solar plus longwave; in W m^{-2}) at the tropopause after allowing for stratospheric temperatures to readjust to radiative equilibrium, but with surface and tropospheric temperatures and state held fixed at the unperturbed values (Forster et al., 2007; Hansen et al., 1997).

When the balance between incoming solar radiation and outgoing longwave radiation is changed, it "forces" the climate from its equilibrium. It is conventionally used only to refer to first order effects. Any consequence of this heating acting to accelerate or decelerate the initial change is not termed a RF but a *climate feedback*. RF is linearly related to

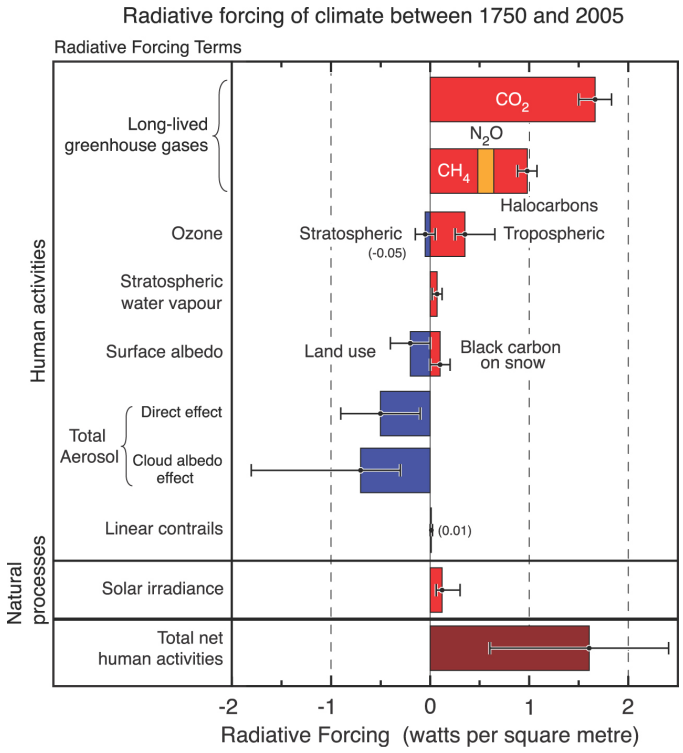

(a)

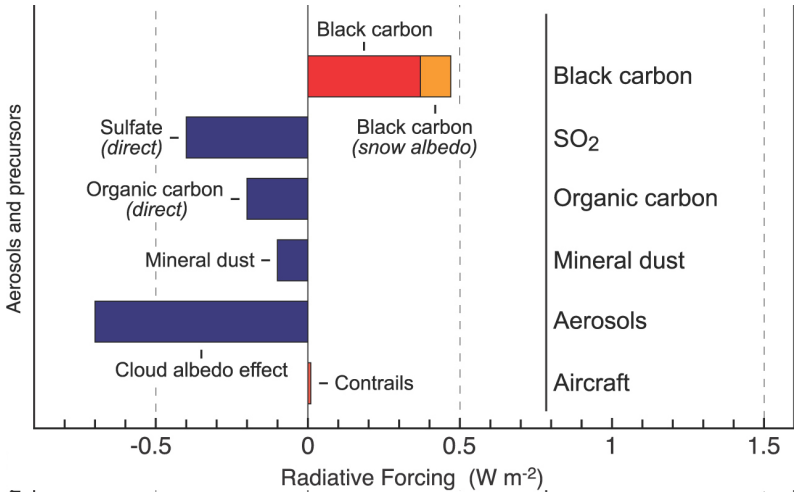

(b)

Figure 1.1: (a) Total radiative forcing of the atmosphere. Aerosol contributions are assessed as having low/medium-low levels of understanding. (b) Radiative forcings of different aerosol effects. Images reproduced from the IPCC AR4 (Forster et al., 2007).

the global mean equilibrium temperature change at the surface through the climate sensitivity parameter (Forster et al., 2007). This is a very simplistic view of climate change and is not meant to completely describe climate response. In reality, both the climate sensitivity parameter and the relationship of radiative forcing to climate change are not well quantified. However, radiative forcing provides some level of quantification that can be useful for ranking influences on the climate.

The IPCC AR4 assesses the contributions of different radiative forcings affecting the global radiation balance (Figure 1.1). The effect of aerosols is the least well understood of

any of the radiative forcings, with levels of scientific understanding of "low" or "medium-low." By far the biggest forcing shown in Figure 1.1 is due to greenhouse gases. While it is not directly related to aerosol climate effects, it is an important part of anthropogenic radiative effects and, as such, is discussed briefly here. A fraction of the solar radiation that is incident on the Earth's surface is absorbed, acting to heat the surface. This results in the emission from the surface of radiation at longer wavelengths, predominantly in the thermal infra-red (IR). Greenhouse gases absorb this IR radiation and, in turn, re-emit it in all directions, including back towards the Earth. This means radiation that otherwise would have been emitted into space remains in the Earth's atmosphere, resulting in an increase in the mean temperature of the Earth — a process known as the *greenhouse effect*. Some gases (such as water vapour) interact with this up-welling radiation strongly, but they do not accumulate in the atmosphere as they have a short atmospheric lifetime. Greenhouse gases that are less reactive (such as carbon dioxide and methane) have long atmospheric lifetimes and accumulate over a period of years (known as long lived greenhouse gases, LLGHG). This means that, despite being less efficient greenhouse gases than some of the shorter lived species, perturbations to their emission causes a larger net effect on climate over their lifetimes. Because of their long atmospheric lifetime, these major greenhouse gases are relatively evenly distributed around the World.

Aerosol Effects on Climate

The effects of aerosols on the Earth's radiative balance are classified into *direct* and *indirect* (Haywood and Boucher, 2000; Twomey, 1977b). The direct effect consists of any direct interaction of radiation with aerosol, such as absorption or scattering. It affects both short and longwave radiation to produce a net negative RF (Charlson et al., 1992). The magnitude of the RF due to the direct effect of an aerosol is dependent on the underlying surface, as this affects the net amount of radiation absorbed or scattered to space. If a highly scattering aerosol is above a surface of low albedo[1] it has a greater RF than if it was above a surface of high albedo. The converse is true of absorbing aerosol, with the greatest RF arising from a highly absorbing aerosol over a surface of high albedo (Haywood and Boucher, 2000).

Aerosols also affect the Earth's climate though their role in cloud formation, known as the indirect effect. Cloud droplets form onto pre-existing particles, known as cloud condensation nuclei (CCN). For any given meteorological conditions, an increase in CCN can increase the number of cloud droplets. This increases the albedo of the cloud, reducing the surface flux of solar radiation in a process known as the *cloud albedo effect* (Twomey, 1977b). Evidence supporting the cloud albedo effect has been seen from the effects of ship tracks (Ackerman et al., 2000b) and biomass burning (Andreae et al., 2004; Kaufman and Fraser, 1997) on cloud albedo compared to ambient clouds. The direct and cloud albedo effect are both first order effects and therefore are classified as radiative

[1]The albedo of an entity is defined as the fraction of incoming radiation reflected by that entity.

forcings by the IPCC (Forster et al., 2007).

An increase in cloud droplet number also acts to reduce the cloud droplet size (for a given amount of water) which suppresses precipitation, increasing the cloud lifetime. This increases the time-averaged cloud albedo and is known as the *cloud lifetime effect* (Forster et al., 2007). This has been observed as the suppression of drizzle in ship tracks (Ferek et al., 2000) compared to ambient clouds and inhibited precipitation in biomass burning plumes (Rosenfeld, 1999). The cloud lifetime effect is classified as a climate feedback (rather than a RF) by the IPCC due to the interdependence between it and the hydrological cycle (Forster et al., 2007). However, it has previously been classified as a negative RF (Hansen et al., 1997).

The *semi-direct effect* concerns the influence of absorbing aerosol, such as soot. It encompasses many individual mechanisms, and in general is more poorly defined and understood than the direct and indirect aerosol effects. However, direct evidence of several of these mechanisms has been reported. If absorbing aerosols are present in a layer aloft in the atmosphere they can heat surrounding air which inhibits the condensation of water vapour resulting in less cloud formation (Ackerman et al., 2000a). Additionally, heating a layer of the atmosphere relative to the surface results in a more stable atmosphere which inhibits convective uplift of moisture (Koren et al., 2004). The heating of the atmosphere aloft also cools the surface resulting in less evaporation of surface water. The semi-direct effect is sometimes classified as a positive RF (Hansen et al., 1997), although strictly it is considered a climate feedback by the IPCC AR4 due to the interdependence between it and the hydrological cycle (Forster et al., 2007).

All the aerosol climate effects have some reliance on the vertical distribution of aerosol in the atmosphere, in particular their altitude in comparison to cloud cover. Aerosol below cloud will interact with less sunlight than aerosol above cloud or in a clear sky, meaning its role in the direct aerosol effect will be less. Absorbing aerosol over cloud cover is also likely to result in a bigger change in albedo than if over cloud free ground. For aerosol to be involved in the semi-direct aerosol effect it must be transported to the altitude of cloud formation. The altitude of absorbing aerosol governs whether it will act to evaporate existing cloud, or if it will stabilise the mixing of the atmosphere, both examples of the semi-direct effect. The atmospheric lifetime of an aerosol (see Section 1.3) is dependent on its altitude (Textor et al., 2006), with aerosol above cloud less likely to be removed, leading to a greater time-averaged radiative forcing.

While there is mounting evidence supporting the significance of these various aerosol effects, the magnitude of their influence remains uncertain. In particular, the semi-direct aerosol effects are not well understood due to the variety of feedbacks which may interact with each other in a complex manner. A schematic of aerosol effects, adapted from the IPCC AR4 (Forster et al., 2007), can be seen in Figure 1.2. Aerosols tend to have short atmospheric lifetimes compared to the long lived greenhouse gases — on the time scale of days or weeks — meaning their distribution round the World is much more heterogeneous.

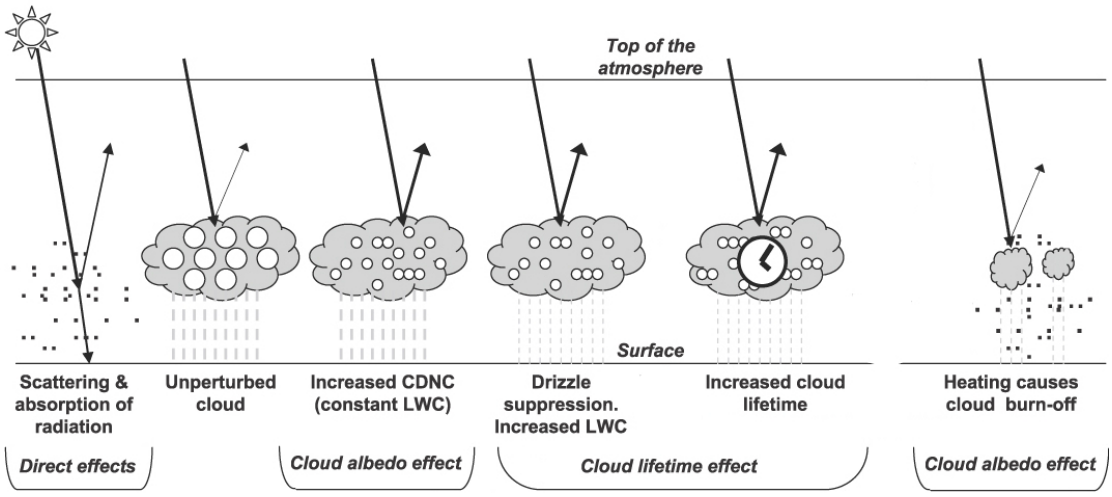

Figure 1.2: Schematic of various aerosol radiative effects. Black dots represent aerosols, white circles represent cloud droplets. Straight lines represent incident and reflected solar radiation, wavy lines represent terrestrial longwave radiation. CDNC stand for cloud droplet number concentration and LWC stands for liquid water concentration. Figure adapted from the IPCC AR4 (Forster et al., 2007).

This leads to dramatically different aerosol radiative forcings in different parts of the World. It is also the case that the localisation of some aerosol effects can have a complex influence on regional meteorology, for instance to the hydrological cycle.

Effects on the Hydrological Cycle

In predicting the human impact of future climate change it is essential to better understand the hydrological cycle which governs rainfall. Changes to the hydrological cycle can lead to drought or flooding, which can have extreme effects on communities. It is difficult to predict the behaviour of the hydrological cycle under future emissions scenarios due to the complex interaction of global heating from greenhouse gases with the cloud micro-physical effects of aerosol. Models and observations indicate that planetary surface heating increases the amount of water vapour in the atmosphere at around 7% K^{-1} due to the increased capacity of the atmosphere to contain water (Wentz et al., 2007, and ref. therein). This in turn is predicted to increase precipitation, although it is uncertain by how much.

Aerosol can both enhance and inhibit precipitation. In some pristine environments cloud droplet formation is thought to be limited by the number of CCN available (Poschl et al., 2010). Precipitation can be caused by inadvertent or intentional "seeding" of clouds with hygroscopic particles. For instance Biswas and Dennis (1971) demonstrated artificial cloud seeding using sodium chloride and Mather (1991) observed an increase of large cloud drops downwind of a paper mill which was hypothesised to affect precipitation rates. However, aerosols also inhibit precipitation through the semi-direct and indirect effects. Koren et al. (2004) found that in Amazonia, heavy smoke from biomass burning completely inhibited cumulus cloud formation, compared to 38% cloud cover in smoke-

less conditions. Rosenfeld (1999) also demonstrated a similar effect in Borneo using satellite data.

It also seems that aerosols can affect the hydrological cycle on a regional scale. As Patra et al. (2005) highlight, change in the Indian monsoon is an important example of hydrological change impacting a wide region. Layers of absorbing pollution aerosol reduce the sea surface temperature, reducing the amount of water vapour entering the monsoon system. Agriculture accounts for around 16% of Indian GDP and employs over half a billion people in India (US Central Intellegence Agency, 2011) and Indian crop yields are historically linked to the monsoon (Parthasarathy et al., 1994). The failure of the Indian monsoon has been linked to anthropogenic aerosol (Chung and Ramanathan, 2006; Patra et al., 2005), with an estimated rainfall suppression of 10-20% (Chung and Ramanathan, 2006). It is also thought that suppression of Indian monsoon rainfall has increased precipitation in the African Sahel (Chung and Ramanathan, 2006), showing the hydrological cycle of the World to be complex and interconnected.

It is still unclear if aerosols cause a net increase or decrease in precipitation (Levin and Cotton, 2008; Rosenfeld et al., 2008). However, there is mounting evidence that aerosol effects can perturb the hydrological cycle on a regional scale, often to the detriment of local populations. Andreae (2007) believes that in virtually all terrestrial environments anthropogenic aerosol emissions modify the hydrological cycle, with pre-industrial aerosol concentrations more similar to those in remote marine environments.

Effects on Atmospheric Chemistry

Aerosols play an important role in the chemistry of the troposphere by providing surfaces upon which chemical reactions can occur. They facilitate *heterogeneous reactions* which are defined as reactions "in which one or more reactants undergo a change at an interface" (Encycopaedia Britannica, 2011). In the context of aerosol this refers to reactions between gas and condensed phase species at an aerosol surface. Such reactions change the nature of the aerosol itself, and also affect concentrations of the gas phase species.

Understanding changes to physical properties of aerosol as a result of heterogeneous reactions is important for predicting how they will affect climate. For instance, if an aerosol becomes more hygroscopic (see Section 1.3) as a result it is more likely play a role in the direct effect due to an increased scattering cross section (through activation or swelling) and the indirect effect as a CCN. Reactions that change aerosol absorbance will change their role in the direct effect. The atmospheric lifetime of an aerosol is also linked to its hygroscopicity, as particles activated as cloud droplets are more likely to be removed by precipitation.

Aerosol appeared to affect gas phase species after the eruption of Mount Pinatubo in 1991 (McCormick et al., 1995) when sulphate aerosol (formed from volcanic emissions of sulphur dioxide; see Section 1.2) affected stratospheric ozone concentrations by increasing the surface area upon which heterogeneous chemistry could occur. A major sink

of stratospheric ozone is through its reaction with chlorine radicals, Cl. It is thought that the sulphuric acid aerosol allowed more conversion of relatively inert forms of chloride into reactive Cl through heterogeneous reactions. Reactive forms of nitrate, which are normally a sink for reactive Cl were also heterogeneously converted to inert forms. Both of these effects appeared to increase the amount of chloride reacting to deplete ozone. The understanding of the heterogeneous chemistry of stratospheric sulphate is reasonably advanced. However, one of the major challenges of aerosol science is to gain an understanding of how these processes govern tropospheric chemistry, particularly in organic aerosol (see Section 1.4).

Other Aerosol Effects

While much aerosol research is currently focused on the climatic influence of aerosols, they have long been studied for other reasons. Urban areas have been known to be major sources of particulate pollution for many years. This was particularly apparent during the industrial revolution where unbridled and inefficient combustion of coal caused buildings to turn black with soot and helped to reduce the average life expectancy in working class cities like Manchester to less 30 years old (Szreter and Mooney, 1998). The effects of aerosol on buildings are not limited to unsightly blackening but also act to degrade the materials through the deposition of acids (Grossi and Brimblecombe, 2002).

1.2 Understanding the Natural Background

In order to predict how anthropogenic activity will affect the Earth, it is necessary to have a good understanding of the biogeochemical cycles which govern the transport and transformation of important elements. Understanding how they affect aerosol formation, evolution and removal is key to properly assessing and predicting atmospheric aerosol climate effects. If we can understand better how we are perturbing these cycles we can make informed decisions about how to manage our interactions with them in the future. In order to assess the influence of anthropogenic aerosol direct, indirect and semi-direct effects, it is essential to first quantify the effects due to the natural, unperturbed system. Only then will the full nature of anthropogenic aerosol climate effects be understood, allowing effective mitigation of their effects.

The Carbon Cycle

The carbon cycle has become increasingly relevant as it is being perturbed to a great extent by anthropogenic activity, leading to the build-up of CO_2 in the atmosphere that is playing a major role in climate change. While this is largely due to the combustion of fossil fuels (especially during the latter part of the 20th Century), a significant amount of carbon has been released from the biosphere as a result of anthropogenic land use change.

The IPCC AR4 estimate that, during the 1990s, about 1.6 Gt C yr^{-1} was released into the atmosphere as a result of the destruction of natural ecosystems, compared to 6.4 Gt C yr^{-1} from fossil fuels (Denman et al., 2007). Half of the carbon emitted due to land use change in the 1990s was from tropical Asia (Denman et al., 2007).

Plants, algae and some bacteria use the energy from sunlight to photosynthesise CO_2 which results in carbon being reserved in the living tissue. This carbon is returned to the atmosphere in the form of CO_2 through respiration in organism cells, decomposition or combustion. Emission of volatile organic compounds (VOC) by vegetation is also a significant natural source of carbon to the atmosphere — it has been estimated that VOC emissions account for 3.5–39% of net ecosytem production of carbon[1] (NEP; Denman et al., 2007; Kesselmeier et al., 2002). Globally, non-methane biogenic emissions of VOCs are 5–10 times the anthropogenic emissions (Guenther et al., 1995; Kanakidou et al., 2005). These VOCs can be oxidised in the atmosphere to form secondary organic aerosol (SOA; see Section 1.4) or gas phase species such as CO_2, both of which can influence climate. Biomass burning is also a major route by which carbon reserved in the biosphere is moved into the atmosphere, both in the form of CO_2 and aerosol.

Isoprene (2-methyl-1,3-butadiene) is emitted naturally by many different types of vegetation and is the most abundant non-methane hydrocarbon in the atmosphere, comprising 44% of all VOC emissions (Guenther et al., 1995). It has long been considered an insignificant source of secondary aerosol (Pandis et al., 1991). However, recent studies have measured isoprene SOA in chambers and in the field (e.g. Chan et al., 2010; Claeys et al., 2004; Surratt et al., 2006). While chamber yields are extremely low, it could be a very important source of SOA as it is present in the atmosphere in such vast quantities.

About half the World's forests are in the tropics (Food and Agriculture Organisation, 2010), however, the region is undergoing rapid land use change, with deforestation for timber and agriculture (Achard et al., 2002; McMorrow and Talip, 2001) changing the amount of carbon released to the atmosphere as VOCs. Tropical rainforests may be affected not just by direct destruction, but by climate change itself. It seems that, as the hydrological cycle (see Section 1.1) becomes more erratic with climate change, the terrestrial biospheric carbon sink may weaken as ecosystems are affected by drought (Zhao and Running, 2010). A recent study by Lewis et al. (2011) highlighted the dangers posed by deforestation of Amazonia. They found evidence to suggest that a reduction in precipitation caused by climate change caused tree mortality, which transferred stored carbon to the atmosphere, exacerbating the initial climate change. It is estimated that tropical forests contribute almost half of all global biogenic non-methane VOC emissions — about 500 Tg C yr^{-1} compared to the global total of 1150 Tg C yr^{-1} (Guenther et al., 1995). They are an important source of carbon to the atmosphere and, as such, they could be an important source of SOA, especially in remote regions where the role of anthropogenic emissions is less.

[1] *Net ecosystem production* is defined as the amount of carbon taken up by the biosphere but not released through other natural processes (decay or natural trauma) or combustion

It is a complicated but important task to characterise the unperturbed biospheric systems, particularly in the tropics where land use change is rapid and widespread. Characterising the unperturbed biospheric systems gives insight into what the implications of future land use change is likely to be, allowing for informed decisions to be made on land use change policy. It also provides a benchmark to measure any future, more extreme perturbations against.

The Sulphur Cycle

Sulphur has a variety of important roles in the Earth's system (Jacobson et al., 2000). The vast majority of sulphur is reserved in the lithosphere, from which large amounts are released through volcanic emissions of sulphur dioxide (SO_2) and hydrogen sulphide (H_2S) (Allen et al., 2002; Graf et al., 1997). Many biological processes also emit sulphur-containing gases. In particular, phytoplankton can move seawater sulphate (SO_4^{2-}) to the atmosphere through the formation of dimethyl sulphide (DMS; CH_3SCH_3). This has been shown to be the dominant sulphur producing process in the open oceans (Andreae and Raemdonck, 1983; Andreae et al., 1985) and, as such, is a major part of the sulphur cycle. It is possible for sulphate to be emitted from biomass burning although the processes are highly uncertain (Gao et al., 2003). Anthropogenic activity introduces sulphur into the atmosphere mainly in the form of sulphur dioxide from the burning of coal (and oil derivatives). Sulphur from ore smelting is also a significant anthropogenic source (Jacobson et al., 2000).

Once emitted into the atmosphere, gaseous sulphurous species tend to have a short lifetime (days) due to oxidation by the hydroxyl radical (OH), with the OH oxidation of sulphur dioxide in particular creating sulphuric acid. Sulphur dioxide is also highly soluble and it readily dissolves in cloud droplets where it can be oxidised, especially under winter conditions when the photochemistry is less (Irwin and Williams, 1988), with subsequent evaporation of the drop leaving the residual sulphate aerosol (Forster et al., 2007; Irwin and Williams, 1988). Sulphuric acid produced from OH oxidation of sulphur dioxide also condenses without the presence of water to form liquid aerosol (Forster et al., 2007). It can then be neutralised by a base (usually ammonia) to form a salt.

Globally about 72% of sulphate aerosol is produced anthropogenically from fossil fuel combustion emissions, with phytoplankton emissions producing around 19% and volcanoes accounting for about 7% (Forster et al., 2007). Most of the anthropogenic sulphate is concentrated in the northern mid-latitudes where fossil fuel combustion emissions are greatest. While anthropogenic emissions are thought to make up more than 80% of sulphate emissions in northern mid-latitudes (Bates et al., 1992) there are large parts of the globe that are unaffected by anthropogenic emissions (Jacobson et al., 2000).

As sulphate aerosol is relatively abundant, it plays an important role in the global climate balance. It scatters light efficiently and is hygroscopic, playing and important

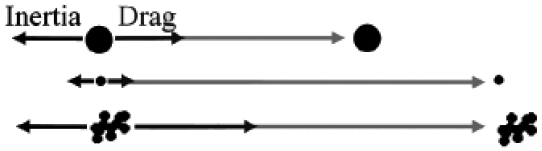

Figure 1.3: A schematic representation of particles of different aerodynamic diameter. Adapted from (DeCarlo et al., 2004). Particles undergo a force imparted by moving air (from left to right). Grey arrows represent the velocity of the particles after an acceleration and black arrows represent the forces imparted. The irregular particle has the same mass as the larger sphere but the same aerodynamic size as the smaller particle. All particles have standard density.

role as CCN (Forster et al., 2007). Although much smaller than anthropogenic emissions, volcanic emissions of sulphate can also significantly affect climate. If sulphurous gas is injected into the stratosphere from the vigorous uplift produced in volcanic eruptions, it can form aerosol with an atmospheric lifetime of years, rather than the days or weeks typical of the tropospheric aerosol. It is then free to affect atmospheric chemistry (see Section 1.1) and climate through the direct effect, and, once it sediments back into the troposphere, the indirect effect through the formation of cirrus clouds (Forster et al., 2007; McCormick et al., 1995). These effects were measured after the eruption of Mount Pinatubo in the early nineties which caused a mean global cooling of around 0.5°C, which lasted for several years (Forster et al., 2007; McCormick et al., 1995; Stowe et al., 1992).

The sulphur cycle significantly affects climate through the biogenic and anthropogenic production of aerosol. While sulphate sources and processes are better understood than those of organic species, the uncertainty in their radiative forcing still remains large when compared to LLGHG (Forster et al., 2007). While legislation has led to much of the sulphur being removed from fossil fuels used in the West, many developing countries still use fuel that is rich in sulphur (International Fuel Quality Center, 2009). A better understanding of the sulphur cycle will lead to more accurate predictions of the effect sulphate aerosols will have under future emissions scenarios.

1.3 Atmospheric Aerosol Properties

Size Definitions

Care has to be taken with the concept of aerosol "size." Mere diameter will only suffice for the cartoon of ball bearing-like particles. In reality aerosols are rarely of uniform shape or density. The simplest size definition is the volume equivalent diameter, D_v, defined as the diameter of a perfect sphere with the same volume as the subject particle. However in practice this is an inconvenient property to quantify.

It is more convenient to define the size of an aerosol in terms of properties that are more easily measured. A useful property of a particle is its aerodynamic diameter, D_a,

which is defined as the diameter of a sphere of unit density (1 g cm^{-3}) with the same terminal velocity[1] as the particle. It is dependent on the density, size (D_v) and shape of the particle (Figure 1.3). It is also dependent on the Cunningham slip factor, which is a correction to the drag predicted by Stoke's law that is significant when the particle is not in the continuum regime[2] (DeCarlo et al., 2004). The application of the Cunningham slip factor for particles in the free molecular regime[3] leads to the definition of the vacuum aerodynamic diameter (D_{va}). This is the size metric used in Aerosol Mass Spectrometer measurements (see Section 2.1). It can be defined as

$$D_{va} = \frac{\rho_p}{\rho_0}\frac{D_v}{\chi} \tag{1.3.1}$$

where ρ_p is the density of the particle, ρ_0 is unit density, D_v is the volume equivalent diameter and χ is the shape factor in the free molecular regime (unity for a sphere and greater for irregular shapes) (Jimenez et al., 2003).

Aerosol Sources and Sinks

Aerosol mass can be thought of as originating in one of two ways: it is either emitted directly into the atmosphere (primary aerosol) or formed in the atmosphere from the condensation of gases (secondary aerosol). Aerosols can be split into the size classes indicated in Figure 1.4. Different sources and sinks are relevant to different sizes of particles, leading to the formations of distinct size modes.

Particles smaller than 10 nm are known as *ultrafine* and are produced from bursts of newly nucleated particles (Kulmala, 2003). Between diameters of around of 10 and 100 nm are the *Aitken mode* particles. These particles are relatively newly formed and often arise from growth on, or coagulation of, ultrafine particles. They are also emitted from internal combustion engines are often a mode indicative of urban locations. As Aitken mode particles age, they tend to increase in size due to coagulation with other particles or condensation of gas phase species, forming the next classification of *Accumulation* particles, which have diameters between about 100 nm and 1 μm. The process of coagulation also serves to decrease the total aerosol number. Accumulation mode particles have a relatively long lifetime in the order of days to weeks and are normally aged (that is oxidised to some degree), with most of their mass being secondary in nature. Particles in this mode are a similar size to the wavelength of most sunlight, meaning they interact strongly through Mie scattering and, as such, are important for climate. They also tend to have the highest total surface area of all the modes making them important when considering heterogeneous chemistry. Aerosols larger than 1 μm are known as *coarse* and are

[1] Velocity at which the gravitational weight of a particle is balanced by drag forces

[2] Particles are defined as being in the continuum regime if the mean free path of the gas molecules is much less than the radius of the particle

[3] Particles are defined as being in the free molecular regime if the mean free path of the gas molecules is much greater than the radius of the particle

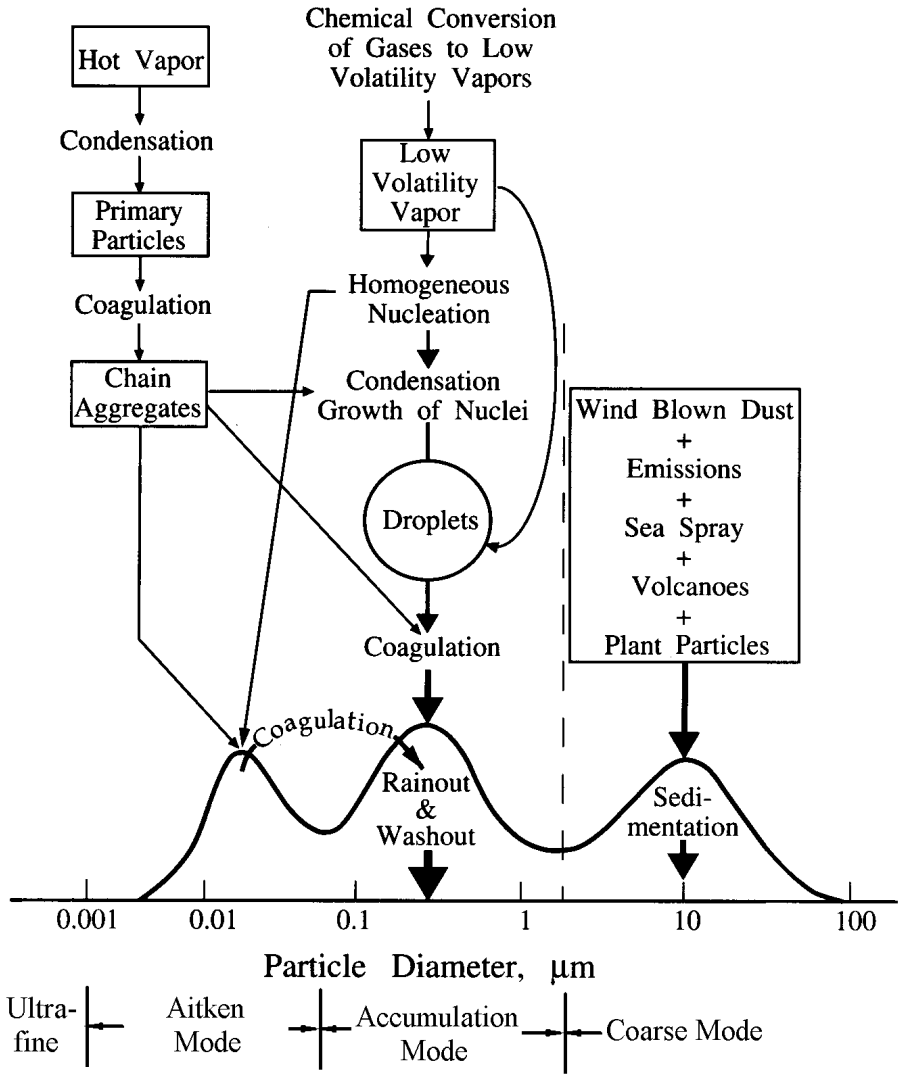

Figure 1.4: Principal aerosol size modes, sources, sinks and processes affecting them. Modified from Seinfeld and Pandis (2006).

generally created during mechanical processes such as vehicle tyre and brake degradation or creation of surface dust.

The lifetime of a particle in the atmosphere is governed by the removal processes that affect it. Aerosols are removed from the atmosphere by two types of process. *Dry deposition* denotes any process that removes an aerosol from the atmosphere without the aid of precipitation, such as gravitational settling, impaction on surfaces or electrostatic deposition. *Wet deposition* denotes any process where the aerosol is removed by precipitation. This can happen through *rain-out*, when particles incorporated in cloud droplets are deposited in precipitation, or by *wash-out*, where particles become incorporated into precipitation after a collision. The deposition route of an aerosol depends on different factors such as its water solubility, its size and the amount of precipitation in its environment. A summary of sources and sinks can be seen in Figure 1.4.

Coarse mode aerosols tend mainly to be removed by settling due to gravitational forces, leading to a typical lifetime in the order of hours, although this can be signif-

icantly longer if injected high into the troposphere, for instance by volcanoes or dust storms (McKendry et al., 2001). They are also more susceptible to removal by impaction on surfaces than smaller particles due to their larger aerodynamic diameters. The smaller particles making up the accumulation mode are less susceptible to gravitational deposition as their weight is small compared to the forces imparted by collisions with the molecules of the suspending gas, that is their terminal velocity is low. These aerosols have an atmospheric lifetime in the order of days to weeks so they accumulate in the atmosphere. Removal of these particles is usually due to precipitation. The smallest particles ($\lesssim$100 nm) diffuse rapidly due to Brownian motion, meaning they are susceptible to removal by random impaction on available surfaces. They also tend to be processed into larger modes, both by condensation of gases and coagulation with other particles.

Condensation of Vapours

Describing the condensation of vapours in the atmosphere is important, both in order to understand the conversion of water vapour to cloud droplets and the conversion of gas phase species to aerosol mass. A vapour is defined as being a substance that is in the gas phase but at a temperature below its boiling point. Vapours often exist in equilibrium with a surface of the same substance, that is when molecules are leaving and joining the surface at the same rate. For instance, when liquid water is introduced to dry air (in a closed system), water molecules will enter the gas phase above the surface of the water. However, until this occurs no water molecules exist in the gas phase that can enter the liquid phase as the air is dry. As more water molecules evaporate and the concentration of gas phase water molecules increases, the likely-hood of water condensing back to the liquid phase increases until an equilibrium is reached. These gas phase water molecules are referred to as a vapour. Given ideal assumptions, a range of terms can be defined to describe the behaviour of vapours. The pressure exerted by a vapour in equilibrium with a surface is known as the *equilibrium vapour pressure*. The *partial pressure* of a vapour is defined as being the "pressure that would be exerted by a constituent gas of a mixture if it alone occupied the space"(Oxford English Dictionary, 2010c). The sum of all the partial pressures of a mixture is equal to the total pressure of the mixture (as stated by Dalton's Law).

Several factors govern the equilibrium vapour pressure of a substance. It increases with temperature until the boiling point is reached, at which point the equilibrium vapour pressure effectively becomes the environmental pressure. The curvature of a surface changes the pressure of the vapour in equilibrium with it, known as the *Kelvin Effect*. This says that the more convexly curved a surface is, the less well bound its molecules are as they have fewer nearest neighbours to bond with. This has the effect of raising the equilibrium vapour pressure. The term *saturation vapour pressure* is sometimes used to refer specifically to the equilibrium vapour pressure above a flat surface. Equilibrium vapour pressure is also affected when particles are composed of a mixture of substances,

known as the *Raoult Effect* which states "the vapour pressure of a solution is proportional to the mole fraction of solute in the solution" (Atkins and de Paula, 2002). It is possible to illustrate this effect by extension of the above example of vapour in equilibrium with a liquid water surface. If a solute, say sodium chloride, is dissolved in the liquid water, then a proportion of the molecules at the surface will be sodium chloride, meaning less of the surface molecules are water. This makes is less likely that an individual water molecule can evaporate from the surface of the water, hence lowering the vapour pressure. This idealised equilibrium thermodynamic description of condensation of water vapour above a surface is known as Köhler theory. An analogous system, known as nano-Köhler theory (Kulmala et al., 2004), can be used to describe the condensation of non-water species such as organic vapours.

A net change of phase begins to occur when the partial pressure of a substance is greater than its equilibrium vapour pressure. The degree to which this is true is measured by *supersaturation*. Net condensation of a gas can happen for three reasons: if the ambient temperature is lowered; if chemical reactions increase the partial pressure of a gas or lower its vapour pressure; and because of an addition to the mixture lowering vapour pressures through the Raoult effect. Gases will preferentially condense onto a surface (which in the context of aerosol is named *heterogeneous nucleation*). In some circumstances, gases may condense without a pre-existing surface in a process known as *homogeneous nucleation*. The supersaturation needed for this to occur with water is higher than occurs naturally in the atmosphere, however, homogeneous nucleation of aerosol has been observed in several environments such as boreal forests (Allan et al., 2006; Laaksonen et al., 2008), the Arctic (Pirjola et al., 1998) and marine environments (O'Dowd et al., 1999).

The size increase of an aerosol as a function of supersaturation is governed by the Kelvin and Raoult terms. At small sizes the gradient of this function is positive due to the dominance of the Raoult effect. At larger sizes the Kelvin term dominates and the gradient becomes negative. The maximum supersaturation (when the two terms are balanced and the gradient is zero) is known as the *critical supersaturation*. This means that when an aerosol surpasses its critical supersaturation, it can grow in size indefinitely (or until mechanical breakup of the droplet occurs) as the supersaturation is always greater than the critical supersaturation for a particle of that size. This is referred to as *activation* of a nucleus. It occurs during the formation of cloud droplets upon aerosol (Twomey, 1977a) and can also occur during the condensation of non-water species such as organic vapours upon aerosol (Kulmala et al., 2004).

The composition of an aerosol also plays an important role in its critical supersaturation, which governs its ability to form cloud droplets (Gysel et al., 2007). Salts and other ionic compounds tend to activate more easily as they readily dissolve in water because it is polar. In general the hygroscopicity[1] of inorganic compounds is relatively well characterised compared to organics. However, recent studies have started to find general trends

[1] *hygroscopic* is "said of bodies which readily absorb moisture from the air, so as to swell up, contract in length, or change form or consistence" (Oxford English Dictionary, 2010d)

in organic hygroscopicity. In particular Jimenez et al. (2009) have combined ambient and chamber data to show that organic aerosol hygroscopicity increases as the aerosol becomes more oxidised (see Section 1.4). In order to accurately predict the indirect aerosol effect, the number of activated CCN must be known. It is also the case that aerosol which absorb water and swell increase their chance of interacting with solar radiation, therefore increasing their role in the direct (and potentially semi-direct) aerosol effect. Therefore it is important to be able to predict the size and compositional evolution of aerosol, and then to be able to effectively relate these to predictions of water affinity.

1.4 Organic Aerosol

The term *organic* refers to any carbon containing molecules other than simple binary compounds and salts. Originally it was used to describe any compound that originates in a living organism and, as such, contains carbon (Oxford English Dictionary, 2010b). Organic aerosols can be a large fraction of the sub-micron aerosol population, ranging from 20 to 90% (Kanakidou et al., 2005), meaning accurately predicting their behaviour is an important part of predicting aerosol climate effects. They can be emitted directly into the atmosphere: sources of primary biogenic aerosols include pollen, fungal spores, viruses, or detritus and primary anthropogenic sources include emissions from fuel combustion or mechanical degradation such as that from vehicle breaks and tyres. These are referred to as primary organic aerosol (POA). Organic aerosol can also be formed through the oxidation of organic vapours, which tends to lower their saturation vapour pressure, causing partitioning to the condensed phase. The volatility of a species i is often expressed as an effective saturation concentration

$$C_i^* = \frac{C_i^{vap}}{C_i^{aer}} C_{OA} \tag{1.4.1}$$

where C_{vap} is the vapour concentration of i, C_{aer} is the condensed phase concentration of i and C_{OA} is the total organic aerosol concentration (Donahue et al., 2006). Atmospheric organic compounds can be classified according to their C^* values. In order of decreasing volatility, they can be present entirely in the gas phase (volatile organic compounds; VOC; $C^* > 10^6 \mu$g m^{-3}), almost entirely in the gas phase but with a very high potential to form aerosol after a reaction (intermediate volatility organic compounds; IVOC; $C^* = 10^3$–$10^6 \mu$g m^{-3}), partitioned between phases with more than 1% of mass condensed (semi-volatile organic compounds; SVOC; $C^* = 10^{-1}$–$10^3 \mu$g m^{-3}) or entirely present in the condensed phase ($C^* < 10^{-1} \mu$g m^{-3}).

SOA has traditionally been thought of as formed from the oxidation of VOCs, however work in the last few years has shown SVOCs and IVOCs may also be significant sources of aerosol through the oxidation of their gas phase components. For instance, organics traditionally considered involatile POA were shown to partition to the gas phase upon

dilution, where they were then oxidised to form SOA (Robinson et al., 2007). Recently it was found that the width of the organic aerosol plume downwind of a large oceanic oil slick was greater than the width of the VOC plume. The VOC plume width was also found to be a function of decreasing volatility. The conclusion was that SOA was formed from the lower volatility species (IVOC) which evaporate more slowly, by which time the slick has spread over a wider area (de Gouw et al., 2011).

Formation of Secondary Organic Aerosol Through Oxidation of Organic Vapours

Kroll and Seinfeld (2008) provide a review of the chemistry of formation of SOA from oxidation of VOCs. This and references therein are the basis for much of this section. The main way VOCs are processed in the atmosphere is through gas phase oxidation reactions. Oxidation of a molecule is defined as the loss of electrons when two or more substances interact, one of which is often, but not always, oxygen. Usually the oxidation of atmospheric VOCs occurs through reaction with the hydroxyl radical[1] ($OH\cdot$), the nitrate radical ($NO_3\cdot$) or ozone (O_3). Oxidation of organic molecules can lower their equilibrium vapour pressure, making them more likely to be present in the condensed phase. This occurs through the addition of functional groups which increases the overall polarity of the molecule (especially if the added group is polar). It can also occur from the increase in molecular weight, especially if the species oligomerises to form a long chain molecule. However, oxidation can also increase the equilibrium vapour pressure of a molecule by fragmenting it into products of smaller molecular weight than the parent molecule.

The most important oxidant in the troposphere is the hydroxyl radical, which has been calculated to destroy about 3.7 Pg of trace gases every year (Prinn, 2005). During the daytime it is primarily formed via the photo-decomposition of ozone in the reaction

$$O_3 + h\nu \rightarrow O_2 + O(^1D) \tag{1.4.2a}$$

$$O(^1D) + H_2O \rightarrow 2OH\cdot \tag{1.4.2b}$$

at wavelengths < 319 nm (Seinfeld and Pandis, 2006). It can also be created by the photolysis of nitrous acid (HONO). Since the main removal reaction for HONO is photo-decomposition, it reaches a maximum at night-time (especially in urban areas because of NO_2 emissions) but can be a source of OH in the morning (Seinfeld and Pandis, 2006). The hydroxyl radical does not react with any of the major atmospheric gases but is highly reactive with most trace gases. It is also often regenerated in catalytic cycles when reacting with trace gases. This means the supply of OH is not exhausted and sustains day time levels of $\sim 10^6$ molecules cm^{-3} (Seinfeld and Pandis, 2006). It has a diurnal cycle as it

[1] A *Free Radical* (often just *radical*) is defined as "an uncharged atom or group of atoms having one or more unpaired electrons"(Oxford English Dictionary, 2010a). They tend to be highly reactive and are denoted by a dot which represents the unpaired electron, as in $OH\cdot$

is produced photolytically, and it is the dominant radical during the day. OH· is of particular importance in the tropics due to the reliance of mechanism 1.4.2 on solar radiation and water vapour. The most important radical at night is the nitrate radical, however it photolyses readily (it has a noontime lifetime of ~ 5 seconds) so is not important during daylight hours (Seinfeld and Pandis, 2006).

One of the most important governing factors in the formation of SOA is the concentration of reactive nitrogen oxides (NO or NO_2, referred to as NO_x). These are produced naturally by lightning and from soil emissions, and anthropogenically from high temperature combustion (such as in vehicle engines). The effect of NO_x levels on SOA formation has been the focus of much work recently but the effects appear to be complex. Generally speaking, NO_x affects the type of reactions that occur in three ways: it affects the relative proportions of the initial oxidants; fate of RO_2 radicals; and fate of RO. Under high NO_x conditions RO_2 reacts with NO_x at the expense of RO_2 + RO_2 or RO_2 + HO_2 reactions. In general, small hydrocarbons (such as isoprene and monoterpenes) show lower SOA yields when oxidised in the presence of NO_x. However the converse seems to be true for larger hydrocarbons (such as sesquiterpenes) that have been studied.

The formation of SOA from isoprene has been a subject of much work in recent years. It was considered an insignificant source of SOA (Pandis et al., 1991) until organic aerosol detected on filter samples from Amazonia (Claeys et al., 2004) was confirmed to be the same as that from the chamber oxidation of isoprene (Surratt et al., 2006). Since then, chamber studies have measured isoprene SOA such as epoxides (Paulot et al., 2009; Surratt et al., 2010), tetrols (Kleindienst et al., 2009; Surratt et al., 2006, 2010) and organosulphates (Surratt et al., 2008). The same species have subsequently been measured on ambient filter samples (Chan et al., 2010; Surratt et al., 2010). Until Froyd et al. (2010) recently measured organosulphate isoprene SOA using the Particle Analysis by Laser Mass Spectrometry (PALMS) technique, isoprene SOA had only been measured on filter samples, leaving the high time resolution behaviour unexplored. Several factors seem to affect the amount and type of isoprene SOA formed, including relative NO_x concentrations and the presence of sulphate (Carlton et al., 2009; Surratt et al., 2010). Isoprene SOA is now considered likely to be a significant source of atmospheric aerosol (Henze and Seinfeld, 2006), however the atmospheric processing of isoprene SOA and burden is still poorly understood (Carlton et al., 2009).

Organic Aerosol Models

Due to the vast number of organic species and reactions present in the atmosphere, the amount of VOC that is partitioned to the condensed phase is highly uncertain. Goldstein and Galbally (2007) estimate that there have been between 10^4 and 10^5 different organic compounds measured in the atmosphere, although many more may be present. They assert that most atmospheric organics have not been directly measured, in either the gaseous or aerosol phase. The sinks of a large proportion of VOCs emitted into the atmosphere

are not known. They suggest that these organics are reacting to become SOA. Consensus over organic aerosol sources has not been reached and there are still significant gaps in our knowledge of the life-cycle of organic aerosol as a whole.

So called bottom-up models rely on detailed knowledge of chemical processing of SOA precursors and associated partitioning. Highly explicit models representing thousands of individual gas phase chemical reactions such as the Master Chemical Mechanism[1] can be coupled with partitioning models (e.g. Johnson et al., 2006). These highly explicit models are computationally expensive making them impractical for predicting SOA on global scales. They rely on a good knowledge of precursor emissions, detailed knowledge of the highly complex chemical processes that occur and accurate prediction of species vapour pressures. However, if they can be made provide an accurate representation of atmospheric organic chemistry they should be highly skilled at predicting chemistry under future perturbations.

Less explicit bottom up models use parameterisations of aerosol yields from chamber experiments. Chamber oxidation experiments can measure the fraction of VOC that partitions as SOA for different precursors and oxidising conditions (e.g. precursor, NO_x and oxidant concentrations, relative humidity). This yield can then be used in SOA modelling schemes. Like the highly explicit models, these models rely on a good knowledge of VOC emissions, which can be a significant source of error. Guenther et al. (1995) estimated the uncertainty in BVOC emission rates to be a factor of three, probably higher in the tropics. These models also rely on the behaviour of SOA chemistry in chambers being representative of atmospheric processes. SOA formed under the conditions typical of many chamber studies can have different composition and yields from that formed under atmospherically representative levels (Shilling et al., 2009). Ng et al. (2010) showed that data from chamber SOA only represented the less oxygenated fraction of atmospheric organic aerosol, with SOA representative of highly aged atmospheric organics (which are ubiquitous in the atmosphere) never reached. It is also impractical to separately parameterise SOA formation for all atmospheric organic compounds so decisions have to be taken about which are the most important sources to study and what generalisations can be made to unstudied species.

Many species in the atmosphere exist in an equilibrium between the condensed and gas phases. Predicting the amount of a species present in each phase is particularly difficult in the case of organics as their volatility constantly changes as it they are oxidised in the atmosphere. Donahue et al. (2006) proposed a framework for the description of the partitioning of aerosol named the Volatility Basis Set (VBS). The volatility of an aerosol can be parameterised in terms of the VBS using measurements of volatility performed in conjunction with chamber experiments. These parameterisations can then be used to describe SOA formation in regional scale models (e.g Lane et al., 2008). The VBS has the advantage of covering a large range of volatilities meaning it can capture partitioning of

[1]The Master Chemical Mechanism at the University of Leeds http://mcm.leeds.ac.uk/MCM

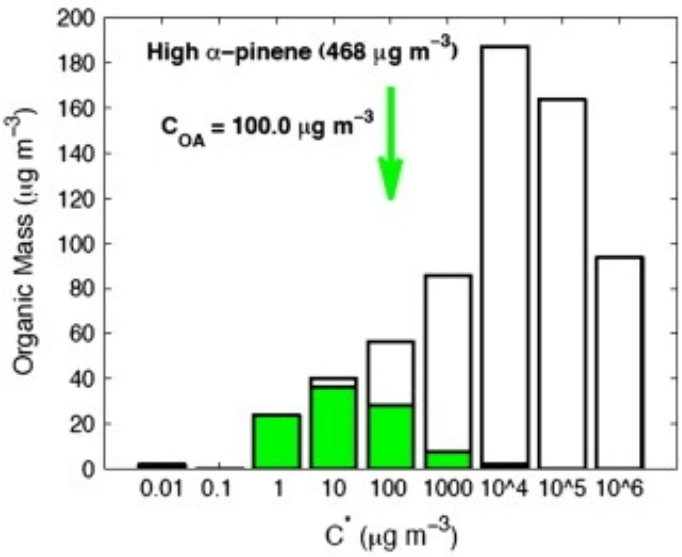

Figure 1.5: Results of chamber oxidation of α-pinene displayed using the VBS. Condensed material is represented by the green portion of the bars and vapours shown by white portion. The point indicated with an arrow is where $C_{OA} = C^*$ i.e. the same amount of vapour and condensed phase is present in that bin. Reproduced from Donahue et al. (2009)

aerosol that was previously considered involatile (Robinson et al., 2007). The description of the vapour component of low volatility species allows for SOA formed from these vapours to be predicted. Terms can be defined that quantify the volatility of a system (Donahue et al., 2009; Shrivastava et al., 2006). The particle fraction (X_p) is defined as being the ratio of the organic particulate mass to the total organic mass (particulate and gas). This can be expressed as

$$X_p = \sum_{i=1}^{n} f_i \left(1 + \frac{C_i^*}{C_{OA}}\right)^{-1} \tag{1.4.3}$$

where f_i is the mass fraction of species i (particulate and gas), C_i^* is the effective saturation concentration of species i, C_{OA} is the mass concentration of the absorbing organic phase, and n is the number of components in the system. By measuring X_i and C_{OA} experimentally, a value of C_i^* can be calculated. C_{OA} can be thought of as the total organic aerosol concentration although there is some debate as to the effects of composition and coatings. The volatility distribution of a species can then be expressed on a basis set of C_i^*: usually 10^{-2}, 10^{-1}, 10^0, 10^1, 10^2, 10^3, 10^4 and 10^5 μg m^{-3}. Figure 1.5 shows α-pinene oxidation products expressed on a VBS. While the VBS provides a framework for quantifying the volatility distribution and partitioning of an organic aerosol population, it is highly empirical. Different approaches used to predict species volatility distributions from first principles give a wide range of values, and little data currently exists to asses which, if any, of these approaches are applicable to atmospheric species (Booth et al., 2010).

Top-down modelling approaches apply estimates of well understood global sources

and sinks in order to assess the likely size of the less well known. While these "back-of-the-envelope" calculations make vast assumptions and have poor predictive skill accordingly, they tend to negate the problems associated with bottom-up approaches such as a lack of knowledge of detailed chemical schemes or extrapolations from laboratory data. As such they often provide a better assessment of source and sink budgets.

Global Estimates of SOA

Hallquist et al. (2009) collated bottom-up and top-down OA estimates from a range of studies in order to better constrain global SOA estimates. Their meta-analysis is summarised here. Recent bottom-up estimates that combine anthropogenic and biogenic fluxes of VOCs with yields from chamber experiments (Henze and Seinfeld, 2006; Henze et al., 2008; Kanakidou et al., 2005) give a total biogenic SOA (BSOA) flux of around 9–50 Tg C yr^{-1}. This is compared to a POA flux of 35 Tg C yr^{-1} (Bond et al., 2004) and an anthropogenic SOA (ASOA) flux of 1.4–8.6 Tg C yr^{-1} (Henze et al., 2008). This gives a total OA budget of around 50–90 Tg C yr^{-1}.

Through various treatments of knowledge of atmospheric emissions and depositions, Goldstein and Galbally (2007) suggest that bottom up estimates of SOA production could be more than an order of magnitude too small. One value is calculated by balancing mass of known sources and sinks of VOCs, by which they estimate the amount of SOA to be 510–910 Tg C yr^{-1}. Another estimate of SOA concentrations is performed by inspecting the relationship of organic to sulphate aerosol. Sulphate aerosol fluxes are better constrained than those of organic aerosol as there is a more complete understanding of the relatively simple chemistry that governs sulphate aerosol formation. By combining an estimate of the global sulphate flux with typical measured sulphate to organic ratios ($\sim$1:1) a final value of 140–540 Tg C yr^{-1} is reached. However, the majority of studies which inform this ratio were performed in the northern mid-latitudes, meaning extrapolating to other areas where the sulphate to organic ratio is likely to be different may introduce error.

This kind of top-down estimate has been updated by Hallquist et al. (2009) which builds on the sulphate scaling approach, which they believe to be the most accurate, to estimate the total SOA flux. They state that the assertion of Goldstein and Galbally (2007) that bottom-up models under-predict SOA fluxes by a factor of 10-100 (requiring 11–70% of VOCs to condense) seems to be "unrealistically high". The top-down sulphate scaling estimates of Hallquist et al. (2009) predict an OA flux of 150 TgC yr^{-1} (60–240 Tg C yr^{-1}). This included primary and secondary OA from both biogenic and anthropogenic sources. By then subtracting best estimates from the literature of POA loadings they estimate SOA fluxes of 115 Tg C yr^{-1} (25–210 Tg C yr^{-1}), or approximately 70% of OA mass. This estimate compares favourably to the meta-analysis of Aerosol Mass Spectrometer (AMS; see Chapter 2) data sets (Zhang et al., 2007) when some broad assumptions about oxidised POA (for instance from biomass burning) are made. The Hallquist et al. (2009) SOA estimate is towards the lower end of the Goldstein

and Galbally (2007) estimates. By subtracting estimated contributions of anthropogenic and biomass burning to SOA flux, Hallquist et al. (2009) arrive at a flux of BSOA of 90 Tg C yr^{-1} (0–185 Tg C yr^{-1}).

Global SOA estimates have been refined further by Spracklen et al. (2011), in discussion at the time of writing. This study uses a set of AMS data form numerous studies (including the results reported in this work in Chapter 4) to constrain SOA production yields in a global chemical transport model. They estimate a total global SOA source of 140$\pm$90 Tg yr^{-1}, of which 13$\pm$8 Tg yr^{-1} is biogenic, 100$\pm$6 Tg yr^{-1} is anthropogenically controlled (a definition of which is included on p.65), 23$\pm$15 Tg yr^{-1} is from conversion of POA to SOA (mostly from biomass burning), and 3$\pm$3 Tg yr^{-1} is from processing of biomass burning VOCs. This translates to mean radiative forcings of -0.26$\pm$0.15 Wm^{-2} for the direct aerosol effect and -0.6$^{0.24}_{-0.14}$ Wm^{-2} for the indirect effect.

Of course, these top down estimates make substantial assumptions, but it does appear that they predict a vastly higher global carbon flux to SOA than is predicted by the bottom-up considerations. The discrepancy implies that chamber experiment yields do not provide a complete picture of atmospheric oxidation processes.

Ensemble Property Models

Explicitly modelling the vast amount of atmospheric organic species that are thought to exist may be difficult due to the computational cost and need to parameterise all relevant processes. Several conceptual models now exist for the description of organic aerosol processing in terms of their ensemble properties, negating the need for a detailed understanding of individual mechanisms and species emissions. Zhang et al. (2005) deconvolved an urban AMS organic mass spectrum using a component analysis algorithm that relates individual marker peaks to source spectra contributing to the ensemble mass spectrum. By using m/z 57 (mostly $C_4H_9^+$) as a marker peak for hydrocarbon-like organic aerosol (HOA; a proxy for primary aerosol from vehicle combustion emissions) and m/z 44 (mostly CO_2^+) as a marker peak for oxygenated organic aerosol (OOA; a proxy for SOA and oxygenated POA) they were able to account for $\sim$99% of the variance in their dataset. This technique was applied to 37 existing data AMS datasets, which showed that OOA was the dominant factor, particularly in rural studies (Zhang et al., 2007).

This deconvolution approach was improved by the introduction of positive matrix factorisation (PMF, see Section 2.3), which Lanz et al. (2007) applied to an urban dataset. They found that the OOA component was itself composed of sub-factors (as speculated by Zhang et al. (2007)). These seemed to represent a highly oxygenated component (named OOA1) and a less oxidised component (named OOA2). Ulbrich et al. (2009) then presented a standardised approach for PMF analysis of AMS data (along with authoring analysis software) the use of which is now widespread in the community.

Jimenez et al. (2009) applied the PMF analysis to 30 datasets resolving up to four factors (corresponding to the HOA, OOA1, OOA2 and any other factor). They proposed that

newly formed semi-volatile aerosol is represented by OOA2 and that this is oxidised to aerosol represented by OOA1. They refer to these as semi-volatile OOA (SV-OOA) and low-volatility OOA (LV-OOA) respectively, and stress that these are points on a continuum of aerosol oxidation rather than distinct aerosol types (Morgan et al., 2010; Ng et al., 2010). This is supported by data they present from the Megacity Initiative: Local and Global Research Observations (MILAGRO) project in Mexico city (DeCarlo et al., 2008). This study compared high resolution AMS data from three ground sites (in Mexico city itself, 30 km downwind and 63 km downwind) and aircraft data to find that the fraction of OOA, O:C ratio and LV-OOA contribution all increased with ageing. By comparing O:C with hygroscopicity measurements from several studies, they show that a generalised link can be made between the two (Figure 1.6(a)). They propose a conceptual framework where organic species evolution can be represented by progression through a 2-D space of O:C vs. volatility. The effect of different types of chemical reactions to an organic species in this space is shown in Figure 1.6(b).

Heald et al. (2010) propose a slightly different conceptual model that represents organic aerosol on a Van Krevelen diagram (H:C vs O:C) (Van Krevelen, 1950). They found that data from a variety of contrasting environments (laboratory and field) populated a very narrow space of the Van Krevelen diagram, characterised by a slope of approximately -1, with aerosol progressing from top left to bottom right as it ages. In addition, Kroll et al. (2011) propose describing the evolution of organic aerosol species in a 2-D space of average carbon oxidation state[1] vs. number of carbon atoms. As organic species are oxidised they tend to progress from bottom left, with low oxidation number and a high number of carbon atoms, to top left, with high oxidation number and a low number of carbon atoms.

Organic aerosols are complex and dynamic which makes prediction of their radiative effects from first principles extremely difficult. The frameworks that have been presented in the recent years go a long way to addressing this issue by aiming to characterise ensemble aerosol properties. The goal is to relate relevant physical properties (e.g. light absorption, number, size) to measurable properties of bulk aerosol, in the same way that hygroscopicity seems to be closely related to the O:C ratio of organic aerosol. This will then allow a better constraint on the way the significant and least well understood component of atmospheric aerosol affects climate through direct interaction with sunlight and its role as CCN. These nascent ensemble models hold huge potential for providing an efficient description of organic aerosol. A fuller characterisation of ambient organic aerosol is essential in order to refine our understanding of organic aerosol processes. These conceptual models have so far mainly or exclusively been tested in the northern mid-latitudes. Aerosol distributions are heterogeneous due to their relatively short atmospheric lifetime. Hence, in order to reach a fuller understanding of global organic aerosol, the pool of

[1]Oxidation state of an atom is defined as the charge it would take if it were to loose all electrons participating in bonds to more electro-negative atoms, but gain all electrons participating in bonds to less electro-negative atoms.

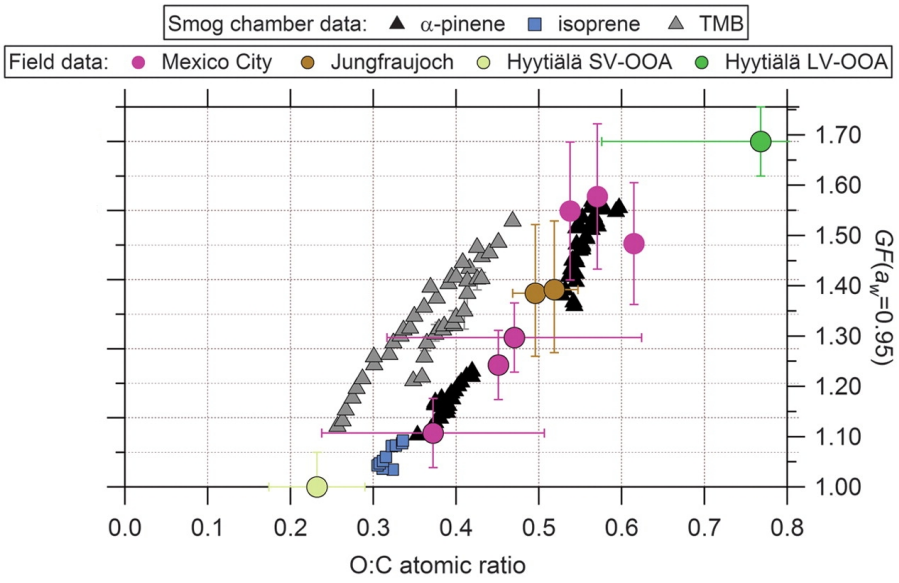

(a)

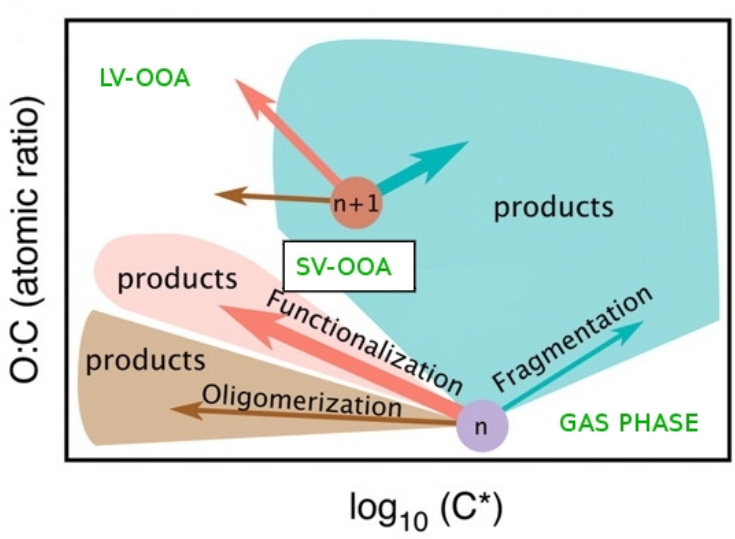

(b)

Figure 1.6: Figures modified from Jimenez et al. (2009). (a) A generalised relation of hygroscopic growth factor (measured with HTDMA) to aerosol O:C ratio (measured with AMS) using data from field projects and chamber studies. (b) Schematic representation of the ways different reactions move an organic species through the 2-D O:C vs C^* (volatility) space. Organic species n can be affected by oligomerisation (volatility decreasing but O:C staying constant), functionalisation (volatility decreasing and O:C increasing) or fragmentation (resulting in at least two fragments with possibly increased volatility and increased aggregate O:C). This results in organic species $n+1$ which can then be evolved further. Labels in green indicate that organic species tend to move from bottom right to top left as they are processed from VOCs to SV-OOA and LV-OOA.

detailed datasets must be expanded to cover the regions which are uncharacterised.

CHAPTER
TWO

THE AERODYNE AEROSOL MASS SPECTROMETER

The Aerodyne Aerosol Mass Spectrometer[1] (AMS) was used to make the majority of the measurements presented in this thesis so its workings, calibration and analysis are presented here. The AMS is a field deployable instrument that can provide quantitative measurements of the chemical composition and aerodynamic size of aerosol particles. It provides much higher time resolution data than off-line techniques, and avoids many of the associated artifacts such as evaporation of volatile species and contamination of samples. Its use has been demonstrated in a variety of field campaigns (e.g. Alfarra et al., 2004; Jimenez et al., 2009), aircraft campaigns (e.g. Bahreini et al., 2003a) and laboratory studies (e.g. Robinson et al., 2007). There have been several different models of the AMS produced, namely the *Quadrupole AMS* (Q-AMS; Jayne et al., 2000), *Compact Time of Flight AMS* (C-AMS; Drewnick et al., 2005) and the *High Resolution Time of Flight AMS* (HR-AMS; DeCarlo et al., 2006). AMS design and techniques have been reviewed by Canagaratna et al. (2007). This Chapter will describe the design, operation and analysis of the two time-of-flight AMSs.

The instrument consists of three main sections: the inlet, particle sizing region and the particle mass spectrometer region (Figure 2.1). The particles are sampled through an aerodynamic lens that focuses the particles into a narrow beam. A supersonic expansion at the exit of the lens imparts size dependent velocity upon the particles, meaning vacuum aerodynamic size (D_{va}) can be inferred from particle time of flight over a specific distance. The particles are then vapourised on a heated surface and ionised by electron impact. The resultant ions are extracted into the ion time of flight (IToF) mass spectrometer where their mass to charge ratio is measured. These can then be grouped by species type and summed to give speciated mass loadings as a function of time.

2.1 Design of the AMS

This section provides a description of the AMS technique, following the an aerosol from entering the instrument to the logging of its data.

[1]Manufactured by Aerodyne Research Inc., 45 Manning Road, Billerica, MA, USA

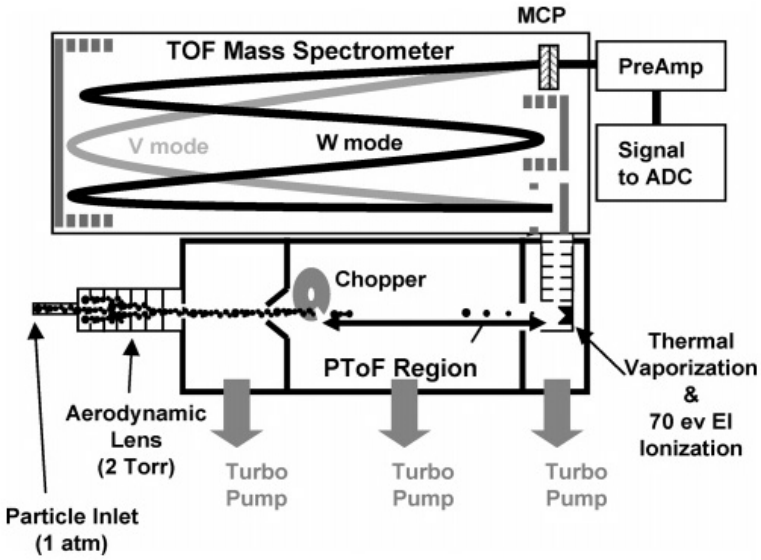

Figure 2.1: Schematic of the HR-AMS with V- and W-mode ion paths indicated. Reproduced from DeCarlo et al. (2006). The C-AMS is comparable to the HR-AMS running in V-mode but with a smaller mass spectrometer (and therefore ion path length).

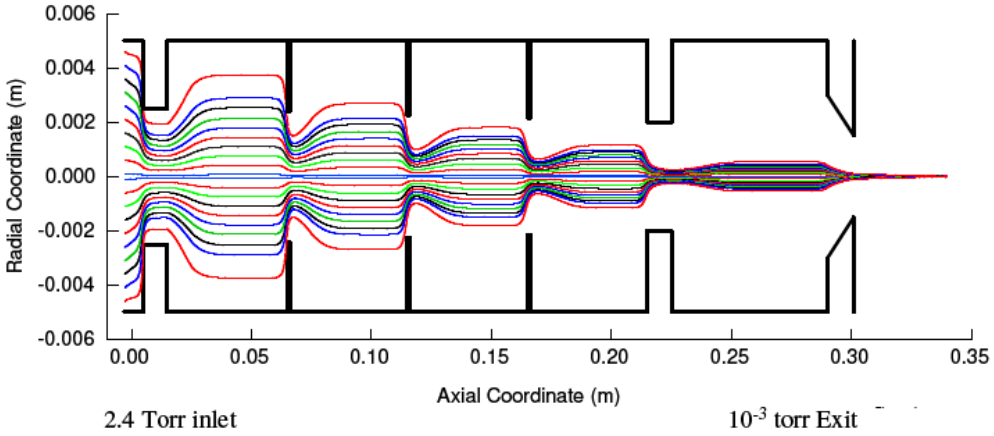

Figure 2.2: Modelled particle trajectories of 100 nm unit density spheres in the aerodynamic lens. Reproduced from Jayne et al. (2000) and Zhang et al. (2002).

Inlet Technology

The aerosols are sampled through a critical orifice, typically 100 or 120 μm in diameter. They then pass through an aerodynamic "lens" consisting of a series of concentric apertures of decreasing diameter. The successive compressions and expansions cause the particle trajectories to converge on the axis of the lens. The gas phase fraction expands upon exiting the lens making it possible to skim the majority of it off with a skimmer cone as it enters the second chamber. However, it is worth noting that even the enriched beam is still dominated by the gas phase (a factor of 10^2 – 10^3 by mass). An extensive fluid dynamics model of the lens (Figure 2.2) has calculated a 100% transmission efficiency for particles between 30 nm and 700 nm, gradually diminishing to $\sim 40\%$ up to 2.5 μm. Particles smaller that this are lost as they follow the gas streamlines and are skimmed

off. Larger particles are lost by impaction on the lens interior. The AMS is kept under vacuum by five turbo-molecular pumps, or *turbo-pumps*. As well as directly evacuating the instrument, several of the turbo-pumps act to back those evacuating higher vacuum sections of the instrument.

Particle Time of Flight Region

The beam then passes into the particle time of flight (PToF) region. It is modulated with a mechanical chopper wheel consisting of a rotating disk with two radial slits. The chopper can be positioned in-line with the beam without rotating so as to block it (the *blocked* position, used for measurements of the background signal), out of line to let it pass freely (the *open* position) or in-line rotating to transmit pulses of particles (the *chopped* position). These positions are changed depending on the mode of operation of the instrument. The flight time of pulses of particles in the chopped mode, from the chopper to detection, can be measured, with the start time established using the signal from an infra-red photo-diode pair monitoring through the chopper slit. As the time between vapourisation and detection is comparatively negligible, the time until detection is equivalent to the time taken for a pulse to travel from the chopper to the vapouriser — a distance of 0.395 m in the Manchester HR-AMS. As the particles have a size dependent velocity this can be used to produce size resolved measurements. The resolution of the size measurement is governed by the size of the packet across time of flight space, a smaller packet giving higher resolution. This can be controlled by changing the rotation frequency or slit width (known as the duty cycle) of the chopper (typically 150 Hz and 2% respectively). However, while reducing the duty cycle increases the sizing resolution, it reduces the singal to noise ratio as a smaller proportion of the particles are analysed. Care also has to be taken that pulses are not so close as to overlap before detection.

Vapourisation and Ionisation

The beam impacts on a heater ($\sim$550°C) at a pressure of $\lesssim 10^{-7}$ Torr. A component of the aerosol population is flash vapourised on impact; these are defined as non-refractory (NR). Some particles, such as black carbon, mineral dust and sea salt do not vapourise (defined as refractory) and are not detected by the AMS. Some particles are also not vapourised as they rebound off the heater. This is mitigated by using an inverted conical heater made from porous tungsten (Figure 2.3). After vapourisation of the particle, the resultant molecules are then ionised using 70 eV electron impact (EI). During ionisation most molecules are fragmented because of the high energy of the electrons. However, if the energy of the ionising electrons is consistent then the distribution of fragment ions is repeatable and can be accounted for in the data analysis (see Section 2.3). 70 eV EI is a standard ionisation method so AMS spectra can be compared to mass spectral

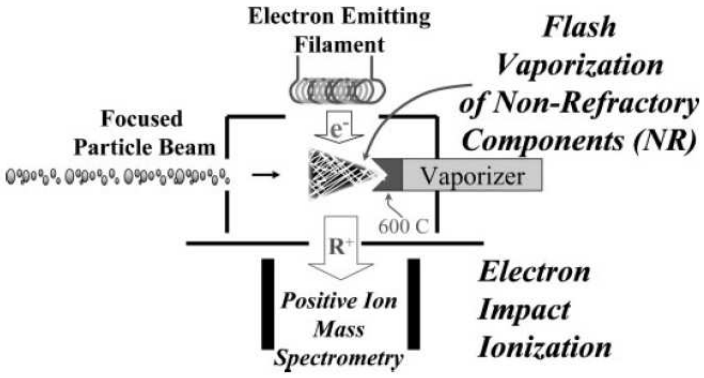

Figure 2.3: Schematic of AMS vapouriser and ioniser (Canagaratna et al., 2007).

databases such as the one run by the National Institute of Standards and Technology[1] (NIST). Studies, for example Alfarra et al. (2004), show that the AMS and NIST spectra are qualitatively comparable. However, two systematic differences have been observed in AMS spectra due to the harsh vapourisation. Firstly, there is a greater tendency for long chain species to fragment, however this does not occur to such an extent as to prevent useful comparison. Secondly, the thermal decomposition of highly oxidised molecules on the surface of the AMS vapouriser has a tendency to form CO_2^+ fragments. This phenomenon allows for insight into the degree of oxidation from inspection of the m/z 44 CO_2^+ peak, a practice now commonplace in the AMS community.

Mass Spectrometer

The ions are focused into a beam using tuned electric fields. Pulses of ions are then extracted orthogonally from this beam into the ion time of flight mass spectrometer[2] where they are detected using a Micro-Channel Plate (MCP). Ions of mass-to-charge ratio m/z, accelerated through a voltage V, have a time of flight t, over a distance L of

$$t = \left(\frac{m}{z}\frac{1}{2V}\right)^{1/2} \tag{2.1.1}$$

A mass spectrum, in terms of m/z, is generated by measuring the ion time of flight (not to be confused with particle time of flight). The mass spectrometer has two different configurations consisting of different ion drift lengths: V-mode with a path length of 1.3 m and W-mode with a path length of 2.9 m (as shown in Figure 2.1). In the V-mode the ion beam is reflected off a reflectron before reaching the MCP. In the W-mode the ion beam is reflected off the reflectron, off a hard mirror and back off the reflectron before arriving at the MCP. As well as reflecting the ion beam, the reflectron also increases the mass resolution by accounting for the kinetic energy distribution of the ions. It consists of

[1]"Mass Spectra" in NIST Chemistry WebBook, NIST Standard Reference Database Number 69. National Institute of Standards and Technology, http://webbook.nist.gov.

[2]Tofwerk AG, H-ToF Platform, Thun, Switzerland

an electrostatic field, and is employed in such a way that ions with a higher kinetic energy travel deeper into the reflectron so have a slightly longer path length, meaning ions of the same m/z arrive over a shorter period of time. The longer path length of the W-mode means ions have greater temporal separation for a given mass difference, providing a higher m/z resolution. However, the ion beam diverges with distance meaning the increased resolution comes at a loss of sensitivity. This means the V-mode is the most sensitive mode and W-mode has the highest resolution. The HR-AMS can be set to run in either V or W-mode. Section 2.3 deals with high resolution mass spectrometry in more detail. The C-AMS has only one configuration, which is similar to the V-mode of the HR-AMS but with a shorter path length of 0.43 m.

Modes of Operation

Custom software is used for data acquisition, real time data pre-processing, display of initial data and timing control. Typical timing settings for the ion extraction pulses are 30 μs (33 kHz) for V-mode and 50 μs (20 kHz) for the W-mode although these can be adjusted to observe different m/z ranges. The signal from the MCP is amplified by a pre-amplifier before being sampled at 1 GHz by an 8-bit analogue-to-digital converter (ADC).[1] The ADC has a digital threshold that is set as part of the routine calibrations. This has the effect of detecting ion pulses but rejecting electronic noise.

The AMS has several different modes of operation (Jimenez et al., 2003). In the mass spectrum (MS) mode the beam is alternately blocked and unblocked by the chopper. The blocked spectrum is subtracted from the open spectrum to account for any background signal ions. Spectra are co-averaged on the ADC to avoid an unmanageable quantity of data. These spectra are then transferred to the computer RAM where they can be averaged further. The time over which the spectra are averaged is defined by the user and is typically of the order of seconds or minutes depending on the time resolution and data burden desired. In the Particle Time of Flight (PToF) mode the spectra from each packet are recorded sequentially on the data acquisition card. This provides mass spectra as a function of PToF for each chopper cycle. The MS and PToF mode are usually routinely interchanged as part of the *general alteration mode* of the logging software. There is a third mode, called the Brute Force Single Particle (BFSP) mode, which is used for recording single particle events. This is similar to the PToF mode except that all the data from a chopper cycle is recorded with no on-board averaging. This data can then be filtered with user definable thresholds for one or more m/z. This mode is not used to record ambient data as it has a very low duty cycle ($\sim$3%) due to the amount of data that has to be transferred from the board to the computer. However this mode is useful for the IE calibration (see Section 2.2).

[1] AP240, Acqiris, Geneva, Switzerland

2.2 Quantitative Measurement and Calibrations

Mass Loading

The following section details the various calibrations that allow the production of quantitative measurements from the AMS. The pure voltages output to the logging computer must be converted into ion rates and then, in turn, to mass concentrations of chemical species. The velocity of the aerosols also needs to be converted into vacuum aerodynamic diameter. These calibrations were originally detailed by Jayne et al. (2000) and Jimenez et al. (2003).

The logging computer receives data in the form of the voltage output by the pre-amplifier which is proportional to current output by the MCP. To remove the voltage signal due to electronic noise, a threshold is applied which is based on the signal detected with the MCP off. The remaining signal is then converted into detected ion rates (in ions per second, Hz) by dividing by the average single ion strength (in V s). This is measured as part of routine calibrations, normally once a day in the field. The particle beam is blocked (either by closing the inlet or by moving the chopper to the blocked position) allowing single ions from background gas phase material to be measured. These single ion peaks are then averaged to find the average single ion strength.

The single ion strength is dependent on the MCP gain which degrades through use meaning the MCP voltage must be increased over time to maintain consistent sensitivity. Care must be taken to set the MCP gain correctly: too low and the single ions may not provide a big enough signal for them to be distinguished from the electronic noise; too high and the output voltage of the pre-amplifier may be above the 0.2 V maximum of the ADC, causing it to saturate. A higher gain also causes the MCP to deteriorate faster.

The amount of ions detected then needs to be converted in to speciated mass concentrations. Ion rates, I, in detected ions per second (Hz) can be converted to ambient mass loadings, C, in μg m^3 by using

$$C = 10^{12} \cdot \frac{MW}{IE\,Q\,N_A} I \tag{2.2.1}$$

where MW is the relative molecular weight of the species in g mol^{-1}, Q is the volumetric flow rate into the instrument in cm^3 s^{-1}, N_A is Avagadro's number[1] and IE is the ionisation efficiency (Bley, 1988; Jimenez et al., 2003). The ionisation efficiency is a dimensionless quantity that equals the ratio of the amount of detected ions to the amount of molecules in the detection region. It depends on the chance of a molecule being ionised, the transmission efficiency of the ion passing through the IToF region and associated DC optics, and the detection efficiency of the MCP. The factor of 10^{12} is included to convert from g cm^{-3} to μg cm^3 (given the use of the other units stated above).

The purpose of the ionisation efficiency calibration (also called the nitrate calibra-

[1] Avagadro's number, $N_A = 6.022 \times 10^{23}$ mol^{-1}.

tion) is to calculate the IE of a specific molecule that can then be used as a comparative standard for other molecules. Ammonium nitrate (NH_4NO_3) aerosols are used as they vapourise very efficiently and do not leave a background signal due to their relatively high volatility. They also yield very few fragment ions making the calculation of resultant signal relatively simple. Nitrate aerosols are generated from a nebuliser and dried, either by dilution with dry air or with a Nafion drier. They are then passed through a Differential Mobility Analyser (DMA; Knutson and Whitby, 1975) which size selects particles with a mobility diameter of 350 nm, a size which has a good transmission efficiency though the AMS and produces significant number of ions per particle. The average mass of the particles is calculated by applying the density of ammonium nitrate (1.752 g cm^3) and a "Jayne" shape factor of 0.8, as described in Jayne et al. (2000). The ionisation efficiency of nitrate, IE_{NO_3}, can then be calculated by comparing the average pulse size of a particle to its mass. Multiply charged particles are filtered out by rejecting particles with too large a vacuum aerodynamic diameter during post processing.

This provides a measure of IE_{NO_3}, but it must be generalised in order to quantify the mass concentrations of other molecules. The ionisation cross section of a molecule is proportional to the number of electrons in that molecule. The molecular weight of the molecule is to a first order also proportional to the number electrons in the molecule for most of the species found in the atmosphere. By assuming the molecular weight of a species, MW_s, is proportional to its ionisation cross section, the equation

$$\frac{MW_s}{IE_s} = RIE_s \frac{MW_{NO_3}}{IE_{NO_3}} \tag{2.2.2}$$

can be used to give a species specific form of Equation 2.2.1 of the form

$$C_s = \left(\frac{1}{RIE_s} \frac{MW_{NO_3}}{IE_{NO_3} Q N_A} I_s \right) \times 10^{12} \tag{2.2.3}$$

where the subscript s denotes a species specific quantity, RIE is the relative ionisation efficiency and all the other symbols have their usual meanings. RIE is a species specific quantity that is established in laboratory experiments (Alfarra, 2004).

Air Beam Correction

The MCP degrades with use, with the effect that the amount of signal produced per ion detected is reduced. This effect is largely accounted for by employing the ion rate calibrations described in Section 2.2. However, because the MCP degrades continuously, the correction can be improved by applying it as a function of time. The degradation in sensitivity can be assumed to be constant as a function of ion mass. This means that the efficiency loss can be quantified by measuring the change of the air beam signal which can be assumed to provide a constant input to the instrument. Conventionally the largest air signal at m/z 28 (N_2^+) is used to calculate a time dependent correction factor which

gives a constant air beam signal (Allan et al., 2003). The air beam correction accounts for any change in sensitivity that affects the gas and particle phases consistently. In addition to MCP degradation this includes any time dependent changes of the filament emission current or the transmission efficiency of ions through the mass spectrometer.

Collection Efficiency

Upon entering the instrument only a fraction of the particles are successfully vapourised and detected. Particles can be lost through deposition in the lens interior, lack of contact with the vapouriser caused by divergence of the aerosol beam, and rebound from the vapouriser surface. These effects are quantified by the ratio of NR particles introduced into the instrument to the amount of particles successfully vapourised, which is known as the *Collection Efficiency* (CE). It is governed by many factors such as composition, phase, humidity and morphology. Measurements of CE have been carried out on many campaigns (e.g. Alfarra et al., 2004; Salcedo et al., 2007) and in most cases is found to be ∼0.5, ranging between 0.43 and 1. Observations have shown that the CE can change suddenly between ∼0.5 and 1. This has been attributed to a change in the phase of the particle surface, with solid aerosol being more likely to rebound than liquid (Matthew et al., 2008). The CE is determined by comparison to an external standard. It is common practice to convolve the AMS total mass series to a total volume series, using assumed organic and inorganic densities (Cross et al., 2007). This can then be compared to total volume series from size distribution instruments such as a DMPS. The inverse of this factor is applied to Equation 2.2.3 to provide quantitative measurements.

Particle Size

The AMS must be calibrated to relate the velocity of a particle through the PToF region to its aerodynamic diameter using the empirical equation

$$v = v_l + \frac{v_a - v_l}{1 + \left(\frac{D_{va}}{D^*}\right)^b} \tag{2.2.4}$$

where v_l is the velocity of gas in the aerodynamic lens, D_{va} is the vacuum aerodynamic diameter, v_a is the gas velocity after the lens (that is the asymptotic velocity as D_{va} tends to zero) and D^* and b are empirical parameters (Jayne et al., 2000). A velocity calibration is done once a campaign using calibration particles of accurately known size, density and shape, usually polystyrene latex spheres (PSLs).[1] The heater temperature must be increased to ∼800 °C in order to rapidly vapourise the PSLs. Even so the resulting ions have a spread in arrival time due to the finite vapourisation time. The leading edge of the arrival peak is taken to be representative of the arrival time at the vapouriser. The four co-

[1]Polystyrene Latex spheres, from Duke Scientific, Palo Alto, California with diameters ranging from 90 to 1000 nm

Group	Molecule/Species		Ion Fragments	Mass Fragments
Water	H_2O	$\xrightarrow{e^-}$	$\mathbf{H_2O^+}$, HO^+ , O^+	**18**, 17, 16
Ammonium	NH_3	$\xrightarrow{e^-}$	NH_3^+, $\mathbf{NH_2^+}$, NH^+	17, **16**, 15
Nitrate	NO_3	$\xrightarrow{e^-}$	HNO_3^+, $\mathbf{NO_2^+}$, $\mathbf{NO^+}$	63, **46**, **30**
Sulfate	H_2SO_4	$\xrightarrow{e^-}$	$H_2SO_4^+$, HSO_3^+, SO_3^+ $\mathbf{SO_2^+}$, $\mathbf{SO^+}$	98, 81, 80 **64**, **48**
Organic *(Oxygenated)*	$C_nH_mO_y$	$\xrightarrow{e^-}$	H_2O^+, CO^+, $\mathbf{CO_2^+}$ $\mathbf{H_3C_2O^+}$, HCO_2^+, $C_{n'}H_{m'}^+$	18, 28, **44** **43**, 45, ...
Organic *(hydrocarbon)*	C_nH_m	$\xrightarrow{e^-}$	$C_{n'}H_{m'}^+$	27,29,**41,** **43,55,57**,69,71...

Table 2.1: The main ion fragments in the AMS and their relation to atmospheric species type. The most useful fragments for identification of species are highlighted in bold. Reproduced from Canagaratna et al. (2007).

efficients are entered into the data acquisition software and used in real time calculations of particle sizes.

The velocity calibration assumes a constant lens pressure. This can be problematic, most commonly if the critical orifice becomes partially blocked or if the environmental pressure changes (normally with altitude of an aircraft). The pressure in the lens is logged by the AMS computer via an auxiliary input, meaning that it is possible to correct for this retrospectively. By performing the standard velocity calibration over a range of inlet pressures it is possible to derive the dependence of the velocity of a particle on both its diameter and the lens pressure (Bahreini et al., 2003b).

2.3 Data Analysis Techniques

Fragmentation

During the vaporisation/ionisation process particles are often split into constituent ions in a process known as *fragmentation* (Chapter IV, McLafferty and Turecek, 1993). One of the major challenges of mass spectrometry is to be able to ascertain the parent molecules of these fragments during data analysis. A signal at any particular integer m/z can be made up from contributions of fragments from several parent ions of different m/z. For instance, nitrate (NO_3) produces two main fragments: m/z = 30 from NO^+ and m/z = 46 from NO_2^+. These are the two signals that are measured during the mass calibration detailed in Section 2.2. There is another smaller signal at m/z = 63 from HNO_3^+ which is not included in the calculation, meaning, somewhat counter intuitively, that the $RIE_{NO_3} > 1$. Table 2.1 shows some of the main fragments produced in the AMS. Complications arise when one m/z channel has contributions from several different

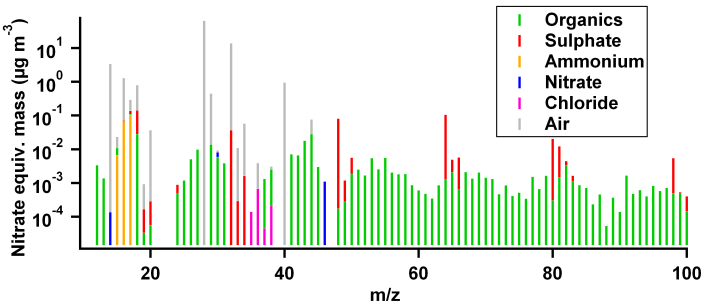

Figure 2.4: A species resolved mass spectrum from OP3 (see Chapter 4). RIE_s has been set to one for all species meaning masses are reported as nitrate equivalent.

species. This can be resolved by relating fragments in mixed peaks to fragments in non-mixed peaks, as described by Allan et al. (2004). The data analysis suite designed by Allan et al. (2003) uses a comprehensive table of predictable fragmentation patterns to resolve fragments onto their parent ions. This can be represented as

$$\vec{I_s} = \mathbf{M_s}\vec{I_{en}} \tag{2.3.1}$$

where the $\vec{I_s}$ is a vector containing the mass spectrum of species s, $\vec{I_{en}}$ is the ensemble mass spectrum and $\mathbf{M_s}$ is a square conversion matrix of the a_i multipliers specific to the species. The conversion matrix is derived from laboratory studies of ion fragmentation ratios. In practice this matrix is fairly simple and a non-circular solution can be found. The analysis software also allows for the construction of a time dependent table.

This gives a new version of Equation 2.2.1 of the form

$$C_s = 10^{12} \cdot \frac{MW_s}{IE_s\, Q\, N_A} \sum_i I_{s,i} \tag{2.3.2}$$

where $\sum_i I_{s,i}$ is the sum of all the elements of the $\vec{I_s}$ vector, that is the sum of all the fragments of species s. An example of a species resolved mass spectrum that was produced using these techniques can be seen in Figure 2.4.

High Resolution Mass Spectrometry

The C-AMS can resolve mass spectra to unit m/z, a resolution of $\sim$1000 (Canagaratna et al., 2007). The HR-AMS has two modes of operation, as detailed in Section 2.1. The V-mode, a similarly shaped but longer ion flight path to that of the C-ToF, can resolve slightly more than unit m/z, a resolution of $\sim$2500 (DeCarlo et al., 2006). The W-mode, with the longest ion path length, has a greater than unit m/z resolution of as high as $\sim$5000 (DeCarlo et al., 2006). All resolutions are quoted for typical working m/z ranges.

Ions are nominally of integer m/z values. However, different ions contributing to the same integer m/z peak have slightly different masses due to the differing mass defects of the constituent ions. A comparison of the resolving power of the C-, V- and W-modes

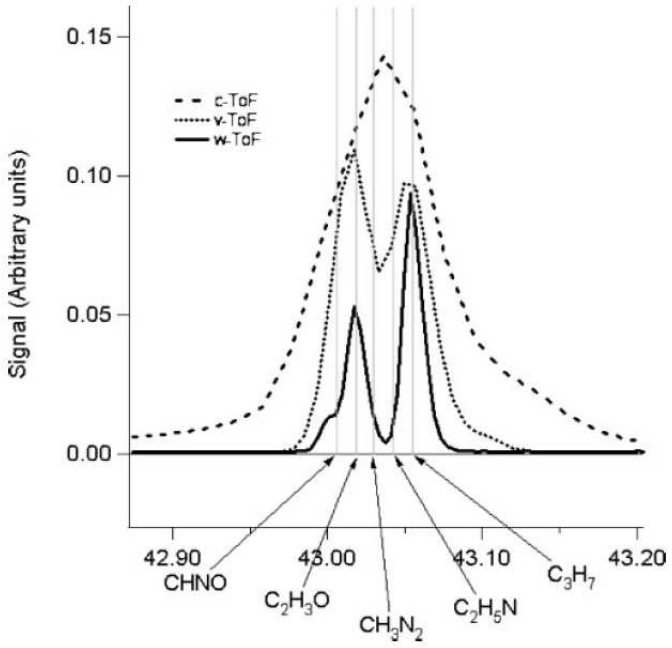

Figure 2.5: The $m/z = 43$ peak resolved using the C-AMS, HR-AMS V-Mode and HR-AMS W-mode. Reproduced from DeCarlo et al. (2006).

can be seen in Figure 2.5, with the resolution of the W-mode great enough to resolve the different constituent ions of the m/z 43 peak.

Aiken et al. (2007, 2008) pioneered work measuring atomic oxygen-to-carbon (O:C), organic-mass-to-organic-carbon (OM:OC), nitrogen-to-carbon (N:C) and hydrogen-to-carbon (H:C) ratios. Elemental analysis software developed by Sueper and quantifies various elemental ratios, and has become an established analysis technique in recent years.

The W-mode can also be useful for fine tuning the fragmentation tables. The default fragmentation table is defined for a typical dataset and, while fine turning the table is part of standard procedures, these unit mass resolution techniques can be inaccurate. The W-mode can be used to directly investigate the relative contributions of different ions to the unit mass resolution peak, and the table can be adjusted accordingly. The V-mode can then be used with the new table to provide more accurate speciated mass loadings.

Positive Matrix Factorisation

In terms of the AMS, Positive Matrix Factorisation (PMF) analysis seeks to represent the time series of mass spectra measured by the AMS as a time dependent combination of a number of static factor spectra. These factors can be attributed to different groups of atmospheric species by comparison of the factor spectra to those identified in previous studies, and by comparison of the factor time series to contemporaneous measurements. It is a statistical technique that has been adapted for the AMS from a general technique first developed by Paatero and Tapper (1994) and refined by Paatero (1997). Specifically, the ensemble mass spectrum time series is represented in a $m \times n$ matrix, $\mathbf{X}$, consisting

of m measurements in time of n m/z values. This matrix can then be resolved into two matrices, $\mathbf{X} = \mathbf{GF}$, where $\mathbf{F}$ is a $p \times n$ matrix and $\mathbf{G}$ is a $m \times p$ matrix. The number of *factors* is denoted by p. These represent the different sources that could be contributing to the ensemble. The source activity is represented by the *score*, denoted by the columns, p, of matrix $\mathbf{G}$. As physically meaningful values of the score cannot be negative, the solution is constrained to positive solutions. The optimum number of factors, p, is not usually known, so in practice solutions are found for a range of different p values. Solutions depend (albeit to varying amounts) on starting parameters (seeds) and rotational ambiguity (fpeak) which are both set by the user. The criterion for the optimum value of p, the starting seed and value of fpeak is how interpretable the factors are, that is, how much they correspond to what the user expects to see. Choosing the most suitable solution requires *a priori* knowledge and is a subjective step.

Proprietary software has been developed for PMF analysis by Paatero, and methods for its application to AMS data are described in Ulbrich et al. (2009). They have gone some way to standardise the analysis procedures used in the PMF analysis of AMS data in an effort to limit the inherent subjectivity. Since being adopted by the AMS community, PMF has proven a useful tool in the analysis of organic mass spectra. Jimenez et al. (2009) successfully applied PMF to 30 datasets from across the northern mid-latitudes, finding that ensemble organic mass spectra are typically composed of three or four factor spectra (see Section 1.4). Details of the PMF analysis performed as part of this thesis can be found in Appendix D.

CHAPTER

THREE

TROPICAL AEROSOLS

3.1 Aerosol Measurements In The Tropics

To date the majority of detailed aerosol studies have been performed in the northern mid-latitudes (Jimenez et al., 2009; Zhang et al., 2007). The paucity of measurements elsewhere in World is a limitation on global aerosol models, as asserted by Spracklen et al. (2011) who state that:

> ...the biogenic and biomass SOA sources [predicted by their work] are not well constrained due to the limited number of organic aerosol observations in regions and periods strongly impacted by these sources. To further improve the constraints by this method, additional observations are needed in the tropics and the Southern Hemisphere.

Those studies which have been performed in the tropics have focused on the continental land masses of Africa and South America. The maritime continent of islands in the western Pacific are largely uncharacterised, despite representing a substantial portion of the tropics. The vertical dispersion of aerosol, whist important for predicting radiative forcing, is not well predicted by models (Heald et al., 2005; Textor et al., 2006). There is a World-wide lack of sufficient in-situ aerosol composition profile data, with no detailed aerosol chemical composition altitude profiles performed over the rainforests of either Amazonia or South East Asia in particular.

Tropical Aerosol Measurements

The African Monsoon Multi-disciplinary Analysis (AMMA; Lebel et al. (2010)) was a large interdisciplinary project that combined long term measurements with intensive measurements from research aircraft and multiple ground sites. This region, which is dominated by savannah, is known to be a large source biomass burning aerosol, mostly from agricultural burning, and is also a source of mineral dust and biogenic aerosol. Aerosol AMS composition measurements were made from the NERC Facility for Airborne Atmospheric Measurement (FAAM) BAe-146 research aircraft during periods dominated by

biomass burning (Capes et al., 2008) and biogenic emissions (Capes et al., 2009). The measurements of biomass burning aerosol showed them to be widespread across the region (in contrast to studies in northern mid-latitudes) and confirmed Africa to be one of the World's largest sources of biomass burning aerosol (Capes et al., 2008). Biogenic organic aerosol loadings in West Africa were found to be in line with the range predicted by global models (Capes et al., 2009). However, when SOA concentrations were predicted from measured VOC data using a similar bulk yield scheme to these models, Capes et al. (2009) found that the ratio of modelled to measured values was 4.5–15. Hence these global models predicted the correct organic aerosol loadings in West Africa due to fortuitous cancelling of errors. Better agreement was achieved by using more up-to-date yields, although they were still highly imprecise, with modelled to measured values ranging from 0.7–6.5. Although it was not focused on in the publish papers, there was also a significant concentration of sulphate aerosol detected which was thought to be from terrestrial or marine DMS emissions or anthropogenic emissions.

All detailed atmospheric aerosol measurements in or above rainforests have been conducted in Amazonia. It is by far the largest rainforest in the World and, as such, plays a very substantial role in the biospheric production of VOCs and associated BSOA (Heald et al., 2008). Since the late 1980s, nine projects have been performed to measure Amazonian aerosol (Martin et al., 2010b). Many of these projects focused on the intense biomass burning in the region, while some that were performed during the wet season focused on biogenic emissions. The Large Scale Biosphere-Atmosphere Experiment in Amazonia (LBA; performed in various intensives between 1998 and 2001) was a long term experiment into the effect of the Amazon rainforest on the atmosphere (Avissar et al., 2002). The most recent study of biogenic aerosol, and also the first to employ an AMS, was the Amazonian Aerosol Characterization Experiment (AMAZE-08; Martin et al., 2010a)) performed in Amazonia in 2008.

Martin et al. (2010b) provide a review of more than 20 years of atmospheric measurements in Amazonia and the salient results are summarised here. In-basin sources across most of Amazonia (apart from some urbanised areas) are dominated by biospheric emissions producing both primary and secondary biogenic aerosol. The primary particles are actively produced by flora (from the ejection of fungal spores and pollen) and passively (as leaf and soil debris). Substantial production of SOA occurs through condensation onto pre-existing particles or possibly nucleation of new particles. The influence of in-basin biomass burning emissions (natural and anthropogenic) is large but intermittent, mostly governed by rainfall. Out-of-basin biomass burning emissions from Africa can influence Amazonia intermittently throughout the year. Long range transport of African dust can also dominate particulate mass concentrations periodically. Marine aerosol from the Atlantic (i.e. sea salt and sulphate from DMS processing) are progressively removed (through wet and dry deposition) as air masses travel from the coast to central Amazonia. However, marine aerosol loadings, while normally present at very low levels, can remain

significant over central Amazonia. During periods not influenced by biomass burning or dust, around half the sub-micron sulphate in general is attributable to marine emissions, with the rest from processing of terrestrial DMS emissions. Due to large seasonal and regional variability in sources and sinks, Amazonian aerosol show large variation across space and time.

Chen et al. (2009) segregated AMS measurements from AMAZE-08 into in- and out-of-basin periods based on levels of correlation between sulphate and organic aerosol concentration, and inspection of back trajectories. It was found that sub-micron aerosol loadings during in-basin periods were dominated by BSOA. This is supported by filter analysis from the same period, which showed that $\sim$85% of the ground level sub-micron aerosol was pure SOA, with another $\sim$10% mixed SOA and inorganic (Poschl et al., 2010). Chen et al. (2009) also observed a minor inorganic contribution from sulphate which was at loadings consistent with production of aerosol from processing of terrestrial DMS emissions. Inspection of high mass resolution AMS data showed that any sub-micron primary biological aerosol present was at undetectably small concentrations. In contrast to this, out-of-basin periods had higher total aerosol loadings and organic aerosol that was more oxidised. While still being dominated by organic aerosol, there was a more significant sulphate aerosol fraction. This suggested the influence of long range transport of biomass burning emissions from West Africa and sulphate from processing of marine emissions. Comparison of organic aerosol loadings to the GEOS-Chem model showed and under-prediction of 35%.

During LBA, the number/size distribution always showed Aitken and accumulation modes, with average diameters of 68 nm and 151 nm respectively and a mean concentration of $\sim$450 cc^{-1} (Zhou et al., 2002). During AMAZE-08 a similar bi-modal number/size distribution was observed but at lower loadings of $\sim$200 cc^{-1}(Poschl et al., 2010). Krejci et al. (2005a) made aerosol size measurements from an aircraft over Surinam, where they attributed 50–85% of accumulation mode aerosol number concentration growth observed in the boundary layer during the day to primary particle emissions from the rainforest. However, the increase in accumulation mode number concentrations (75–130 cc^{-1}) seems anomalously high when compared to those measured it in an environment rich in bioaerosol of a similar size ($<$10 cc^{-1}) (Matthias-Maser and Jaenicke, 1995). It seems more likely that the growth of the accumulation mode Krejci et al. (2005a) observed was due to SOA formation. Martin et al. (2010b) state that it is likely that both primary and secondary aerosol are transported throughout and above the surface mixed layer.

Fisch et al. (2004) characterised boundary layer heights in Amazonia during the wet and dry seasons (less than 1500 m and up to 2000 m respectively). Krejci et al. (2005a) found that the Amazonian turbulent convective boundary layer grows from a nocturnal height of $\sim$250 m to $\sim$1500 m by the early afternoon. In general, late afternoon convective boundary layer depths $>$1000 m are typical in the Amazon Basin, although the variability is high Martin et al. (2010b). Martin et al. (2010b) state that the nocturnal boundary layer

is "typically a few hundred meters or less" with a residual layer above that is usually preserved until the next morning. Surface emissions get rapidly mixed throughout the convective boundary layer in the afternoon, acting to dilute their concentrations (Martin et al., 2010b). In fair weather conditions turbulence at the top of the boundary layer entrains cleaner air from aloft and in rainy weather convective clouds act to lift aerosol to higher levels (Martin et al., 2010b).

There are no high time resolution in-situ aerosol profile composition measurements in the tropics, with the only composition data available from filter samples. Krejci et al. (2005b) performed single particle analysis of filter samples from three atmospheric layers, however characterisation of chemical species was poor, with the composition of 64% of the particles "not determined". Only particle number concentrations were reported, however they showed that a significant number of sub-micron aerosol in the boundary layer over the rainforest and ocean was "mineral dust", probably transported from West Africa. The majority of particles above the marine and terrestrial mixed layers were "not determined", however Krejci et al. (2005b) hypothesise that they are biogenic in nature. Detailed characterisation of sub-micron aerosol composition above rainforest remains very poorly characterised during biogenically dominated periods.

3.2 Current Issues with Tropical Organic Aerosols

A large fraction of global organic aerosol mass has been shown to be secondary in nature, however, despite recent advances, the mechanisms by which they are formed are still poorly understood (de Gouw et al., 2005; Hallquist et al., 2009; Heald et al., 2005; Jimenez et al., 2009; Volkamer et al., 2006; Zhang et al., 2007). The comparison of top-down to bottom-up organic aerosol estimates (see Section 1.4) leads to two major questions: is there evidence that there exist organic aerosol precursors that are not currently being measured; and what proportion of VOCs are processed to SOA in the atmosphere? Goldstein and Galbally (2007) cite evidence that VOCs are routinely being under measured, for instance laboratory chamber studies commonly show discrepancies between the amount of precursor VOC and total measured amount of oxidised gas and particle phase carbon. There is also indirect evidence that there are unmeasured VOCs in the atmosphere. The presence of VOCs can be inferred by observing their chemical influence on oxidant levels and their stable products. Goldstein et al. (2004) argued that observed ozone loss in a forest canopy was due to oxidation of terpenes which was corroborated by the discovery of oxidation products of ozone and terpenes. However, these terpenes have not been measured directly, perhaps because they are so unstable as to be hard to measure without affecting their composition with conventional techniques (Goldstein et al., 2004).

Other studies have measured SOA with unknown VOC precursors. For example Heald et al. (2008) reported that bottom-up models under-predicted organic aerosol concentrations in the free troposphere by a factor of 10–100, despite correctly predicting black

carbon and sulphate aerosol concentrations. It is thought that this could be due to formation of SOA not included in current models that is long lived enough to be transported into the free troposphere. Similarly, Volkamer et al. (2006) reported that bottom-up SOA models based on chamber yields vastly under-predict loadings in a range of polluted environments (by almost an order of magnitude after a few hours of VOC oxidation). This is a surprising result in that conditions in chambers (precursor and oxidant levels, RH, temp etc.) would be expected to be relatively representative of this environment compared to pristine environments. Volkamer et al. (2006) suggest that a significant amount of missing SOA in models could be due to inaccurately represented oxidation of anthropogenic VOCs. By extrapolating from field data from Mexico City, they estimate that anthropogenic SOA could account for as much as one third of global SOA levels (3–25 Tg yr^{-1}), despite AVOC emissions making up only around 10–20% of global VOC emissions (Guenther et al., 1995; Kanakidou et al., 2005).

Recent work has blurred the line between the definitions of "anthropogenic" and "biogenic" organic aerosol, implying that anthropogenic emissions could be increasing the aerosol yields of BVOCs, which may go some way to explain the larger under-prediction of SOA in polluted regions (Hoyle et al., 2011). While the mechanisms are as yet unclear, it was hypothesised that anthropogenic aerosol emissions could provide an increased surface area for biogenic species to partition onto, or provide surface area upon which heterogeneous reactions could occur. It was also though that anthropogenic emissions of NO_x may increase biogenic organic mass yields (see Section 1.4). The anthropogenic enhancement of biogenic aerosol formation has been further elucidated by Spracklen et al. (2011). By inspecting measurements of ^{14}C in organic aerosol they were able to constrain the amount of aerosol that was directly from processing of AVOCs compared to the amount produced from anthropogenically enhanced formation from BVOCs. They found 10% of organic aerosol in the northern mid-latitudes was formed from processing of AVOCs and 90% formed from anthropogenic enhancement of BVOC processing. The term *anthropogenically controlled* organic aerosol has been coined to refer to the fraction produced from the enhanced processing of BVOCs.

Another potential source of missing BSOA is from the oxidation of isoprene (Carlton et al., 2009; Henze and Seinfeld, 2006). Previously considered an insignificant source of SOA (Pandis et al., 1991), it now seems that, despite low chamber yields, it is significant by virtue of its abundance in the atmosphere. In fact, Henze and Seinfeld (2006) modelled that its inclusion could increase the global SOA burden by more than a factor of two. However, significant uncertainties in isoprene SOA formation processes and atmospheric yields still remain (Carlton et al., 2009).

Whilst ubiquitous in the atmosphere, SOA is clearly poorly understood. The SOA burden, assuming the IPCC A1B[1] scenario, has been predicted to increase by 36% over the

[1]The A1B scenario describes a future World of rapid economic growth, population that peaks mid-21st century, a reduction in the polarisation of wealth and a balanced reliance on fossil fuel and non-fossil fuel energy sources (Parry et al., 2007).

next century due to increased biological and anthropogenic emissions and so will only become of more importance in coming years (Heald et al., 2008). Hallquist et al. (2009) estimate that bottom-up models are under-predicting BSOA by a factor of two and Volkamer et al. (2006) estimate they are under-predicting ASOA by a factor of between ∼5–50. The tropics are an essential part of the global biosphere (see Section 1.2), emitting around half of all gas phase non-methyl organic species released into the atmosphere. Previous studies have tended to measure higher aerosol concentrations in anthropogenically dominated environments then in biogenically dominated (Jimenez et al., 2009), however, rescent studies suggest much of this may be from anthropogenic processing of BVOCs (Hoyle et al., 2011; Spracklen et al., 2011). This suggests that, while remote tropical aerosol burdens may currently be relatively low, there is a large latent source of SOA that will develop as regional anthropogenic pollution increases. Given the current high rate of land use change across the tropics, this is an important issue for predictions of tropical aerosol loadings in the future.

3.3 Remaining Challenges

Aerosols are clearly an important and uncertain factor in the prediction of climate change under future emission scenarios. In order to improve these predictions, it is necessary to better understand the physical properties of aerosol that govern their interaction with climate such as optical absorbance and hygroscopicity. To predict the extent of these interactions we need to understand aerosol sources, sinks and evolution in the atmosphere, as well as the both their horizontal and vertical distributions. In particular, organic aerosol constitutes a substantial part of these uncertainties due to the complex and dynamic processes that govern their lifetimes. To mitigate the effects of anthropogenic emissions, it is first necessary to gain an understanding of the pre-industrial atmosphere. Once the unperturbed system is constrained, a better understanding of the effects of perturbations to the system will follow.

Anthropogenic activity is changing the aerosol climate forcing through destruction of natural sources and introduction of new sources of aerosol. Accurate prediction of aerosol climate effects under future land use and emissions scenarios relies on the accurate characterisation of the natural systems that underly anthropogenic perturbations. It is important, then, that the pre-industrial particulate burden is known (or as close to it as is possible) so that any anthropogenic changes can be quantified. While much progress has been made in recent years, the formation and evolution of organic aerosol is still shrouded in uncertainty. In particular the formation of SOA from isoprene is a pivotal issue. This is due in part to the large amounts of isoprene that the biosphere emits, which means that even small changes in our understanding of the processes can have a significant impact on the global picture of isoprene SOA.

The tropics are an essential part of the World's climatological system due to the high

solar flux. They are also home to a highly active, complex and substantial portion of the World's biosphere. However, this system is being rapidly affected by active deforestation for agriculture, timber and general urbanisation. Such rapid and drastic changes to such an important part of the biosphere is likely to significantly affect the atmosphere. Indeed, Rockström et al. (2009) highlight land use change as one of the "planetary boundaries" that must be controlled if mankind is to thrive in the future. While the tropics as a whole have been under-represented in previous aerosol studies (with only a handful of studies in Amazonia and Africa) there have been no detailed composition studies performed in South East Asia in particular. Despite being a vital part of the tropical biosphere, atmospheric composition in a rainforest has only been studied in Amazonia. The patchwork of islands that make up South East Asia is home to substantial amounts of rainforest, however the regional atmospheric make-up could be significantly different to that of Amazonia.

CHAPTER

FOUR

THE OP3 PROJECT

4.1 Overview and Objectives

The patchwork of tropical islands that make up the "maritime continent" of South East Asia represents a significant portion of the tropics. This region is home to substantial amounts of tropical rainforest but it is likely its atmospheric composition and dynamics are different to those of the Amazon Rainforest. The influence of the sea may be much greater — addition of marine species is likely to result in different atmospheric composition to Amazonia and may also affect the chemical processing of rainforest emissions. While much of the region is covered in rainforest, there is also potentially significant urbanisation. This is in contrast to the Amazon Rainforest where huge areas of the forest remain uninterrupted. The rainforests of South East Asia are being destroyed at a greater absolute rate than those of South America, despite being only about 40% the size (Achard et al., 2002). South East Asian deforestation is mostly motivated by the cultivation of palm oil plantations (McMorrow and Talip, 2001). In 2007 palm oil was responsible for almost 60% of the global vegetable oil market and its production has been increasing at a rate of 8% per year (between 1974 and 2007; Carter et al., 2007). It is widely used in high street products and is also increasingly in demand for use as biofuel (Carter et al., 2007).

The Oxidant and Particulate Project Above a South East Asian Rainforest project (OP3) was a large National Environmental Research Council (NERC) funded consortium project consisting of eight UK institutions, three Malaysian institutions and other partners from around the World. It was conducted in Sabah, the Malay region of Northern Borneo in South East Asia between April and July 2008. Ground measurements were performed in Danum Valley, an area of protected primary and secondary rainforest. The ground site was around 40 km from the coast of Borneo at its closest. Aircraft measurements were also carried out during June 2008 using the FAAM aircraft. A detailed overview of the project can be found in Hewitt et al. (2010).

The key objectives of the project as a whole were

1. to understand how emissions of reactive trace gases from a tropical rainforest mediate the production and processing of oxidants and particles in the troposphere,

and

2. to better understand the impact of these processes on local, regional and global scale atmospheric composition, chemistry and climate.

In contrast to the Amazonian projects, OP3 provided an opportunity to study the influence of a local marine emission source on terrestrial biogenic emissions. The proximity of local oil palm plantations also gave the opportunity to assess the influence of their emissions — the first step in gauging the effect of regional land use change on aerosol. This thesis endeavours to meet the above objectives through using on-line ground and aircraft AMS measurements of aerosol composition to answer the following questions:

1. Are regional aerosol sources in this marine influenced tropical rainforest environment different from the previously studied tropical environments and, if so, what are the individual source contributions?

2. If sources are different, is the atmospheric processing of aerosol affected?

3. Is there any evidence that the land use change is affecting atmospheric aerosol?

4. What effect does Borneo have on regional aerosol concentrations, both from terrestrial emissions and island dynamics?

The three included papers present: an analysis of regional sources that influence the ground site, using two distinct but complimentary back trajectory analysis techniques; a description of the effect transport of air over Borneo has on aerosol populations and their altitude distribution throughout the troposphere; and identification of a novel isoprene SOA signal in AMS mass spectra, including quantification of the amount of isoprene SOA in Borneo and comparison to other projects in regions dominated by biogenic isoprene and terpene emissions.

4.2 Paper I: Source attribution during the OP3 project using backwards air mass trajectories

N. H. Robinson, H. M. Newton, J. D. Allan, M. Irwin, J. F. Hamilton, G. Mills, C. E. Reeves, G. McFiggans and H. Coe

Under discussion for the Atmospheric Chemistry and Physics OP3 special issue

Supporting Material reproduced in Appendix B

Overview

This paper uses backwards air mass trajectories to assess the dependence on air mass origin of species abundance and physical properties measured from the ground site in Boreno during the OP3 project. Established marine halocarbon tracers showed marine origins, implying the techniques are applicable in this setting and emphasising the importance of marine sources of aerosols. A period dominated by biomass burning emissions was identified from in-situ measurements, supported by the MODIS fire-count product. Off-island air masses were characterised by: marine halocarbon tracers; strongly correlating sulphate and ammonium aerosol, probably from marine DMS emissions, volcanoes and/or long range transport of anthropogenic emissions; strongly correlating nitrate and chloride aerosol, probably from marine sodium chloride reacting with terrestrial nitrate; and highly aged organic aerosol, from long range transport of biogenic or anthropogenic aerosol. On-island air was characterised by: biomass burning aerosol and gases; and fresh organic aerosol from oxidation of rainforest emissions. Organic aerosol thought to be from isoprene oxidation shows signs of originating over the oil palm plantations, which have been shown to emit five times as much isoprene as the rainforest. It appears that transit across the interior of Borneo results in depletion of regional aerosol and enhancement of terrestrial aerosol.

This work provides the first characterisation of aerosol composition in this region of the tropics and highlights how different it is from that in other parts of the World. Aerosol loadings were much lower than has been measured in the northern mid-latitudes and, while total aerosol loadings are similar, composition is markedly different to that measured in Amazonia, with much greater sulphate loadings in Borneo. This is likely to be due to the greater marine influence in South East Asia. This paper shows that atmospheric composition is heterogeneous through the tropics, and that it is likely the "maritime-continent" region is significantly different to the continental regions previously studied. More subsequent studies need to be performed to characterise this significant portion of the tropics better. This study also acts to characterise atmospheric composition in a location that is beginning to be affected by land use change. This can act as a benchmark

for the assessment of future more severe changes to atmospheric composition caused by regional land use change.

Contribution of authors

Newton performed measurements, initial analysis and interpretation of halocarbon data and wrote the halocarbon section. Allan assisted with aerosol measurements, interpretation of results and preparation of the manuscript. Irwin performed measurements and initial analysis of hygroscopicity data. Hamilton performed measurements and initial analysis of carbon monoxide data. Mills performed measurements and initial analysis of halocarbon data. Reeves performed measurements and initial analysis of the halocarbon data and assisted in preparation of the manuscript. McFiggans and Coe assisted with preparation of the manuscript and interpretation of the results.

Robinson performed aerosol measurements and analysis, developed the back trajectory analysis techniques, interpreted data and wrote the manuscript.

Atmos. Chem. Phys., 11, 9605–9630, 2011
www.atmos-chem-phys.net/11/9605/2011/
doi:10.5194/acp-11-9605-2011

Atmospheric Chemistry and Physics

Source attribution of Bornean air masses by back trajectory analysis during the OP3 project

N. H. Robinson[1], H. M. Newton[2], J. D. Allan[1,3], M. Irwin[1], J. F. Hamilton[4,5], M. Flynn[1], K. N. Bower[1], P. I. Williams[1,6], G. Mills[2], C. E. Reeves[2], G. McFiggans[1], and H. Coe[1]

[1]Centre for Atmospheric Science, University of Manchester, Manchester, UK
[2]School of Environmental Sciences, University of East Anglia, Norwich, UK
[3]National Centre for Atmospheric Science, University of Manchester, Manchester, UK
[4]Department of Chemistry, The University of York, York, UK
[5]National Centre for Atmospheric Science, University of York, York, UK
[6]Facility for Groundbased Atmospheric Measurements, University of Manchester, UK

Received: 4 May 2011 – Published in Atmos. Chem. Phys. Discuss.: 18 May 2011
Revised: 5 September 2011 – Accepted: 13 September 2011 – Published: 16 September 2011

Abstract. Atmospheric composition affects the radiative balance of the Earth through the creation of greenhouse gases and the formation of aerosols. The latter interact with incoming solar radiation, both directly and indirectly through their effects on cloud formation and lifetime. The tropics have a major influence on incoming sunlight however the tropical atmosphere is poorly characterised, especially outside Amazonia. The origins of air masses influencing a measurement site in a protected rainforest in Borneo, South East Asia, were assessed and the likely sources of a range of trace gases and particles were determined. This was conducted by interpreting in situ measurements made at the site in the context of ECMWF backwards air mass trajectories. Two different but complementary methods were employed to interpret the data: comparison of periods classified by cluster analysis of trajectories, and inspection of the dependence of mean measured values on geographical history of trajectories. Sources of aerosol particles, carbon monoxide and halocarbons were assessed. The likely source influences include: terrestrial organic biogenic emissions; long range transport of anthropogenic emissions; biomass burning; sulphurous emissions from marine phytoplankton, with a possible contribution from volcanoes; marine production of inorganic mineral aerosol; and marine production of halocarbons. Aerosol sub- and super-saturated water affinity was found to be dependent on source (and therefore composition), with more hygroscopic aerosol and higher numbers of cloud condensation nuclei measured in air masses of marine origin. The prevailing sector during the majority of measurements was south-easterly, which is from the direction of the coast closest to the site, with a significant influence inland from the south-west. This analysis shows that marine and terrestrial air masses have different dominant chemical sources. Comparison with the AMAZE-08 project in the Amazon basin shows Bornean composition to arise from a different, more complex mixture of sources. In particular sulphate loadings are much greater than in Amazonia which is likely to mainly be the result of the marine influence on the site. This suggests that the significant region of the tropics made up of island networks is not well represented by extrapolation from measurements made in the Amazon. In addition, it is likely that there were no periods where the site was influenced only by the rainforest, with even the most pristine inland periods showing some evidence of non-rainforest aerosol. This is in contrast to Amazonia which experienced periods dominated by rainforest emissions.

Correspondence to: H. Coe
(hugh.coe@manchester.ac.uk)

1 Introduction

In order to assess and predict the anthropogenic influence on climate, it is also important to understand the natural role of the biosphere. One way the biosphere can affect climate is through its role in aerosol production. This aerosol can then interact with solar radiation directly, acting to scatter shortwave radiation to space, and indirectly through its role as cloud condensation nuclei (CCN) acting to influence cloud brightness and persistence (Denman et al., 2007).

The tropics have a large influence on global climate due to the high surface flux of solar radiation, however to date the comprehensive data needed to fully characterise the gas and aerosol composition in these environments has been scarce. The tropics contain about half the World's forests (Food and Agriculture Organisation, 2010), playing a major role in the global biosphere. This natural background is being affected by anthropogenic activity such as deforestation and land use changes. It is important to assess the extent to which anthropogenic activities are affecting tropical aerosol, and their subsequent effects on climate.

Intensive field studies have been performed in Amazonia (ACP special issue OP3/ACES: Oxidant and particle photochemical processes above a south-east Asian tropical rain forest), Martin et al., 2010; JGR special issue 107, Avissar et al., 2002) and West Africa (ACPD special issue AMMA Tropospheric Chemistry and Aerosols; Lebel et al., 2010) but until now data from South East Asia has been limited. Specifically, the AMAZE-08 project in Amazonia found that sub-micron aerosol was dominated by biogenic secondary organic aerosol (BSOA) with elevated levels of oxidised organic aerosol (OOA) and sulphate during periods influenced by out-of-basin sources, which were attributed to biomass burning transport from Africa or a marine influence (Chen et al., 2009). The major source of submicron aerosol in West Africa is from biomass burning during the dry season and BSOA during the monsoon season (Capes et al., 2009, 2008). It also experiences high sulphate loadings which may be due to the influence of the Atlantic Ocean, although data coverage and quality did not allow this to be drawn as a conclusion.

Borneo is home to one of the largest expanses of rainforest in the world making it an important part of the biosphere and a potentially large source of volatile organic compounds (VOC) and associated BSOA. There is widespread deforestation on Borneo where land is being given over to logging and, particularly, palm oil production (McMorrow and Talip, 2001), meaning the role of the biosphere in the region is changing. Global palm oil production grew by 8 % per year between 1976 and 2006, with the majority of production in Malaysia and Indonesia (Carter et al., 2007). It has been shown that oil palms are a large source of isoprene in Borneo (five times more than the rainforest; Hewitt et al., 2009). Isoprene has previously been found to produce secondary organic aerosol (SOA) in chambers and field studies (Claeys et al., 2004; Surratt et al., 2006, 2008; Paulot et al., 2009; Kleindienst et al., 2009; Surratt et al., 2010; Chan et al., 2010) and is thought to produce a substantial fraction of the SOA in Borneo (Robinson et al., 2011). As Borneo is an island, marine influences could be much larger than that in Amazonia and Africa. The oceans are a source of dimethyl sulphide (DMS) produced by phytoplankton (Kloster et al., 2006), minerals contained in sea water (Millero, 1974), halocarbons (Butler et al., 2007) and OA (O'Dowd et al., 2004; Novakov et al., 1997; Facchini et al., 2008). Borneo has a population of around 16 million people, mostly inhabiting regions around the coast, so there is potential for influence of anthropogenic pollution in the form of combustion related emissions from transport, power stations or biomass burning. There is an abundance of volcanoes near Borneo which are a known source of sulphurous gases that are processed in the atmosphere to form aerosol (Pandis et al., 1995; Allen et al., 2002), which may contrast to other tropical studies that have not reported a volcanic influence (Chen et al., 2009; Capes et al., 2008).

Measurements were made as part of the Oxidant and Particulate Photochemical Processes Above a South East Asian Rainforest (OP3) project in protected rainforest in Sabah, Borneo (Hewitt et al., 2010). This region extends from around 4° N to the north coast of the island. Investigating the relationship between composition and synoptic flow can provide insight into significant regional sources. Two different but complementary methods employing back trajectories are used to attribute geographical sources, which can then be linked to likely emission sources. The focus of the paper is on species with a long enough atmospheric lifetime (hours or more) to be suitable for the analyses; mainly submicron aerosol composition and physical property measurements, but also long lived trace gases such as CO and halocarbons. Specifically the issues dealt with are the separation of atmospheric species originating on- and off-island and the attribution of likely sources.

2 Methods

2.1 Instrumentation

Measurements were performed at the Bukit Atur site (4°58′49.33″ N, 117°50′39.05″ E, 426 m a.s.l.) during two periods: 7 April–4 May (OP3-I) and 23 June–23 July (OP3-III). Measurements from the intervening period (OP3-II) were made from a different measurement site and are not detailed here. An overview of measurement techniques and a description of the measurement site can be found in the OP3 overview paper, Hewitt et al. (2010). There was poor data coverage during OP3-I and, though air mass characterisations of both periods are presented in Sect. 2 for reference, results presented here focus on OP3-III.

Aerosol composition was measured using a High Resolution Aerodyne Aerosol Mass Spectrometer (AMS; DeCarlo et al., 2006; Canagaratna et al., 2007) – a state of the art instrument capable of providing detailed bulk composition and aerodynamic sizing measurements of aerosols with a time resolution of minutes. It is limited to measurements of submicron non-refractory aerosol, where non-refractory (NR) is operationally defined as a species that volatilises quickly (on time-scales of less than a second) after impaction on the tungsten vaporiser (nominally run at 600 °C). Conversion of AMS aerosol mass loadings into total aerosol volume (assuming organic and inorganic densities as in Cross et al., 2007) allowed for comparison with a DMPS sampling from the same

inlet, and limited to the same size range. The instruments agreed and correlated well ($r = 0.92$) and a linear regression of AMS vs. DMPS volume series gave a gradient of 0.45. The collection efficiency (CE) factor accounts for the likelihood that a particle will be successfully vapourised and detected once in the AMS, and has typically been found to be around 0.5 in other projects (Matthew et al., 2008). The gradient of the linear regression is consistent with this and a CE of 0.5 has been applied to all the AMS data.

Despite extensive fragmentation, individual peaks in the mass spectrum provide more information about aerosol composition. Insight into the photochemical age of organic aerosols (OA) can be gained from the *m/z* 44 (mainly CO_2^+) to 43 (mainly $C_2H_3O^+$ and $C_3H_7^+$) peaks (Ng et al., 2010; Jimenez et al., 2009; Morgan et al., 2010). Organic spectra with a low f_{44} and high f_{43} (where f_x denotes the fraction of the organic mass at $m/z = x$) are less oxidised and can be thought of as semi-volatile aerosol (SV-OOA) which exist in an equilibrium between the gas and condensed phases. Aerosol with high f_{44} and low f_{43} are more oxidised and can be thought of as low volatility aerosol (LV-OOA) which exists mainly in the condensed phase.

In reality organic aerosol exist in a continuum between these two endpoints that can be expressed by points on a 2-D f_{44} vs. f_{43} space. The peak at *m/z* 60 can be used as a marker for fresh biomass burning (Alfarra et al., 2007; Capes et al., 2008), being a peak associated with levoglucosan and other anhydrous sugars which are compounds widely reported to be emitted during biomass burning (Simoneit et al., 1999; Jordan et al., 2006). It has been shown that as organic aerosol ages (with increasing f_{44} and decreasing f_{43}) its mass spectral signature becomes similar and dominated by *m/z* 44 regardless of source (McFiggans et al., 2005; Ng et al., 2010; Morgan et al., 2010).

The unit mass resolution organic aerosol data from the AMS were analysed using positive matrix factorisation (PMF). This is a multivariate technique that endeavours to explain the bulk organic AMS mass spectral time series in terms of time series of differing amounts of static "factor" spectra which can then be linked to distinct components of the ensemble organic aerosol mass (Paatero and Tapper, 1994; Paatero, 1997; Ulbrich et al., 2009). The details of the PMF analysis of the OP3 data were originally published in Robinson et al. (2011). The dependence of the solution on starting parameters (seeds) and rotational ambiguity (fpeak) was explored. In short, the most satisfactory solution was found to be the four factor solution. The results of the PMF analysis are discussed in more detail in Sect. 2.3. The high mass resolution of the AMS also enables the separation of ions at the same unit mass resolution by resolving the ion mass defects.

Subsaturated aerosol water affinity was measured as a function of size using a single column Hygroscopicity Tandem Differential Mobility Analyser (HTDMA; Cubison et al., 2005; Gysel et al., 2009), which measures the size change of an aerosol experiencing a certain change in relative humidity (RH). This is expressed in terms of the growth factor (GF) defined as the ratio of the "dry" to "wet" size – in this case the sizes at <15 % and 90 % RH, respectively (GF_{90}). The supersaturation needed to activate a particle to a cloud droplet (critical supersaturation; SS_{crit}) was measured as a function of size using a Droplet Measurement Technologies dual column Cloud Condensation Nucleus counter (CCNc; DMT model 100; Roberts and Nenes, 2005; Lance et al., 2006; Irwin et al., 2011, 2010; Good et al., 2010a) downstream of a differential mobility particle sizer (DMPS; Williams et al., 2000, 2007). Both the HTDMA and CCNc perform measurements as a function of dry (<15 % RH) aerosol size, selected using Vienna style differential mobility analysers (DMA; Winklmayr et al., 1991). The HTDMA measured at six sizes between 32 and 258 nm and the CCNc measured at 11 diameters between 57 and 224 nm. Aerosol optical absorption was measured with a Thermo Scientific model 5012 Multi Angle Absorption Photometer (MAAP; Petzold and Schonlinner, 2004) which reports in black carbon equivalent loading.

The halocarbon measurements were made using gas chromatography-mass spectrometry (GC-MS). The analysis was conducted on-site at Bukit Atur. Whole air samples were dried using a Nafion contra-flow drier and were preconcentrated using a Markes International UNITY and Online Air Server with a Carbograph B and Carboxen 1000 trap. The UNITY was coupled to the Agilent 6890 GC and the MS5973 N mass spectrometer. The results presented here are from analysis on this GC-MS system in negative ion chemical ionization (NICI) mode (Worton et al., 2008). Litre samples were taken hourly (collected over a period of 40 min) from a position 30 m up the GAW tower (Hewitt et al., 2010) and separated on a Restek RTX-502.2 column. Calibrations were performed every 8 samples using the UEA 2006 Standard reference gas which is calibrated against the "NOAA 2003" scale for $CHBr_3$, CH_2Br and CH_3Br and the "NOAA 2004" scale for CH_3I (Laboratory Earth Systems Research Global Monitoring Division, 2008). Gas phase CO measurements were made using an Aerolaser AL5002 fluorescence instrument (Gerbig et al., 1999).

2.2 Analysis of back trajectories

Backwards air mass trajectories (back trajectories) were generated using the British Atmospheric Data Centre Web Trajectory Service using European Centre for Medium-Range Weather Forecasts (ECMWF) wind fields (BADC, 2006a) at $1.125° \times 1.125°$ resolution. These trajectories show the modelled history of an air mass from a particular time and place in terms of geographical position and pressure altitude. One trajectory per hour was generated for the whole of the OP3 project – a total of 720 trajectories for OP3-I and 794 for OP3-III. Trajectories originate at the latitude and longitude

of the ground measurement site and a pressure altitude of 950 hPa, and were calculated backwards for the preceding seven days with a 30 min time resolution. No trajectories impacted the surface during the time-scales investigated.

Two distinct but complementary methods were used to interpret back trajectories: construction of a map showing the dependence of the mean value of the studied quantity measured at the site on air mass residence time in specific regions; and a comparison of periods classified by cluster analysis of trajectories. These methods provide a means of separating influences of different geographical locations on measurements made from the ground site. Elevated measurement values associated with regions can in turn be attributed to likely sources. Similar approaches have been used in the past to assess sources: for example, in Mace Head, Western Ireland, Cape et al. (2000) used trajectory cluster analysis to interpret trace gas measurements and Bassford et al. (1999) used a residence time analysis to separate two discrete sources of methyl iodide – a coastal source and a sub-tropical Atlantic ocean source. The trajectory residence time analysis was pioneered by Ashbaugh (1985) who used it to attribute measurements of sulphate aerosols made in the Grand Canyon National Park to source regions. These methods are particularly useful in analysing the OP3 data as the complex local topography at the measurement site means local wind vector data are likely not to be representative of the direction of air mass origin. While ECMWF trajectories do not explicitly represent complex terrain and boundary layer processes, they should still be a good indicator of regional synoptic transport over the time scales presented here. The analyses presented are suited to analysis of species with a long atmospheric lifetime compared to the trajectory durations used, i.e. for species such as aerosol particles, carbon monoxide and halocarbons which are the focus of this paper.

Typically, of the seven day trajectories, only the 36 h closest to the measurement site were used, although the seven day trajectories are discussed for context in Sect. 3.1. Many of the species studied here have atmospheric lifetimes longer than this and it is possible that more insight into far field sources could be gained from their use, however we focus on shorter trajectories to minimise the introduction of erroneous analysis. This is caused by: the "shadowing" effect demonstrated in Sect. 2.2.1 below; the dependence of the density of trajectory data points on proximity to the receptor site which is inherent in the polar geometry; and the increase in the error of modelled trajectories with increased time calculated backwards.

2.2.1 Residence time analysis of back trajectories

The statistical method first described by Ashbaugh (1985) was extended to give an indication of geographical origins of measurements made at the ground site. For a given measurement, a geographical grid is constructed – all grids presented here used a cell size of $0.1^\circ \times 0.1^\circ$. Maps of trajectory residence time are shown in Fig. 1 for 36 h back trajectories during OP3-I and OP3-III. These are calculated by counting the number of trajectory data points in each cell for all trajectories and normalising to the probability density function inherent in the polar geometry. The polar probability density function can be calculated using

$$f_{ij}(r) = \frac{1}{2\pi Rr} \quad (1)$$

where R is the limit of the radial distance from the origin of the trajectories and r is the mean distance of each cell from origin of the trajectories (Ashbaugh, 1985). To assess the dependence of a measured quantity on air mass history, the value at the observing site at the time of arrival of a given trajectory is added to the grid cell that contains each trajectory point. Doing this for all trajectories and dividing by the total number of trajectory points in each cell gives the mean value measured at the ground site for an air mass that has passed over that cell. These plots are henceforth referred to as mean value maps.

Figure 2 shows an example mean value map of bromoform ($CHBr_3$) during OP3-III. Measurement techniques are detailed in Sect. 2.1. In interpreting mean value maps it is important to remember that air mass trajectories that regularly travel through a non-source region before travelling through a source region will show artificially elevated levels in the non-source region, henceforth called "shadowing". For example, in Fig. 2 there appears to be bromoform south of the site in the region around 1.5° N, 117° E, however this may be artificial if the east coast is a source region. A similar argument can be made if trajectories regularly travel through a source region before travelling through a removal region (for example a region of elevated levels of precipitation acting to remove aerosol) resulting in the source region not being resolved. As a wider range of conditions are sampled, these artificial data would be expected to be of less importance with unaffected data dominating. It is also the case in general that increasing data coverage will tend to resolve sources more accurately as the influence of isolated events is outweighed by representative conditions. In order to assess the potential extent of these effects, the percentage of the entire set of calculated back trajectories that was used in the construction of each mean value map is displayed. It is also important to be able to quantify the degree of similarity between different mean value maps. This is done by calculating the Pearson's r of a scatter plot of the intensities of corresponding grid points.

2.2.2 Agglomerative hierarchical cluster analysis of back trajectories

Trajectories were processed using the custom made cluster analysis routine described in Morgan et al. (2009) based on the method described in Cape et al. (2000). At the start of the analysis, each trajectory is assigned its own cluster. An

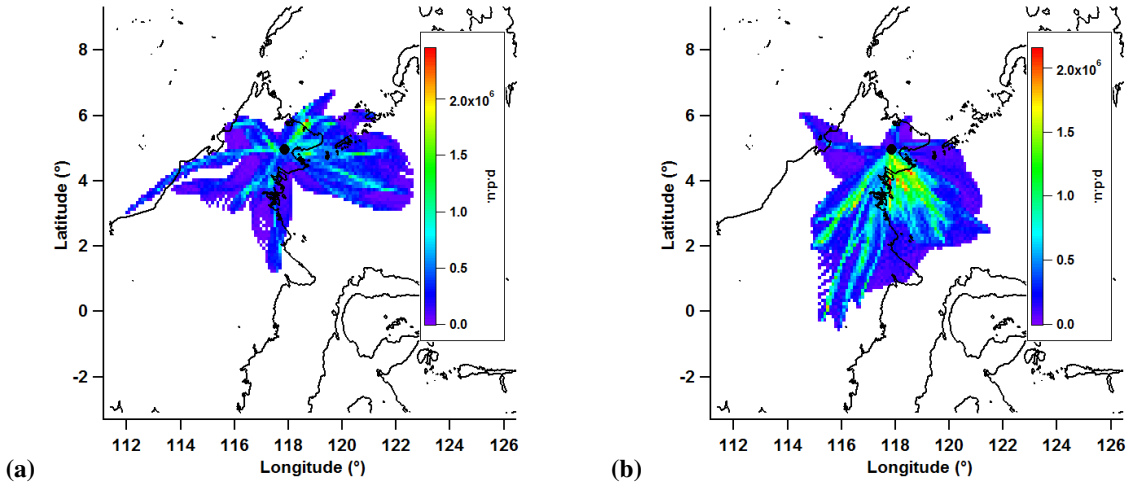

Fig. 1. Residence time of air masses in previous 36 h for all trajectories during **(a)** OP3-I and **(b)** OP3-III. Colour is number of trajectory data points (normalised to geometric probability density function), expressed in the resulting procedure defined units (p.d.u.). Trajectory receptor site (the measurement site) marked with a black dot.

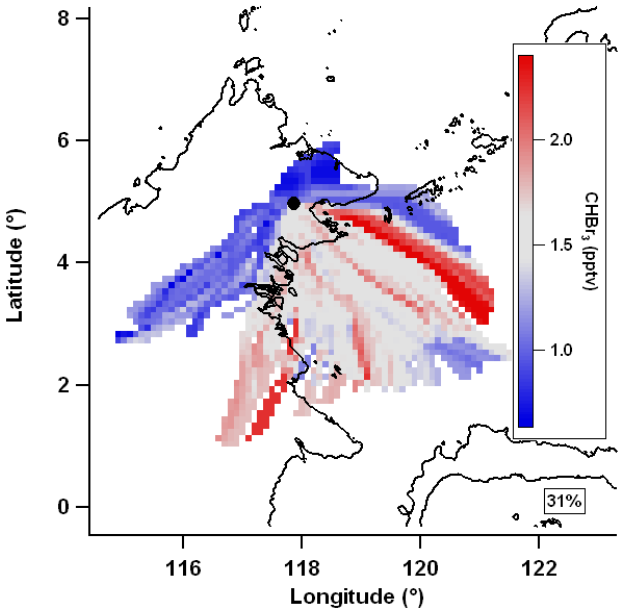

Fig. 2. Example mean value map of bromoform ($CHBr_3$) during OP3-III using 36 h trajectories. Grey is median value, red is greater than median, blue is less than median and white denotes no data coverage. Percentage of trajectories used denoted below key.

average linkage method was used based on calculating the squared distance between trajectories at each time step using

$$d(x_i, x_j) = \sum_k \left\{ (x_{ki} - x_{kj})^2 + (y_{ki} - y_{kj})^2 + (p_{ki} - p_{kj})^2 \right\} (2)$$

where x_k, y_k and p_k are the coordinates of x_i or x_j. At each step in the analysis the two clusters with the lowest squared distance are agglomerated. This continues until all trajectories are in one cluster. The optimum number of clusters may then be chosen, so as to maximize between cluster variance and minimize within cluster variance (Cape et al., 2000). The choice of the optimum number of clusters is subjective, however this has been shown to be the most appropriate technique for analysing meteorological trajectories (Kalkstein et al., 1987). The suitability of a solution of N clusters can be assessed using several scores. An increase in the root mean squared (RMS) distance between clusters indicates that two dissimilar clusters have been agglomerated (Cape et al., 2000). A sharp decrease of the coefficient of determination R^2, defined as

$$R^2 = 1 - \sum_N \frac{\text{(within cluster variance)}}{\text{(variance of all trajectories)}} \quad (3)$$

is a subjective indicator of the number of clusters to retain (Kalkstein et al., 1987). Similarly to Morgan et al. (2009) and Cape et al. (2000), an indication of the number of major clusters is defined as the number of clusters containing more than 3 % of the total number of trajectories.

The project was split into a series of successive twelve hour periods. These were classified according to the clusters that their constituent trajectories belonged to, similar to Cape et al. (2000): if trajectories belonging to more than one cluster were present, the period was deemed "unclassified", otherwise it was deemed to be influenced by that cluster. This removes periods of transition between air mass cluster, leaving comparatively stable conditions and enabling comparison between measurements influenced by different clusters. Mean, median and percentiles of measured quantities were calculated for data influenced by each cluster. These cluster

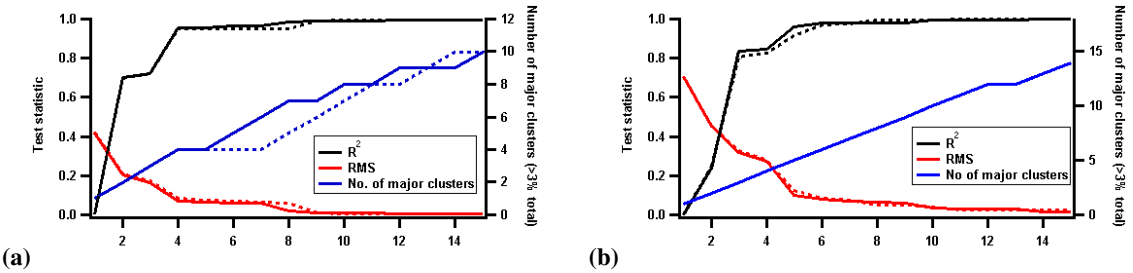

Fig. 3. R^2, RMS and number of major clusters (containing > 3 % of trajectories) as a function of number of clusters in solution for **(a)** OP3-I and **(b)** OP3-III. Solid lines are for one subset of trajectories and dashed lines are for the other.

averages are discussed in Sect. 3 and presented in full in Table 4.

In order to establish the robustness of the solution, the trajectories were split into two subsets: two day back trajectories of one hour time resolution released every two hours were used, with the alternate set similar but using trajectories from the intervening hours. The reduction in trajectory time resolution was necessary to improve computational efficiency. For both OP3-I and OP3-III, cluster scores (Fig. 3) and means (Figs. 4 and 5) show little difference between trajectory subset showing the cluster analysis solutions to be stable to perturbations, and are combined for classification and all subsequent analysis.

The scores for OP3-I (Fig. 3a) show the first major step change at the four cluster solution which is summarised in Fig. 4 and Table 1. Italics will be used for clarity when referring to cluster names, which are defined in Figs. 4 and 5. The main influence on the site is split evenly between the *North-easterly*, *Easterly* and *Terrestrial* clusters. Air masses associated with the *Westerly* cluster. Air masses associated with the *Westerly* cluster are of minor influence, making up only 3 % of the classified periods, and can generally be disregarded.

The scores from OP3-III (Fig. 3b) show the first major step change at the five cluster solution which is summarised in Fig. 5 and Table 2. The major influence on the site was from the south-westerly Marine cluster. The Coastal cluster from the south and the Terrestrial cluster from the south-west also had significant influence. There were two more clusters; the *North-easterly* and *Westerly* but both are of minor influence (consisting of 3 % and 5 % of classified periods, respectively) and can generally be disregarded. Figure 10, Sect. 3.1, shows the clusters influencing the measurement site during OP3-III (displayed as a coloured bar) for comparison to the aerosol composition data.

Table 1. Details of four cluster solution and resultant period classification for OP3-I.

Cluster name	No. of constituent trajectories (%)	No. of 12 h periods (%) attributed
North-easterly	221 (31 %)	15 (25 %)
Easterly	208 (29 %)	15 (25 %)
Terrestrial	236 (33 %)	18 (31 %)
Westerly	51 (7 %)	2 (3 %)
Unclassified		9 (15 %)

Table 2. Details of five cluster solution and resultant period classification for OP3-III.

Cluster name	No. of constituent trajectories (%)	No. of 12 h periods (%) attributed
North-easterly	41 (5 %)	2 (3 %)
Marine	460 (58 %)	33 (50 %)
Coastal	107 (14 %)	5 (8 %)
Terrestrial	141 (18 %)	10 (15 %)
Westerly	41 (5 %)	3 (5 %)
Unclassified		13 (20 %)

2.3 Positive matrix factorisation of organic aerosol mass spectra

Different PMF solutions were explored as a function of starting conditions (seed) and rotational ambiguity (fpeak) as detailed in Robinson et al. (2011), and the most satisfactory solution was a four factor solution with fpeak = −1. This solution was found to have negligible dependence on starting seed. Solutions with greater than four factors were found to be unsatisfactory due to "mixing" of factors (as described in Ulbrich et al., 2009), unrealistic factor spectra consisting of one or two peaks with little signal at other *m/z*s, or lack of convergence. The factor mass spectra are shown in Fig. 6 with the time series shown in Fig. 10.

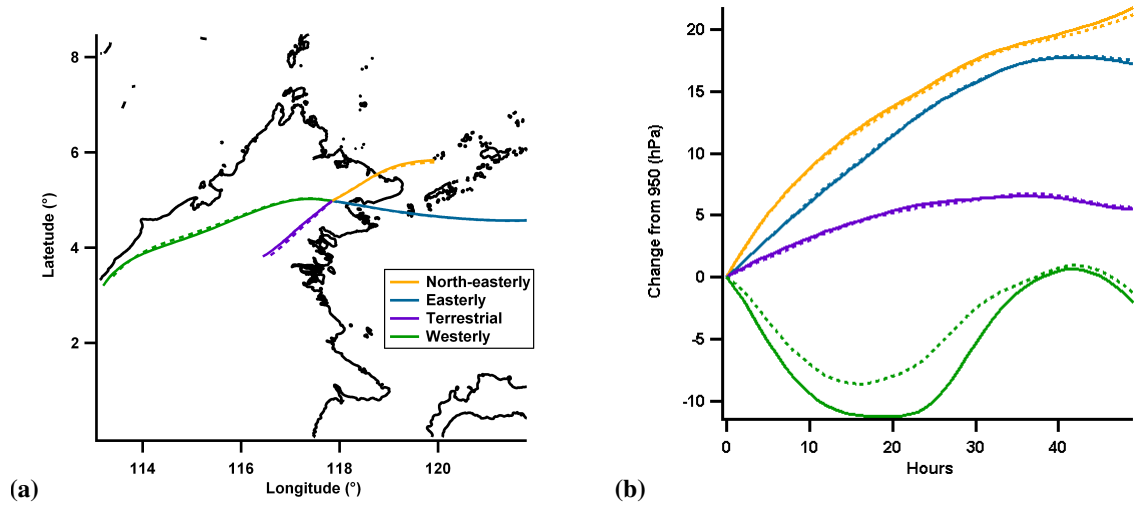

Fig. 4. OP3-I cluster mean **(a)** latitude and longitude and **(b)** pressure altitude in units of hPa different from starting altitude of 950 hPa. Colours are consistent between plots. Solid and dashed lines show solutions from each subset.

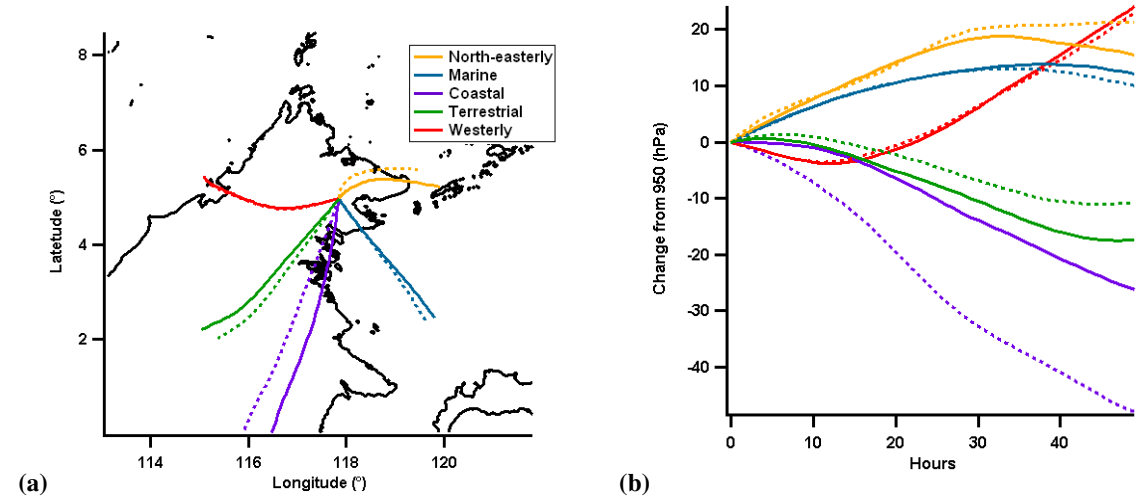

Fig. 5. OP3-III cluster mean **(a)** latitude and longitude and **(b)** pressure altitude in units of hPa different from starting altitude of 950 hPa. Colours are consistent between plots. Solid and dashed lines show solutions from each subset.

The four factors can be attributed sources from inspection of the mass spectral signature as follows. The first factor, named 91Fac, shows some similarities to previously published mass spectra of biomass burning emissions (Alfarra et al., 2007; Allan et al., 2010) for instance a prominent *m/z* 91 peak, which can be indicative of aromatic species. It does not show the *m/z* 60 and 73 peaks normally associated with levoglucosan, an established biomass burning marker in AMS measurements (Alfarra et al., 2007). However these levoglucosan peaks have been shown to reduce with ageing of biomass burning aerosol (Capes et al., 2008), implying the 91Fac may be from far field biomass burning emissions.

The second and third factors are named OOA1 and OOA2 respectively because of their similarity to previously published spectra (Lanz et al., 2007; Zhang et al., 2007). Spectra such as OOA1 are considered highly oxidised and have been linked to low volatility oxygenated organic aerosol (LVOOA; McFiggans et al., 2005); similarly, spectra such as OOA2 are considered less oxidised and have been linked to semi-volatile organic aerosol (SVOOA; Jimenez et al., 2009). However such assertions are impossible without a direct volatility measurement. While these factors are resolved as separate factors, they represent what are in reality different ends of a continuum of OA oxidations (Ng et al., 2010; Morgan et al., 2010). OA is gradually oxidised from OOA2-like to OOA1-like aerosol over time, which would be represented by the PMF factors as a reduction in OOA2 and a concurrent increase in OOA1.

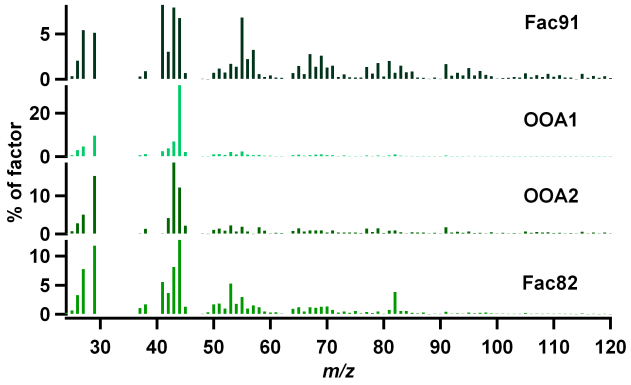

Fig. 6. Factor spectra for the four factor, fpeak = −1 solution of PMF analysis of organic mass spectra. From top to bottom, spectra are 91Fac, OOA1, OOA2 and 82Fac.

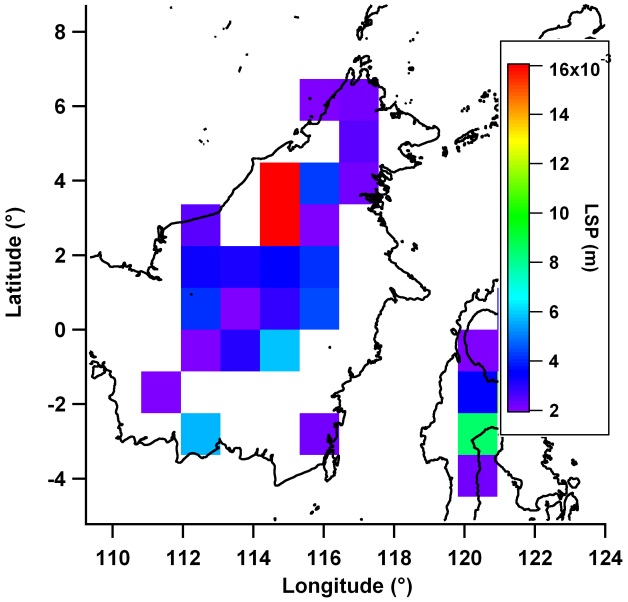

Fig. 7. Average daily large scale precipitation (m) from the European Centre for Medium-Range Weather Forecast Integrated Forecasting System model reanalysis (BADC, 2006b) at 1.125° × 1.125° resolution during OP3-III. Values below 2×10^{-3} m are not shown for clarity.

The last factor, named 82fac because of its prominent *m/z* 82 peak, is not similar to any mass spectra widely reported in the literature. Its measurement during the OP3 project was reported in Robinson et al. (2011) who provide evidence that it is associated that it is the product of isoprene oxidation. A similar factor has since been reported in rural North America where it was also associated with isoprene oxidation (Slowik et al., 2011). Further investigation into the likely sources linked to these factors will be made through the analysis presented in this paper.

3 Results

3.1 Overview of measurements and their regional setting

The major cities in Borneo are all located on the coast, with the biggest settlements on the south west of the island. The interior of Borneo is a mountainous unsettled and undeveloped region of rainforest. Average daily large scale precipitation from the ECMWF Integrated Forecasting System model reanalysis shows increased precipitation in the interior of Borneo (Fig. 7; BADC, 2006b). It is likely that this increased precipitation is due to the orography inland. Precipitation inhibits long range transport of aerosol. This means air masses from the southwest of the site will tend to have reduced concentrations of background aerosol. These air masses will have relatively greater amounts of locally produced aerosol.

Figure 8 shows a trajectory residence time plot, and the average minimum pressure (maximum altitude) of the trajectories passing through each cell, both using seven day back trajectories. These provide context for the more detailed analyses presented herein which use shorter (36 h) trajectories. This means the more detailed analyses only use trajectory data from relatively close to the receptor site where they are most accurate and their density is highest. The residence time plot shows that the site is mostly influenced by air masses from the south east. There is no influence from the major urbanised regional areas in mainland Malaysia (around Kuala Lumpur, east of Borneo), Singapore (south west of Borneo) and Indonesia (around Jakarta, south west of Borneo). Many air masses travel over Sulawesi (around 2° S, 121° E). The majority of the 16 million people inhabiting Sulawesi live at the far south. The plot showing the average minimum pressure of trajectories passing over each cell shows trajectories travelling over the island to generally be from a greater maximum altitude than trajectories transported from the east coast of Borneo. The distribution of trajectory minimum pressures has a mean of 909 hPa, median of 938 hPa and a tenth percentile value of 821 hPa. This corresponds to a ninetieth percentile maximum altitude of approximately 1.8 km a.s.l. with the majority of trajectories having a maximum altitude close to that of the receptor site.

The Moderate Resolution Imaging Spectroradiometer (MODIS) fire count (Davies et al., 2009; Justice et al., 2002; Giglio, 2003) shows hotspots/open fires detected in the wider region during OP3-III in Fig. 9. The majority of fires are concentrated to the south west of the measurement site in Vietnam, mainland Malaysia, Sumatera, Indonesia and South Western Borneo. The seven day trajectories show none of these regions to be an influence on the measurement site. The trajectories that travel up from the south of the island (largely associated with the *Terrestrial* and Coastal clusters) are likely

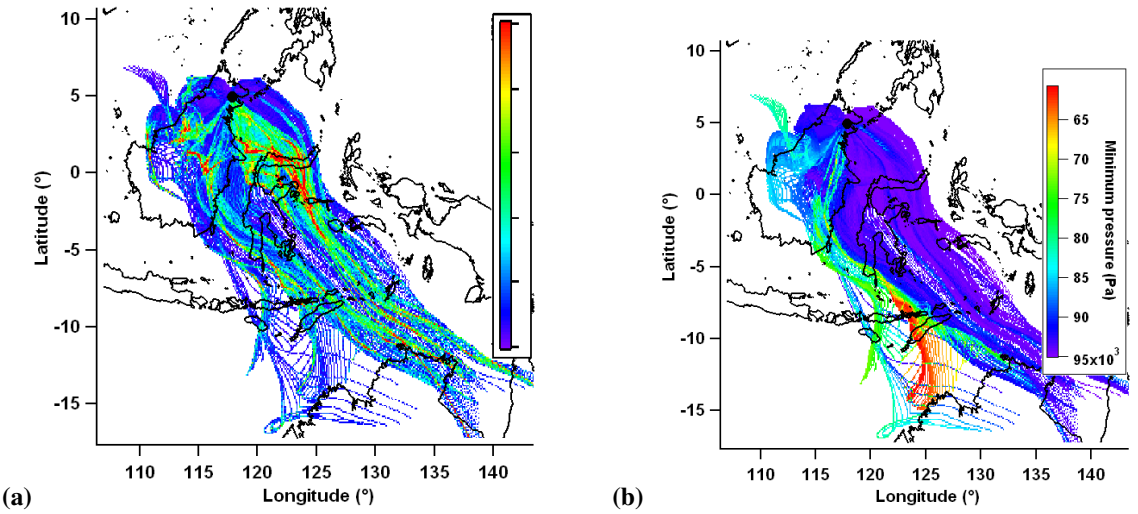

Fig. 8. **(a)** Residence time of air masses in previous 7 d for all trajectories during OP3-III. Colour is number of trajectory data points (normalised to geometric probability density function). **(b)** mean minimum pressure of trajectories passing through that cell in in previous 7 d. Trajectory receptor site (the measurement site) marked with a black dot.

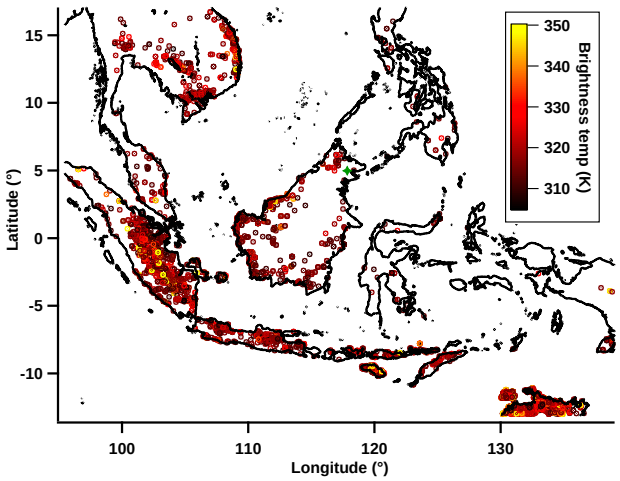

Fig. 9. MODIS hotspot/active fires coloured by temperature of event during OP3-III. Site marked with green star.

to have the most biomass burning influence due to on-island fires, and perhaps fires further afield on the Lesser Sunda Islands in South East Indonesia (around 7° S by 125° E).

Aerosol measurements made in Borneo show a contrasting situation to Amazonia with much higher sulphate and ammonium loadings, much more similar to those measured in West Africa (Table 3). The time series of aerosol composition is shown in Fig. 10 with a bar indicating the classification of the air mass (see Sect. 2.2.2) influencing the measurement site.

3.2 Halocarbons

The bromoform (shown previously in Fig. 2) and dibromomethane (CH_2Br_2; not shown) mean value maps show very similar profiles ($r = 0.90$) which is unsurprising as these compounds are well correlated in the atmosphere (Butler et al., 2007; Yokouchi et al., 2005; Zhou et al., 2008). The time series collected at Bukit Atur also confirms this as their time series are well correlated. Bromoform and dibromomethane show elevated levels over coastal and marine regions compared to terrestrial regions, this is consistent with other studies which have shown them to be produced by macro-algae (Carpenter and Liss, 2000; Goodwin et al., 1997; Quack et al., 2007). In particular the south-east coast of Sabah is a region of seaweed cultivation which is reflected in the high concentration seen in air masses from this region.

The methyl iodide mean value map (Fig. 11a) is similar to those of the polybrominated compounds, however, there are some differences in features (mean value map correlations of $r = 0.70$ with bromoform and with dibromomethane). Like the polybrominated compounds, the methyl iodide map shows high values to be predominantly attributable to off-island sources. This is consistent with whole air samples collected in the boundary layer during the OP3 flight campaign on the FAAM BAe-146 aircraft (Hewitt et al., 2009; Newton et al., 2011), and analysed on the same GC-MS system set-up as described in Sect. 2.1 of this paper. Data from this aircraft campaign showed a clear concentration gradient from sea-to-land, with highest concentrations of methyl iodide seen off the south-east coast of Sabah. The pattern of high values seen over the sea in the methyl iodide mean value map is similar to that seen in the polybrominated compound mean

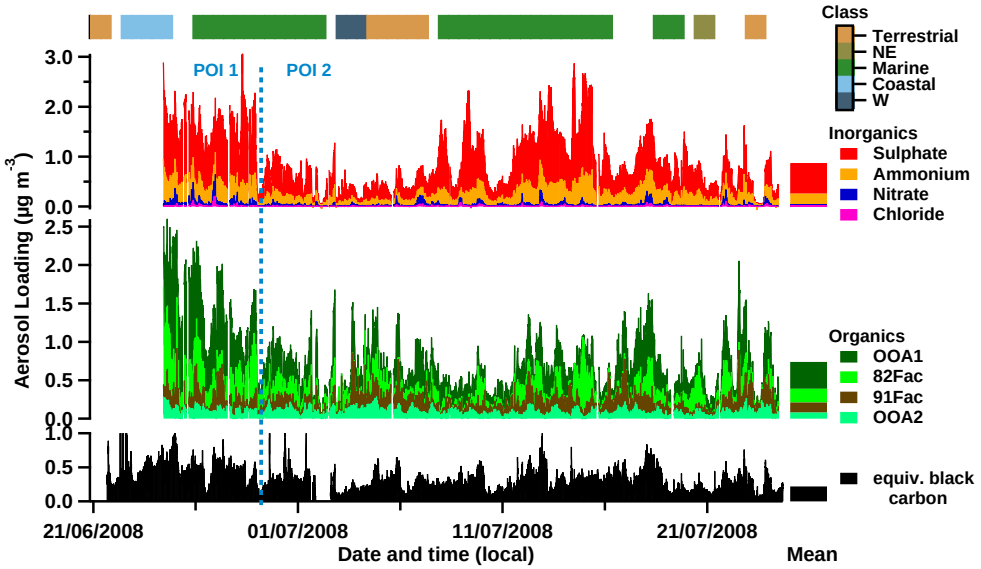

Fig. 10. Stacked time series of total sub-micron non-refractory aerosol split by composition (see Sect. 2.1) for OP3-III. The inorganics and organics are shown on separate axes, with the organics split into their constituent PMF factors. The split point between Period Of Interest (POI) One and Two is marked with a dashed blue line (see Sect. 3.6). The campaign mean aerosol loadings are shown as stacked bars to the right of the time series. Colour of bar at top indicates class of air mass influencing site (see Sect. 2). No bar indicates unclassified (changeable) air mass.

value maps. In particular the methyl iodide and polybrominated mean value maps all show a region of high values off the coast to the immediate east of Bukit Atur which extends east (to around 4° N, 120° E). This shared feature suggests a co-located source of methyl iodide and the polybrominated compounds; possibly it is even the same source, potentially macro algae, which have been shown to produce all three of these compounds (Carpenter and Liss, 2000; Manley et al., 1992). Other studies have observed correlations between methyl iodide and these polybrominated compounds, but noted the inconsistency of their correlation, suggesting different production mechanisms for the methyl iodide and polybrominated compounds (Butler et al., 2007). Methyl iodide shows less separation between terrestrial and marine air masses than the polybrominated compounds. This consistent with previous studies, which have shown methyl iodide to have a mixture of marine and terrestrial sources (Bell et al., 2002; Smythe-Wright et al., 2006; Sive et al., 2007) and be emitted during biomass burning (Cox et al., 2005; Mead et al., 2008).

In stark contrast to the other three halocarbons presented here the waters immediately east of Bukit Atur around 4° N, 120° E do not appear to be a productive region for methyl bromide (Fig. 11b). There is some marine contribution, predominantly from the coastal zone south of Sabah included in the extent of these maps, which is consistent with known marine sources of methyl bromide such as macro algae (Baker, 2001; Cox et al., 2005). Higher values (8–9 pptv) are seen over an area to the north of Bukit Atur (5.4–6° N) covering

Table 3. Comparison of sub-micron non-refractory aerosol loadings ($\mu g\,m^{-3}$) from different tropical campaigns. Bornean and Amazonian (Chen et al., 2009) measurements are campaign averages of ground site intensives. West African measurements are averages of low altitude data over several flights, screened to remove (local) biomass burning and anthropogenic influence (Capes et al., 2008, 2009).

	Borneo	Amazonia	West Africa
Organic	0.74	0.64	1.01
Sulphate	0.61	0.15	0.82
Ammonium	0.21	0.02	0.36
Total	1.6	0.82	2.26

both land and coastal areas. This area is known to comprise oil palm plantations and there are similarities between the methyl bromide mean value map and 82Fac (Fig. 14a) discussed in Sect. 3.4 although overall correlation is not high ($r = 0.32$). It is currently unknown whether oil palm trees are actually a source of methyl bromide. However, other activities associated with the oil palm plantations such as biomass burning, a known source of methyl bromide (Mead et al., 2008; Reeves, 2003), may also contribute to the localised high values. Moreover, a coastal source cannot be discounted as responsible for this feature, possibly a macro algae source. The mean value plot for methyl bromide shows an elevated feature to the south west of the measurement site,

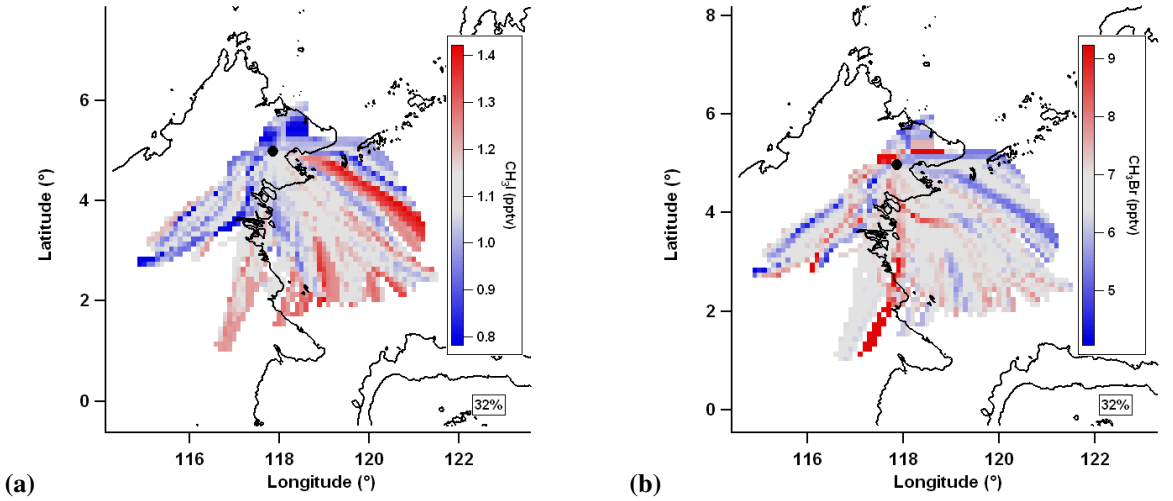

Fig. 11. Mean value maps for **(a)** methyl iodide, CH_3I and **(b)** methyl bromide CH_3Br. Grey is median value, red is greater than median, blue is less than median and white denotes no data coverage. 36 h trajectories used.

in a similar location to that seen in the methyl iodide map though the exact grid boxes differ. As discussed earlier small scale biomass burning may be a contributing factor to this feature, in addition tropical vegetation has been suggested as a weak source of methyl bromide (Blei et al., 2010).

3.3 Nitrate and chloride aerosol

The nitrate (Fig. 12) and chloride (not shown) mean value maps and time series are similar ($r = 0.76$) suggesting the two species may be components of the same aerosol. The greatest aerosol loadings are mostly associated with marine air from the south-east. Elevated loadings shown to the far south over the Sangkulirang Peninsula (around 1° N, 117.5° E) may be artificial, caused by the preceding or subsequent transit of the air mass over the sea. Cluster averages show nitrate and chloride to be associated with air of marine origin, with greater loadings in the *Marine* cluster than the *Terrestrial*. Campaign average loadings of nitrate (0.03 µg m^{-3}) and chloride (0.01 µg m^{-3}) are very low however they are high when compared to Amazonia (0.01 µg m^{-3} and 0.00 µg m^{-3}, respectively). The diurnal profile of nitrate and chloride loadings shows them to be strongly elevated around midnight with low levels throughout the day.

Nitrate (NO_3^-) is produced in the atmosphere by oxidation of NO_x on the time-scale of hours. Hewitt et al. (2009) found that NO_x levels in Borneo, while typically lower than those found in more developed countries such as USA and Europe, were highest over the oil palm plantations where the sources were vehicle emissions, combustion and crop fertilisation. The AMS nitrate loading is derived from two fragments (NO^+ and NO_2^+ at *m/z* 30 and 46) and during OP3 these varied, indicating that the nitrate that is detected is unlikely to be purely in the form ammonium nitrate (NH_4NO_3), as this is

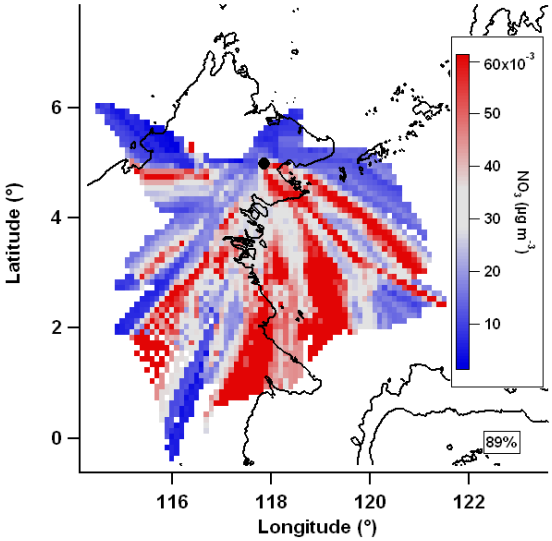

Fig. 12. Mean value map for nitrate. Grey is median value, red is greater than median, blue is less than median and white denotes no data coverage. 36 h trajectories are used.

known to fragment consistently. The ratio of the mean ambient NO^+ and NO_2^+ signals is significantly greater than during calibrations using ammonium nitrate (5.4 vs. 2.6). The AMS has been shown to be poor at measuring organic nitrates directly as $C_xH_yN^+$ or $C_xH_yO_zN^+$ (Farmer et al., 2010), with significant mass (30 %) detected at the NO_x^+ peaks (Rollins et al., 2010), which make up AMS "nitrate" measurements usually associated with inorganic nitrate. However the majority of organic nitrate mass is still thought to be measured at the $C_xH_yN^+$ and $C_xH_yO_zN^+$ peaks (Rollins et al., 2010) and there is little correlation of these signals with the NO^+

and NO_2^+ ($r = 0.29$), implying any role of organic nitrates to be low.

A likely source of chloride containing aerosol is sodium chloride particles from sea water, however the AMS cannot measure sea salt particles well as they are usually too large to be successfully sampled and they vapourise slowly (Allan et al., 2004). There is no excess ammonium (NH_4) detected after the neutralisation of sulphate in Borneo, meaning nitric acid will not readily be neutralised. The introduction of nitric acid (HNO_3) to aqueous sodium chloride particles would force the chloride to partition to the gas phase in the form of hydrogen chloride (HCl). This leads to aqueous sodium nitrate particles that are more easily volatilised by the AMS. The liberated hydrogen chloride can then react to form aerosol which is detected by the AMS. While there are no direct measurements of the composition of the chloride containing aerosol, it is likely that they are in the form ammonium chloride.

The nitrate and chloride diurnal profiles show a very strong increase at night, which may be driven by partitioning of vapours as the temperature reduces. A dense layer of fog formed across the forest every night which may have facilitated nitrate and chloride aerosol reformation occurring in the aqueous phase. Furthermore, the measurement site, located on a ridge top, protruded above the planetary boundary layer top every night (Pearson et al., 2010) which may have introduced more marine influenced aerosol that would be typical of the regional background.

3.4 Organic aerosol

The OOA1 mean value map shows both off-island and on-island sources (Fig. 13a). The *Marine* and *Terrestrial* period averages (0.33 and 0.29 $\mu g\,m^{-3}$, respectively) show, while both sources are significant, the off island source is larger. The greatest concentrations of OOA1 are in marine/coastal air masses. These are likely to be the result of long range transport of highly oxidised regional emissions with a possible contribution from processed biomass burning at the start of the measurement period (see Sect. 3.6). It is likely that the on island source of OOA1 represents the aged component of BSOA from the rainforest and the components of regional long range transport aerosol that is not removed through wet deposition during transit across the island. The inland OOA1 is changeable, showing both high and low loadings, and it is conceivable that the amount of inland OOA1 is driven by the level of precipitation inland.

The OOA2 mean value map (Fig. 13b) shows a strongly terrestrial source of aerosol, with *Marine* and *Terrestrial* period loadings of 0.11 and 0.07 $\mu g\,m^{-3}$, respectively. It shows elevated loadings across much of the island with the exception of the known oil palms to the immediate north and south of the measurement site. This suggests the rainforest is a source of freshly produced BSOA from the oxidation of rainforest VOC emissions which are represented by the OOA2 factor. OOA2 is a relatively minor fraction of the total organic aerosol, making up only 11 % compared to OOA1 which makes up 47 %. This is expected in an environment such as Borneo where there are influences from far field sources such as off-island anthropogenic sources and OA from oceanic emissions, meaning more aged organic aerosol could dominate.

The ratio of mean value maps of OOA1 to OOA2 (extent of oxidation; Fig. 13) shows the oxidised aerosol to be originating externally to the island compared to the less oxidised aerosol which originates in the island interior. This implies the highly oxidised OA is from long range transport of aerosols that are emitted from sources external to the island, either biogenic or anthropogenic. Figure 13 shows low OA oxidation in air masses travelling across the centre of the island, a region of enhanced precipitation (Fig. 7). Wet removal of aerosol is likely to lead to depleted concentrations of regional aerosol (highly aged OA) and relatively increased concentrations of more locally produced aerosol. This local aerosol is likely to be BSOA generated from rainforest produced precursors as there were not any other major sources known to be nearby (e.g. biomass burning, large settlements), especially in the inland region.

The oil palm plantations in Borneo have been shown to be a substantial source of isoprene, with emissions per unit area five times higher than the rainforest (Hewitt et al., 2009). Robinson et al. (2011) showed that isoprene was a significant source of BSOA at the measurement site in Bukit Atur, linking isoprene derived BSOA to a distinctive *m/z* 82 peak in the AMS organic aerosol mass spectrum and the associated 82Fac PMF factor. The mean value map of 82Fac (Fig. 14a) shows higher than average loadings in air masses from the immediate north, north-east and south-east. These are all areas of oil palm agriculture, as shown in Fig. 1b of Hewitt et al. (2010). The air masses associated with these areas also have particularly low maximum altitudes meaning they are likely to be particularly influence by local surface emissions (Fig. 8). The cluster averages show higher 82Fac loadings from air masses associated with the *Marine* cluster than *Terrestrial* (0.18 vs. 0.12 $\mu g\,m^{-3}$, respectively), which in this case corresponds to air masses from the Semporna Peninsula region to the immediate south-east of the site (approximately 4.5° N, 118° E). The north-easterly cluster, which corresponds to air mass from the oil palms to the north, shows high average loadings (0.14 $\mu g\,m^{-3}$), although there is a low amount of data from this period as stated earlier. Loadings are periodically high across the rest of the island signifying additional inland sources. The 82Fac OA makes up a significant proportion of the total OA (24 %). Robinson et al. (2011) speculated that the formation of isoprene SOA may be catalysed by the high sulphate loadings in Borneo: acidic sulphate has been shown to affect isoprene SOA formation in chambers (although through a mechanism unlikely to yield the *m/z* 82 marker detected in Borneo; Surratt et al., 2010) and acidic aerosol has been shown to catalyse the

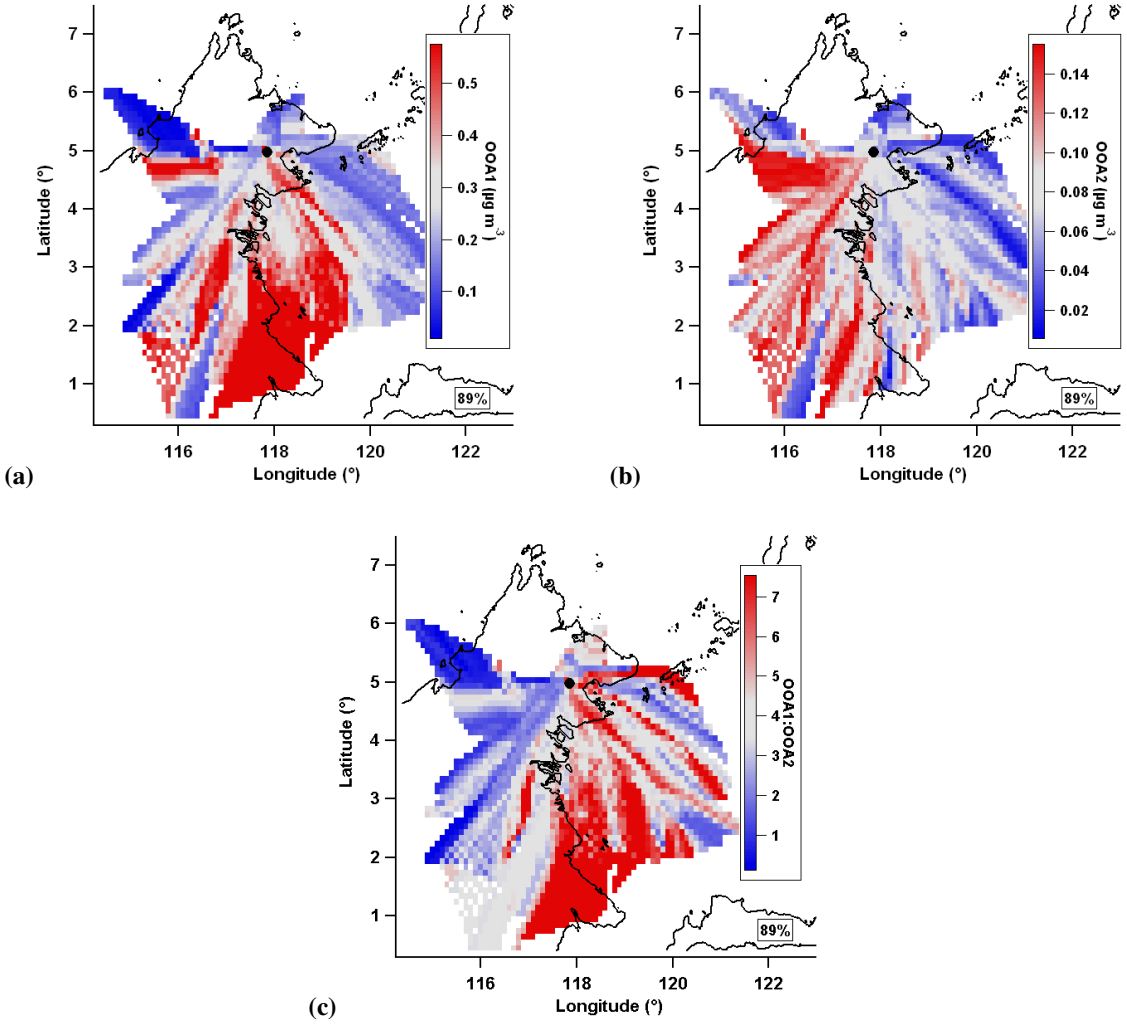

Fig. 13. (a) OOA1, **(b)** OOA2 and **(c)** the ratio of the OOA1 and OOA2 mean value maps, equivalent to OA oxidation. Grey is median value, red is greater than median, blue is less than median and white denotes no data coverage. 36 h trajectories are used.

heterogeneous reactive uptake of 1,4-hydroxycarbonyls (established isoprene oxidation products) to condensed phase species likely to yield the *m/z* 82 peak (Lim and Ziemann, 2009). The mean value map of excess sulphate (Fig. 14) shows the main source to the south-east of the site, in one of the regions associated with isoprene SOA. It should be noted that sulphate aerosol that is neutralised by the time of arrival at the measurement may be acidic closer to the coast where it has had less time to be neutralised by terrestrial ammonium sources.

3.5 Sulphate aerosol

The mean value map correlation ($r = 0.93$) suggests that sulphate (Fig. 15) and ammonium are components of the same aerosol, with the ion balance indicating this is likely in the form of ammonium sulphate. Cluster averages of ammonium and sulphate show greater loadings in the *Marine* cluster than in the *Terrestrial* cluster (0.25 vs. 0.09 $\mu g\,m^{-3}$ for ammonium and 0.75 vs. 0.25 $\mu g\,m^{-3}$ for sulphate, respectively), which is consistent with the mean value maps.

Ammonia is produced from the natural breakdown of urea and uric acid excretion from animals and emissions from fertiliser. It is the primary basic gas in the atmosphere and would be expected to be present in Borneo. Sulphate aerosol is often produced from processing of anthropogenic emissions of SO_2 from fossil fuel combustion. South East Asia uses more sulphur rich vehicle fuel (International Fuel Quality Center, 2009) than western countries meaning anthropogenic fossil fuel combustion may be of particular influence in the region. Sulphate is also produced naturally by processing of phytoplankton DMS emission (Kloster et al., 2006) and gaseous sulphur emitted by volcanoes (Allen et al., 2002). Previous studies have used the methane sulphonic

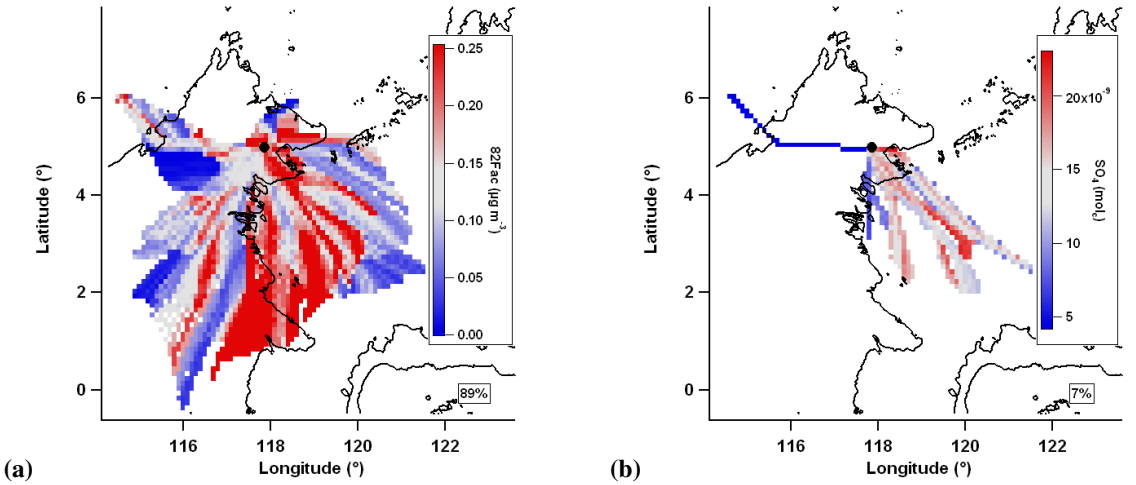

Fig. 14. Mean value maps of **(a)** 82Fac and **(b)** excess sulphate (defined as moles of charge of sulphate greater than moles of charge of ammonium plus 3×10^{-9} to account for spread of neutral values). Grey is median value, red is greater than median, blue is less than median and white denotes no data coverage. 36 h trajectories are used.

acid peak (MSA; CH_3SO_3H) of the high resolution AMS mass spectrum as a marker for DMS derived sulphate aerosol (Zorn et al., 2008). The yield of MSA relative to sulphate from atmospheric DMS oxidation has been shown to be much lower in tropical conditions (Bates et al., 1992; Allan et al., 2009) and no MSA signal was apparent in the Borneo dataset.

Volcanic activity was reported around the time of the OP3 project from Ruang (735 m), an island north of Sulawesi, Indonesia, East of Borneo and Mount Papandayan (2665 m) on Java, Indonesia, to the South of Borneo (Venzke et al., 2010), and could be responsible for some of the sulphate aerosol detected. However, if the back trajectories are assumed to be reliable when extended to the seven day limit (Fig. 8), these regions did not influence the site.

A scatter plot of sulphate loading vs. OA loading, coloured by cluster, is shown in Fig. 16, similar to the method used in Chen et al. (2009) when analysing aerosol composition in Amazonia. Figure S1 of the Supplement shows the same scatter plot coloured by *m/z* 44:43 (OA oxidation). Lines indicate the modal centres of the histogram of values of the sulphate to OA ratio. It should be noted that some level of correlation is to be expected between aerosol loadings due to shared removal processes, hence points at all three lines show a degree of correlation. Line A indicates points of high sulphate concentration with little dependence on OA loading, which are characteristically associated with the *Marine* cluster. They also show a varied level of OA oxidation. They are consistent with sources of sulphate external to Borneo that are not necessarily associated with production of OA – such as marine DMS production or volcanic emissions.

Line B indicates points of correlated high sulphate and OA concentration which are characteristically associated with

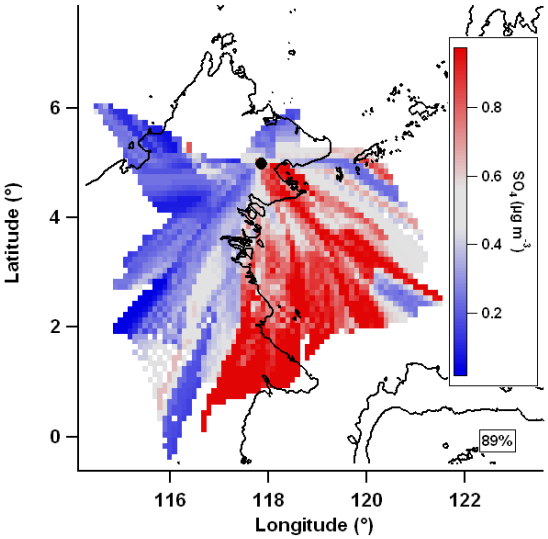

Fig. 15. Sulphate mean value map. Grey is median value, red is greater than median, blue is less than median and white denotes no data coverage. 36 h trajectories are used.

the *Marine*, *Coastal* and *North-easterly* clusters. These points show generally higher oxidation. This is consistent with an internally mixed regional background that is removed through wet deposition in inland Borneo. It is possible that the aerosol associated with line B could be sulphate from similar sources to that associated with line A, but with OA mass added during transit over conurbations on the east coast of Borneo, however this is not likely given the high level of OA oxidation which suggests long atmospheric lifetime, and the lack of association with individual cities. Most likely,

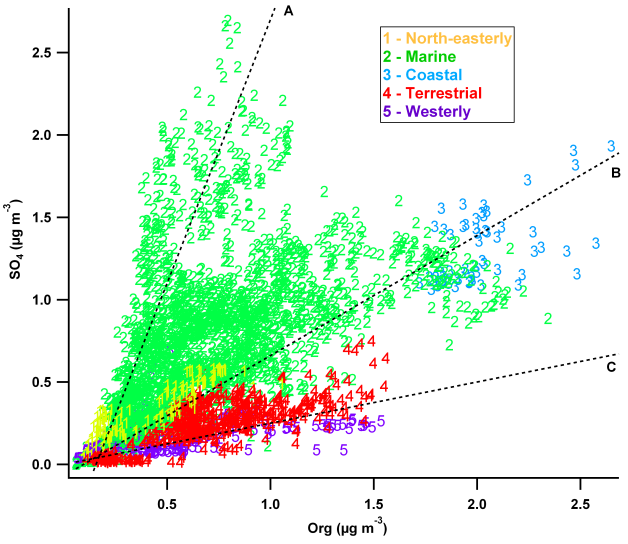

Fig. 16. SO_4 loading vs. OA loading coloured and numbered by cluster. Lines, labelled with letters, indicate different proposed dependencies. Lines represent modes of the SO_4:org ratio histogram of values.

the aerosol whose sulphate and organic mass correlate along line B result from long range transport, which may well be a combination of anthropogenic and biogenic sources. Biogenic sources of organic matter are most likely to be of terrestrial origin and those of sulphate are likely to be marine in nature.

Line C indicates points of high OA loading with a weaker dependence on sulphate loading, which are characteristically associated with the *Terrestrial* and *Westerly* clusters. They show a range of levels of OA oxidation. This is consistent with biogenic production of SOA, providing a mixture of more and less aged OA.

For the region including the measurement site and the sea to the south-east, where the majority of sulphate containing air masses came from: DMS emissions from phytoplankton are predicted to contribute around 30–40 % of total column sulphate (Gondwe, 2003; Kloster et al., 2006); around 40–50 % of surface sulphate is predicted to be from anthropogenic emissions (Tsai et al., 2010) with < 10 % of surface sulphate concentrations predicted to be from shipping emissions (Capaldo et al., 1999); and around 30 % of surface sulphate predicted from volcanic emissions (Graf et al., 1997).

It is likely that the apparent elevated sulphate loadings over the oil palms to the south-east of the site are mainly due to the preceding transport of the air across marine source regions. There may also be elevated sulphate loadings due to the proximity of marine sources such as DMS production and shipping as well as an increased anthropogenic influence. The fact that sulphate and ammonium loadings are depleted inland is probably due to the wet removal of the aerosols as they are transported through these regions of enhanced precipitation (Fig. 7).

3.6 Combustion emissions

High aerosol loadings at the beginning of the measurement period are associated with air masses from the south of the measurement site. This can be seen by splitting the data set into two periods of interest (POI): POI1 before 00:01 a.m. 29 June 2008 UTC and POI2 after. This point was chosen because of the drop in both organic and inorganic aerosol loadings and is indicated in Fig. 10. POI1 was influenced by air from the east coast of Borneo, and experienced greater amounts of OA (1.34 vs. 0.62 µg m^{-3}), OOA1 (0.76 vs. 0.27 µg m^{-3}), CO (177 vs. 98 ppb; Fig. 17), BC (0.36 vs. 0.18 µg m^{-3}; Fig. 18) and 91Fac (0.15 vs. 0.12 µg m^{-3}; Fig. 19) than POI2. These quantities are all indicative of pollution. The 91Fac factor may suggesting biomass burning specifically due to its resemblance to previously reported biomass burning spectra (Alfarra et al., 2007; Allan et al., 2010), although it is a minor factor making up only 18 % of total OA mass over the whole project. Trajectories also tended to be influenced by air masses that have higher maximum altitudes during POI1 compared to POI2, with median minimum trajectory pressures of 880 hPa vs. 946 hPa and tenth percentile pressures of 653 hPa vs. 886 hPa, respectively.

During POI2, CO and 91Fac show strongly on-island sources implying that biomass burning still influences the site, albeit to a lesser extent. It is less evident that an on-island source of BC dominates during POI2, with elevated amounts to the south, both on and off-island. There is a disparity between inland BC and CO measurements during POI2, with the dominant CO source being inland and the dominant BC source being more coastal and marine. This would be explained if the BC and CO were emitted from biomass burning on the south coast of Borneo (or even further upwind) and then transported across the island. The BC would be depleted inland through wet removal but the CO concentrations would be largely unaffected. Any BC from shipping off the east coast that was insignificant compared to biomass burning emissions in POI1 would then be apparent in POI2. Modelled loadings of BC (0.2–0.5 µg m^{-3} for the region; Koch et al., 2009) are consistent with the BC equivalent loadings for POI1 and POI2.

The MODIS fire count shows more open fire activity on Borneo at the beginning of the campaign, with an average of 42 events per day in POI1 compared to 10 in POI2. The fires are mainly confined to the coast with particularly high activity on the south-west of the island. This is also true of the wider region as a whole, with an average of 193 events per day in POI1 compared to 176 in POI2 (for the region shown in Fig. 9). This is consistent with POI1 being particularly heavily influenced by aged biomass burning in the region, either transport of aged off-island biomass burning emissions,

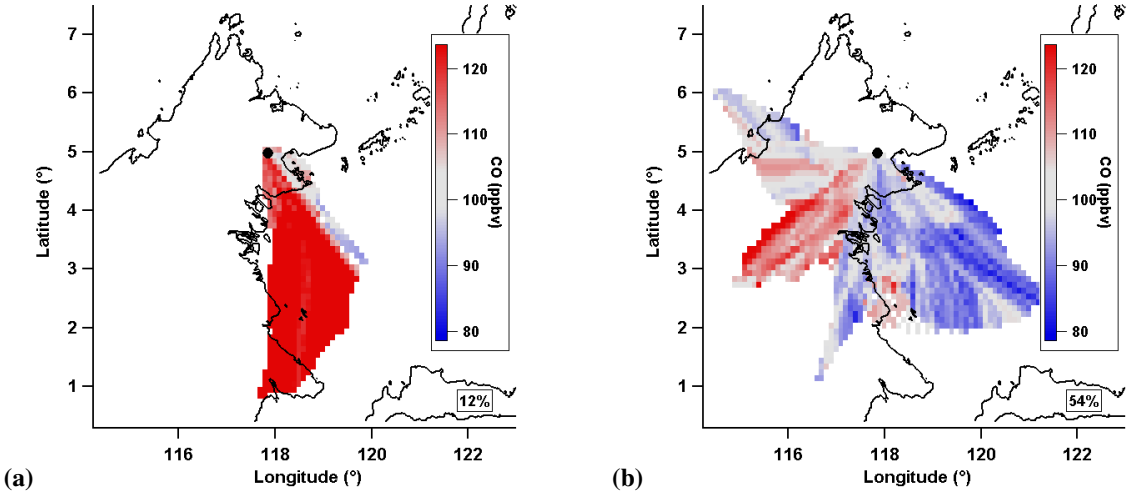

Fig. 17. Mean value maps of CO during **(a)** POI 1 and **(b)** POI 2. Colour scale is centred round the median value of the CO mean value map for the whole campaign.

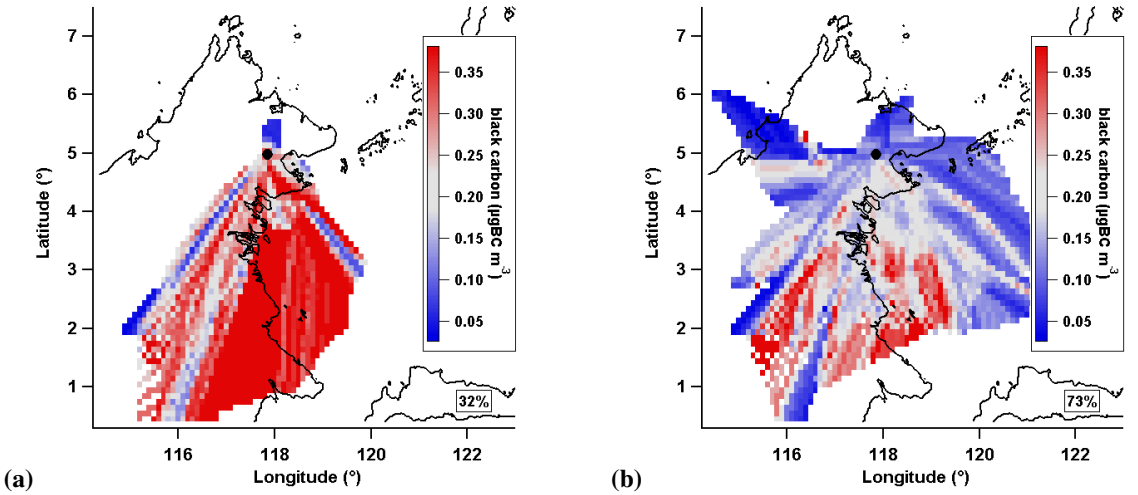

Fig. 18. Mean value maps of aerosol absorbance (expressed as black carbon equivalent loading) during **(a)** POI 1 and **(b)** POI 2. The colour scale is centred round the median value of the BC mean value map for the whole campaign.

or more local on-island biomass burning emissions. It is also the case that air masses during POI1 descended from higher altitudes than POI2, with mean minimum pressures of 838 hPa and 931 hPa and tenth percentile values of 652 hPa and 886 hPa, respectively. The introduction of free tropospheric air may increase the dominance of biomass burning species which are likely to be transported from their source to the upper troposphere by pyroconvection.

It is possible that there is an oxidised aerosol influence from the south eastern coast of the island, particularly during POI1. The enhanced OOA1 loadings during POI1 may be due to processed emissions from biomass burning. In POI2 the majority of oxidised aerosol is in air masses external to the island, implying long range transport of OA. Taking this into consideration, it is likely that the OOA1 in POI1 is from a combination of long range transport of OA and on-island production and ageing of biomass burning OA. Further separation of these sources during POI1 is not possible given the short time scale and small range of trajectories sampled.

The inorganic aerosol components and 82Fac are also all greater in POI1 than POI2. There has been some evidence in the literature that sulphate gases produced from biomass burning can condense onto biomass burning aerosol downwind of fires, so this could be a potential sulphate source (Gao et al., 2003). However, coastal and marine air masses dominate POI1 compared to POI2, which has a more balanced mixture of coastal/marine and inland air masses. This would explain the greater inorganic loadings in POI1, as

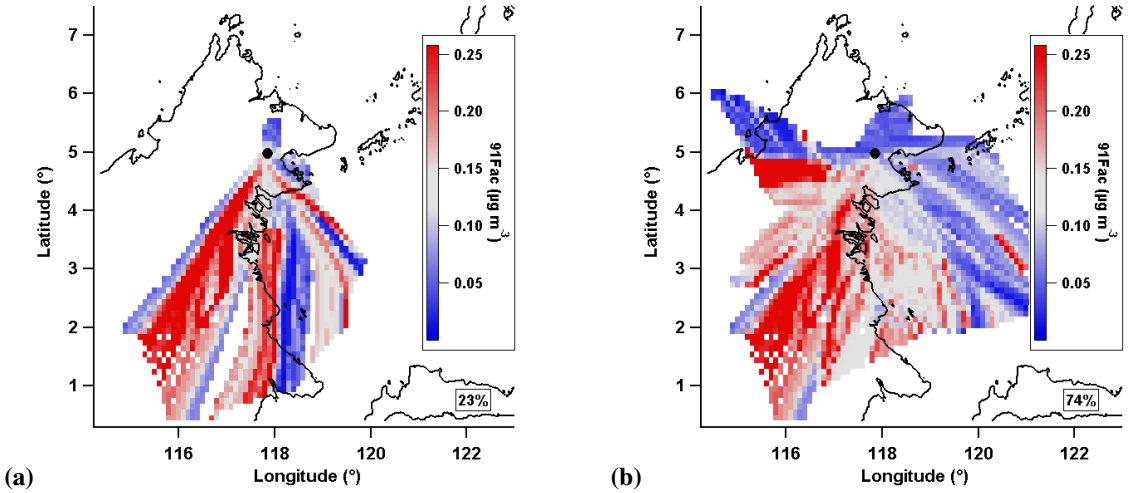

Fig. 19. Mean value maps of 91Fac during **(a)** POI 1 and **(b)** POI 2. Colour scale is the consistent between plots and is centred round the median value of the 91Fac mean value map for the whole campaign.

these aerosols are thought to be marine in origin (sulphate and chloride) or formed by reaction with marine aerosol (ammonium and nitrate). While 82Fac is not thought to be marine in origin, it is associated with marine air masses as these pass over the oil palm plantation to the south east of the site. It can also be speculated that some other controlling factor involved in the 82Fac OA was increased during POI1 (e.g. sulphate aerosol acidity or oxidation rates). Acidic sulphate has previously been shown to affect isoprene SOA formation and (Slowik et al., 2011) also showed their *m/z* 82 containing PMF factor may be associated with elevated sulphate concentrations. However, it appears that 82Fac shows little relation to the biomass burning markers throughout the project, suggesting that the increase during POI1 is unrelated to biomass burning. OOA2 showed a very slight decrease in loadings between POI1 and POI2 (0.09 vs. 0.08 µg m^{-3}), however this change is so small as to be within the uncertainty of the instrument and analysis methods.

3.7 Dependence of hygroscopicity on regional source

Figure 20 shows mean value maps of hygroscopicity measurements for two given aerosol sizes. These are representative of other measured sizes, with an average $r = 0.9$ for six sizes between 32 and 258 nm for the GF_{90} mean value maps and an average $r = 0.7$ for ten sizes between 57 and 202 nm for the SS_{crit} mean value map. A complete discussion of aerosol hygroscopicity and its relation to composition and size is detailed in Irwin et al. (2010). The subsaturated growth factor (between 0 and 90 % relative humidity; GF_{90}) shows good separation between terrestrial and marine air masses for both sizes, with higher aerosol GF_{90} measured in air of marine origin. Critical supersaturation (SS_{crit}) shows highest values from the south-west and east over Bongao island (5° N, 120° E), which are air masses associated with low sulphate levels (Fig. 13) and less oxidised aerosol (Fig. 13). As previously stated, the AMS does not efficiently measure sea salt, however if primary externally mixed sea salt aerosol was present it would be expected to be apparent in HTDMA data as a population of particles with a high (>2) growth factor in the upper dry size channels (Good et al., 2010a). Such a mode was not observed, justifying the comparison of AMS and hygroscopicity data. The hygroscopicity mean value maps are supported by the cluster averages. The hygroscopicity instruments have less data coverage than the AMS, not making measurements during the beginning of the measurement period when aerosol loadings were high in air mass from due south over the Sangkulirang Peninsula (1° N, 117.5° E). Taking this into account, higher GF_{90} and lower SS_{crit} values are measured in air masses associated with higher ammonium sulphate mass fraction, and conversely lower GF_{90} and higher SS_{crit} values are measured in air mass associated with lower ammonium sulphate mass fraction. This is consistent with the literature which shows ammonium sulphate to be more hygroscopic than atmospheric OA in both sub- and supersaturated regimes (Petters and Kreidenweis, 2007; Swietlicki et al., 2008). If a single hygroscopicity parameter can be used to explain water uptake then GF and SS_{crit} mean value plots would be expected to anti-correlate. While there is generally good anti-correlation, there are some exceptions. These should be the subject of further investigation to establish if this is due merely to instrumental or inversion artifacts, or if it is indicative of limitations of single variable parameterisations (as discussed by Good et al., 2010b; Irwin et al., 2010).

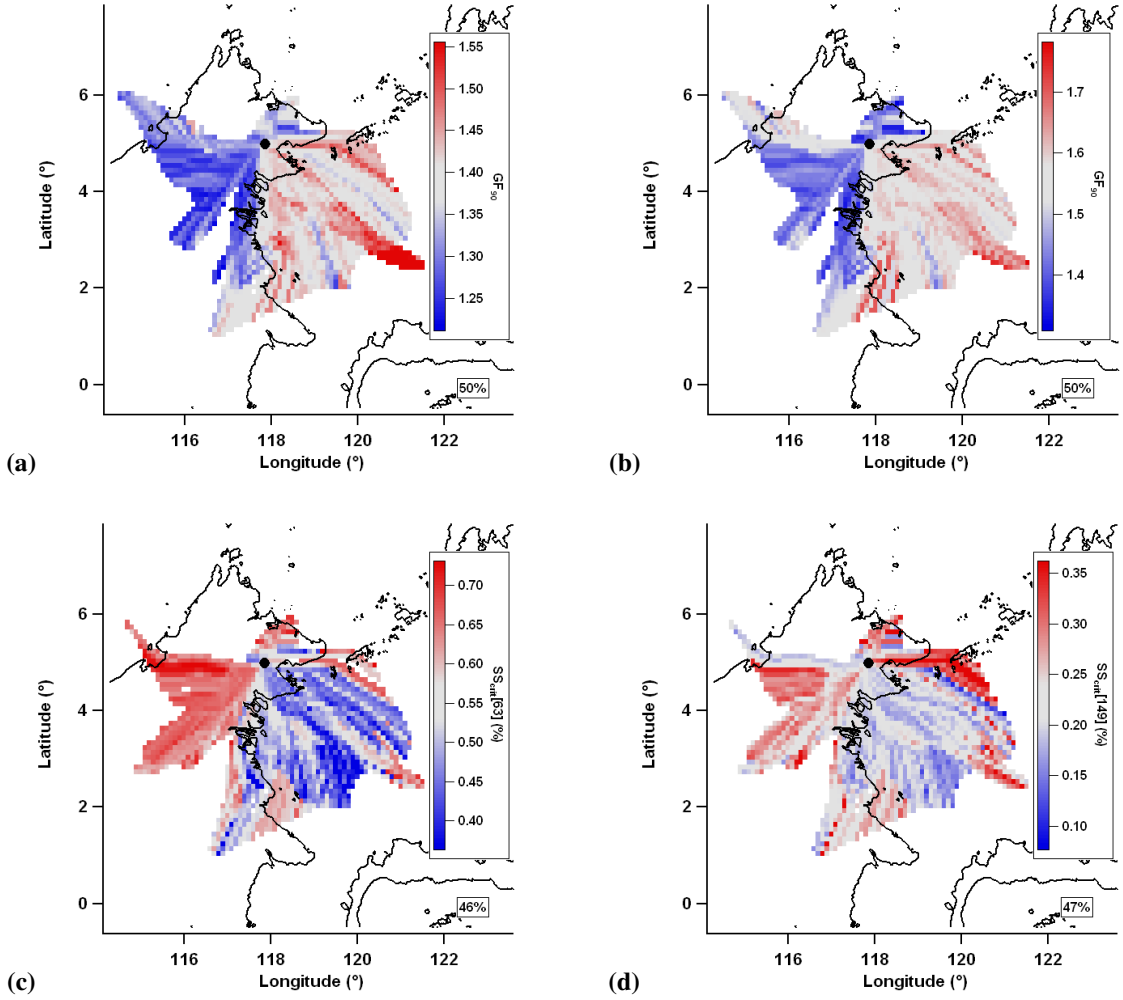

Fig. 20. Mean value maps of: sub-saturated growth factor for **(a)** 53 nm particles and **(b)** 155 nm particles; and critical supersaturation for **(c)** 63 nm particles and **(d)** 149 nm particles. Grey is median value, red is greater than median, blue is less than median and white denotes no data coverage. 36 h trajectories are used.

4 Summary

In general, many species demonstrated an association with either terrestrial or marine air masses. These are represented by data from the *Terrestrial* and *Marine* clusters which are displayed in Table 4. The analysis of halocarbons shows bromoform and dibromomethane to be strongly associated with coastal and marine air mass. These species are established marine tracers and this result provides validation for the back trajectory analysis presented here. Particularly high mixing ratios were observed in air masses associated with an area of seaweed cultivation directly east of the site. Methyl iodide was associated with similar air masses as the polybrominated compounds but it is unclear if it is produced from similar sources or by a different mechanism. It shows some departure from the polybrominated compounds, with inland levels not as uniformly low. Elevated inland values are also present in the methyl bromide mean value map. Methyl iodide has previously been reported from terrestrial vegetation and soil as well as biomass burning, all of which may contribute to the inland sources. Biomass burning has been reported as a source of methyl bromide and there is some evidence for emission from tropical vegetation. In contrast to the other halocarbons, the methyl bromide mean value map showed low mixing ratios in air masses directly east of the site. There does seem to be some marine contribution, specifically from the coast directly south of the site. It also showed some elevated mixing ratios in air masses from directly north and south of the site. This may be due to biomass burning associated with the oil palm plantations however other biomass burning markers were not observed to be significant of this region. It could also be due to the proximity of coastal sources such as macro algae. It is unclear if the oil palms themselves are a source of methyl bromide.

Table 4. Averages of data during 12 h periods classified as belonging to the *Marine* and *Terrestrial* clusters. Values quoted in the form mean (median$^{75\text{th }\%\text{ile}}_{25\text{th }\%\text{ile}}$). *Marine* and *Terrestrial* data sets that are significantly different with a 95% confidencelevel (using the two tailed Mann-Whitney U test (Cheung et al., 1997), which is nonparametric) are marked with an asterisk.

	Borneo			Amazonia		
	Terrestrial	Marine	All	In basin	Out of basin	All
Aerosol composition						
Organics ($\mu g\,m^{-3}$)	0.68 ($0.64^{0.89}_{0.47}$)	0.70 ($0.62^{0.90}_{0.41}$)	0.74 ($0.63^{0.95}_{0.43}$)	0.50	0.80	0.67
OOA1* ($\mu g\,m^{-3}$)	0.29 ($0.25^{0.44}_{0.16}$)	0.33 ($0.27^{0.43}_{0.16}$)	0.35 ($0.27^{0.46}_{0.16}$)			
OOA2* ($\mu g\,m^{-3}$)	0.11 ($0.10^{0.14}_{0.07}$)	0.07 ($0.07^{0.10}_{0.04}$)	0.08 ($0.07^{0.11}_{0.04}$)			
82Fac* ($\mu g\,m^{-3}$)	0.12 ($0.09^{0.18}_{0.05}$)	0.18 ($0.14^{0.25}_{0.06}$)	0.18 ($0.13^{0.25}_{0.06}$)			
91Fac* ($\mu g\,m^{-3}$)	0.16 ($0.15^{0.21}_{0.09}$)	0.12 ($0.09^{0.15}_{0.05}$)	0.13 ($0.10^{0.17}_{0.05}$)			
Sulphate* ($\mu g\,m^{-3}$)	0.27 ($0.26^{0.35}_{0.19}$)	0.75 ($0.71^{0.99}_{0.40}$)	0.61 ($0.50^{0.89}_{0.28}$)	0.04	0.30	0.15
Ammonium* ($\mu g\,m^{-3}$)	0.09 ($0.09^{0.12}_{0.05}$)	0.25 ($0.24^{0.35}_{0.13}$)	0.21 ($0.19^{0.31}_{0.09}$)			0.02
Nitrate* ($\mu g\,m^{-3}$)	0.03 ($0.02^{0.04}_{0.01}$)	0.04 ($0.03^{0.05}_{0.02}$)	0.04 ($0.02^{0.05}_{0.01}$)			0.01
Chloride* ($\mu g\,m^{-3}$)	0.01 ($0.00^{0.01}_{0.00}$)	0.01 ($0.01^{0.01}_{0.00}$)	0.01 ($0.01^{0.01}_{0.00}$)			0.00
Absorbance* ($\mu g\,m^{-3}$)	0.19 ($0.16^{0.28}_{0.09}$)	0.21 ($0.17^{0.29}_{0.09}$)	0.22 ($0.18^{0.31}_{0.09}$)			
Hygroscopicity						
GF_{90}* [53 nm]	1.30 ($1.29^{1.34}_{1.27}$)	1.42 ($1.41^{1.45}_{1.36}$)	1.38 ($1.38^{1.43}_{1.32}$)			
GF_{90}* [155 nm]	1.46 ($1.49^{1.52}_{1.41}$)	1.58 ($1.58^{1.62}_{1.53}$)	1.53 ($1.54^{1.60}_{1.46}$)			
SS_{crit}* [63 nm]	0.63 ($0.63^{0.67}_{0.61}$)	0.48 ($0.47^{0.55}_{0.41}$)	0.53 ($0.54^{0.63}_{0.45}$)			
SS_{crit}* [149 nm]	0.26 ($0.25^{0.31}_{0.18}$)	0.20 ($0.17^{0.23}_{0.15}$)	0.22 ($0.20^{0.27}_{0.16}$)			
Gas composition						
CO* (ppbv)	111 (110^{116}_{105})	98.4 ($94.3^{108}_{86.8}$)	101 ($100^{110}_{89.4}$)			
$CHBr_3$* (pptv)	1.10 ($1.13^{1.28}_{0.96}$)	1.61 ($1.56^{1.79}_{1.38}$)	1.48 ($1.45^{1.75}_{1.17}$)			
CH_2Br_2* (pptv)	0.81 ($0.83^{0.85}_{0.80}$)	0.95 ($0.95^{0.99}_{0.91}$)	0.91 ($0.93^{0.98}_{0.85}$)			
CH_3I* (pptv)	1.03 ($1.08^{1.12}_{0.97}$)	1.09 ($1.08^{1.18}_{0.99}$)	1.08 ($1.08^{1.18}_{0.99}$)			
CH_3Br (pptv)	6.73 ($6.68^{7.39}_{6.23}$)	6.92 ($6.90^{7.23}_{6.35}$)	6.80 ($6.69^{7.21}_{6.16}$)			

Particulate nitrate and chloride show very similar time series trends and their mean value maps show their association with marine air. They exhibit a consistent diurnal profile with sharply elevated levels around midnight. Inspection of the AMS mass spectral information shows that the nitrate is unlikely to be present as ammonium nitrate or organic nitrates. The sea is an established source of sodium chloride aerosol, however this is not generally detected due to its slow vapourisation time in the AMS. Nitric acid may be produced by processing of biogenic NO_x from soil (particularly from the fertilised oil palms plantations) and anthropogenic NO_x emissions from settlements on the coast. This nitric acid could displace chloride from marine sodium chloride particles to give aqueous sodium nitrate aerosol that is more efficiently vapourised by the AMS than sodium chloride. It is likely that the liberated chloride is detected in the form of ammonium chloride although it is unclear if this is the case. The nocturnal profile may be caused by the reformation of nitrate and chloride aerosols in nocturnal fog droplets or their likely partitioning to the gas phase as the temperature increases during the day. It may also be associated with sampling of free tropospheric air when the boundary layer dropped below the measurement site, as was observed by LIDAR measurements (Pearson et al., 2010). While loadings of nitrate and chloride are small, they are higher than were measured in Amazonia which is consistent with greater influence of a marine source.

Levels of sulphate and ammonium are much higher than in the AMAZE-08 project in the rainforest of the Central Amazon basin where Chen et al. (2009) performed a similar analysis of sulphate and OA correlation to assess aerosol origin. This led to the classification of "in-basin" and "out-of-basin" influences. 40 % of the AMAZE-08 project was classified as being influenced by in-basin periods which were dominated by (relatively unoxidised) OA (0.5 $\mu g\,m^{-3}$), with

little sulphate influence ($0.04\,\mu g\,m^{-3}$). These were deemed to be influenced mainly by BSOA freshly produced from rainforest VOC emissions. The out-of-basin periods, comprising 30 % of the project, were less dominated by OA ($0.8\,\mu g\,m^{-3}$), which was more oxidised, with more sulphate influence ($0.3\,\mu g\,m^{-3}$). During these periods the measurement site was more influenced by long range transport of emissions from a variety of sources, probably processed DMS emissions from the Atlantic and biomass burning from West Africa. This is in contrast to Borneo which experienced much higher sulphate loadings ($0.61\,\mu g\,m^{-3}$). A study in West Africa measured similarly high levels of sulphate as were observed during OP3, which may be due to the marine influences during the West African monsoon phase.

Organic aerosol is most oxidised in marine air masses. Sulphate was associated with marine air masses and showed varying levels of correlation with organic aerosol. Sulphate unassociated with organic aerosol showed an off-island source and is likely to be mainly from the processing of marine DMS emissions. Air masses travelling over the mountainous interior of Borneo show depressed levels of regional background aerosol which is probably due to greater wet removal by orographically induced convective precipitation. These air masses are also associated with less oxygenated OA, presumably because the removal of regional aerosol increases the relative dominance of BSOA produced close to the measurement site. It should be noted that the sulphate loading in *Terrestrial* air masses (which are most representative of rainforest conditions) is even greater than the out-of-basin classified data from Amazonia. This implies that, while regional aerosol is probably being depleted inland through wet deposition, a significant amount of aerosol is transported across the length of the island. Emissions from agriculture seemed to influence the site with isoprenoid BSOA showing elevated levels over the major oil palm plantations to the north and south of the site, which is consistent with measurements showing oil palm to emit five times as much isoprene as the natural rainforest (Hewitt et al., 2009).

OA associated with sulphate also showed an off-island source and an increased level of oxidation. This is likely to be long range transport of internally mixed aerosol. The sources are likely to be a combination of both anthropogenic and biogenic sources of both OA and sulphate but the OA has aged considerable during transport. It is unclear how much of this background signal is biogenic, anthropogenic or pyrogenic. It is also possible that the organic background may be wholly or in part due to marine biological sources (O'Dowd et al., 2004). A fraction of the OA showed only a weak association with sulphate. This predominantly arose during air periods influenced by on-island air masses and is likely to be biogenic aerosol from processing of VOCs emitted by the rainforest. Emissions from the rainforest in Borneo are likely to be measured at Bukit Atur as relatively fresh aerosol and so would be expected to be represented by OOA2 and 82Fac, plus some fraction of OOA1. Considering only periods influenced by *Terrestrial* air masses, this gives an estimated loading of between 0.23 and $0.52\,\mu g\,m^{-3}$, compared to $0.5\,\mu g\,m^{-3}$ of OA seen in-basin in Amazonia. This lower contribution from the Bornean rainforest is likely to be mainly due to the difference in the size of the source regions.

The beginning of the campaign was dominated by high aerosol loadings, due in particular to sulphate and the organic OOA1 and 82Fac PMF factors. This period was also associated with increased CO, BC, 91Fac and all inorganic species. The MODIS satellite shows this to be a period of enhanced fire activity around the coast of Borneo, particularly on the southwest of the island. The beginning of the measurement period is influenced by coastal air running up the east coast of Borneo. It is likely that the increased biomass burning activity caused the increased CO, BC and 91Fac loadings. It is also likely that processed organic biomass burning emissions contributed to the increased OOA1 loadings. It is possible that some of the sulphate aerosol is from condensation of gases emitted from biomass burning. However, the correlation is not high ($r = 0.45$) between the OOA1 and sulphate time series during POI1 suggesting that, if this is occurring, it is a relatively small contribution. In addition to aerosol emissions from biomass burning, the enhanced inorganic and OOA1 aerosol loadings during POI1 could be due to the dominance of coastal air, a reduction in precipitation causing less wet removal, or an increase in oxidation rates. The latter two could themselves be consequences of biomass burning emissions.

Aerosol hygroscopicity showed marked differences between terrestrial and marine air masses, however the data coverage does not include the period of more intense biomass burning. The most hygroscopic aerosol associated with the same air masses as high ammonium sulphate concentrations. As sulphate aerosol is more hygroscopic than (even highly oxidised) organic aerosol, the sulphate to organic mass ratio would be expected to be the driving factor in the aerosol hygroscopicity.

5 Conclusions

The results are consistent with a regional background of sulphate and aged organic aerosol that is removed by wet deposition in the interior of Borneo. This may be expected on an island, where off-island sources are likely to be distant enough to contribute to an aged background. Seven day air mass trajectories show the site was influenced by the least populated areas with the least amount of detected fires, when compared to the wider region. Given this it is likely that biological sources dominated the regional background.

Both the Marine and Terrestrial clusters had much higher sulphate loadings (0.75 and $0.27\,\mu g\,m^{-3}$, respectively) than were measured in Amazonia ($0.15\,\mu g\,m^{-3}$), which is probably due to a greater marine influence. The rainforest ecosystem has also been reported as a minor source

of sulphur gases (and associated aerosol) in the Amazon (Andreae et al., 1990), but the analysis presented here shows if this is present it is a comparatively minor source, with *Terrestrial* air masses containing 65 % less sulphate than *Marine*.

The sulphate appears to be largely neutralised to ammonium sulphate by time of arrival at the site, probably by terrestrial ammonium. The rainforest and oil palms appear to be sources of BSOA, with an estimated mean concentration of $0.26\,\mu g\,m^{-3}$, however there are no periods where local BSOA dominates as was the case in the AMAZE-08 project. The region is influenced by some level of biomass burning, although, apart from the beginning of the measurement period, this appears to be a relatively minor source. Far field biomass burning emissions may be so aged as to be part of the regional background, however inspection of seven day back trajectories were not associated with areas of particularly high fire activity in the region. There also appears to be a minor influence at night from marine chloride reacting with terrestrial nitrate.

In general Borneo shows a wider range of influences than Amazonia. Despite data coverage lower than other comparable analyses the methods proved useful in assessing the origin of species measured. This study shows that the Amazon, whilst clearly an important part of the biosphere, is not representative of the tropics as a whole. The "maritime continent" region needs to be considered separately from the Amazon, as being a heterogeneous and complex mixture of biogenic, marine and anthropogenic influence.

Supplementary material related to this article is available online at: http://www.atmos-chem-phys.net/11/9605/2011/acp-11-9605-2011-supplement.pdf.

Acknowledgements. Thanks to Gavin McMeeking (Colorado State University) and Mathew Evans (The University of Leeds) for useful conversations in the preparation of this manuscript. Thanks also to Minnie Wong (Fire Information and Resource Management System) for providing archived MODIS fire data. The OP3 project was funded by the UK Natural Environment Research Council [grant number NE/D002117/1]. We thank the Malaysian and Sabah Governments for their permission to conduct research in Malaysia; the Malaysian Meteorological Department (MMD) for access to the Bukit Atur Global Atmosphere Watch station and their long term ozone record; Leong Chow Peng (formerly of MMD) for her support in the early stages of the project; Waidi Sinun of Yayasan Sabah and his staff and Glen Reynolds of the Royal Society's South East Asian Rain Forest Research Programme and his staff for logistical support at the Danum Valley Field Centre; the NERC Facility for Ground-based Atmospheric Measurements and Halo Photonics for support with the LIDAR deployment; Phua Mui How of the University Malaysia Sabah for his help with the land cover map; and the rest of the OP3 project team for their individual and collective efforts. This is paper number 525 of the Royal Society's South East Asian Rainforest Research Programme.

Edited by: R. MacKenzie

References

Alfarra, M. R., Prevot, A. S. H., Szidat, S., Sandradewi, J., Weimer, S., Lanz, V. A., Schreiber, D., Mohr, M., and Baltensperger, U.: Identification of the mass spectral signature of organic aerosols from wood burning emissions, Environ. Sci. Technol., 41, 5770–5777, doi:10.1021/es062289b, 2007.

Allan, J. D., Bower, K. N., Coe, H., Boudries, H., Jayne, J. T., Canagaratna, M. R., Millet, D. B., Goldstein, A., Quinn, P. K., Weber, R. J., and Worsnop, D. R.: Submicron aerosol composition at Trinidad Head, California, during ITCT 2K2: its relationship with gas phase volatile organic carbon and assessment of instrument performance, J. Geophys. Res., 109, D23S24, doi:10.1029/2003JD004208, 2004.

Allan, J. D., Topping, D. O., Good, N., Irwin, M., Flynn, M., Williams, P. I., Coe, H., Baker, A. R., Martino, M., Niedermeier, N., Wiedensohler, A., Lehmann, S., Müller, K., Herrmann, H., and McFiggans, G.: Composition and properties of atmospheric particles in the eastern Atlantic and impacts on gas phase uptake rates, Atmos. Chem. Phys., 9, 9299–9314, doi:10.5194/acp-9-9299-2009, 2009.

Allan, J. D., Williams, P. I., Morgan, W. T., Martin, C. L., Flynn, M. J., Lee, J., Nemitz, E., Phillips, G. J., Gallagher, M. W., and Coe, H.: Contributions from transport, solid fuel burning and cooking to primary organic aerosols in two UK cities, Atmos. Chem. Phys., 10, 647–668, doi:10.5194/acp-10-647-2010, 2010.

Allen, A. G., Oppenheimer, M. F., Baxter, P. J., Horrocks, L. A., Galle, B., McGonigle, A. J. S., and Duffell, H. J.: Primary sulfate aerosol and associated emissions from Masaya Volcano, Nicaragua, J. Geophys. Res., 107, 4682, doi:10.1029/2002JD002120, 2002.

Andreae, M. O., Berresheiem, H., Bingemer, H., Jacob, D. J., Lewis, B. L., Li, S.-M., and Talbot, R. W.: The atmospheric sulfur cycle over the Amazon Basin. II. Wet season, J. Geophys. Res., 95, 16813–16824, doi:10.1029/JD095iD10p16813, 1990.

Ashbaugh, L.: A residence time probability analysis of sulfur concentrations at grand Canyon National Park, Atmos. Environ., 19, 1263–1270, doi:10.1016/0004-6981(85)90256-2, 1985.

Avissar, R., Silva Dias, P., Silva Dias, M., and Nobre, C. A.: The Large-Scale Biosphere-Atmosphere Experiment in Amazonia (LBA): insights and future research needs, J. Geophys. Res., 107, 8086, doi:10.1029/2002JD002704, 2002.

British Atmospheric Data Centre: European Centre for Medium-Range Weather Forecasts back trajectories, http://badc.nerc.ac.uk/data/ecmwf-op/ (last access: January 2010), 2006a.

British Atmospheric Data Centre: European Centre for Medium-Range Weather Forecasts. ECMWF Operational Analysis data, http://badc.nerc.ac.uk/view/badc.nerc.ac.uk_ATOM_dataent_ECMWF-OP (last access: October 2010), 2006b.

Baker, J.: Emissions of CH_3Br, organochlorines, and organoiodines from temperate macroalgae, Glob. Change Sci., 3, 93–106, doi:10.1016/S1465-9972(00)00021-0, 2001.

Bassford, M. R., Nickless, G., Simmonds, P. G., Lewis, A. C., Pilling, M. J., and Evans, M. J.: The concurrent observation of methyl iodide and dimethyl sulphide in marine air; implications for sources of atmospheric methyl iodide, Atmos. Environ., 33, 2373–2383, doi:10.1016/S1352-2310(98)00403-8, 1999.

Bates, T. S., Calhoun, J. A., and Quinn, P. K.: Variations in the methanesulfonate to sulfate molar ratio in submicrometer marine

aerosol particles over the South Pacific Ocean, J. Geophys. Res., 95, 813–816, 1992.

Bell, N., Hsu, L., Jacob, M., Schultz, M. G., Blake, D. R., Butler, J. H., King, D. B., Lobert, J. M., and Maier-Reimer, E.: Methyl iodide: atmospheric budget and use as a tracer of marine convection in global models, J. Geophys. Res., 107, 4340, doi:10.1029/2001JD001151, 2002.

Blei, E., Hardacre, C. J., Mills, G. P., Heal, K. V., and Heal, M. R.: Identification and quantification of methyl halide sources in a lowland tropical rainforest, Atmos. Environ., 44, 1005–1010, doi:10.1016/j.atmosenv.2009.12.023, 2010.

Butler, J. H., King, D. B., Lobert, J. M., Montzka, S. A., Yvon-Lewis, S. A., Hall, B. D., Warwick, N. J., Mondeel, D. J., Aydin, M., and Elkins, J. W.: Oceanic distributions and emissions of short-lived halocarbons, Global Biogeochem. Cy., 21, GB1023, doi:10.1029/2006GB002732, 2007.

Canagaratna, M. R., Jayne, J. T., Jimenez, J. L., Allan, J. D., Alfarra, M. R., Zhang, Q., Onasch, T. B., Drewnick, F., Coe, H., Middlebrook, A., Delia, A., Williams, L. R., Trimborn, A. M., Northway, M. J., DeCarlo, P. F., Kolb, C. E., Davidovits, P., and Worsnop, D. R.: Chemical and microphysical characterization of ambient aerosols with the aerodyne aerosol mass spectrometer., Mass Spectrom. Rev., 26, 185–222, doi:10.1002/mas.20115, 2007.

Capaldo, K., Corbett, J. J., Kasibhatla, P., Fischbeck, P., and Pandis, S. N.: Effects of ship emissions on sulphur cycling and radiative climate forcing over the ocean, Nature, 400, 743–746, doi:10.1038/23438, 1999.

Cape, J. N., Methven, J., and Hudson, L. E.: The use of trajectory cluster analysis to interpret trace gas measurements at Mace Head, Ireland, Atmos. Environ., 34, 3651–3663, doi:10.1016/S1352-2310(00)00098-4, 2000.

Capes, G., Johnson, B., McFiggans, G., Williams, P. I., Haywood, J., and Coe, H.: Aging of biomass burning aerosols over West Africa: aircraft measurements of chemical composition, microphysical properties, and emission ratios, J. Geophys. Res., 113, D00C15, doi:10.1029/2008JD009845, 2008.

Capes, G., Murphy, J. G., Reeves, C. E., McQuaid, J. B., Hamilton, J. F., Hopkins, J. R., Crosier, J., Williams, P. I., and Coe, H.: Secondary organic aerosol from biogenic VOCs over West Africa during AMMA, Atmos. Chem. Phys., 9, 3841–3850, doi:10.5194/acp-9-3841-2009, 2009.

Carpenter, L. J. and Liss, P. S.: On temperate sources of bromoform and other reactive organic bromine gases, J. Geophys. Res., 105, 20539–20547, doi:10.1029/2000JD900242, 2000.

Carter, C., Finley, W., Fry, J., Jackson, D., and Willis, L.: Palm oil markets and future supply, Eur. J. Lipid Science Technol., 109, 307–314, doi:10.1002/ejlt.200600256, 2007.

Chan, M. N., Surratt, J. D., Claeys, M., Edgerton, E. S., Tanner, R. L., Shaw, S. L., Zheng, M., Knipping, E. M., Eddingsaas, N. C., Wennberg, P. O., and Seinfeld, J. H.: Characterization and quantification of isoprene-derived epoxydiols in ambient aerosol in the Southeastern United States, Environ. Sci. Technol., 44, 4590–4596, 2010.

Chen, Q., Farmer, D. K., Schneider, J., Zorn, S. R., Heald, C. L., Karl, T. G., Guenther, A., Allan, J. D., Robinson, N., Coe, H., Kimmel, J. R., Pauliquevis, T., Borrmann, S., Pöschl, U., Andreae, M. O., Artaxo, P., Jimenez, J. L., and Martin, S. T.: Mass spectral characterization of submicron biogenic organic particles in the Amazon Basin, Geophys. Res. Lett., 36, L20806, doi:10.1029/2009GL039880, 2009.

Cheung, Y. K., and Klot, J. H.: The Mann Whitney Wilcoxon Distribution Using Linked Lists, Statistica Sinica, 7, 805-813, , 1997.

Claeys, M., Graham, B., Vas, G., Wang, W., Vermeylen, R., Pashynska, V., Cafmeyer, J., Guyon, P., Andreae, M. O., Artaxo, P., and Maenhaut, W.: Formation of secondary organic aerosols through photooxidation of isoprene, Science, 303(5661), 1173–1176, doi:10.1126/science.1092805, 2004.

Cox, M. L., Sturrock, G. A., Fraser, P. J., Siems, S. T., and Krummel, P. B.: Identification of regional sources of methyl bromide and methyl iodide from AGAGE observations at Cape Grim, Tasmania, J. Atmos. Chem., 50, 59–77, doi:10.1007/s10874-005-2434-5, 2005.

Cross, E., Slowik, J., Davidovits, P., Allan, J., Worsnop, D., Jayne, J., Lewis, D., Canagaratna, M., and Onasch, T.: Laboratory and ambient particle density determinations using light scattering in conjunction with aerosol mass spectrometry, Aerosol Sci. Technol., 41, 343–359, doi:10.1080/02786820701199736, 2007.

Cubison, M., Coe, H., and Gysel, M.: A modified hygroscopic tandem DMA and a data retrieval method based on optimal estimation, J. Aerosol Sci., 36, 846–865, doi:10.1016/j.jaerosci.2004.11.009, 2005.

Davies, D. K., Ilavajhala, S., Wong, M. M., and Justice, C. O.: Fire information for resource management system: archiving and distributing MODIS active fire data, IEEE Trans. Geosci. Remote S., 47, 72–79, doi:10.1109/TGRS.2008.2002076, 2009.

DeCarlo, P. F., Kimmel, J. R., Trimborn, A., Northway, M. J., Jayne, J. T., Aiken, A. C., Gonin, M., Fuhrer, K., Horvath, T., Docherty, K. S., Worsnop, D. R., and Jimenez, J. L.: Field-deployable, high-resolution, time-of-flight aerosol mass spectrometer, Anal. Chem., 78, 8281–8289, 2006.

Denman, K., Brasseur, G., Chidthaisong, A., Ciais, P., Cox, P., Dickinson, R., Hauglustaine, D., Heinze, C., Holland, E., Jacob, D., Lohmann, U., Ramachandran, S., Dias, P. D. S., Wofsy, S., and Zhang, X.: Couplings Between Changes in the Climate System and Biogeochemistry, Chap. Couplings, Cambridge University Press, Cambridge, UK and New York, NY, USA, 2007.

Facchini, M. C., Decesari, S., Rinaldi, M., Carbone, C., Finessi, E., Mircea, M., Fuzzi, S., Moretti, F., Tagliavini, E., Ceburnis, D., and O'Dowd, C. D.: Important source of marine secondary organic aerosol from biogenic amines, Environ. Sci. Technol., 42, 9116–9121, doi:10.1021/es8018385, 2008.

Farmer, D. K., Matsunaga, A., Docherty, K. S., Surratt, J. D., Seinfeld, J. H., Ziemann, P. J., and Jimenez, J. L.: Response of an aerosol mass spectrometer to organonitrates and organosulfates and implications for atmospheric chemistry, P. Natl. Acad. Sci. USA, 107, 6670–6675, doi:10.1073/pnas.0912340107, 2010.

Food and Agriculture Organisation: Global Forest Resources Assessment 2010: Main Report, Bernan Assoc, Rome, http://books.google.com/books?id=vEcJTwEACAAJ\&pgis=1 (last access: January 2011), 2010.

Froyd, K. D., Murphy, S. M., Murphy, D. M., de Gouw, J. A., Eddingsaas, N. C., and Wennberg, P. O.: Contribution of isoprene-derived organosulfates to free tropospheric aerosol mass., P. Natl. Acad. Sci. USA, 107, 21360–21365,

doi:10.1073/pnas.1012561107, 2010.

Gao, S., Hegg, D. A., Hobbs, P. V., Kirchstetter, T. W., Magi, B. I., and Sadilek, M.: Water-soluble organic components in aerosols associated with savanna fires in Southern Africa: identification, evolution, and distribution, J. Geophys. Res., 108, 8491, doi:10.1029/2002JD002324, 2003.

Gerbig, C., Schmitgen, S., Kley, D., Volz-Thomas, A., Dewey, K., and Haaks, D.: An improved fast-response vacuum-UV resonance fluorescence CO instrument, J. Geophys. Res., 104, 1699–1704, doi:10.1029/1998JD100031, 1999.

Giglio, L.: An enhanced contextual fire detection algorithm for MODIS, Remote Sens. Environ., 87, 273–282, doi:10.1016/S0034-4257(03)00184-6, 2003.

Gondwe, M.: The contribution of ocean-leaving DMS to the global atmospheric burdens of DMS, MSA, SO_2, and NSS $SO_4^=$, Global Biogeochem. Cy., 17, 1056, doi:10.1029/2002GB001937, 2003.

Good, N., Topping, D. O., Allan, J. D., Flynn, M., Fuentes, E., Irwin, M., Williams, P. I., Coe, H., and McFiggans, G.: Consistency between parameterisations of aerosol hygroscopicity and CCN activity during the RHaMBLe discovery cruise, Atmos. Chem. Phys., 10, 3189–3203, doi:10.5194/acp-10-3189-2010, 2010a.

Good, N., Topping, D. O., Duplissy, J., Gysel, M., Meyer, N. K., Metzger, A., Turner, S. F., Baltensperger, U., Ristovski, Z., Weingartner, E., Coe, H., and McFiggans, G.: Widening the gap between measurement and modelling of secondary organic aerosol properties?, Atmos. Chem. Phys., 10, 2577–2593, doi:10.5194/acp-10-2577-2010, 2010b.

Goodwin, K. D., North, W. J., and Lidstrom, M. E.: Production of bromoform and dibromomethane by giant kelp: factors affecting release and comparison to anthropogenic bromine sources, Limnol. Oceanogr., 42, 1725–1734, 1997.

Graf, H.-F., Feichter, J., and Langmann, B.: Volcanic sulfur emissions: estimates of source strength and its contribution to the global sulfate distribution, J. Geophys. Res., 102, 10727–10738, doi:10.1029/96JD03265, 1997.

Gysel, M., McFiggans, G., and Coe, H.: Inversion of tandem differential mobility analyser (TDMA) measurements, J. Aerosol Sci., 40, 134–151, doi:10.1016/j.jaerosci.2008.07.013, 2009.

Hewitt, C. N., MacKenzie, A. R., Di Carlo, P., Di Marco, C. F., Dorsey, J. R., Evans, M., Fowler, D., Gallagher, M. W., Hopkins, J. R., Jones, C. E., Langford, B., Lee, J. D., Lewis, A. C., Lim, S. F., McQuaid, J., Misztal, P., Moller, S. J., Monks, P. S., Nemitz, E., Oram, D. E., Owen, S. M., Phillips, G. J., Pugh, T. A. M., Pyle, J. A., Reeves, C. E., Ryder, J., Siong, J., Skiba, U., and Stewart, D. J.: Nitrogen management is essential to prevent tropical oil palm plantations from causing ground-level ozone pollution., P. Natl. Acad. Sci. USA, 106, 18447–18451, doi:10.1073/pnas.0907541106, 2009.

Hewitt, C. N., Lee, J. D., MacKenzie, A. R., Barkley, M. P., Carslaw, N., Carver, G. D., Chappell, N. A., Coe, H., Collier, C., Commane, R., Davies, F., Davison, B., DiCarlo, P., Di Marco, C. F., Dorsey, J. R., Edwards, P. M., Evans, M. J., Fowler, D., Furneaux, K. L., Gallagher, M., Guenther, A., Heard, D. E., Helfter, C., Hopkins, J., Ingham, T., Irwin, M., Jones, C., Karunaharan, A., Langford, B., Lewis, A. C., Lim, S. F., MacDonald, S. M., Mahajan, A. S., Malpass, S., McFiggans, G., Mills, G., Misztal, P., Moller, S., Monks, P. S., Nemitz, E., Nicolas-Perea, V., Oetjen, H., Oram, D. E., Palmer, P. I., Phillips, G. J., Pike, R., Plane, J. M. C., Pugh, T., Pyle, J. A., Reeves, C. E., Robinson, N. H., Stewart, D., Stone, D., Whalley, L. K., and Yin, X.: Overview: oxidant and particle photochemical processes above a south-east Asian tropical rainforest (the OP3 project): introduction, rationale, location characteristics and tools, Atmos. Chem. Phys., 10, 169–199, doi:10.5194/acp-10-169-2010, 2010.

International Fuel Quality Center: International Desil Rankings – Top 100 Sulphur, http://www.ifqc.org/UserFiles/file/Misc/DieselRankings0909(1).pdf, (last access: April 2010), 2009.

Irwin, M., Good, N., Crosier, J., Choularton, T. W., and McFiggans, G.: Reconciliation of measurements of hygroscopic growth and critical supersaturation of aerosol particles in central Germany, Atmos. Chem. Phys., 10, 11737–11752, doi:10.5194/acp-10-11737-2010, 2010.

Irwin, M., Robinson, N., Allan, J. D., Coe, H., and McFiggans, G.: Size-resolved aerosol water uptake and cloud condensation nuclei measurements as measured above a Southeast Asian rainforest during OP3, Atmos. Chem. Phys. Discuss., 11, 3117–3159, doi:10.5194/acpd-11-3117-2011, 2011.

Jimenez, J. L., Canagaratna, M. R., Donahue, N. M., Prevot, A. S. H., Zhang, Q., Kroll, J. H., DeCarlo, P. F., Allan, J. D., Coe, H., Ng, N. L., Aiken, A. C., Docherty, K. S., Ulbrich, I. M., Grieshop, A. P., Robinson, A. L., Duplissy, J., Smith, J. D., Wilson, K. R., Lanz, V. A., Hueglin, C., Sun, Y. L., Tian, J., Laaksonen, A., Raatikainen, T., Rautiainen, J., Vaattovaara, P., Ehn, M., Kulmala, M., Tomlinson, J. M., Collins, D. R., Cubison, M. J., Dunlea, E. J., Huffman, J. A., Onasch, T. B., Alfarra, M. R., Williams, P. I., Bower, K. N., Kondo, Y., Schneider, J., Drewnick, F., Borrmann, S., Weimer, S., Demerjian, K., Salcedo, D., Cottrell, L., Griffin, R., Takami, A., Miyoshi, T., Hatakeyama, S., Shimono, A., Sun, J. Y., Zhang, Y. M., Dzepina, K., Kimmel, J. R., Sueper, D., Jayne, J. T., Herndon, S. C., Trimborn, A. M., Williams, L. R., Wood, E. C., Middlebrook, A. M., Kolb, C. E., Baltensperger, U., and Worsnop, D. R.: Evolution of organic aerosols in the atmosphere, Science, 326, 1525–1529, doi:10.1126/science.1180353, 2009.

Jordan, T., Seen, A., and Jacobsen, G.: Levoglucosan as an atmospheric tracer for woodsmoke, Atmos. Environ., 40, 5316–5321, doi:10.1016/j.atmosenv.2006.03.023, 2006.

Justice, C., Giglio, L., Korontzi, S., Owens, J., Morisette, J., Roy, D., Descloitres, J., Alleaume, S., Petitcolin, F., and Kaufman, Y.: The MODIS fire products, Remote Sens. Environ., 83, 244–262, 2002.

Kalkstein, L. S., Tan, G., and Skindlov, J. A.: An evaluation of three clustering procedures for use in synoptic climatological classification, J. Appl. Meteorol., 26, 717–730, 1987.

Kleindienst, T. E., Lewandowski, M., Offenberg, J. H., Jaoui, M., and Edney, E. O.: The formation of secondary organic aerosol from the isoprene + OH reaction in the absence of NO_x, Atmos. Chem. Phys., 9, 6541–6558, doi:10.5194/acp-9-6541-2009, 2009.

Kloster, S., Feichter, J., Maier-Reimer, E., Six, K. D., Stier, P., and Wetzel, P.: DMS cycle in the marine ocean-atmosphere system – a global model study, Biogeosciences, 3, 29–51, doi:10.5194/bg-3-29-2006, 2006.

Koch, D., Schulz, M., Kinne, S., McNaughton, C., Spackman, J. R., Balkanski, Y., Bauer, S., Berntsen, T., Bond, T. C., Boucher, O., Chin, M., Clarke, A., De Luca, N., Dentener, F., Diehl, T.,

Dubovik, O., Easter, R., Fahey, D. W., Feichter, J., Fillmore, D., Freitag, S., Ghan, S., Ginoux, P., Gong, S., Horowitz, L., Iversen, T., Kirkevåg, A., Klimont, Z., Kondo, Y., Krol, M., Liu, X., Miller, R., Montanaro, V., Moteki, N., Myhre, G., Penner, J. E., Perlwitz, J., Pitari, G., Reddy, S., Sahu, L., Sakamoto, H., Schuster, G., Schwarz, J. P., Seland, Ø., Stier, P., Takegawa, N., Takemura, T., Textor, C., van Aardenne, J. A., and Zhao, Y.: Evaluation of black carbon estimations in global aerosol models, Atmos. Chem. Phys., 9, 9001–9026, doi:10.5194/acp-9-9001-2009, 2009.

Laboratory Earth Systems Research Global Monitoring Division: NOAA Calibration Scales for Various Trace Gases, http://www.esrl.noaa.gov/gmd/ccl/scales.html (last access: August 2008), 2008.

Lance, S., Medina, J., Smith, J. N., and Nenes, A.: Mapping the operation of the DMT continuous flow CCN counter, Aerosol Sci. Technol., 40, 242–254, 2006.

Lanz, V. A., Alfarra, M. R., Baltensperger, U., Buchmann, B., Hueglin, C., and Prévôt, A. S. H.: Source apportionment of submicron organic aerosols at an urban site by factor analytical modelling of aerosol mass spectra, Atmos. Chem. Phys., 7, 1503–1522, doi:10.5194/acp-7-1503-2007, 2007.

Lebel, T., Parker, D. J., Flamant, C., Bourlès, B., Marticorena, B., Mougin, E., Peugeot, C., Diedhiou, A., Haywood, J. M., Ngamini, J. B., Polcher, J., Redelsperger, J.-L., and Thorncroft, C. D.: The AMMA field campaigns: multiscale and multidisciplinary observations in the West African region, Q. J. Roy. Meteor. Soc., 136, 8–33, doi:10.1002/qj.486, 2010.

Lim, Y. B. and Ziemann, P. J.: Kinetics of the heterogeneous conversion of 1,4-hydroxycarbonyls to cyclic hemiacetals and dihydrofurans on organic aerosol particles., Phys. Chem. Chem. Phys., 11, 8029–8039, doi:10.1039/b904333k, 2009.

Manley, S. L., Goodwin, K., and North, W. J.: Laboratory production of bromoform, methylene bromide, and methyl iodide by macroalgae and distribution in nearshore Southern California waters, Limnol. Oceanogr., 37, 1652–1659, 1992.

Martin, S. T., Andreae, M. O., Althausen, D., Artaxo, P., Baars, H., Borrmann, S., Chen, Q., Farmer, D. K., Guenther, A., Gunthe, S. S., Jimenez, J. L., Karl, T., Longo, K., Manzi, A., Müller, T., Pauliquevis, T., Petters, M. D., Prenni, A. J., Pöschl, U., Rizzo, L. V., Schneider, J., Smith, J. N., Swietlicki, E., Tota, J., Wang, J., Wiedensohler, A., and Zorn, S. R.: An overview of the Amazonian Aerosol Characterization Experiment 2008 (AMAZE-08), Atmos. Chem. Phys., 10, 11415–11438, doi:10.5194/acp-10-11415-2010, 2010.

Matthew, B., Middlebrook, A., and Onasch, T.: Collection efficiencies in an aerodyne aerosol mass spectrometer as a function of particle phase for laboratory generated aerosols, Aerosol Sci. Technol., 42, 884–898, doi:10.1080/02786820802356797, 2008.

McFiggans, G., Alfarra, M. R., Allan, J., Bower, K., Coe, H., Cubison, M., Topping, D., Williams, P., Decesari, S., Facchini, C., and Fuzzi, S.: Simplification of the representation of the organic component of atmospheric particulates, Faraday Discuss., 130, 341, 341–362, doi:10.1039/b419435g, 2005.

McMorrow, J. and Talip, M. A.: Decline of forest area in Sabah, Malaysia: relationship to state policies, land code and land capability, Global Environ. Change, 11, 217–230, doi:10.1016/S0959-3780(00)00059-5, 2001.

Mead, M., Khan, M., White, I., Nickless, G., and Shallcross, D.: Methyl halide emission estimates from domestic biomass burning in Africa, Atmos. Environ., 42, 5241–5250, doi:10.1016/j.atmosenv.2008.02.066, 2008.

Millero, F. J.: The physical chemistry of seawater, Annu. Rev. Earth Planet. Sci., 2, 101–150, doi:10.1146/annurev.ea.02.050174.000533, 1974.

Morgan, W. T., Allan, J. D., Bower, K. N., Capes, G., Crosier, J., Williams, P. I., and Coe, H.: Vertical distribution of sub-micron aerosol chemical composition from North-Western Europe and the North-East Atlantic, Atmos. Chem. Phys., 9, 5389–5401, doi:10.5194/acp-9-5389-2009, 2009.

Morgan, W. T., Allan, J. D., Bower, K. N., Highwood, E. J., Liu, D., McMeeking, G. R., Northway, M. J., Williams, P. I., Krejci, R., and Coe, H.: Airborne measurements of the spatial distribution of aerosol chemical composition across Europe and evolution of the organic fraction, Atmos. Chem. Phys., 10, 4065–4083, doi:10.5194/acp-10-4065-2010, 2010.

Ng, N. L., Canagaratna, M. R., Zhang, Q., Jimenez, J. L., Tian, J., Ulbrich, I. M., Kroll, J. H., Docherty, K. S., Chhabra, P. S., Bahreini, R., Murphy, S. M., Seinfeld, J. H., Hildebrandt, L., Donahue, N. M., DeCarlo, P. F., Lanz, V. A., Prévôt, A. S. H., Dinar, E., Rudich, Y., and Worsnop, D. R.: Organic aerosol components observed in Northern Hemispheric datasets from Aerosol Mass Spectrometry, Atmos. Chem. Phys., 10, 4625–4641, doi:10.5194/acp-10-4625-2010, 2010.

Newton, H. M., Reeves, C. E., Mills, G. P., and Oram D. E.: Organohalogens in and above the rainforest of Borneo, to be submitted to Atmos. Chem. Phys., 2011.

Novakov, T., Corrigan, C., Penner, J., Chuang, C., Rosaria, O., and Bracero, O. M.: Organic aerosols in the Caribbean trade winds: a natural source?, J. Geophys. Res.-Atmos., 102, 21307–21313, 1997.

O'Dowd, C. D., Facchini, M. C., Cavalli, F., Ceburnis, D., Mircea, M., Decesari, S., Fuzzi, S., Yoon, Y. J., and Putaud, J.-P.: Biogenically driven organic contribution to marine aerosol, Nature, 431, 676–680, 2004.

Paatero, P.: Least squares formulation of robust non-negative factor analysis, Chemometr. Intell. Lab., 37, 23–35, doi:10.1016/S0169-7439(96)00044-5, 1997.

Paatero, P. and Tapper, U.: Positive matrix factorization: a non-negative factor model with optimal utilization of error estimates of data values, Environmetrics, 5, 111–126, doi:10.1002/env.3170050203, 1994.

Pandis, S. N., Wexler, A. S., and Seinfeld, J. H.: Dynamics of tropospheric aerosols, J. Phys. Chem., 99, 9646–9659, doi:10.1021/j100024a003, 1995.

Paulot, F., Crounse, J. D., Kjaergaard, H. G., Kürten, A., St. Clair, J. M., Seinfeld, J. H., and Wennberg, P. O.: Unexpected epoxide formation in the gas-phase photooxidation of isoprene., Science, 325, 730–733, doi:10.1126/science.1172910, 2009.

Pearson, G., Davies, F., and Collier, C.: Remote sensing of the tropical rain forest boundary layer using pulsed Doppler lidar, Atmos. Chem. Phys., 10, 5891–5901, doi:10.5194/acp-10-5891-2010, 2010.

Petters, M. D. and Kreidenweis, S. M.: A single parameter representation of hygroscopic growth and cloud condensation nucleus activity, Atmos. Chem. Phys., 7, 1961–1971, doi:10.5194/acp-7-1961-2007, 2007.

Petzold, A. and Schonlinner, M.: Multi-angle absorption photome-

ter – a new method for the measurement of aerosol light absorption and atmospheric black carbon, J. Aerosol Sci., 35, 421–441, doi:10.1016/j.jaerosci.2003.09.005, 2004.

Quack, B., Peeken, I., Petrick, G., and Nachtigall, K.: Oceanic distribution and sources of bromoform and dibromomethane in the Mauritanian upwelling, J. Geophys. Res., 112, C10006, doi:10.1029/2006JC003803, 2007.

Reeves, C. E.: Atmospheric budget implications of the temporal and spatial trends in methyl bromide concentration, J. Geophys. Res., 108, 4343, doi:10.1029/2002JD002943, 2003.

Roberts, G. and Nenes, A.: A continuous-flow streamwise thermal-gradient CCN chamber for atmospheric measurements, Aerosol Sci. Technol., 39, 206–221, doi:10.1080/027868290913988, 2005.

Robinson, N. H., Hamilton, J. F., Allan, J. D., Langford, B., Oram, D. E., Chen, Q., Docherty, K., Farmer, D. K., Jimenez, J. L., Ward, M. W., Hewitt, C. N., Barley, M. H., Jenkin, M. E., Rickard, A. R., Martin, S. T., McFiggans, G., and Coe, H.: Evidence for a significant proportion of Secondary Organic Aerosol from isoprene above a maritime tropical forest, Atmos. Chem. Phys., 11, 1039–1050, doi:10.5194/acp-11-1039-2011, 2011.

Rollins, A. W., Fry, J. L., Hunter, J. F., Kroll, J. H., Worsnop, D. R., Singaram, S. W., and Cohen, R. C.: Elemental analysis of aerosol organic nitrates with electron ionization high-resolution mass spectrometry, Atmos. Meas. Tech., 3, 301–310, doi:10.5194/amt-3-301-2010, 2010.

Simoneit, B., Schauer, J. J., Nolte, C. G., Oros, D. R., Elias, V. O., Fraser, M. P., Rogge, W. F., and Cass, G. R.: Levoglucosan, a tracer for cellulose in biomass burning and atmospheric particles, Atmos. Environ., 33, 173–182, doi:10.1016/S1352-2310(98)00145-9, 1999.

Sive, B. C., Varner, R. K., Mao, H., Blake, D. R., Wingenter, O. W., and Talbot, R.: A large terrestrial source of methyl iodide, Geophys. Res. Lett., 34, L17808, doi:10.1029/2007GL030528, 2007.

Slowik, J. G., Brook, J., Chang, R. Y.-W., Evans, G. J., Hayden, K., Jeong, C.-H., Li, S.-M., Liggio, J., Liu, P. S. K., McGuire, M., Mihele, C., Sjostedt, S., Vlasenko, A., and Abbatt, J. P. D.: Photochemical processing of organic aerosol at nearby continental sites: contrast between urban plumes and regional aerosol, Atmos. Chem. Phys., 11, 2991–3006, doi:10.5194/acp-11-2991-2011, 2011.

Smythe-Wright, D., Boswell, S. M., Breithaupt, P., Davidson, R. D., Dimmer, C. H., and Eiras Diaz, L. B.: Methyl iodide production in the ocean: implications for climate change, Global Biogeochem. Cy., 20, GB3003, doi:10.1029/2005GB002642, 2006.

Surratt, J. D., Murphy, S. M., Kroll, J. H., Ng, N. L., Hildebrandt, L., Sorooshian, A., Szmigielski, R., Vermeylen, R., Maenhaut, W., Claeys, M., Flagan, R. C., and Seinfeld, J. H.: Chemical composition of secondary organic aerosol formed from the photooxidation of isoprene, J. Phys. Chem. A, 110, 9665–9690, 2006.

Surratt, J. D., Gomez-Gonzalez, Y., Chan, A. W. H., Vermeylen, R., Shahgholi, M., Kleindienst, T. E., Edney, E. O., Offenberg, J. H., Lewandowski, M., Jaoui, M., Maenhaut, W., Claeys, M., Flagan, R. C., and Seinfeld, J. H.: Organosulfate formation in biogenic secondary organic aerosol, J. Phys. Chem. A, 112, 8345–8378, doi:10.1021/jp802310p, 2008.

Surratt, J. D., Chan, A. W. H., Eddingsaas, N. C., Chan, M., Loza, C. L., Kwan, A. J., Hersey, S. P., Flagan, R. C., Wennberg, P. O., and Seinfeld, J. H.: Atmospheric chemistry special feature: reactive intermediates revealed in secondary organic aerosol formation from isoprene., P. Natl. Acad. Sci. USA, 15, 6640–6645, doi:10.1073/pnas.0911114107, 2010.

Swietlicki, E., Hansson, H.-C., Hameri, K., Svenningsson, B., Massling, A., McFiggans, G., McMurry, P. H., Petaja, T., Tunved, P., Gysel, M., Topping, D., Weingartner, E., Baltensperger, U., Rissler, J., Wiedensohler, A., and Kulmala, M.: Hygroscopic properties of submicrometer atmospheric aerosol particles measured with H-TDMA instruments in various environments – a review, Tellus B, 60, 432–469, doi:10.1111/j.1600-0889.2008.00350.x, 2008.

Tsai, I.-C., Chen, J.-P., Lin, P.-Y., Wang, W.-C., and Isaksen, I. S. A.: Sulfur cycle and sulfate radiative forcing simulated from a coupled global climate-chemistry model, Atmos. Chem. Phys., 10, 3693–3709, doi:10.5194/acp-10-3693-2010, 2010.

Ulbrich, I. M., Canagaratna, M. R., Zhang, Q., Worsnop, D. R., and Jimenez, J. L.: Interpretation of organic components from Positive Matrix Factorization of aerosol mass spectrometric data, Atmos. Chem. Phys., 9, 2891–2918, doi:10.5194/acp-9-2891-2009, 2009.

Venzke, E., Wunderman, R. W., McClelland, L., Simkin, T., Luhr, J. F., Siebert, L., and Mayberry, G. (Eds.): Global Volcanism, 1968 to the Present, Smithsonian Institution, Global Volcanism Program Digital Information Series, GVP-4, http://www.volcano.si.edu/reports/ (last access: February 2009), 2010.

Williams, I., Gallagher, M. W., Choularton, T. W., Coe, H., Bower, K. N., and McFiggans, G.: Aerosol development and interaction in an urban plume, Aerosol Sci. Technol., 32, 120–126, doi:10.1080/027868200303821, 2000.

Williams, P. I., McFiggans, G., and Gallagher, M. W.: Latitudinal aerosol size distribution variation in the Eastern Atlantic Ocean measured aboard the FS-Polarstern, Atmos. Chem. Phys., 7, 2563–2573, doi:10.5194/acp-7-2563-2007, 2007.

Winklmayr, W., Reischl, G. P., Lindner, A. O., and Berner, A.: A new electromobility spectrometer for the measurement of aerosol size distributions in the size range from 1 to 1000 nm, J. Aerosol Sci., 22, 289–296, 1991.

Worton, D. R., Mills, G. P., Oram, D. E., and Sturges, W. T.: Gas chromatography negative ion chemical ionization mass spectrometry: application to the detection of alkyl nitrates and halocarbons in the atmosphere, J. Chromatogr. A, 1201, 112–119, 2008.

Yokouchi, Y., Hasebe, F., Fujiwara, M., Takashima, H., Shiotani, M., Nishi, N., Kanaya, Y., Hashimoto, S., Fraser, P., Toom-Sauntry, D., Mukai, H., and Nojiri, Y.: Correlations and emission ratios among bromoform, dibromochloromethane, and dibromomethane in the atmosphere, J. Geophys. Res., 110, D23309, doi:10.1029/2005JD006303, 2005.

Zhang, Q., Jimenez, J. L., Canagaratna, M. R., Allan, J. D., Coe, H., Ulbrich, I., Alfarra, M. R., Takami, A., Middlebrook, A. M., Sun, Y. L., Dzepina, K., Dunlea, E., Docherty, K., DeCarlo, P. F., Salcedo, D., Onasch, T. B., Jayne, J. T., Miyoshi, T., Shimono, A., Hatakeyama, S., Takegawa, N., Kondo, Y., Schneider, J., Drewnick, F., Borrmann, S., Weimer, S., Demerjian, K., Williams, P., Bower, K. N., Bahreini, R., Cottrell, L., Griffin, R. J., Rautiainen, J., Sun, J. Y., Zhang, Y. M., and Worsnop, D. R.: Ubiquity and dominance of oxygenated species in organic aerosols in anthropogenically-influenced Northern

Hemisphere midlatitudes, Geophys. Res. Lett., 34, 101029, doi:10.1029/2007GL029979, 2007.

Zhou, Y., Mao, H., Russo, R. S., Blake, D. R., Wingenter, O. W., Haase, K. B., Ambrose, J., Varner, R. K., Talbot, R., and Sive, B. C.: Bromoform and dibromomethane measurements in the seacoast region of New Hampshire, 2002–2004, J. Geophys. Res., 113, D08305, doi:10.1029/2007JD009103, 2008.

Zorn, S. R., Drewnick, F., Schott, M., Hoffmann, T., and Borrmann, S.: Characterization of the South Atlantic marine boundary layer aerosol using an aerodyne aerosol mass spectrometer, Atmos. Chem. Phys., 8, 4711–4728, doi:10.5194/acp-8-4711-2008, 2008.

4.3 Paper II: The elevation of Western Pacific regional aerosol by island thermodynamics as observed around Borneo

N. H. Robinson, J. D. Allan, G. Allen and H. Coe

Published September 2011

Supporting Material reproduced in Appendix C

Overview

An assessment of the effect transport of air mass over Borneo has on regional aerosol was performed by inspecting aircraft aerosol composition profiles in the context of atmospheric thermodynamic data. Profiles were performed upwind over the ocean, in East Sabah over the ground site and oil palm plantations, and downwind during take-off and landing at the airport on the west coast. It was found that the upwind aerosol population was confined to a shallow marine boundary layer. As the air mass advected over East Sabah it appears that it is lofted above the well mixed surface layer, identifiable from inspection of tephigrams. As the day progresses, this lofted layer progresses from being sulphate dominated to also having a significant organic aerosol population. This is likely to be due to the photochemical production of SOA from processing of both rainforest and oil palm VOC emissions, providing evidence that the upper troposphere is influenced by island sources. By the time of arrival on the west coast of Borneo, the lofted aerosol is often dominated by organic aerosol.

These are the first reported vertical profile aerosol measurements in South East Asia. The change in altitude relative to cloud cover has implications for the direct, indirect and semi-direct aerosol climate effects. It also has implications for the atmospheric lifetime of these aerosol as they are more likely to be above precipitation that would otherwise remove them through wet deposition, extending their atmospheric lifetime, and therefore their time averaged radiative effects. This paper provides evidence that the long chain of islands stretching from continental South East Asia to Australia may provide a significant regional source of aerosol to the free troposphere.

Contributions of authors

Allan assisted with performing measurements, interpretation of the data and preparation of the manuscript. Allen prepared the synoptic charts and tephigrams, assisted with interpretation of the data and preparation of the manuscript including writing some text interpreting the synoptic meteorology. Coe assisted in preparation of the manuscript.

Robinson performed aerosol measurements and analysis, collation of profiles, interpreted the data and wrote the manuscript.

Manuscript prepared for Atmos. Chem. Phys.
with version 3.2 of the LaTeX class copernicus.cls.
Date: 3 November 2011

The elevation of Western Pacific regional aerosol by island thermodynamics as observed around Borneo

N.H. Robinson[1], J.D. Allan[1,2], G. Allen[1], and H. Coe[1]

[1]The Centre for Atmospheric Science, School of Earth Atmospheric and Environmental Science, The University of Manchester, UK
[2]The National Centre for Atmospheric Science, The University of Manchester, UK

Correspondence to: H. Coe
(hugh.coe@manchester.ac.uk)

Abstract. Vertical profiles of aerosol chemical composition were measured throughout the lower troposphere of Borneo, a large tropical island in the western Pacific Ocean. Aerosol measurements were made both upwind and downwind of Borneo, as well as over the island itself, using an Aerodyne Aerosol Mass Spectrometer on board the UK BAe-146 research aircraft. Two meteorological regimes were identified — one dominated by isolated terrestrial convection (ITC) which peaked in the afternoon, and the other characterised by more regionally active mesoscale convective systems (MCS). Upwind profiles show aerosol to be confined to a shallow marine boundary layer below 930±10 hPa. As this air mass advects over the island with the mean near-surface synoptic flow during the ITC-dominated regime, it is lofted above the terrestrial surface mixed layer to altitudes of between 945±22 and 740±44 hPa, consistent with a coupling between the synoptic steering level flow and island sea breeze circulations. Terrestrial aerosol was observed to be lofted into this higher layer through both moist convective uplift and transport through turbulent diurnal sea-breeze cells. At the peak of convective activity in the mid-afternoons, organic aerosol loadings in the lofted layer were observed to be substantially higher than in the morning (by a factor of three). This organic matter is dominated by secondary aerosol from processing of biogenic gas phase precursors. By the time the air mass reaches the west coast of the island, terrestrial aerosol is enhanced in the lofted layer. Such uplift of aerosol in Borneo is expected to increase aerosol lifetimes downwind, as they are above the boundary layer and therefore less likely to be lost by wet or dry deposition. It is also likely to change the role they play in the semi-direct and direct aerosol effects. The long chain of islands extending from Malaysia to Australia may all similarly be expected to present an orographic barrier to low level mean flow. This would lead to significant transport of aerosol into the tropical free troposphere across the western Pacific region.

1 Introduction

Aerosol particles interact with incoming solar radiation directly by absorbing and scattering sunlight and indirectly by affecting the properties of clouds through their role as cloud condensation nuclei (CCN). In order to accurately predict their influence on climate it is important to be able to effectively model their residence time in the atmosphere, as well as their effects on the Earth's radiative balance. The altitude of aerosol is a governing factor of their atmospheric lifetime, with aerosol at lower altitudes more likely to be removed through wet deposition (Balkanski et al., 1993). Aerosol altitude relative to cloud cover affects the direct aerosol effect (Liao and Seinfeld, 1997), with absorbing aerosol above cloud (which has a high albedo) tending to have a greater net radiative influence, and aerosol below cloud tending to interact with less incoming solar radiation. Aerosol altitude also plays a role in the semi-direct aerosol effects (Johnson et al., 2004), with local heating of different levels of the atmosphere causing a decrease in relative humidity and potentially an increase in atmospheric stability.

The tropics experience a higher top of the atmosphere flux of sunlight than any other region of the Earth meaning they play an important role in governing global climate. They are estimated to contribute almost half of global biogenic volatile organic carbon (BVOC) emissions (Guenther et al., 1995). BVOCs are oxidised in the atmosphere and condense as biogenic secondary organic aerosol (BSOA) (Hallquist et al., 2009). The emissions profiles of BVOCs and the processes by which they are oxidised to SOA are uncertain (Kanakidou et al., 2005; Hallquist et al., 2009) making modelling of organic aerosol challenging. Understanding the way BSOA is formed from tropical BVOC emissions is an important part of modelling the global radiative influence of aerosol. Despite this, there is a paucity of detailed in-situ aerosol measurements made in the tropics (e.g. Jimenez et al., 2009). Some studies have been performed in the large tropical continents of South America (Martin et al., 2010a) and Africa (Lebel et al., 2010), however until now the significant region of the tropics in the "maritime continent" of South East Asia has remained uncharacterised. The behaviour of aerosol around tropical islands is potentially very different to the continental locations previously studied: an increased influence of marine species could make SOA chemistry very different, and the thermodynamics of the local atmosphere may be complicated by the interaction of marine and terrestrial boundary layers with sea breeze systems.

Detailed measurements of aerosol have been performed in West Africa and Amazonia. The African Monsoon Multidisciplinary Analysis (AMMA; Lebel et al., 2010) campaign in West Africa made measurements of aerosol composition and physical properties. Airborne aerosol composition measurements showed influences from biomass burning and biogenic secondary organic aerosol (BSOA) (Capes et al., 2008, 2009). It was found that biomass burning played a role in elevating aerosol high into the troposphere. Several experiments have also been performed in Amazonia. The Large-Scale Biosphere-Atmosphere (LBA) experiment (Avissar et al., 2002) consisted of several measurement intensives that observed aerosol properties in Amazonia, during both periods domi-

nated by biomass burning (e.g. Chand et al., 2006) and the natural background (e.g. Claeys et al., 2004). In particular, Krejci et al. (2005) made airborne measurements of aerosol size distributions and composition over the ocean east of French Guyana and the Amazon rainforest. They found aerosol over the ocean to be confined to a shallow boundary layer of around 600 m. Over the rainforest the nocturnal boundary layer was less than 250 m, the lowest altitude flown. Three hours after sunrise the rain forest mixed layer was observed to be 800 m, growing to 1200-1500 m by early afternoon. Aerosol was measured in and above this layer and was attributed to primary biogenic aerosol and aerosol produced from processing in shallow convective clouds. Martin et al. (2010b) assert that mixing of surface aerosol high into the atmosphere by shallow and deep convective clouds is ubiquitous throughout Amazonia. More recently the Amazonian Aerosol Characterization (AMAZE-08) experiment made detailed ground based measurements of aerosol chemical and physical properties (Martin et al., 2010a). They classified periods of in-basin influence which were dominated by production of rainforest BSOA, and periods of out-of-basin influence that had additional marine and biomass burning aerosol (Chen et al., 2009).

The role tropical islands play in generating convection as isolated heat sources has been investigated previously in the Tiwi Islands, off the north cost of Australia (Crook, 2001). This is the location of a large convective storm named Hector which forms daily during the transition seasons. Crook (2001) modelled convection due to an elliptical isolated heat source representing the Tiwi islands and found that convection was most vigorous when the synoptic flow was slow and aligned with the major axis of the heat source. They also found that isolated heat sources such as tropical islands cause more convective uplift than continental coastlines. This island convection was thought to be generated in two different ways. Firstly, when low-level moisture is great, evaporatively produced cold pools prevent the inland progression of sea breezes. The interaction of these cold pools and the sea breeze cell then forms further convection. Secondly, when low-level moisture is less, the sea breeze cells can progress inland until they converge, generating more convection between the cells. Crook (2001) propose the question of what size of island is the most conducive to forming convection, with islands that are too large preventing the interaction between sea breeze cells on opposing coasts and islands that are too small reducing the residence time of air masses over land where they can be heated and become unstable. Its is not clear what the optimal island size is, however the convection associated with Hector is great, suggesting that their maximum width of around 150 km is an efficient size.

This paper reports findings from the Oxidant and Particulate Photochemical Processes Above a South East Asian Rainforest (OP3) project (Hewitt et al., 2010). This large consortium project was performed on the island of Borneo, South East Asia, between April and July 2008 and consisted of intensive studies from both ground and airborne measurement platforms. Borneo is one of the largest islands in the World and the interior is widely populated with rainforest. This is despite increasing settlement and logging of the exterior, mainly due to oil palm cultivation (McMorrow and Talip,

2001). The Crocker Mountain Range runs down the centre of the island, with the tallest peak, Mount Kinabalu (4095 m), situated near the region where measurements reported here were made. Previous studies from this project have reported a large off-island aerosol influence with much greater sulphate concentrations than were measured in other similar studies in Amazonia, and an on-island influence of BSOA from oxidation of isoprene and other BVOCs (Robinson et al., 2011a,b). The terrestrial boundary layer was characterised using doppler lidar measurements (Pearson et al., 2010) which detected an aerosol layer up to around 450 m above ground level during the day, although they state interpretation of mixed layer height is complicated by the influence of clouds and humidity. They also suggest that an observed decrease in aerosol concentration throughout the day may be caused by the mixing of cleaner air aloft into the boundary layer through cloud processes.

Here we report measurements of aerosol composition made during aircraft altitude profiles, in the context of corresponding thermodynamic measurements. By comparing profiles upwind over the ocean, over the island and over the downwind coast of the island we provide insight into the effect that transportation of regional air mass over Borneo has on the distribution of aerosol throughout the local troposphere, and its implications downwind.

2 Methods and instrumentation

Measurements were made on board the UK's BAe-146-301 large Atmospheric Research Aircraft (ARA) operated by the Facility for Airborne Atmospheric Measurements (FAAM), hereafter the BAe-146. This aircraft is equipped with a range of instrumentation to measure trace gas composition, cloud microphysics and standard thermodynamic data as well as aerosol size, composition and physical properties (Hewitt et al., 2009, 2010). The BAe-146 measurements were performed in conjunction with ground measurements made in the Danum Valley conservation area (4.981°N,117.844°E). A full description of the ground based aerosol measurements can be found in Robinson et al. (2011b).

2.1 Overview of aircraft flight plans

Each research flight lasted approximately five hours and usually consisted of sets of profiles over adjacent regions of rainforest and oil palm agriculture, hereafter collectively referred to as "East Sabah" (Fig. 1; Tab. 1; flight plans summarised in Hewitt et al. (2010)). This region is approximately 40 km away from the coast at the nearest point, with air masses influencing the region tending to travel over coastline approximately 90 km away (Fig. 1(a)). Deep profiles, from $\sim$1000 hPa (150 m) to $\sim$460 hPa (6500 m) were interrupted by stacked straight and level runs (SLR; at 100-250, 1500, 3000 and 6500 m). Flying through clouds was avoided when possible. Data from profiles performed when taking off and landing at Kota Kinabalu airport on the west coast are also used in this study. Two flights were performed each day (before and after local noon), with a total of ten flights during which the aerosol instrumentation was successfully operated. Six of these flights were in East Sabah

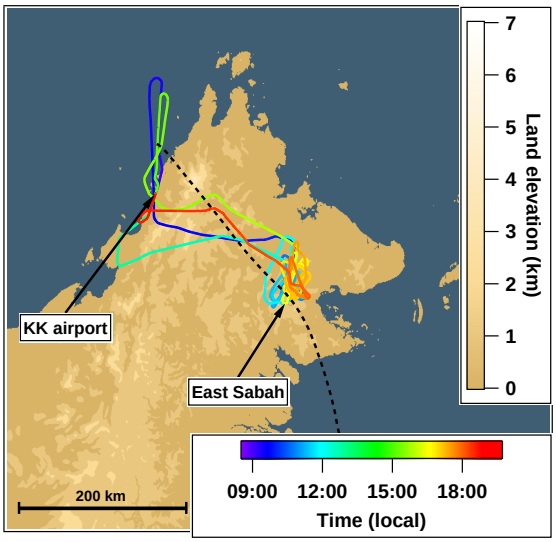

(a)

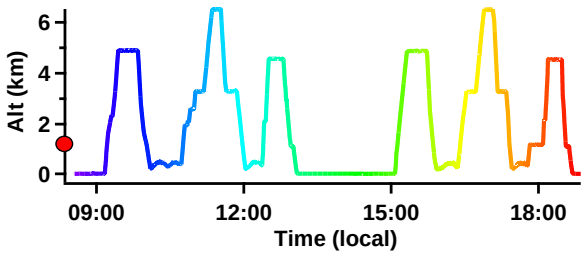

(b)

Fig. 1. Typical research flights B385a and b on the 11/07/08. (a) topographic map of Borneo with flight track coloured by time. Kota Kinabalu (KK) airport and "East Sabah" are indicated. A typical back trajectory is marked by the dashed black line. Air mass is moving from east to west and has a transit time of ∼30 hrs from coast to coast. (b) flight altitude showing a series profiles interrupted by straight and level runs. The red dot on the y-axis marks the trajectory release altitude of 880 hPa or 1.26 km (above the well mixed surface layer) descending to around 903 hPa upwind of Borneo. Both plots have lines coloured on the same time scale.

and two were upwind. Another two were in a region of heavy agro-industrial activity in the south of Sabah and are not included here, with the exception of the profiles above the airport described above. Each day was assigned one flight number with the morning and afternoon flights indicated with the suffixes "a" and "b."

3 Synoptic Meteorology

Two meteorological regimes were identified from inspection of satellite images during the flying campaign, with the 11th, 13th and 14th July showing isolated disorganised convection form-

Flight name	Date	Region	No. of profiles used	Meteorological Regime
B385	11/07/08	East Sabah	6	ITC
B386	13/07/08	East Sabah	7	ITC
B387	14/07/08	Agro-industrial region in south Sabah (airport profiles used)	4	ITC
B388	16/07/08	East Sabah	5	MCS
B389	17/07/08	Upwind	6	MCS

Table 1. Details of flights performed

ing over Borneo (isolated terrestrial convection; ITC), and the 16th and 17th showing the dominance of mesoscale convective systems (MCS). Synoptic 3-D wind reanalyses charts from the Integrated Forecast System (IFS, cycle 33r1) European Center for Medium Range Weather Forecasting (ECMWF) for the Tropical Western Pacific region are plotted in Fig. 2. Examples are shown of the 11 July 2008 and 16 July 2008, both at 0600 UTC (2 pm local time), corresponding to flights B385 and B389, respectively. Operational reanalyses of horizontal and vertical wind data evaluated on hybrid model sigma levels were interpolated onto the 900 hPa isobar to illustrate 3-dimensional motion diagnosed by the model in a plane of upper boundary layer vertical dynamics in the mid-afternoon. It is important to emphasise that vertical dynamics in the ECMWF model are parameterised from large-scale horizontal wind divergence fields and are therefore not expected to capture local scale (sub-degree) circulations such as see-breeze circulations explicitly. Rather, such analyses are useful in illustrating mean ascent and descent of airmasses due to synoptic weather patterns and large scale uplift. The large size of Borneo and therefore large mean influence on convection through surface heating can be expected to manifest in the reanalysis divergence field and therefore to capture mean ascent and descent over the island well. We use ECMWF fields to this end alone.

Fig. 2(a) shows the typical synoptic regime during much of the OP3 campaign; with black arrows showing near-surface easterly trades over Borneo and blue contours illustrating net uplift of air through the 900 hPa level, consistent with active convection during afternoon solar heating of the land surface. Several areas of strong downward motion are observed around the island, which are suggestive of the potential capture of larger see-breeze circulations, seen as closed cells between the warmer land and cooler sea surface around the island. The horizontal and vertical extent of such circulations can be expected to be controlled by the horizontal wind direction and strength and the buoyancy of land-heated air parcels. Satellite images corresponding to the thermodynamic charts in Fig. 2, are shown in Figure 3. These show thermal infrared (10.4 μm) radiances from Channel 4 of the Multi-Functional Transport Satellite (MTSAT-1R) geostationary satellite operated by the Japanese Meteorological Agency (JMA) and provided by the National Environmental Research Council (NERC) Earth Observation and Data Acquisition and Analysis Service (NEODAAS). Fig.

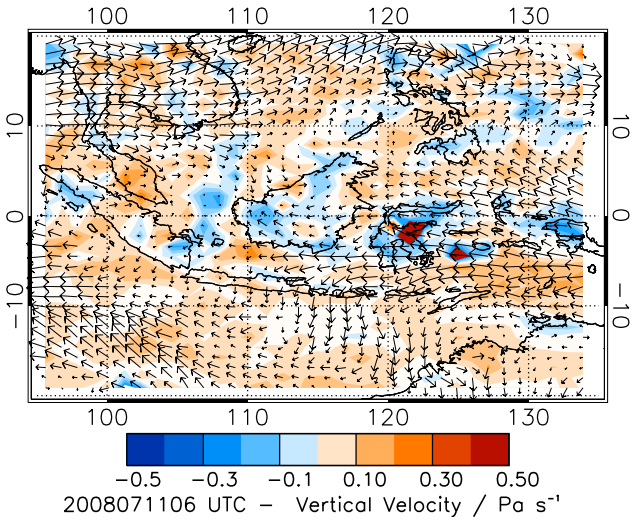

(a)

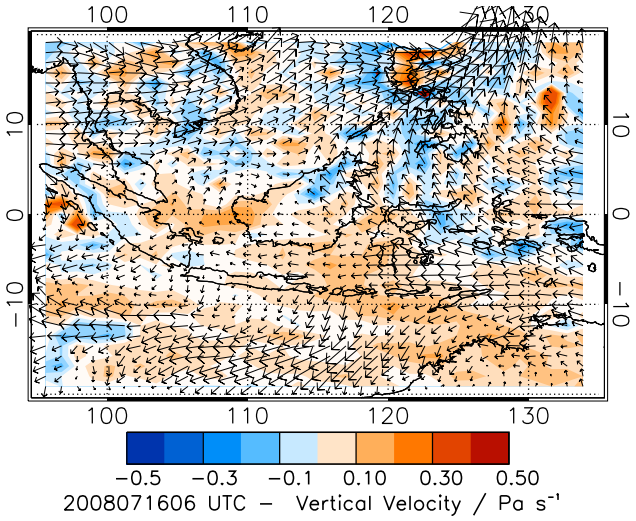

(b)

Fig. 2. Horizontal winds (scaled arrows) and vertical winds (coloured contours as per legend) in the Tropical Western Pacific region from ECMWF reanalyses, interpolated to the 850 hPa isobar for (a) 11/07/08 and (b) 16/07/08, both at 2 pm local time.

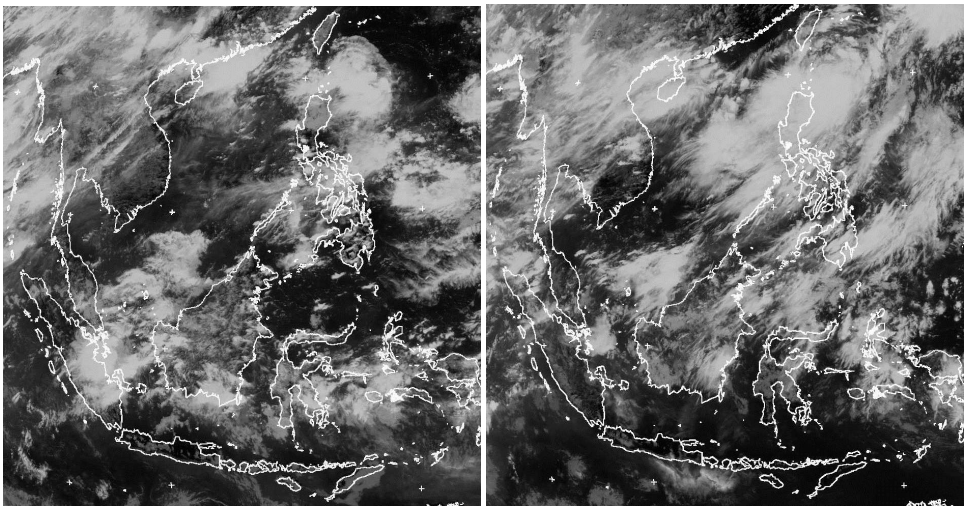

(a) (b)

Fig. 3. Thermal infra-red images from the Multi-Functional Transport Satellite (MT-SAT-1R), operated by the Japanese Meteorological Agency (JMA) and provided by the National Environmental Research Council (NERC) Earth Observation and Data Acquisition and Analysis Service (NEODAAS). Images are of (a) the 11/07/08 and (b) 16/07/08, both at 2 pm local time. (a) shows little cloud cover upwind of Borneo to the south-east, with clouds forming over the island, particularly downwind of the Crocker Mountain range, suggesting the role of orographically induced convection. (b) shows the dominance of an MCS system to the north-east of Borneo, with little convective activity over the island. (a) is typical of conditions on the 13th and 14th of July and (b) is typical of conditions on the 17th of July.

3(a) shows the cloud regime on the afternoon of 11 July 2008. Over Borneo a number of small, isolated clouds are observed, representative of shallow moist convection and consistent with the mean ascent seen in ECMWF reanalysis in Fig 2(a). A larger-scale cloud feature to the South West of the island with cirrus advecting to the South West with the upper level flow represents an area of deeper, more organised convection. Satellite images for the 13th and 14th of July (see supplementary material) show similar ITC as the 11th so, herein, we refer to this period as the ITC-dominated regime.

Fig. 2(b) shows the synoptic picture on 16 July 2008. This is very different to that seen on the 11 July 2008 in Fig. 2(a). On this day, there is net descent over Borneo. Fig. 3(b) shows the likely explanation for this deviation from the typical convective regime over Borneo — a number of upper level cirrus streaks are observed across the island, aligned on a roughly southwest/northeast vector and parallel to the upper level wind direction (not shown here). This mature cirrus is consistent with the active MCS seen to the northeast associated with the convergence seen in Fig 2(b). The extensive cirrus over Borneo is consistent with a much-reduced surface insolation and therefore weaker surface convection. It should be noted that, while Fig 2(b) shows mean descent over the island, there is still a region of uplift in the northwest of Borneo which is co-located with the Crocker Mountain Range

and, as such, is likely to be caused by orographic uplift. Satellite images for the 17th July (see supplementary material) show a similar influence from regional MCS systems so, herein, we refer to this period as the MCS-dominated regime.

4 Data Handling

The boundaries between atmospheric layers were estimated from inspection of aerosol profiles and tephigrams (constructed from thermodynamic data recorded from the BAe-146, and presented in Section 5 and the supplementary material). The estimated altitudes of the boundaries between different air mass layers were based on sudden changes in aerosol loadings and inversions in tephigram profiles. The majority of the time, boundaries were based on discernible changes in both these diagnostics. Occasionally a change was only discernible in one diagnostic, in which case this was used as the boundary level. Average aerosol concentrations were calculated from the data in the discreet diagnosed atmospheric layers for each aircraft profile, which were then subsequently averaged to gain a quantity representative of all corresponding profiles. Stated uncertainties are quoted as the standard deviation of the set of individual profile averages, and therefore reflects the variability between profiles. As such, values based on single profiles are not stated with standard deviations. All aerosol loadings are reported in μg sm^{-3}, defined as μg m^{-3} at 273 K and 1013 hPa with no condensation or evaporation of aerosol matter. Average aerosol loading and wind profiles are reported here with the individual profiles included in the Supplementary Material. Tephigrams were not averaged to facilitate analysis of fine-scale structure in the vertical. Representative tephigrams are displayed alongside the averaged profiles, with all other tephigrams displayed in the Supplementary Material.

4.1 Instrumentation

A GPS-aided Inertial Navigation (GIN) system, consisting of an Applanix POS AV 510 system provided attitude, position and BAe-146 velocity data. The GIN sampled data at 50 Hz and recorded data at 32 Hz. A 5-hole turbulence probe mounted on the aircraft nose was used in conjunction with the GIN system to provide 3-D wind fields and high frequency (32 Hz) turbulence measurements. Thermodynamic instruments include a General Eastern GE 1011B Chilled Mirror Hygrometer measuring dew-point temperature and a Rosemount/Goodrich type-102 True Air Temperature sensor, which recorded data at 32 Hz using a non de-iced Rosemount 102AL platinum resistance immersion thermometer mounted outside of the boundary layer of the aircraft near the nose. The turbulence probe also used measurements from the GIN and measurements of the ambient air temperature to correct for kinetic effects. These thermodynamic instruments are used here to calculate tephigrams and wind direction profiles (see Section 5).

Aerosol was sampled through a Rosemount inlet (Foltescu et al., 1995) via approximately 0.7 m of stainless steel tubing with a total residence time of $\sim$4 s in the inlet system. Accumulation mode

aerosol losses have previously been shown to be negligible (Osborne et al., 2007). Aerosol composition was measured using a Compact Time-of-flight Aerodyne Aerosol Mass Spectrometer (C-AMS; Drewnick et al. (2005); Canagaratna et al. (2007)). This instrument provides online size resolved aerosol composition data. It is limited to sub-micron aerosol that is non-refractory (NR), a term operationally defined to mean the aerosol vaporises rapidly at a temperature of 600°C. Although other aerosol types were present in Borneo, measurements reported here focus on organic and sulphate aerosol which were the most abundant species. The C-AMS was operated in two modes: a $\sim$10 s time resolution mode for profiles and a $\sim$30 s time resolution mode during SLRs and transit. Aerosol number size distributions were measured using a wing mounted Passive Cavity Aerosol Spectrometer Probe (PCASP), an optical sizing instrument (Walter Strapp et al., 1992; Liu et al., 1992).

4.2 Establishing the AMS collection efficiency

The C-AMS data were processed using standard calibration and data analysis techniques (Allan et al., 2003; Allan, 2004). Upon contact with the C-AMS vaporiser, a proportion of the particulate matter is undetected due to rebound from the vapouriser. This effect is quantified by the collection efficiency (CE), which is defined as the fraction of aerosol introduced to the instrument that is successfully vapourised and detected. The CE has previously been shown to be a function of particle phase, composition, shape, relative humidity and heater geometry, and in previous studies has been found to be between 0.43 and 1 with a typical CE ≈ 0.5 (Salcedo et al., 2007). The CE of the C-AMS was determined by convolving the speciated mass loading time series into a total volume time series using assumed organic and inorganic densities determined by Cross et al. (2007). This was then compared to total sub-micron volume measured by the PCASP. The CE of the High Resolution AMS (HR-AMS; DeCarlo et al., 2006) used at the ground site was previously determined to be $\sim$0.5 after a similar comparison to the associated Differential Mobility Particle Sizer (DMPS; Williams et al., 2000) total volume time series. Applying a similar CE of 0.5 to the FAAM C-AMS leads to over-measurement compared to the PCASP and a CE of 1 is found to give better agreement (Figure 4(a)). Comparison of total aerosol volume measured from the ground site and the BAe-146 show good agreement during fly-bys of the ground site when a CE of 1 is applied to the C-AMS data (Figure 4(b)).

A likely reason for different observed CEs in the ground and BAe-146 AMSs is that aerosol sampled in the BAe-146 is more humid due to the lack of a drying system. This has been observed to cause a CE closer to unity at RHs greater than around 80% (Allan et al., 2004; Matthew et al., 2008). The RH in the BAe-146 AMS sample line can be estimated from the ambient RH, the differential between cabin and ambient temperatures, and the pressure increase caused by the motion of the aircraft using Equation 1.

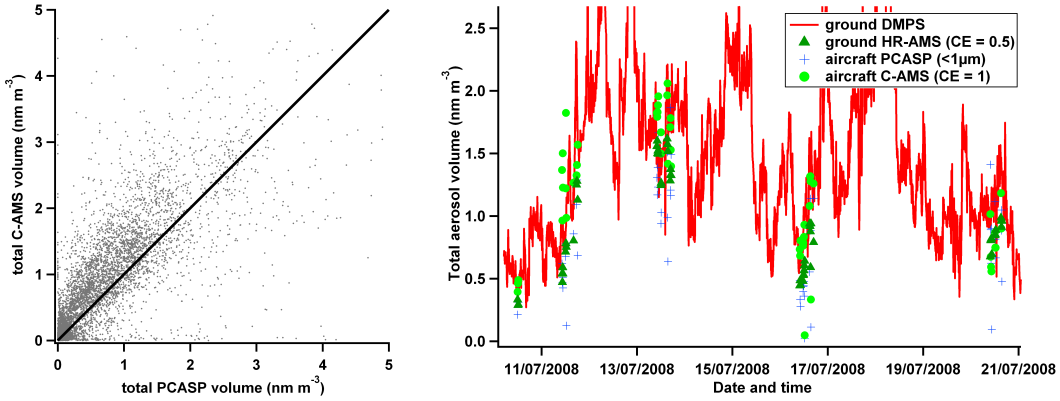

(a) (b)

Fig. 4. (a) Total sub-micron aerosol volume measured by the C-AMS vs. the PCASP. Plot using all available data from the BAe-146. 1:1 line shown in black. (b) comparison of total sub-micron aerosol volume measured from the ground site (DMPS and HR-AMS) and BAe-146 (PCASP and C-AMS) during ground site fly-bys. Conversion of AMS particulate mass to volume uses assumed organic and inorganic densities (Cross et al., 2007). Data shown with BAe-146 C-AMS CE = 1 and ground HR-AMS CE = 0.5.

$$q = \frac{1}{2}\rho v^2 \tag{1a}$$

$$p(\mathrm{H_2O})_{int} = \frac{q}{p} p(\mathrm{H_2O})_{amb} \tag{1b}$$

$$p^*(\mathrm{H_2O})_{int} = e^{A - \frac{B}{C+T_{int}}} \tag{1c}$$

$$RH_{int} = \frac{p(\mathrm{H_2O})_{int}}{p^*(\mathrm{H_2O})_{int}} \tag{1d}$$

where q is the dynamic pressure, p is the static pressure, ρ is the density of ambient air, v is the aircraft velocity, $p(\mathrm{H_2O})_{amb}$ is the ambient partial pressure of water, $p(\mathrm{H_2O})_{int}$ is the internal partial pressure of water, p^* is similarly the saturation vapour pressure, A, B and C are constants (8.07131, 1730.63 and 233.426 respectively), T_{int} is the cabin temperature and RH_{int} is the relative humidity in the line at the time of sampling. This gives an estimated median inlet line RH of 79% for all data, 98% below an altitude of 1 km, 83% between 1-3 km and 56% above 3 km meaning much of the sampled aerosol was humid enough that it may have been sampled with a CE of 1. In contrast, the AMS at the ground site sampled air dried using a 780 tube Nafion counter flow drier, with a resultant median sample RH of 76% (Whitehead et al., 2010; Robinson et al., 2011a). A CE of 1 is used for all BAe-146 measurements reported herein. It should be noted that this will lead to under-reporting of aerosol loading in circumstances where the CE is less than unity, by as much as 50% assuming a lower bound CE of 0.5. This may be particularly relevant in the upper free troposphere where the inlet RH was likely to be lower due to the positive internal/external temperature differential, however it is impossible to determine this effect accurately through a total mass closure given the low aerosol

loadings at higher altitude.

5 Results

5.1 Upwind

Flight B389 (17/07/08) is notable in that measurements were performed upwind of the island. Four upwind profiles were preformed between 09:45 and 12:00 local time. Upwind aerosol profiles show a shallow surface layer up to an average estimated height of 930±10 hPa (770 m). Corresponding wind vector profiles show some shear at the same level and tephigrams indicate weak mixing with a capping inversion at the same level, or no mixing at all. Of the four upwind profiles, one has notably lesser aerosol loadings in the surface layer, however light rain was observed when this low altitude data was sampled which may have been responsible for depleting local aerosol concentrations through wet deposition. Taking data in the surface layer across the four profiles gives average aerosol loadings of 0.74±0.48 μg sm^{-3} of organic aerosol and 0.88±0.22 μg sm^{-3} of sulphate aerosol, with data above the surface layer giving averages of 0.06±0.04 μg sm^{-3} for organic aerosol and 0.26±0.06 μg sm^{-3} of sulphate. Discounting the rain affected flight gives surface layer averages values of 0.88±0.32 and 0.97±0.12 μg sm^{-3} for organic and sulphate aerosol respectively. Averages of the three profiles unaffected by rain are shown in Fig. 5.

5.2 East Sabah — ITC-dominated regime

The morning profiles over East Sabah were performed between 10:00 and 12:00 and the afternoon profiles between 16:00 and 18:00 local time. In total, four morning profiles and five afternoon profiles were successfully recorded in this region during the ITC-dominated regime. The morning aerosol profiles show a shallow surface layer below an average estimated height of 922±14 hPa (890 m) containing organic (0.90±0.50 μg sm^{-3}) and sulphate (1.05±0.24 μg sm^{-3}) aerosol. Above this is a layer up to an average estimated height of 714±20 hPa (3050 m) that contains elevated sulphate aerosol loadings (1.07±0.18 μg sm^{-3}) and relatively low organic aerosol loadings (0.28±0.15 μg sm^{-3}). Very low organic and sulphate aerosol loadings were measured above this (0.02±0.03 and 0.08±0.04 μg sm^{-3} respectively). These layers are referred to (in order of increasing altitude) as Layer One, Layer Two and Layer Three. Tephigrams indicate that Layer One is typically well mixed with a capping inversion at the top. The boundary between Layers One and Two was observed to be regularly marked by a layer of cumulus clouds, consistent with the expected lifting condensation level seen in the tephigrams. The tephigrams show little indication of vertical mixing in Layer Two with occasional weak inversions throughout the layer. The wind vector profile tends to show a change from southerly to easterly winds through Layer Two, sometimes with strong shear but usually with a gradual transition. Average profiles and an example tephigram are shown in Figure 6.

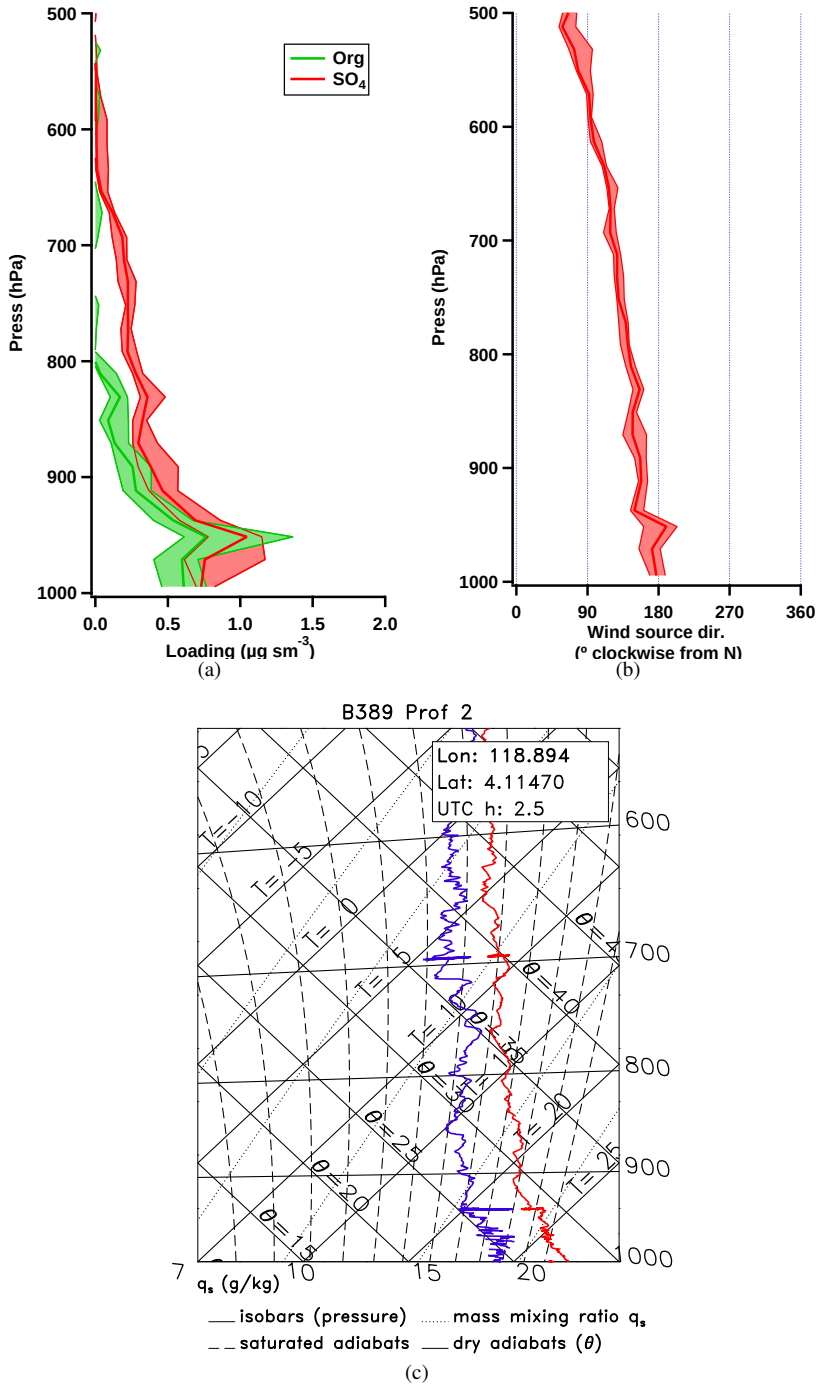

Fig. 5. Averaged altitude profiles (median and interquartile ranges) **(a)** organic and sulphate aerosol loading and **(b)** wind direction. **(c)** shows a typical tephigram detailing ambient temperature (red) and dewpoint temperature (blue). Averages comprise three profiles (during the MCS-dominated regime) from flight B389 in the morning of 17/07/08, and the tephigram is was performed at 10:30 local.

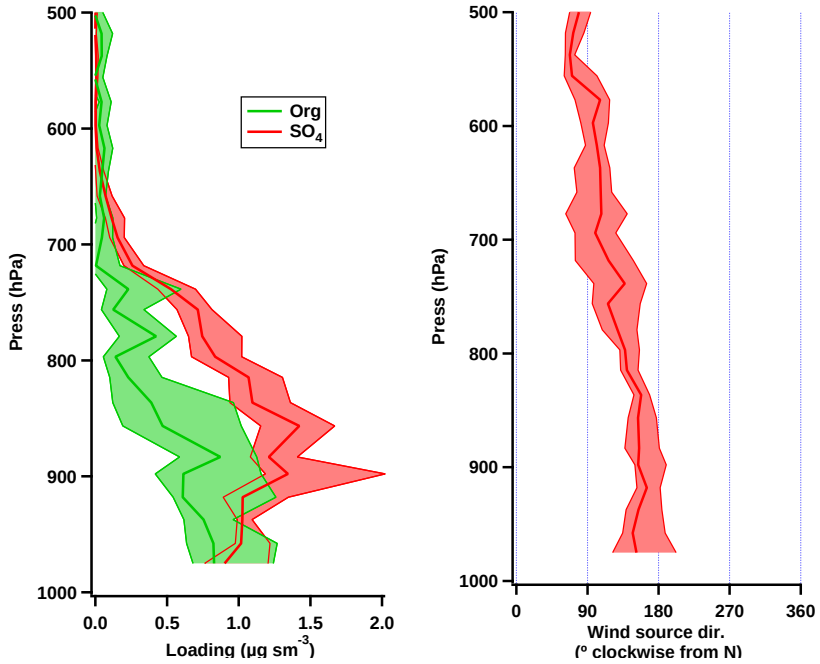

(a) (b)

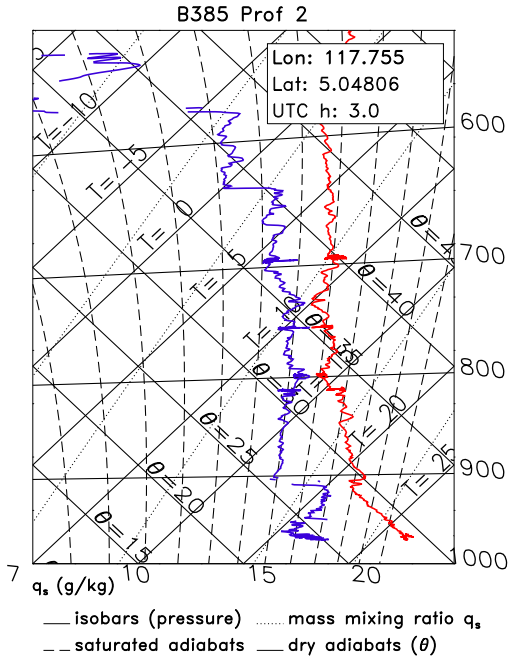

(c)

Fig. 6. Average altitude profiles (median and interquartile ranges) during mornings of the ITC-dominated regime over East Sabah of **(a)** organic and sulphate aerosol loading and **(b)** wind direction. **(c)** shows a tephigram detailing ambient temperature (red) and dewpoint temperature (blue). Averages comprised four profiles on 11/07/08 and 13/07/08. Tephigram from 11/07/08, 11:01 local.

Afternoon profiles show a slightly deeper well mixed layer up to an average estimated height of 914±10 hPa (960 m) and a similar change in wind shear through Layer Two, compared to the morning profiles. Layer One has similar aerosol loadings as in the morning (1.01±0.22 and 0.89±0.12 μg sm^{-3} of organics and sulphate respectively). Layer Two tends to show and increase in organic aerosol loadings compared to the morning (to 0.85±0.09 μg sm^{-3}, an increase by a factor of 3), to amounts similar to the average sulphate loadings in Layer Two (0.91±0.19 μg sm^{-3}). Layer Three still shows low aerosol loadings of both organics and sulphate (0.07±0.02± and 0.07±0.07 μg sm^{-3} respectively). Average aerosol and wind direction profiles and an example tephigram are shown in shown in Fig. 7.

Two of the afternoon profiles (Fig. 8) were performed in the vicinity of intense cumulonimbus formation (such as can be seen in the satellite images in Fig. 3(a)), which were not included in the group of profiles discussed above. They show aerosol profiles that have relatively constant loadings to a height of at least 700 hPa (no AMS data exists above this altitude), consistent with strong mixing. The tephigrams indicate boundary layer mixing to a height of above 900 hPa, possibly to as high as ∼830 hPa.

6 East Sabah — MCS-dominated regime

Only one morning and one afternoon profile was recorded over East Sabah during the MCS-dominated regime. The morning profile (Fig. 9) shows a well mixed Layer One with approximately half the organic and sulphate loadings measured during the ITC-dominated regime (0.51 and 0.42 μg sm^{-3} respectively) up to a similar altitude (920 hPa, 890 m). Layer Two shows a very strong sulphate layer (0.73 μg sm^{-3}) with low organic concentrations (0.19 μg sm^{-3}), again up to a similar altitude (690 hPa, 3330 m) as observed during the ITC-dominated regime. Sulphate and organic loadings (0.01 and 0.02 μg sm^{-3} respectively) were very low in Layer Three, similar to the ITC-dominated regime.

The afternoon profile (Fig. 10) was markedly different to the morning profile with similar sulphate loadings to the morning (0.59 μg sm^{-3}) but a large increase in organic loadings (1.40 μg sm^{-3}) in Layer One. Compared to the morning profile, Layer Two showed an increase in organics (to 0.38 μg sm^{-3}) and a substantial decrease in sulphate (to 0.39 μg sm^{-3}). Layer Three was at a similar altitude (690 hPa) as the morning, with similarly low organic and sulphate (0 and 0.11 μg sm^{-3}) loadings.

6.1 Kota Kinabalu — ITC-dominated regime

Profiles from take-off and landing at Kota Kinabalu airport on the west coast of Borneo (Fig. 12) also often show three distinct layers. In total 15 such profiles were performed, of which nine were during the ITC-dominated period (consisting of three morning, five early afternoon and one late afternoon

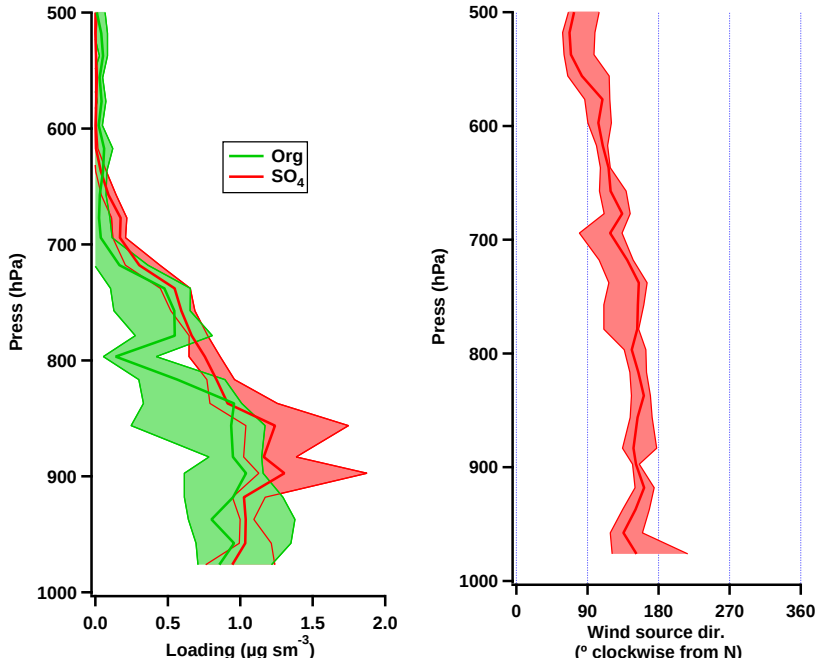

(a) (b)

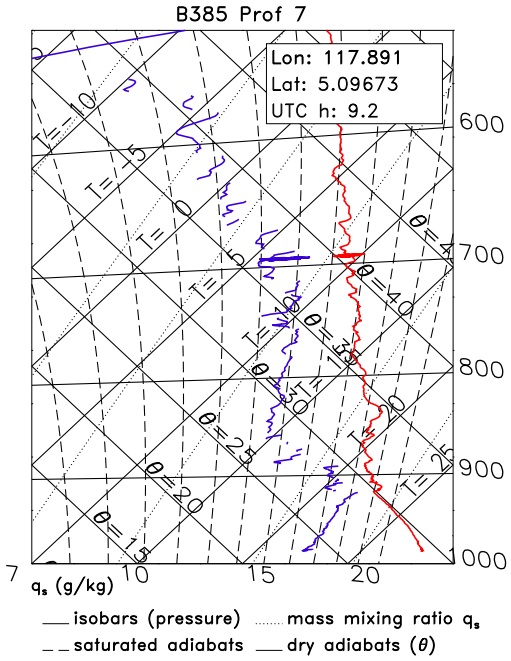

(c)

Fig. 7. Average altitude profiles (median and interquartile ranges) during the afternoons of the ITC-dominated regime over East Sabah of **(a)** organic and sulphate aerosol loading and **(b)** wind direction. **(c)** shows a tephigram detailing ambient temperature (red) and dewpoint temperature (blue). Averages comprised three profiles on 11/07/08 . Tephigram from 11/07/08, 17:11 local.

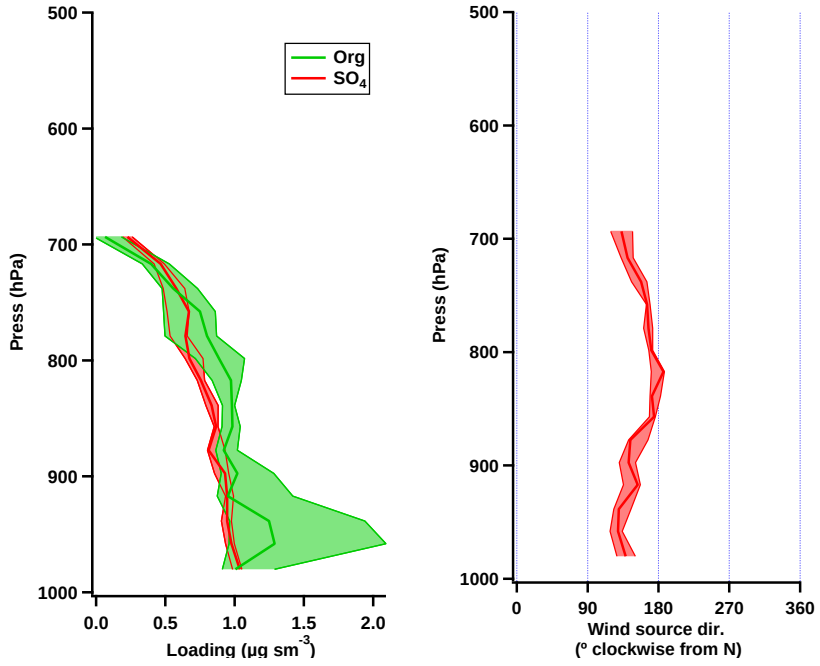

(a) (b)

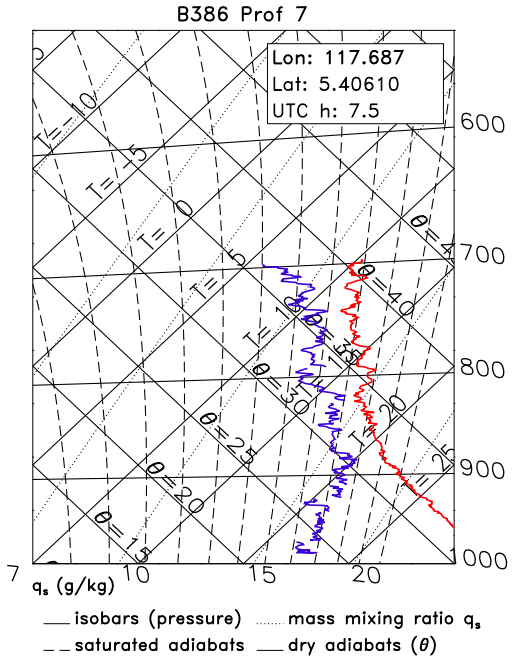

(c)

Fig. 8. Average altitude profile (median and interquartile ranges) during a period of cumulonimbus activity over East Sabah of **(a)** organic and sulphate aerosol loading (only partial data coverage) and **(b)** wind direction. **(c)** shows a tephigram detailing ambient temperature (red) and dewpoint temperature (blue). Averages of two profiles on 13/07/08, with the tephigram at 15:30 local.

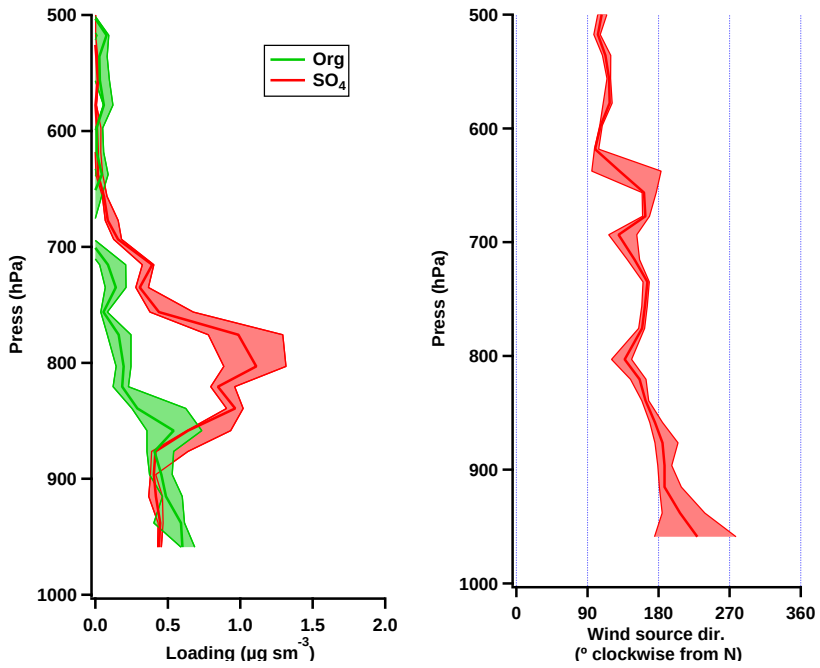

(a) (b)

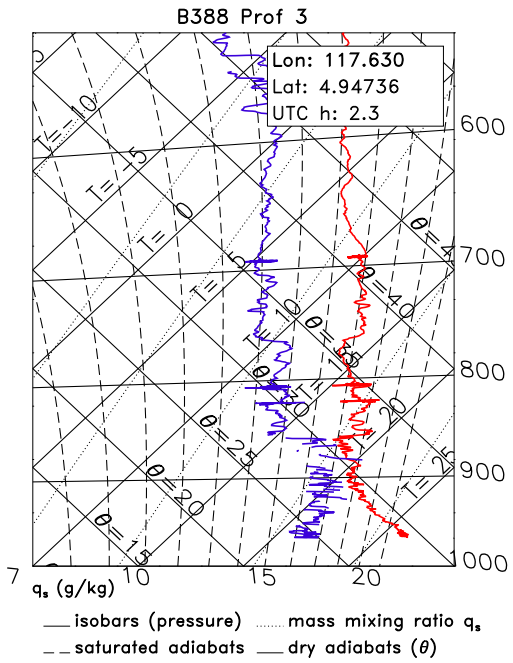

(c)

Fig. 9. Average altitude profile (median and interquartile ranges) during the mornings of the MCS-dominated regime over East Sabah of **(a)** organic and sulphate aerosol loading and **(b)** wind direction. **(c)** shows a tephigram detailing ambient temperature (red) and dewpoint temperature (blue). One profile on 16/07/08, 10:30 local.

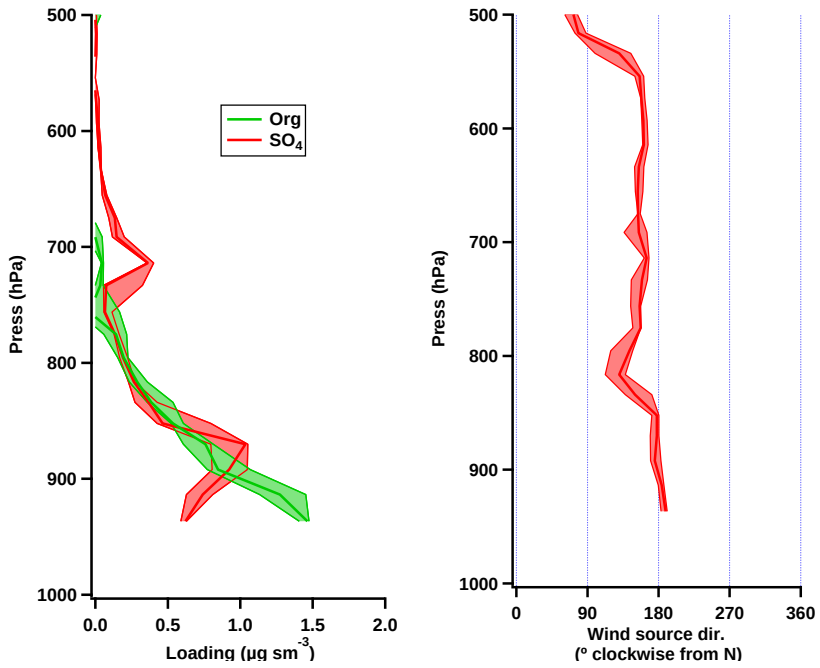

(a) (b)

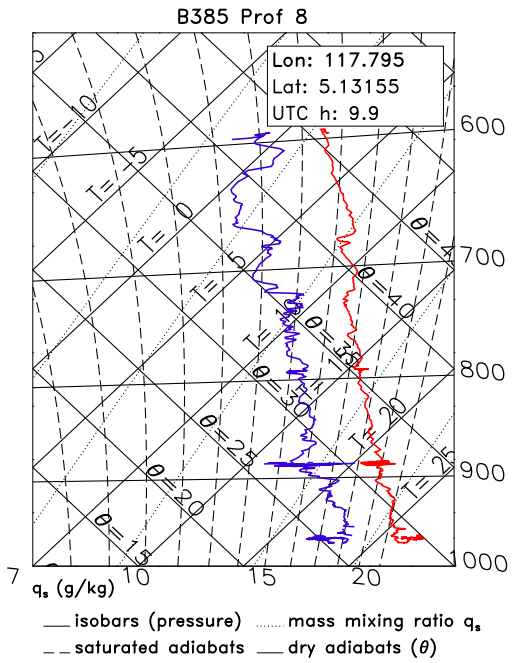

(c)

Fig. 10. Average altitude profile (median and interquartile ranges) during the afternoons of the MCS-dominated regime over East Sabah of **(a)** organic and sulphate aerosol loading and **(b)** wind direction. **(c)** shows a tephigram detailing ambient temperature (red) and dewpoint temperature (blue). One profile on 16/07/08, 15:38 local.

profiles). The tephigrams tend to show Layer One to be a very shallow mixed layer to an average estimated height of 940±25 hPa (670 m), slightly lower than was seen over East Sabah. The level of organic and sulphate aerosol in Layer One (1.52±0.77 and 0.77±0.21 μg sm^{-3}) stayed relatively constant throughout the day, although the large stated standard deviations reflect that there was significant variation between days. Layer Two extended above this to an average estimated height of 768±45 hPa (2430 m). There also appears to be stronger wind shear in layer two on the west coast than over East Sabah and upwind of the island, with an onshore wind in Layer One shearing 180° to be an offshore wind through Layers Two and Three. Sulphate aerosol concentrations in Layer Two showed no significant change during the day, though they were slightly greater in the afternoon than in the morning (0.68±0.32 μg sm^{-3} and 0.52±0.14 μg sm^{-3} respectively). Organic aerosol in Layer Two was observed to increase more substantially throughout the day, with morning and early afternoon profile averages of 0.94±0.32, 1.74±0.78 respectively. Layer Three had low aerosol loadings for organic and sulphate aerosol of 0.08±0.09 and 0.13±0.11 μg sm^{-3} respectively. Average profiles and an example tephigram are shown in Figure 11. This tephigram shows Layer Two is strongly separated from Layer One, with a layer of dry air around 930 hPa and humid air above this up to 800 hPa.

6.2 Kota-Kinabalu — MCS-dominated regime

Six profiles were performed over Kota Kinabalu during the MCS-dominated regime (consisting of two morning, three early afternoon and one late afternoon). The profiles are markedly different from those of the ITC-dominated regime. A shallow well mixed layer is often poorly defined by the tephigrams and there is little wind shear. Sulphate is present in very low concentrations, with no growth through the day and little difference between Layers One and Two (0.36±0.19 and 0.31±0.19 μg sm^{-3} respectively when averaged over the day). Organics concentrations are also not observed to grow significantly through the day, but are present in greater concentrations in Layer One than Layer Two (1.41±0.71 and 0.88±0.63 μg sm^{-3} respectively when averaged over the day).

7 Discussion

Altitude profiles were performed upwind, over and downwind of Borneo from east to west, approximately following air mass trajectories. Profiles recorded upwind of Borneo show a shallow surface layer of sulphate, and sometimes organic, aerosol. Synoptic charts (Fig. 2) and satellite images (Fig. 3) indicate that there are two regimes present — one dominated by ITC and the other dominated by the influence of MCS. A total of 19 profiles were recorded during the ITC-dominated regime, with 12 during the MCS-dominated regime. Profiles over East Sabah and the west coast of Borneo tend to show three layers (numbered with increasing altitude for reference). Average aerosol loadings and layer division heights for the different regions and meteorological conditions are displayed in

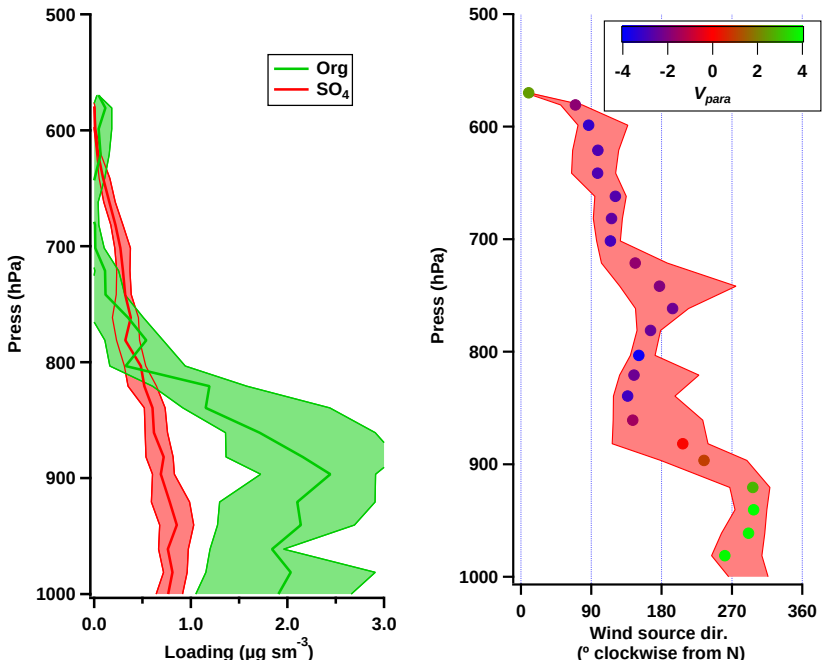

Fig. 11. Averaged altitude profiles (median and interquartile ranges) during the ITC-dominated regime over Kota Kinabalu on the west coast of Borneo of **(a)** organic and sulphate aerosol loading and **(b)** wind direction, coloured by component of direction parallel to the onshore wind, V_{para}, (i.e. positive values onshore and negative offshore) to emphasise the sea-breeze wind shear. **(c)** shows a tephigram detailing ambient temperature (red) and dewpoint temperature (blue). Averages comprised nine profiles from 11/07/08, 13/07/08 and 14/07/08. Tephigram from 13/07/08, 14:20 local.

	Upwind	E. Sabah (AM)	E. Sabah (PM)	E. Sabah (cb)	KK (AM)	KK (midday)	KK (PM)
ITC-dominated regime							
Org L1 (μg sm^{-3})	—	0.90±0.50	1.01±0.22	0.84±0.08	1.72±0.81	1.40±0.81	2.82
Sulph L1 (μg sm^{-3})	—	1.05±0.24	0.89±0.12	0.84±0.21	0.87±0.17	0.71±0.22	0.76
L1/L2 alt (hPa)	—	922±14	914±10	assumed 915	945±22	937±29	963
Org L2 (μg sm^{-3})	—	0.28±0.15	0.85±0.09	1.12±0.53	0.94±0.32	1.74±0.78	2.29
Sulph L2 (μg sm^{-3})	—	1.07±0.18	0.91±0.19	0.81±0.21	0.52±0.14	0.68±0.32	0.74
L2/L3 alt (hPa)	—	714±20	734±51	—	740±44	786±41	747
Org L3 (μg sm^{-3})	—	0.02±0.03	0.07±0.02	—	0.02±0.02	0.09±0.10	0.14
Sulph L3 (μg sm^{-3})	—	0.08±0.04	0.07±0.07	—	0.13±0.02	0.22±0.14	0.27
n profs	0	4	3	2	3	5	1
MCS-dominated regime							
Org L1 (μg sm^{-3})	0.74±0.48	0.51	1.40	—	1.41±0.19	1.20±0.33	0.63
Sulph L1 (μg sm^{-3})	0.88±0.22	0.42	0.59	—	0.28±0.05	0.28±0.07	0.30
L1/L2 alt (hPa)	930±10	920	920	—	949±4	953±24	908
Org L2 (μg sm^{-3})	0.06±0.04	0.19	0.38	—	0.53±0.10	0.66±0.08	0.87
Sulph L2 (μg sm^{-3})	0.26±0.06	0.73	0.39	—	0.21±0.01	0.25±0.02	0.24
L2/L3 alt (hPa)	—	690	690	—	723±30	689±115	723
Org L3 (μg sm^{-3})	—	0.01	0	—	0.15±0.18	0.07±0.08	0.00
Sulph L3 (μg sm^{-3})	—	0.02	0.11	—	0.03±0.00	0.05±0.02	0.08
n profs	4	1	1	0	2	3	1

Table 2. Summary of average estimated heights of layer boundaries, and average aerosol loadings in different layers. Uncertainties on figures represent standard deviation of averages from each individual profile and represent variability between profiles. No clear divide in layers was seen during cumulonimbus activity (cb) in East Sabah so a division was assumed at the same height as other local profiles.

Table 2.

7.1 ITC-dominated regime

During the ITC-dominated regime, the profiles over East Sabah show that at the start of the day Layer One has small but significant sulphate and organic aerosol loadings while Layer Two is dominated by sulphate. As the day progresses organic aerosol loading tended to increase in Layer Two until it was at a similar concentrations to the sulphate aerosol. A smooth transition between aerosol loadings at the normal heigh of divide between Layers One and Two was observed in profiles that were taken during periods of observed cumulonimbus formation. Profiles over Kota Kinabalu on the west coast of Sabah showed Layer Two to have high organic loadings which increased throughout the day, in contrast to the surface loadings which did not.

The sulphate loadings in Layer Two over East Sabah suggest that the air was influenced by off island sources. The origin of sulphate in Borneo has been extensively discussed in Robinson et al. (2011b) which shows surface sulphate loadings to be greater in back trajectories that originate externally to the island. They conclude that the sulphate is potentially from a variety of sources, with

the most likely source being the production of dimethyl sulphide (DMS) from processing of phytoplankton emissions (Kettle and Andreae, 2000). Comparison to the upwind profiles suggests that the shallow marine boundary layer aerosol was being lofted by the time it reaches East Sabah. While the upwind profiles were performed during the MCS-dominated regime, they are likely to be representative of prevailing marine conditions, with high sulphate concentrations confined to a shallow boundary layer. The tephigrams over East Sabah show it was likely that Layer One represents a boundary layer well mixed by turbulence and shallow convection. The direction of synoptic winds has been shown to weaken sea-breeze circulations where it opposes the direction of the seaward branch of the sea-breeze outflow (Gahmberg et al., 2010; Atkins and Wakimoto, 1997). This appeared to be the case in East Sabah as wind profiles, while showing a gradual wind shear, did not show sudden shear associated with strong sea breeze circulations.

Doppler lidar measurements performed at the ground site (an altitude of 198 m above sea level) in East Sabah (Pearson et al., 2010) show a maximum gradient in backscatter (associated with the top of the surface layer of aerosol) at an average heigh of $\sim$650 m above sea level between 09:00 and 18:00 local. Those measurements also observed an average cloud base height that started increasing from 09:00 to a relatively constant height of $\sim$1050 m between 12:00 and 17:00. The lidar measurements were performed during 10 weeks of April and June, earlier than the flying period of OP3 which was in July. The surface layer height derived from cloud base height is consistent with the in-situ BAe-146 measurements, which give an average estimated surface layer height of $\sim$960 m during the afternoon. However, substantial amounts of aerosol were observed above the maximum backscatter gradient level during the flying campaign

As the day progresses there was less segregation between aerosol concentrations in Layers One and Two over East Sabah. However, the tephigrams suggest that there was still a relatively shallow well mixed surface layer. It is likely that aerosol was being mixed from Layer One into Layer Two in discreet events. The aerosol profiles recorded during periods of cumulonimbus formation show a smooth transition in aerosol loadings at the normal height of divide between Layers One and Two. The associated tephigrams also show a very deep mixed layer. This strongly supports mixing of aerosol, and aerosol precursors, from Layers One to Two by convection events as the day progressed. It might be expected that a proportion of the uplifted sulphate aerosol is lost to wet deposition where deep convection is active, which is indeed observed as a smooth decreasing vertical gradient. It should be noted that wet removal would be likely to be less significant for gas phase aerosol precursors. Previous work has attributed the daily increase in tropospheric organic aerosol loadings during OP3 to photochemical processing of BVOCs (Robinson et al., 2011a). These may form aerosol after being lofted, either though photochemical processing or, if they are semi-volatile, condensation due to the reduced temperature higher in the troposphere. It is likely that orographically induced deep convection is even more common downwind of East Sabah where there is more elevated topography, as is highlighted in Fig. 2(b).

Synoptic winds aligned with the seaward branch of a sea-breeze outflow (such as were present on the west coast of Borneo) have been shown to strengthen sea breezes (Gahmberg et al., 2010; Atkins and Wakimoto, 1997). This generally seemed to be the case in Kota Kinabalu, with $\sim$180° wind shear between on and offshore winds seen in the average altitude profile. A more stable sea breeze may also have been created by the relatively straight west coast of Borneo, compared to the east coast which is made up of several bays and peninsula. Aerosol was almost always present to a height of between 800 hPa and 700 hPa. The amount of organic aerosol in Layer Two increased throughout the day, with the average profiles showing a distinct layer of high aerosol concentrations in Layer Two over Kota Kinabalu by midday. These layers are often associated with comparatively humid air. This is consistent with Layer Two being influenced by BSOA which would be expected to be associated with water vapour due to transpiration and evaporation alongside the emission of SOA precursor gases from vegetation. While Borneo is large, the east and west coast of Sabah are only around 250 km apart and it is not clear if this is close enough to allow interaction between the opposing sea breeze cells such as that seen on the Tiwi islands, which are smaller at around 150 km (Crook, 2001). It is also not clear what effect the intervening orography would have on Borneo, compared to the Tiwi islands which are relatively flat.

The profile-to-profile variability is great over Kota Kinabalu when compared to east Borneo (which is apparent from the larger standard deviations). It is likely that aerosol transported across the width of the island ($\sim$300 km) experiences a varying amount of wet removal in the inland mountainous region of Borneo, where orographically induced convective precipitation may be greater. This would also explain the relative dominance of organic aerosol, which is replenished en-route through processing of terrestrial vegetation emissions, in contrast to off island sulphate (and organics) which are not. This suggests that mixing processes over the island increase the aerosol loadings in Layer Two by introducing upwind boundary layer aerosol and aerosol produced from on-island sources during transit across the island.

This suggests that Layer Two represents air mass transported across the width of the island, which undergoes conversion from being dominated by off-island sulphate and organics to being dominated by BSOA. It should be noted that air sampled above 3 km was estimated to have an RH of 56%, meaning it is likely that the reported loadings for Layer Three should be doubled due to a reduced CE.

Figure 13 shows a conceptual illustration of the dynamical processes expected to be active in the local afternoon during periods dominated by ITC. The synoptic winds in the lower troposphere were consistent westerly trades throughout the course of the campaign (Fig. 2). The steep central island topography of Borneo and the open plains on the east of the island have the effect of regularly forcing deep convective development to the east of the Crocker Mountain range. This is consistent with the ECMWF reanalysis shown in Fig. 2(a) which shows mean assent of air over the island, and the satellite image shown in Fig. 3(a) which shows what appear to be isolated convective clouds

over Borneo. In our conceptual picture, the rich source of organic aerosol over the region of oil palm and rainforest is mixed with maritime air already relatively rich in off-island aerosol (Fig.5(a)) and uplifted in deep moist convection. However, the seaward convective outflow of the sea-breeze cell induced by this convection opposes the direction of the synoptic flow and is therefore likely to be weak and turbulent, with uplifted air instead advected westward over the island. The net effect on the eastern side of Borneo is a very efficient ventilation of the island surface layer in the local afternoon, with uplift and westward advection of air rich in organic aerosol and partially depleted in sulphate aerosol.

On the western side of the island, the thermodynamic picture is very different. In this case, the upper boundary layer seaward convective outflow of the sea-breeze cell is aligned with the synoptic flow, thus strengthening the sea-breeze circulation and elongating the cell along its horizontal axis (Gahmberg et al., 2010; Atkins and Wakimoto, 1997). The net effect of this alignment is a weaker surface return flow, resulting in weaker convergence inland and therefore reduced convection and a greater degree of recirculation within the sea-breeze cell and overall a weaker ventilation of the western side of the island. Overall, the effect of the island on the regional background aerosol composition is to lift surface air rich in marine sulphates and add biogenic organics. It is not clear what aerosol profiles are like downwind of the west coast sea breeze, however it would be expected that the aerosol would remain lofted.

7.2 MCS-dominated regime

The majority of profiles performed during the MCS-dominated regime were upwind of Borneo (four) or over Kota Kinabalu of the west coast (nine). Only two profiles were performed over East Sabah (one morning and one afternoon) making it difficult to generalise about the effect this regime has on aerosol transport across the island. The substantial sulphate concentrations in Layer Two in the morning are largely removed by the afternoon, possibly by heavy rain events associated with an MCS. Organic aerosol loadings grow between morning and afternoon but the highest concentrations are near the surface, with a more rapid drop-off with altitude than seen in the ITC-dominated regime. This suggests surface emissions that are inefficiently mixed through the troposphere. This is consistent with the ECMWF reanalysis shown in Fig. 2(b) which shows no mean ascent of air mass, and the satellite image shown in Fig. 3(b) which shows Borneo to be covered by cirrus outflow from an MCS, which would be expected to reduce insolance and therefore terrestrial convection. It is also likely that higher heavy precipitation associated with the MCS system act to remove aerosol.

The averaged profile of Kota Kinabalu on the west coast, which does consist of a significant number of profiles, is markedly different from that of the ITC-dominated regime. Tephigrams tend to show little mixing and the wind profiles show far less wind shear than in the convective-dominated regime. This may be associated with extensive cirrus advecting from the active MCS to the northwest differential heating of land and sea to set up a sea breeze, such as that which was observed in the ITC-

dominated regime. It should be noted that, despite lower loadings in Layer Two over Kota Kinabalu than in the ITC-dominated regime, there were still significant aerosol loadings up to 712±71 hPa. Surface level back trajectories during the MCS-dominated regime were deemed "unclassified" by Robinson et al. (2011b), meaning they were highly changeable, which may be significant of MCS influence. Borneo is influenced by the south edge of the MCS, which might be expected to bring westerly winds, however trajectories released from 800 hPa (the altitude of Layer Two) show a south-easterly influence, similar to those in the ITC-dominated regime. It may be that the trajectory wind field inaccurately captures the MCS, or it may be that the clouds are being released from the rotation of the MCS and carried by the synoptic flow over Borneo.

8 Conclusions

Aerosol were being lofted higher into the atmosphere as a result of transit over Borneo, both by local direct convection and interactions with the local island circulation. This was regularly observed during OP3 in ITC-dominated periods. In contrast, periods when Borneo was affected by nearby MCS systems and their cirrus outflows were observed to result in less convective uplift due to reductions in insolation. Aerosol profiles upwind of Borneo show the vast majority of aerosol to be present below 930±10 hPa. During the ITC-dominated regime, aerosol was present in substantial quantities up to an average estimated height of 768±45 hPa as it leaves the west coast of the island, although substantial aerosol concentrations were occasionally observed up to ∼680 hPa, often with low sulphate loadings above this up to a height of ∼600 hPa. The surface mixed layer over the downwind coast was estimated to be below 947±23 hPa. The aerosol population in the layer above this showed a slight increase in sulphate aerosol concentrations throughout the day of 0.52±0.14, 0.68±0.32 and 0.74 μg sm^{-3} around 10:00, 13:00 and 18:00 respectively. Organic aerosol loadings in in this upper layer showed a more substantial increase of 0.94±0.32, 1.74±0.78 and 2.29 μg sm^{-3} around 10:00, 13:00 and 18:00 respectively.

A similar elevated layer of high aerosol concentrations was seen in profiles upwind of this over the island during the ITC-dominated regime. This layer tended to be dominated by sulphate aerosol in the morning (1.07±0.18 μg sm^{-3}) with organic aerosol concentrations growing throughout the day (from 0.28±0.15 to 0.85±0.09 μg sm^{-3}). Profiles in the vicinity of cumulonimbus clouds show very smooth transitions in aerosol loadings between the normal surface mixed layer height and above, strongly implying that moist convective uplift helps loft terrestrial aerosol above the turbulent mixed layer.

Transit of air masses over Borneo during periods dominated by ITC appears to deplete concentrations of regional aerosol though wet removal, whilst enhancing concentrations of SOA from terrestrial VOC emissions emissions. During periods influenced by MCS systems, there is less efficient transport of aerosol through the troposphere, either due to a reduction of surface insolation and asso-

ciated convection or a greater amount of wet removal of aerosol. Aerosol that is elevated by its transit over Borneo will have a longer atmospheric lifetime as it is more likely to be above precipitation that would deplete it through wet removal. It is possible that this interaction between marine boundary layer aerosol and terrestrial emissions and dynamics, is spread across the whole of the "maritime continent" network of tropical islands. This would present a regional orographic barrier to westerly marine air flowing from the Pacific. Widespread elevation of aerosol could have implications downwind, especially if the air masses travel to the pristine south Indian Ocean. The change in aerosol composition, from being dominated by sulphate to being dominated by fresh organic aerosol will lower the hygroscopicity of the aerosol population, affecting CCN concentrations downwind. This is the first comprehensive study in this region to analyse regional aerosol composition in the context of dynamical interactions between a tropical island and synoptic flow patterns, both in terms of local emissions and lofting. Assessing the effects of islands such as Borneo on regional aerosol allows effective modelling of aerosol lifetimes and, therefore, their impact on cloud formation, atmospheric chemistry and ultimately climate.

Acknowledgements. This work was supported by the UK Natural Environment Research Council through the OP3 (grant NE/D002117/1) and ACES (grant NE/E011179/1) projects. We thank the Malaysian and Sabah Governments for their permission to conduct research in Malaysia; the Malaysian Meteorological Department for access to the measurement site; Yayasan Sabah and the Royal Society's South East Asian Rain Forest Research Programme for logistical support; and the ground staff, engineers, scientists and flight crew of the FAAM aircraft. The authors thank the NERC Earth Observation Data Acquisition and Analysis Service (NEODAAS) for supplying data for this study, and the British Atmospheric Data Centre (BADC) and the European Centre for Medium Range Weather Forecasting (ECMWF) for the archiving service of ECMWF reanalysis data.

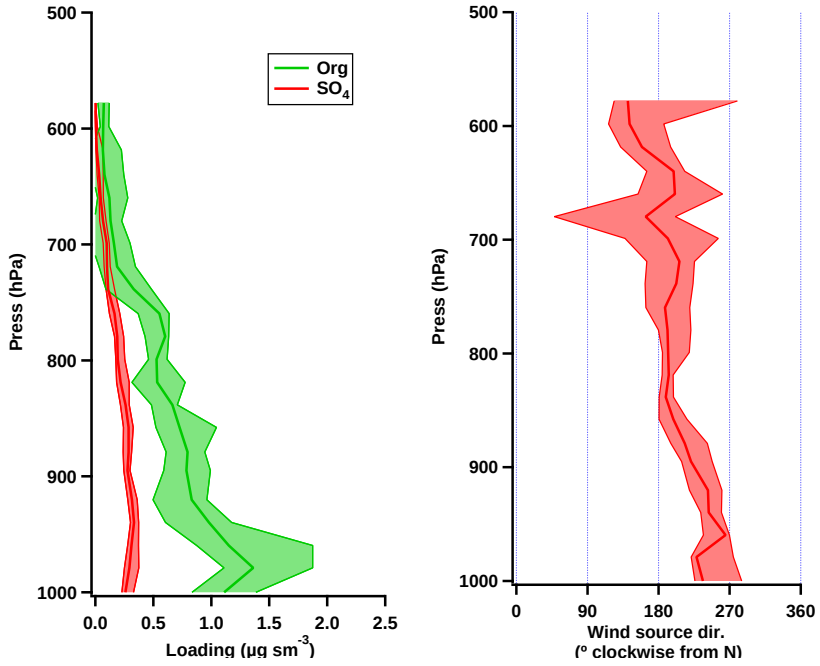

(a) (b)

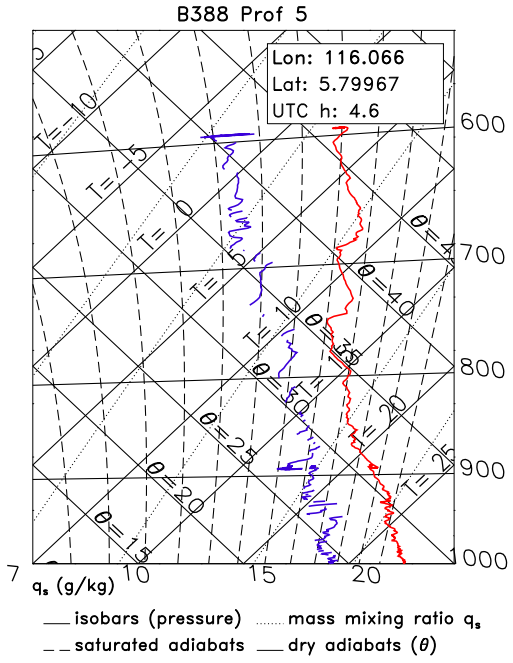

(c)

Fig. 12. Averaged altitude profiles (median and interquartile ranges) during the MCS-dominated regime over Kota Kinabalu on the west coast of Borneo of **(a)** organic and sulphate aerosol loading and **(b)** wind direction. **(c)** shows a tephigram detailing ambient temperature (red) and dewpoint temperature (blue). Averages comprised eight profiles from 16/07/08 and 17/07/08. Tephigram from flight 16/07/08 12:38 local.

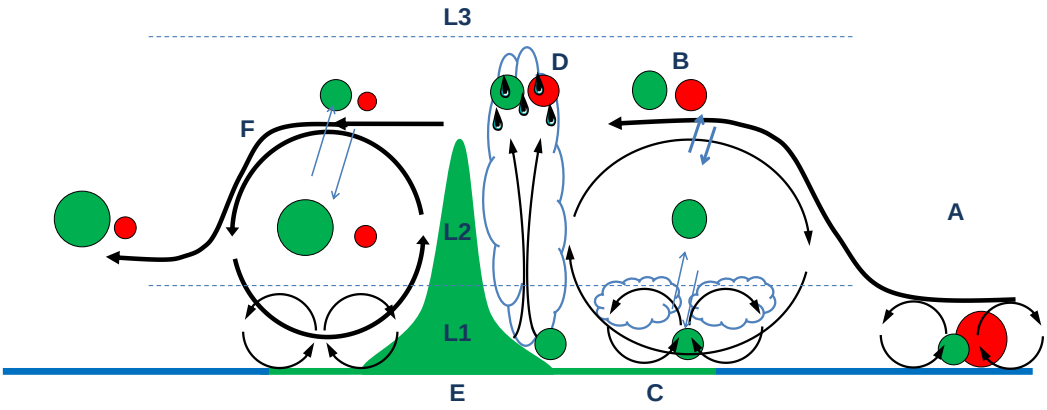

Fig. 13. Conceptual illustration of the dynamical processes as would be expected in local afternoon. Air mass travels from east (right) to west (left). Layers One, Two and Three indicated by L1, L2 and L3 with divisions marked with dashed line. It should be noted that the layer divisions were different between place and time. **(A)** sulphate and organics in a shallow marine boundary layer carried by synoptic flow. **(B)** synoptic flow is opposed to the sea-breeze circulation which is weekend. Turbulent mixing occurs between top of cell and synoptic flow. **(C)** shallow well mixed layer capped with cumulus clouds. **(D)** deep convective uplift lofts more organic aerosol, with precipitation events removing the regional aerosol. **(E)** orography induces uplift. **(F)** synoptic flow strengthens sea-breeze circulation. Some transfer of aerosol from synoptic flow to sea-breeze circulation which is recirculated.

References

Allan, J. D.: An Aerosol Mass Spectrometer: Instrument Development, Data Analysis Techniques and Quantitative Atmospheric Particulate Measurements, Phd, The University of Manchester, 2004.

Allan, J. D., Jimenez, J. L., Williams, P. I., Alfarra, M. R., Bower, K. N., Jayne, J. T., Coe, H., and Worsnop, D. R.: Quantitative sampling using an Aerodyne aerosol mass spectrometer 1. Techniques of data interpretation and error analysis, Journal of Geophysical Research, 108, 1–10, doi:10.1029/2002JD002358, http://www.agu.org/pubs/crossref/2003/2002JD002358.shtml, 2003.

Allan, J. D., Bower, K. N., Coe, H., Boudries, H., Jayne, J. T., Canagaratna, M. R., Millet, D. B., Goldstein, A., Quinn, P. K., Weber, R. J., and Worsnop, D. R.: Submicron aerosol composition at Trinidad Head, California, during ITCT 2K2: Its relationship with gas phase volatile organic carbon and assessment of instrument performance, Journal of Geophysical Research, 109, doi:10.1029/2003JD004208, http://www.agu.org/pubs/crossref/2004/2003JD004208.shtml, 2004.

Atkins, N. T. and Wakimoto, R. M.: Influence of the Synoptic-Scale Flow on Sea Breezes Observed during CaPE, Monthy Weather Review, 125, 2112–2130, doi:10.1175/1520-0493(1997)125⟨2112:IOTSSF⟩2.0.CO;2, 1997.

Avissar, R., Silva Dias, P., Silva Dias, M., and Nobre, C. A.: The Large-Scale Biosphere-Atmosphere Experiment in Amazonia (LBA): Insights and future research needs, Journal of Geophysical Research, 107, doi:10.1029/2002JD002704, http://www.agu.org/pubs/crossref/2002/2002JD002704.shtml, 2002.

Balkanski, Y. J., Jacob, D. J., Gardner, G. M., Graustein, W. C., and Turekian, K. K.: Transport and residence times of tropospheric aerosols inferred from a global three-dimensional simulation of Pb-210, 98, 20 573–20 586, 1993.

Canagaratna, M. R., Jayne, J. T., Jimenez, J. L., Allan, J. D., Alfarra, M. R., Zhang, Q., Onasch, T. B., Drewnick, F., Coe, H., Middlebrook, A., Delia, A., Williams, L. R., Trimborn, A. M., Northway, M. J., DeCarlo, P. F., Kolb, C. E., Davidovits, P., and Worsnop, D. R.: Chemical and microphysical characterization of ambient aerosols with the aerodyne aerosol mass spectrometer., Mass spectrometry reviews, 26, 185–222, doi:10.1002/mas.20115, http://www.ncbi.nlm.nih.gov/pubmed/17230437, 2007.

Capes, G., Johnson, B., McFiggans, G., Williams, P. I., Haywood, J., and Coe, H.: Aging of biomass burning aerosols over West Africa: Aircraft measurements of chemical composition, microphysical properties, and emission ratios, Journal of Geophysical Research, 113, doi:10.1029/2008JD009845, http://www.agu.org/pubs/crossref/2008/2008JD009845.shtml, 2008.

Capes, G., Murphy, J. G., Reeves, C. E., McQuaid, J. B., Hamilton, J. F., Hopkins, J. R., Crosier, J., Williams, P. I., and Coe, H.: Secondary organic aerosol from biogenic VOCs over West Africa during AMMA, Atmospheric Chemistry and Physics, 9, 3841–3850, doi:10.5194/acp-9-3841-2009, http://www.atmos-chem-phys.net/9/3841/2009/, 2009.

Chand, D., Guyon, P., Schmid, O., Frank, G., Rizzo, L., Mayol-Bracero, O., Gatti, L., and Andreae, M. O.: Optical and physical properties of aerosols in the boundary layer and free troposphere over the Amazon Basin during the biomass burning season, Atmospheric Chemistry and Physics, 6, 2911–2925, doi:10.5194/acp-6-2911-2006, 2006.

Chen, Q., Farmer, D. K., Schneider, J., Zorn, S. R., Heald, C. L., Karl, T. G., Guenther, A., Allan, J. D., Robinson, N., Coe, H., Kimmel, J. R., Pauliquevis, T., Borrmann, S., Pöschl, U., Andreae, M. O., Artaxo,

P., Jimenez, J. L., and Martin, S. T.: Mass spectral characterization of submicron biogenic organic particles in the Amazon Basin, Geophysical Research Letters, 36, doi:10.1029/2009GL039880, http://www.agu.org/pubs/crossref/2009/2009GL039880.shtml, 2009.

Claeys, M., Graham, B., Vas, G., Wang, W., Vermeylen, R., Pashynska, V., Cafmeyer, J., Guyon, P., Andreae, M. O., Artaxo, P., and Maenhaut, W.: Formation of secondary organic aerosols through photooxidation of isoprene., doi:10.1126/science.1092805, http://www.ncbi.nlm.nih.gov/pubmed/14976309, 2004.

Crook, N. A.: Understanding Hector: The Dynamics of Island Thunderstorms, Monthly Weather Review, 129, 1550–1563, doi:10.1175/1520-0493(2001)129⟨1550:UHTDOI⟩2.0.CO;2, http://journals.ametsoc.org/doi/abs/10.1175/1520-0493(2001)129⟨1550:UHTDOI⟩2.0.CO;2, 2001.

Cross, E., Slowik, J., Davidovits, P., Allan, J., Worsnop, D., Jayne, J., Lewis, D., Canagaratna, M., and Onasch, T.: Laboratory and Ambient Particle Density Determinations using Light Scattering in Conjunction with Aerosol Mass Spectrometry, Aerosol Science and Technology, 41, 343–359, doi:10.1080/02786820701199736, http://www.informaworld.com/openurl?genre=article\&issn=0278-6826\&volume=41\&issue=4\&spage=343, 2007.

DeCarlo, P. F., Kimmel, J. R., Trimborn, A., Northway, M. J., Jayne, J. T., Aiken, A. C., Gonin, M., Fuhrer, K., Horvath, T., Docherty, K. S., Worsnop, D. R., and Jimenez, J. L.: Field-deployable, high-resolution, time-of-flight aerosol mass spectrometer., Analytical chemistry, 78, 8281–9, http://www.ncbi.nlm.nih.gov/pubmed/17165817, 2006.

Drewnick, F., Hings, S. S., Decarlo, P., Jayne, J. T., Gonin, M., Fuhrer, K., Weimer, S., Jimenez, J. L., Borrmann, K. L. D. S., and Worsnop, D. R.: A new time-of-flight aerosol mass spectrometer TOF-AMS - Instrument description and first field deployment, Aerosol Science & Technology, 39, 637–658, 2005.

Foltescu, V. L., Selin, E., and Below, M.: Corrections for particle losses and sizing errors during aircraft aerosol sampling using a rosemounts inlet and the PMS LAS-X, Atmospheric environment, 29, 449–453, 1995.

Gahmberg, M., Savijarvi, H., and Leskinen, M.: The influence of synoptic scale flow on sea breeze induced surface winds and calm zones, Tellus A, 62, 209–217, doi:10.1111/j.1600-0870.2009.00423.x, http://doi.wiley.com/10.1111/j.1600-0870.2009.00423.x, 2010.

Guenther, A., Hewitt, C., Erickson, D., Fall, R., Geron, C., Graedel, T., Harley, P., Klinger, L., Lerdau, M., McKay, W., Pierce, T., Scholes, B., Steinbrecher, R., Tallmaraju, R., Taylor, J., and Zimmerman, P.: A global model of natural volatile organic compound emissions, Journal of Geophysical Research-Atmospheres, 100, 8873–8892, http://www.agu.org/pubs/crossref/1995/94JD02950.shtml, 1995.

Hallquist, M., Wenger, J. C., Baltensperger, U., Rudich, Y., Simpson, D., Claeys, M., Dommen, J., Donahue, N. M., George, C., Goldstein, A., Hamilton, J. F., Herrmann, H., Hudson, L. E., Iinuma, Y., Jang, M., Jenkin, M. E., Jimenez, J. L., Kiendler-Scharr, A., Maenhaut, W., McFiggans, G., Mentel, T. F., Monod, A., Prévôt, A. S. H., Seinfeld, J. H., Surratt, J. D., Szmigielski, R., and Wildt, J.: The formation, properties and impact of secondary organic aerosol: current and emerging issues, Atmospheric Chemistry and Physics, 9, 5155–5235, http://www.atmos-chem-phys.net/9/5155/2009/, 2009.

Hewitt, C., Lee, J., Barkley, M. P., Carslaw, N., Chappell, N. A., Coe, H., Collier, C., Commane, R., Davies, F., Di Carlo, P., Marco, C. F. D., Edwards, P. M., Evans, M. J., Fowler, D., Furneaux, K. L., Gallagher, M. W., Guenther, A., Heard, D. E., Helfter, C., Hopkins, J., Ingham, T., Irwin, M., Jones, C., Karunaharan, A., Langford, B., Lewis, A. C., Lim, S. F., Macdonald, S. M., Mackenzie, A. R., Mahajan, A. S., Malpass, S.,

Mcfiggans, G., Mills, G., Misztal, P., Moller, S., Monks, P. S., Nemitz, E., Oetjen, H., Oram, D., Palmer, P. I., Phillips, G. J., Plane, J. M. C., Pugh, T., Pyle, J. A., Reeves, C. E., Robinson, N. H., Stewart, D., Stone, D., and Whalley, L. K.: Oxidant and particle photochemical processes above a south-east Asian tropical rain forest (the OP3 project): introduction, rationale, location characteristics and tools, Atmospheric Chemistry and Physics, 163, 18 899–18 963, http://www.atmos-chem-phys.net/10/169/2010/acp-10-169-2010.pdf, 2010.

Hewitt, C. N., MacKenzie, A. R., Di Carlo, P., Di Marco, C. F., Dorsey, J. R., Evans, M., Fowler, D., Gallagher, M. W., Hopkins, J. R., Jones, C. E., Langford, B., Lee, J. D., Lewis, A. C., Lim, S. F., McQuaid, J., Misztal, P., Moller, S. J., Monks, P. S., Nemitz, E., Oram, D. E., Owen, S. M., Phillips, G. J., Pugh, T. A. M., Pyle, J. A., Reeves, C. E., Ryder, J., Siong, J., Skiba, U., and Stewart, D. J.: Nitrogen management is essential to prevent tropical oil palm plantations from causing ground-level ozone pollution., Proceedings of the National Academy of Sciences of the United States of America, 106, 18 447–51, doi:10.1073/pnas.0907541106, http://www.ncbi.nlm.nih.gov/pubmed/19841269, 2009.

Jimenez, J. L., Canagaratna, M. R., Donahue, N. M., Prevot, A. S. H., Zhang, Q., Kroll, J. H., DeCarlo, P. F., Allan, J. D., Coe, H., Ng, N. L., Aiken, A. C., Docherty, K. S., Ulbrich, I. M., Grieshop, A. P., Robinson, A. L., Duplissy, J., Smith, J. D., Wilson, K. R., Lanz, V. A., Hueglin, C., Sun, Y. L., Tian, J., Laaksonen, A., Raatikainen, T., Rautiainen, J., Vaattovaara, P., Ehn, M., Kulmala, M., Tomlinson, J. M., Collins, D. R., Cubison, M. J., Dunlea, E. J., Huffman, J. A., Onasch, T. B., Alfarra, M. R., Williams, P. I., Bower, K. N., Kondo, Y., Schneider, J., Drewnick, F., Borrmann, S., Weimer, S., Demerjian, K., Salcedo, D., Cottrell, L., Griffin, R., Takami, A., Miyoshi, T., Hatakeyama, S., Shimono, A., Sun, J. Y., Zhang, Y. M., Dzepina, K., Kimmel, J. R., Sueper, D., Jayne, J. T., Herndon, S. C., Trimborn, A. M., Williams, L. R., Wood, E. C., Middlebrook, A. M., Kolb, C. E., Baltensperger, U., and Worsnop, D. R.: Evolution of organic aerosols in the atmosphere., Science, 326, 1525–9, doi:10.1126/science.1180353, http://www.ncbi.nlm.nih.gov/pubmed/20007897, 2009.

Johnson, B., Shine, K., and Forster, P.: The semi-direct aerosol effect: Impact of absorbing aerosols on marine stratocumulus, Quarterly Journal of the Royal Meteorological Society, 130, 1407–1422, doi:10.1256/qj.03.61, http://doi.wiley.com/10.1256/qj.03.61, 2004.

Kanakidou, M., Seinfeld, J., Pandis, S. N., Barnes, I., Dentener, F., Facchini, M., Van Dingenen, R., Ervens, B., Nenes, A., and Nielsen, C.: Organic aerosol and global climate modelling: a review, Atmospheric Chemistry and Physics, 5, 1053–1123, http://authors.library.caltech.edu/620/1/KANacp05.pdf, 2005.

Kettle, A. J. and Andreae, M. O.: Flux of dimethylsulfide from the oceans: A comparison of updated data sets and flux models, Journal of Geophysical Research, 105, 26 793–26 808, doi:10.1029/2000JD900252, http://www.agu.org/pubs/crossref/2000/2000JD900252.shtml, 2000.

Krejci, R., Reus, M. D., Williams, J., Fischer, H., and Andreae, M. O.: Spatial and temporal distribution of atmospheric aerosols in the lowermost troposphere over the Amazonian tropical rainforest, Atmospheric Chemistry and Physics, 1985, 1527–1543, http://hal.archives-ouvertes.fr/docs/00/30/13/22/PDF/acpd-4-3565-2004.pdf, 2005.

Lebel, T., Parker, D. J., Flamant, C., Bourlès, B., Marticorena, B., Mougin, E., Peugeot, C., Diedhiou, A., Haywood, J. M., Ngamini, J. B., Polcher, J., Redelsperger, J.-L., and Thorncroft, C. D.: The AMMA field campaigns: multiscale and multidisciplinary observations in the West African region, Quarterly Journal of the Royal Meteorological Society, 136, 8–33, doi:10.1002/qj.486, http://doi.wiley.com/10.1002/qj.486,

2010.

Liao, H. and Seinfeld, J.: Effect of clouds on direct aerosol radiative forcing of climate, Journal of Geophysical Research, 105, 3781–3788, doi:10.1016/S0021-8502(97)85212-3, http://linkinghub.elsevier.com/retrieve/pii/S0021850297852123, 1997.

Liu, P. S. K., Leaitch, W. R., Strapp, J. W., and Wasey, M. A.: Response of Particle Measuring Systems Airborne ASASP and PCASP to NaCl and Latex Particles, Aerosol Science and Technology, 16, 83–95, doi:10.1080/02786829208959539, http://www.informaworld.com/openurl?genre=article\&doi=10.1080/02786829208959539\&magic=crossref||D404A21C5BB053405B1A640AFFD44AE3, 1992.

Martin, S. T., Andreae, M. O., Althausen, D., Artaxo, P., Baars, H., Borrmann, S., Chen, Q., Farmer, D. K., Guenther, a., Gunthe, S. S., Jimenez, J. L., Karl, T., Longo, K., Manzi, a., Müller, T., Pauliquevis, T., Petters, M. D., Prenni, a. J., Pöschl, U., Rizzo, L. V., Schneider, J., Smith, J. N., Swietlicki, E., Tota, J., Wang, J., Wiedensohler, a., and Zorn, S. R.: An overview of the Amazonian Aerosol Characterization Experiment 2008 (AMAZE-08), Atmospheric Chemistry and Physics, 10, 11 415–11 438, doi:10.5194/acp-10-11415-2010, http://www.atmos-chem-phys.net/10/11415/2010/, 2010a.

Martin, S. T., Andreae, M. O., Artaxo, P., Baumgardner, D., Chen, Q., Goldstein, A. H., Guenther, A., Heald, C. L., Mayol-Bracero, O. L., McMurry, P. H., Pauliquevis, T., Pöschl, U., Prather, K. A., Roberts, G. C., Saleska, S. R., Silva Dias, M. A., Spracklen, D. V., Swietlicki, E., and Trebs, I.: Sources and properties of Amazonian aerosol particles, Reviews of Geophysics, 48, doi:10.1029/2008RG000280, http://www.agu.org/pubs/crossref/2010/2008RG000280.shtml, 2010b.

Matthew, B., Middlebrook, A., and Onasch, T.: Collection Efficiencies in an Aerodyne Aerosol Mass Spectrometer as a Function of Particle Phase for Laboratory Generated Aerosols, Aerosol Science and Technology, 42, 884–898, doi:10.1080/02786820802356797, http://www.informaworld.com/smpp/content~db=all~content=a902918478, 2008.

McMorrow, J. and Talip, M. A.: Decline of forest area in Sabah, Malaysia: Relationship to state policies, land code and land capability, Global Environmental Change, 11, 217–230, doi:10.1016/S0959-3780(00)00059-5, http://linkinghub.elsevier.com/retrieve/pii/S0959378000000595, 2001.

Osborne, S. R., Haywood, J. M., and Bellouin, N.: In situ and remote-sensing measurements of the mean microphysical and optical properties of industrial pollution aerosol during ADRIEX, Quarterly Journal of the Royal Meteorological Society, 133, 17–32, doi:10.1002/qj.92, http://doi.wiley.com/10.1002/qj.92, 2007.

Pearson, G., Davies, F., and Collier, C.: Remote sensing of the tropical rain forest boundary layer using pulsed Doppler lidar, Atmospheric Chemistry and Physics, 10, 5891–5901, doi:10.5194/acp-10-5891-2010, http://www.atmos-chem-phys.net/10/5891/2010/, 2010.

Robinson, N. H., Hamilton, J. F., Allan, J. D., Langford, B., Oram, D. E., Chen, Q., Docherty, K., Farmer, D. K., Jimenez, J. L., Ward, M. W., Hewitt, C. N., Barley, M. H., Jenkin, M. E., Rickard, A. R., Martin, S. T., McFiggans, G., and Coe, H.: Evidence for a significant proportion of Secondary Organic Aerosol from isoprene above a maritime tropical forest, Atmospheric Chemistry and Physics, 11, 1039–1050, doi:10.5194/acp-11-1039-2011, http://www.atmos-chem-phys.net/11/1039/2011/, 2011a.

Robinson, N. H., Newton, H., Allan, J. D., Irwin, M., Hamilton, J. F., Chen, Q., Martin, S. T., McFiggans, G., and Coe, H.: Source attribution during the OP3 project using backwards air mass trajectories (in prep.), Atmos. Chem. Phys., 2011b.

Salcedo, D., Onasch, T. B., Canagaratna, M. R., Dzepina, K., Huffman, J. A., Jayne, J. T., Worsnop, D. R., Kolb, C. E., Weimer, S., Drewnick, F., Allan, J. D., Delia, A. E., and Jimenez, J. L.: Technical Note: Use of a beam width probe in an Aerosol Mass Spectrometer to monitor particle collection efficiency in the field, Atmospheric Chemistry and Physics, 7, 549–556, http://www.atmos-chem-phys.net/7/549/2007/, 2007.

Walter Strapp, J., Leaitch, W., and Liu, P.: Hydrated and Dried Aerosol-Size-Distribution Measurements from the Particle Measuring Systems FSSP-300 Probe and the Deiced PCASP-100X Probe, Journal of Atmospheric and Oceanic Technology, 9, 548–555, doi:10.1175/1520-0426(1992)009⟨0548:HADASD⟩2.0.CO;2, http://journals.ametsoc.org/doi/abs/10.1175/1520-0426(1992)009⟨0548:HADASD⟩2.0.CO;2, 1992.

Whitehead, J. D., Gallagher, M. W., Dorsey, J. R., Robinson, N., Gabey, A. M., Coe, H., McFiggans, G., Flynn, M. J., Ryder, J., Nemitz, E., and Davies, F.: Aerosol fluxes and dynamics within and above a tropical rainforest in South-East Asia, Atmospheric Chemistry and Physics, 10, 9369–9382, doi: 10.5194/acp-10-9369-2010, http://www.atmos-chem-phys.net/10/9369/2010/, 2010.

Williams, I., Gallagher, M. W., Choularton, T. W., Coe, H., Bower, K. N., and McFiggans, G.: Aerosol Development and Interaction in an Urban Plume, Aerosol Science & Technology, 32, 120–126, doi: 10.1080/027868200303821, http://www.informaworld.com/10.1080/027868200303821, 2000.

4.4 Paper III: Evidence for a significant proportion of secondary organic aerosol from isoprene above a maritime tropical forest

N. H. Robinson, J. F. Hamilton, J. D. Allan, B. Langford, D. E. Oram, Q. Chen, K. Docherty, D. K. Farmer, J. L. Jimenez, M. W. Ward, C. N. Hewitt, M. H. Barley, M. E. Jenkin, A. R. Rickard, S. T. Martin, G. McFiggans and H. Coe

Atmospheric Chemistry and Physics, 11, 1039-1050, doi:10.5194/acp-11-1039-2011

Supporting Material reproduced in Appendix D

Published February 2011

Overview

This paper describes evidence that a significant proportion of organic aerosol in Borneo is from oxidation of isoprene. It also speculates that it may be produced through a formerly unreported mechanism. PMF analysis of the ground site AMS organic mass spectral data yielded four factors: named OOA1, OOA2, 91Fac and 82Fac. In particular the 82Fac, which was highly robust to changes in initial settings in the PMF analysis, showed a distinctive peak at m/z 82. Inspection of high-resolution AMS data showed the majority of this signal to be from $C_5H_6O^+$, and off-line GC×GC/ToF-MS analysis of filter samples further identified it as methylfuran. The m/z 82 signal in the aircraft data set was found to correlate with gas phase isoprene oxidation products. Comparison with other projects showed the m/z 82 signal, both in terms of fraction of total mass and peak prominence, was larger in data sets from isoprene dominated environments then in terpene dominated environments.

This work shows that isoprene SOA makes up and unusually large fraction of the organic aerosol population in Borneo. As the oil palm plantations are high isoprene emitters, this has implications for the organic aerosol burden under future land use change. It is also the first time that isoprene SOA has been identified using an AMS, opening up the opportunity for other in-situ high time resolution measurements in subsequent studies.

Contributions of authors

Hamilton performed filter sampling and associated GC×GC/ToF-MS analysis. Allan assisted with field AMS measurements and data analysis. Langford gathered and analysed ground PTRMS data. Oram gathered and analysed aircraft PTRMS data. Docherty, Farmer and Jimenez gathered and analysed AMS data from the BEARPEX project. Farmer

also wrote Appendix A. Ward performed GC×GC/ToF-MS analysis of filters. Hewitt assisted with manuscript preparation. Barley performed aerosol partitioning modelling and provided relevant text for Section 4. Jenkin and Rickard assisted with preparation of the manuscript and with interpretation of the data. Martin assisted with preparation of the manuscript. McFiggans and Coe assisted with preparation of the manuscript and interpretation of the data.

Robinson performed and analysed AMS aerosol measurements, interpreted the data and wrote the manuscript.

Atmos. Chem. Phys., 11, 1039–1050, 2011
www.atmos-chem-phys.net/11/1039/2011/
doi:10.5194/acp-11-1039-2011

Atmospheric Chemistry and Physics

Evidence for a significant proportion of Secondary Organic Aerosol from isoprene above a maritime tropical forest

N. H. Robinson[1], J. F. Hamilton[2], J. D. Allan[1,3], B. Langford[4], D. E. Oram[5], Q. Chen[6], K. Docherty[7,8], D. K. Farmer[7,8], J. L. Jimenez[7], M. W. Ward[2], C. N. Hewitt[4], M. H. Barley[1], M. E. Jenkin[9], A. R. Rickard[10], S. T. Martin[6], G. McFiggans[1], and H. Coe[1]

[1]Centre for Atmospheric Science, School of Earth Atmospheric and Environmental Science, University of Manchester, UK
[2]Department of Chemistry, University of York, UK
[3]National Centre for Atmospheric Science, University of Manchester, UK
[4]Lancaster Environment Centre, Lancaster University, Lancaster, UK
[5]National Centre for Atmospheric Science, University of East Anglia, UK
[6]School of Engineering and Applied Sciences, Harvard University, USA
[7]Department of Chemistry and Biochemistry, and CIRES, University of Colorado at Boulder, CO, USA
[8]Cooperative Institute for Research in Environmental Sciences, University of Colorado at Boulder, CO, USA
[9]Atmospheric Chemistry Services, Okehampton, UK
[10]National Centre for Atmospheric Science, School of Chemistry, University of Leeds, UK

Received: 4 October 2010 – Published in Atmos. Chem. Phys. Discuss.: 1 November 2010
Revised: 14 January 2011 – Accepted: 29 January 2011 – Published: 4 February 2011

Abstract. Isoprene is the most abundant non-methane biogenic volatile organic compound (BVOC), but the processes governing secondary organic aerosol (SOA) formation from isoprene oxidation are only beginning to become understood and selective quantification of the atmospheric particulate burden remains difficult. Organic aerosol above a tropical rainforest located in Danum Valley, Borneo, Malaysia, a high isoprene emission region, was studied during Summer 2008 using Aerosol Mass Spectrometry and offline detailed characterisation using comprehensive two dimensional gas chromatography. Observations indicate that a substantial fraction (up to 15% by mass) of atmospheric sub-micron organic aerosol was observed as methylfuran (MF) after thermal desorption. This observation was associated with the simultaneous measurements of established gas-phase isoprene oxidation products methylvinylketone (MVK) and methacrolein (MACR). Observations of MF were also made during experimental chamber oxidation of isoprene. Positive matrix factorisation of the AMS organic mass spectral time series produced a robust factor which accounts for an average of 23% (0.18 $\mu g\,m^{-3}$), reaching as much as 53% (0.50 $\mu g\,m^{-3}$) of the total oraganic loading, identified by (and highly correlated with) a strong MF signal. Assuming that this factor is generally representative of isoprene SOA, isoprene derived aerosol plays a significant role in the region. Comparisons with measurements from other studies suggest this type of isoprene SOA plays a role in other isoprene dominated environments, albeit with varying significance.

Correspondence to: H. Coe
(hugh.coe@manchester.ac.uk)

1 Introduction

In order to assess the regional and global impacts of anthropogenic aerosols, it is necessary to quantify the contribution of the natural background. Aerosols can interact directly with incoming radiation by scattering or absorption, or indirectly through their effect on cloud formation and lifetime. A large fraction of the background particulate matter in the atmosphere is composed of organics thought to be formed by secondary processes from biogenic precursors (Kanakidou et al., 2005). Isoprene (2-methyl-1,3-butadiene) is potentially a major source of secondary organic aerosol (SOA) (Henze and Seinfeld, 2006), but highly time resolved atmospheric identification of isoprene derived SOA have so far proven elusive (Hallquist et al., 2009). In Amazonia, 2-methyltetrols identified on ambient filter samples were hypothesised to arise from isoprene oxidation (Claeys et al., 2004), and subsequently found to be present

in chamber photo-oxidation of isoprene under low NO_x conditions (<1 ppb of NO_x with isoprene:NO_x ~500:1; Surratt et al., 2006). Low NO_x isoprene chamber studies have identified reactive photo-oxidation products in the gaseous and particulate phases such as epoxides (Paulot et al., 2009; Surratt et al., 2010), tetrols (Surratt et al., 2006, 2010; Kleindienst et al., 2009) and organosulphates (Surratt et al., 2008). These isoprene derived SOA species have also been measured offline in field studies (Chan et al., 2010; Surratt et al., 2008).

While previous work has identified a number of potentially important mechanisms (Chan et al., 2010; Paulot et al., 2009), the ambient measurements are largely based on offline analysis of bulk samples. These measurements are limited by low time-resolution, which prevents detailed photochemical analysis and comparison to rapidly changing parameters, such as photolysis rates and oxidant concentrations. However, one recent study has measured isoprene SOA online, with IEPOX-derived organosulphates being detected using Particle Analysis by Laser Mass Spectrometry (PALMS; Froyd et al., 2010).

The Aerodyne Aerosol Mass Spectrometer (AMS; Canagaratna et al., 2007) allows for online measurements of organic aerosols with a high time resolution and has been used previously for studies concerning isoprene oxidation (e.g. Capes et al., 2009). While the AMS reports bulk organic matter, the indentification of specific chemical markers is required for more comprehensive biogenic source apportionment.

Here we present results from intensive measurements in an isoprene-dominated tropical forest environment and attempt to interpret a previously unreported chemical marker within the measurements. Factor analysis and comparisons with other datasets are used to estimate its importance both locally and in a global context.

2 Measurements

Measurements were made above a South East Asian Rainforest at the Danum Valley Conservation Area Global Atmospheric Watch (GAW) station, Sabah, in Malaysian Borneo (4.981° N, 117.844° E) as part of both the Oxidant and Particulate Photochemical Processes Above a South East Asian Rainforest project (OP3) (Hewitt et al., 2009, 2010) and the Aerosol Coupling in the Earth's System (ACES) project, during June and July 2008. A wide suite of aerosol, gas, radical and meteorological instruments were deployed in order to study the local atmospheric chemical processes as comprehensively as possible. In addition to the ground-based measurements, airborne measurements were made using instruments aboard the Facility for Airborne Atmospheric Measurements (FAAM) BAe 146 aircraft.

At the ground site, air was sampled from a height of 33 m above ground level on the top of a ridge surrounded by rainforest. The inlet sampled at a rate of 1500 l min^{-1} through a 30 m long, 15 cm i.d. diameter polypropylene tube insulated against solar heating. Air was then sub-sampled isokinetically from the centre of this flow at 35 l min^{-1}. To avoid condensation in the lines, sampled air was dried using a 780 tube Nafion drier using a dry air counter flow, where the air was decelerated to the laminar flow regime. After drying the air was decelerated further before being sampled by the suite of online instruments. Comparison of size distributions at the top and bottom of the inlet show that the aerosol transmission efficiency is approximately 70% in the size range 0.3–1 µm and comparison of total number series show a transmission efficiency of >96% for the smaller particles that dominate the number mode (Whitehead et al., 2010). The aircraft missions consisted of two separate sets of stacked straight and level runs (at 100–250, 1500, 3000 and 6000 m) over regions of rainforest (centred around the ground site) and homogeneous agro-industrial region of oil palm agriculture (centred around 5.25° N, 118.25° E). Aerosol was sampled on board the FAAM through a Rosemount inlet (Foltescu et al., 1995) and approximately 0.7 m of stainless steel tubing with a total residence time of ~4 s in the inlet system.

Filter samples (Thermo Scientific Partisol) were collected at the ground site from a height of 10 m. Particles less than 2.5 µm were collected onto pre-fired quartz filters which were transported and stored at −20 °C until analysis. Organic aerosol material was thermally desorbed from the filter for off-line analysis by comprehensive two dimensional gas chromatography with detection by Time-of-Flight Mass Spectrometry (GC × GC/ToF-MS) (Phillips and Beens, 1999; Hamilton et al., 2004). A dual stage commercial thermal desorption injector was used incorporating a thermal desorption unit (TDU) connected to a programmable-temperature vaporisation (PTV) injector, CIS-4 plus (Gerstel, Mulheim an der Ruhr, Germany), using a heated transfer line. 10–20 mg of filter paper containing each different sample was loaded into cleaned thermodesorption tubes using tweezers to ensure no contamination of the sample. The GC × GC/ToF-MS system consisted of an Agilent 6890 (Agilent Technologies, Palo Alto, CA, USA) gas chromatograph and a Pegasus III TOF-MS (LECO, St. Joseph, MI, USA). The first column was a non-polar DB5 (29 m × 0.32 mm i.d. ×0.25 µm film thickness) and the second column a DB17 (1.5 m × 0.10 mm i.d. ×0.10 µm film thickness).

Ground and airborne VOC measurements were made using Proton Transfer Reaction Mass Spectrometry (PTRMS) (Lindinger et al., 1998). Ground VOC measurements were made using an inlet separate to the one described above and further details can be found in Langford et al. (2010) and Murphy et al. (2010). The PTRMS can measure methylvinylketone (MVK) and methacrolein (MACR), both first generation isoprene oxidation products. These species have the same molecular mass and cannot be separated using this technique, so are reported as the sum of the two, referred to as MVK + MACR.

Online aerosol composition was measured using two Aerodyne time of flight Aerosol Mass Spectrometers; a high mass resolution version (HR-AMS) (DeCarlo et al., 2006) for measurements at the 33 m level of the ground site measurement tower, and a compact version (C-AMS) (Drewnick et al., 2005) for airborne measurements on the FAAM. The AMS provides quantitative online measurements of submicron non-refractory aerosol composition and size. Despite extensive fragmentation of particulate matter species, compositional information can be gained from inspection of ions in the mass spectra. For example, the ratio of *m/z* 44 (mainly CO_2^+) to *m/z* 43 (mainly $C_2H_3O^+$) can be used as a proxy for the oxidation of organic aerosols (Morgan et al., 2010; Ng et al., 2010) and *m/z* 60 can be used as a marker for fresh biomass burning (Alfarra et al., 2007; Capes et al., 2008). The high resolution mode of the HR-AMS can resolve ion mass at a higher resolution (∼4300) than the C-AMS, allowing separation of ions with different elemental composition detected at the same *m/z*.

Positive matrix factorisation (PMF) analysis was also performed on the organic HR-AMS unit mass resolution data. This multivariate technique attempts to explain the AMS ensemble organic mass spectral time series as the sum of time series of differing amounts of static "factor" spectra which can then be linked to distinct contributions to the total organic mass (Paatero and Tapper U., 1994; Paatero, 1997; Ulbrich et al., 2009). Details of this analysis are included in the Supplement. In short, a variety of solutions were calculated exploring different starting parameters and rotational ambiguities, and the most satisfactory solution was obtained when four factors were used. A detailed discussion of the results of PMF analysis will be included in Robinson et al. (2011a).

3 Results

Total sub-micron non-refractory organic aerosol mass was less in Borneo than typical measurements in the Northern mid latitudes, which have an average of 2.8 µg m^{-3} for remote sites (Zhang et al., 2007). A mean organic matter loading of 0.74 µg m^{-3} was measured from the ground site, which is comparable to a mean loading of 0.64 µg m^{-3} measured in Amazonia (Chen et al., 2009). A time series of organic and inorganic sub-micron non-refractory aerosol loading is shown in Fig. 1. The ambient organic spectra from both AMS instruments shows a distinctive peak at *m/z* 82 (Fig. 2a and b), a feature not seen in the mid-latitude environments that make up the majority of ambient AMS observations to date. Furthermore, the high mass resolution capability of the HR-AMS was able to attribute the majority of the *m/z* 82 peak of the AMS mass spectrum to the $C_5H_6O^+$ ion (Fig. 2b and c). One of the PMF factors exhibited strong signals at *m/z* 82 and 53, henceforth called 82Fac, which was found to be very robust when subjected to variations in the starting conditions

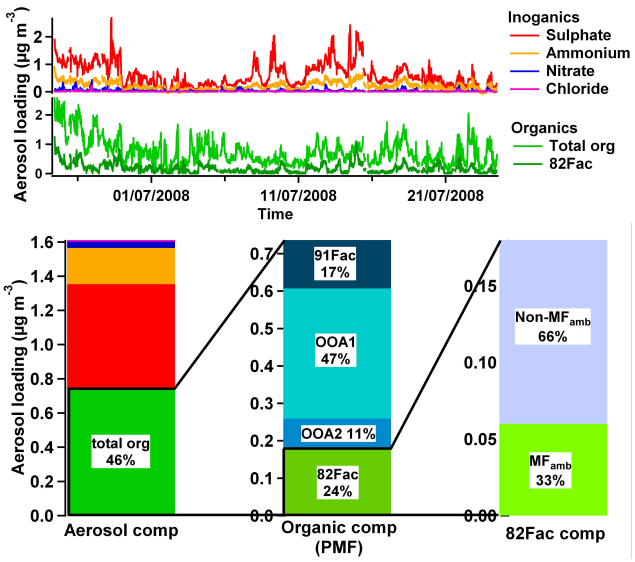

Fig. 1. Top, time series of inorganic and, below that, organic aerosol loading as measured by the AMS. The organic time series also details the *m/z* 82 containing PMF factor (82Fac). On the bottom are bars showing: the mean aerosol composition (with same colour scheme as in the time series legend); an expansion of the organic component to show the individual PMF factors; and an expansion of the 82Fac to show the contribution from MF which is calculated from the $C_5H_6O^+$ signal using Eq. (1).

(starting seed) or when rotational ambiguity in the solutions was explored (fpeak; see Supplement and Fig. 1). It was closely correlated with the *m/z* 82 peak with an r^2 of 0.86. Also, the other factors contained largely insignificant contributions from this *m/z*.

GC × GC chromatography was used to investigate the source of the *m/z* 82 ion, as shown in Fig. 3. The dominant peak was identified as methylfuran (MF) based on a standard solution retention time and electron ionisation mass spectrum, although under this column set, the 2- and 3-methylfuran isomers cannot be separated. It is clear that there are no other substantial contributions to $C_5H_6O^+$. The AMS *m/z* 82 peak was found to occur in conjunction with a prominent *m/z* 53 peak (Pearson's r^2 of 0.96) corresponding to $C_4H_5^+$, the most abundant electron ionisation fragment ion of MF (NIST mass spec database, Stein, 2009). Combined with the GC × GC/ToF-MS results, this suggests that the *m/z* 82 fragment in the AMS can be attributed to the MF molecular ion, and confirms that the filter-identified MF was particulate and was not attributable to a gaseous artifact.

An AMS spectrum of pure 3-methylfuran (3MF) (Fig. 2e) was obtained by nebulising commercially available 3MF (Fisher Scientific, UK; 98% pure) suspended in deionized water in the laboratory. A background spectrum of deionized water measured using the same equipment was subtracted to remove any influences from contamination sources. The measured sample spectrum compared well to the 3MF

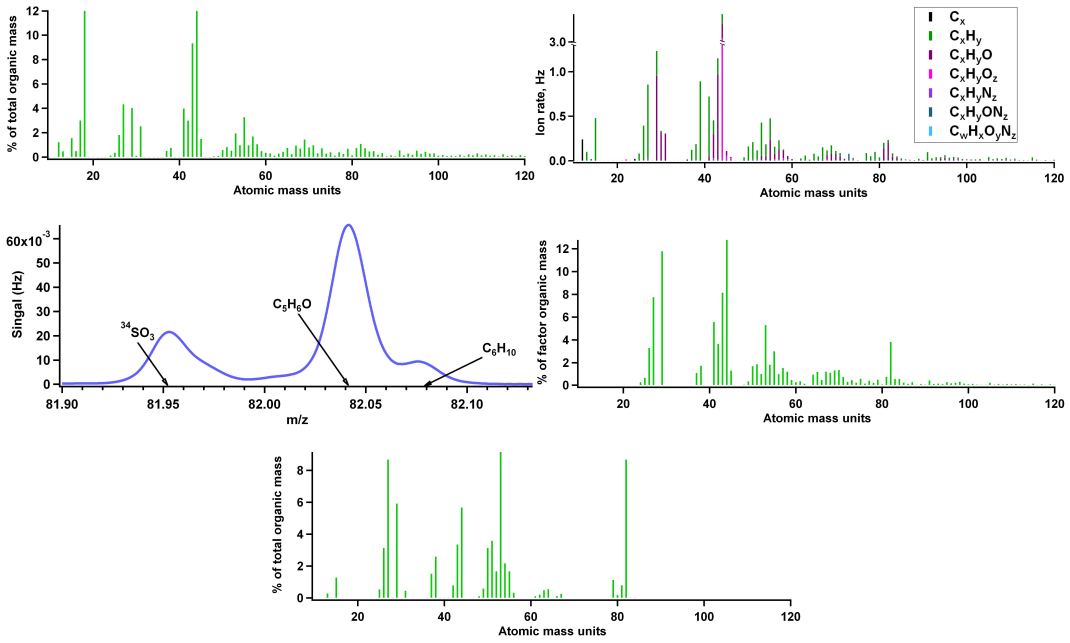

Fig. 2. Various AMS mass spectra showing a MF peak at *m/z* 82, including **(a)** a C-AMS mass spectrum measured aboard the FAAM aircraft during a period of high *m/z* 82 signal, **(b)** a high resolution mass spectrum measured from the ground site during a period of high MF signal, **(c)** detail of the *m/z* 82 peaks during the same period of high MF signal, **(d)** the 82Fac organic aerosol factor from PMF analysis of the ground site mass spectra and **(e)** a mass spectrum of 3MF suspended in water and measured in the laboratory.

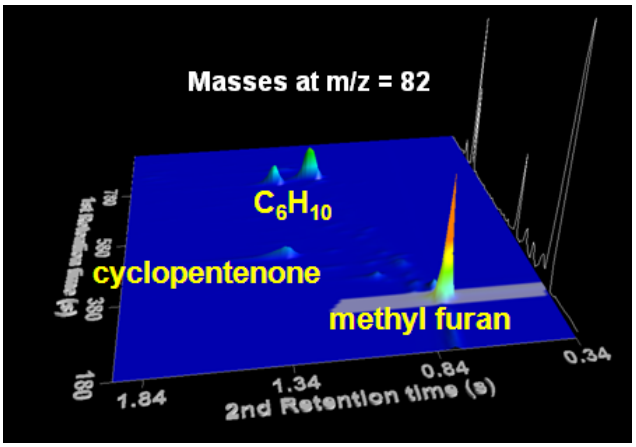

Fig. 3. GC × GC chromatogram of *m/z* 82. The first and second retention times (s) are plotted against the y- and x-axis respectively. The dominant peak is based on methyfuran.

reference spectrum (NIST mass spec database, Stein, 2009) and the unusual features of the ambient organic spectrum, such as the prominent *m/z* 82 and 53 peaks. Inspection of the high resolution *m/z* 82 peak of the pure 3MF mass spectrum showed only $C_5H_6O^+$ ions to be present, comprising 13% of the total organic mass.

The average diurnal profile of the $C_5H_6O^+$ signal shows an increase throughout the day with a maximum in the early evening (Fig. 4a). This is also the case for the diurnal profile of the fraction of organic aerosol at $C_5H_6O^+$ (Fig. 4b). These elevated levels in the evening may be caused by partitioning of semi-volatile aerosol as the ambient temperature drops. They may also be transported from the isoprene rich oil palm plantations (Hewitt et al., 2009) close to the site (around 30 km), causing a time lag between production and measurement. The first-generation isoprene oxidation products MVK+MACR, also show a strong diurnal cycle linked to the peak in the emission of isoprene at midday with the delay caused by the photochemical reaction rate. If it is assumed that the $C_5H_6O^+$ signal has a similar precursor, the fact it peaks later in the day could imply that it is produced by a longer or slower sequence of reactions.

Airborne PTRMS measurements of MVK+MACR, and AMS measurements of *m/z* 82 were also compared (Fig. 5). The median of the AMS *m/z* 82 and *m/z* 53 peaks measured in the boundary layer over each of eight individual flights correlated well with gas phase MVK+MACR, with respective Pearson's r^2 values of 0.92 and 0.87. This shows that both measurements exhibited systematically similar daily increases, which would be expected if they shared a common precursor. A substantial *m/z* 82 signal was observed throughout the surface mixed layer to a height of 3000 m, with little signal observed in the lower free troposphere above (Fig. 6a). That MF was measured throughout the boundary layer shows

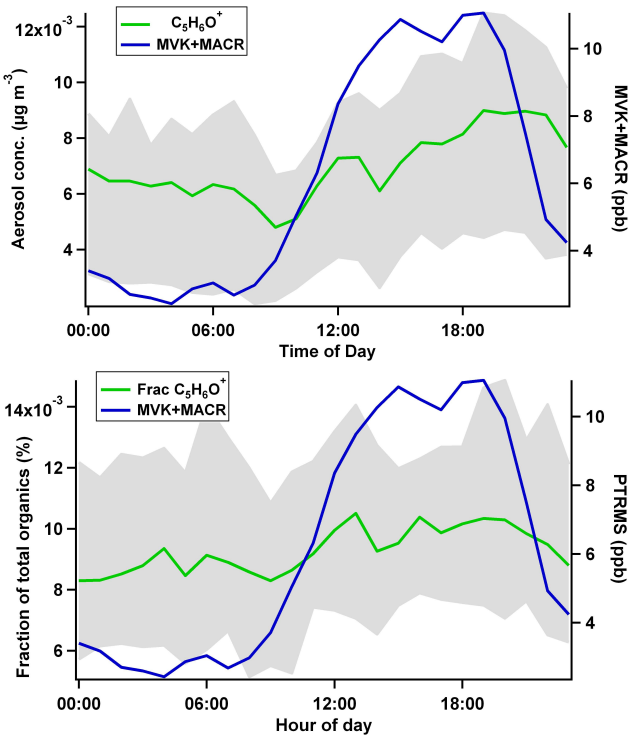

Fig. 4. Diurnal averages of **(a)** $C_5H_6O^+$ signal and MVK+MACR and **(b)** fraction of organic signal at $C_5H_6O^+$ and MVK+MACR. $C_5H_6O^+$ interquartile ranges are shown by shaded regions.

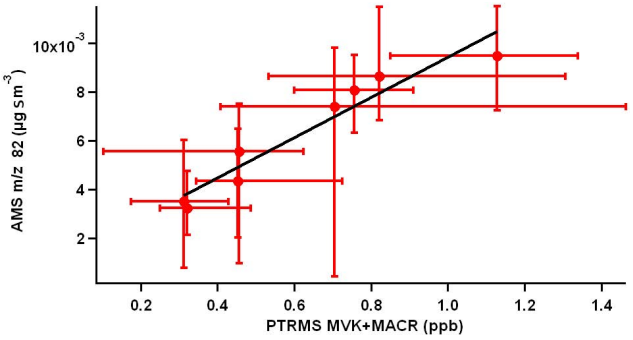

Fig. 5. AMS *m/z* 82 aerosol loading (in $\mu g\ sm^{-3}$, defined as $\mu g\ m^{-3}$ at 273 K and 1013 hPa with no condensation of evaporation) vs. PTRMS gas phase MVK + MACR as measured in the boundary layer from the FAAM research aircraft. Each data point represents the median of all boundary layer data collected during a single flight. Bars are 25th and 75th percentiles.

that it is of regional importance. Altitude profiles show the AMS aerosol signal at *m/z* 82 increases throughout the day, at all altitudes in the boundary layer, which is consistent with production from photochemical processing of precursors rather than direct emission from the surface. This increase in the afternoon is also observed in the altitude profile of gas phase MVK+MACR (Fig. 6b), although this increase is mostly below 2000 m. The averaged values of organic mass and *m/z* 82 at the lowest altitudes are similar to those measured at the ground site at the same time of day. The altitude profiles are consistent with semi-volatile aerosol partitioning at the top of the boundary layer where it is cooler, with a change of temperature of 298 K at ∼500 m to 283 K at ∼3000 m. This may also explain the disparity between the MVK+MACR profile and the *m/z* 82 profile at the top of the boundary layer.

4 Possible sources of MF

Previous studies have presented evidence of gas-phase methylfuran formation through oxidation of isoprene by OH radicals: MF has been measured in simulation chamber studies of isoprene oxidation (Atkinson et al., 1989; Ruppert and Becker, 2000; Sprengnether et al., 2002) and, in a study of a rural US forest, ambient measurements of gaseous MF were found to correlate with isoprene (Montzka et al., 1995). The likelihood of MF being present in the condensed phase was investigated using methods to estimate first the normal boiling point (Nannoolal et al., 2004), and then the vapour pressure (Nannoolal et al., 2008), evaluated as being the best available for atmospheric purposes (Barley and McFiggans, 2010). A literature boiling point was used (Burness, 1956) (338.65 K) with the above vapour pressure method to give an estimated value of 0.217 atm at 298.15 K. This value was then used to estimate the abundance of MF that would be expected to be present in secondary organic aerosol under equilibrium conditions at 298.15 K. Using a partitioning model (Barley et al., 2009) with a reasonable and representative set of assumptions ($2\ \mu g\ m^{-3}$ of completely involatile, perfectly organic core of molar mass $320\ g\ mol^{-1}$ with total concentration of the considered molecule set to $2\ \mu g\ m^{-3}$), it was estimated that MF contributed $1.41 \times 10^{-9}\ \mu g\ m^{-3}$ to the condensed mass (7.05×10^{-8}% by mass). Based upon an equilibrium partitioning consideration, MF should not be present in the condensed phase in detectable quantities under reasonable atmospheric conditions.

That MF is measured from condensed material may be explained if it is directly incorporated into the particles by some means other than absorptive partitioning, such as reversible reactive uptake. However, no such mechanism is known. Instead, we hypothesise that MF measurements are a result of decomposition of some condensed phase isoprene photo-oxidation product upon the thermal vaporisation used in the GC × GC and AMS analyses reported here. This is supported by the association of detected MF with the gas-phase isoprene photo-oxidation products MVK + MACR. The diurnal profiles shown in Fig. 4 also support this, being consistent with comparisons of day and night filter samples from previous studies which show greater levels of isoprene SOA markers during the day when isoprene emissions and photochemistry are greatest (Kourtchev et al., 2008; Ion et al.,

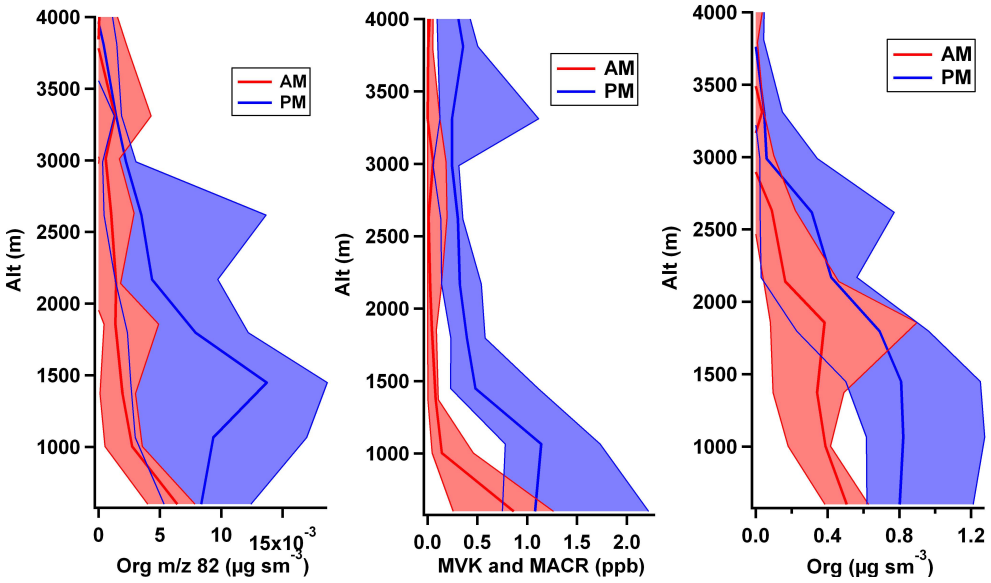

Fig. 6. Average altitude profiles of **(a)** *m/z* 82 signal, **(b)** gas phase MVK+MACR and **(c)** organic aerosol loading as measured from the FAAM research aircraft. Red lines from data before midday and blue lines from data after midday, local time. Thick lines are median values and shaded areas (outlined with thin lines) denote interquartile ranges.

2005). Known potential sources of isoprene SOA include epoxides (Paulot et al., 2009; Surratt et al., 2010), tetrols (Surratt et al., 2006, 2010; Kleindienst et al., 2009), peroxides (Surratt et al., 2006) or oligomers (Surratt et al., 2010) (formed through accretion reactions) but at present it is unclear how they would produce MF upon volatilisation. It is conceivable that this relation of MF to MVK+MACR could be caused by terpene photo-oxidation products produced at a similar rate to isoprene products. However, there is no evidence in the literature for MF formation from terpene photo-oxidation, in contrast to various isoprene mechanistic studies. This suggests that the MF could be a product of a form of isoprene SOA not previously identified.

The previously reported isoprene:NO_x ratio measured during OP3 had a typical value of 20:1 (Hewitt et al., 2009) which is comparable to ratios in NO_x-limited chamber oxidation studies of isoprene (e.g. Lane et al., 2008). The formation of gas-phase 3MF during isoprene photo-oxidation studies has previously been attributed to cyclisation/dehydration of unsaturated C_5 1,4-hydroxycarbonyls formed (Sprengnether et al., 2002; Dibble, 2007), in a process that would also be possible during the heating involved in the analyses reported here. A $C_5H_8O^+$ ion has been attributed to the fragmentation of 1,4-hydroxycarbonyls in previous isoprene photo-oxidation studies (Zhao et al., 2004). This signal was present in the ambient mass spectrum in Borneo and was covariant with the molecular ion of MF with a Pearson's r^2 of 0.57 but absent in the laboratory 3MF spectrum, consistent with the hypothesis that unsaturated 1,4-hydroxycarbonyls are the source of the ambient MF measurements. While these studies were performed at NO_x levels higher than in Borneo, they do provide a possible candidate for a mechanism that yields MF measurements. Two unsaturated C_5-hydroxycarbonyls (4-hydroxy-2-methyl-but-2-enal and 4-hydroxy-3-methyl-but-2-enal), are known to be formed as substantial first generation products of the OH-initiated degradation of isoprene, with their collective molar yield reported to be approximately 15–20% in a number of studies performed in the presence of NO_x, albeit at higher concentrations than in the atmosphere (Kwok et al., 1995; Zhao et al., 2004; Baker et al., 2005). Hydroxycarbonyls have also been observed in NO_x-free systems with a collective yield approaching 20% (Ruppert and Becker, 2000), with the dominant contribution estimated to be attributable to the above 1,4 isomers (Jenkin et al., 1998) and substantial formation may occur under the range of conditions of the OP3 field campaign.

Similar partitioning calculations as for MF were performed for C_5-hydroxycarbonyls. They were estimated to have a boiling point of 463.06 K and a vapour pressure at 298.15 K of 3.38×10^{-5} atm. The C_5-hydroxycarbonyls contributed $9.05 \times 10^{-6} \mu g\,m^{-3}$ to the condensed mass (4.5×10^{-4}% by mass). It is apparent from these calculations that, if either or both of the C_5-hydroxycarbonyls are degrading upon measurement to give MF, it must itself be a degradation product of another, less volatile compound. Again it is unclear how C_5-hydroxycarbonyls could be formed from established isoprene or terpene SOA species. One possibility is that some isoprene SOA could be in the form of peroxyhemiacetals which produce MF upon analysis. Hydroperoxide species (ROOH), such as isoprene derived hydroxyhydroperoxides, can be formed under (low

NO_x) NO_x-limited conditions where RO_2+HO_2 reactions become important. Under such conditions peroxyhemiacetals can be formed from the (reversible) reactions of isoprene derived 1,4-hydroxycarbonyls with hydroperoxides and hydroperoxides with aldehydes. The formation of high molecular weight peroxyhemiacetals has been characterised in previous studies of condensed organic material formed from the ozonolysis of alkene and monoterpene systems (Tobias and Ziemann, 2000; Docherty et al., 2005). Future chamber studies investigating isoprene SOA should seek to identify the potential sources of C_5-hydroxycarbonyls and MF in analytical measurements.

5 Mass estimates of MF related aerosol

The fraction of the ambient *m/z* 82 peak present as $C_5H_6O^+$ was calculated as a function of time using the high resolution AMS data. Averaged over the whole data set, these time series have a ratio of mean values of 80%, showing the $C_5H_6O^+$ ion to be the major contributor to the *m/z* 82 mass. This high resolution time series was scaled to the unit mass resolution data to ensure consistency with calibrations, and used to derive a quantitative estimate of the $C_5H_6O^+$ signal (used in Fig. 1). By scaling the laboratory 3MF spectrum so its *m/z* 82 peak is the same magnitude as the ambient $C_5H_6O^+$ signal, it is possible to estimate an upper limit to the MF loading detected, MF_{amb}, using

$$MF_{amb} = \frac{3MF_s}{C_5H_6O_s^+} C_5H_6O_{amb}^+ \quad (1)$$

where $3MF_s$ is the total organic loading of the laboratory sample spectrum, $C_5H_6O_{amb}^+$ is the $C_5H_6O^+$ signal in the ambient spectrum and $C_5H_6O_s^+$ is the $C_5H_6O^+$ signal in the laboratory 3MF sample spectrum (*m/z* 82 loading). This estimation method assumes that $C_5H_6O^+$ is entirely from the molecular ion of a thermal fragment rather than a fragment ion produced during ionization. Given that the GC-MS retention times of the *m/z* 82 peak from analysis of field and laboratory samples were the same, and the tendency of oxygenated organic species to generate odd *m/z* fragments under ionization (McLafferty and Turecek, 1993), this is considered to be a reasonable assumption. The mean ambient $C_5H_6O^+$ signal measured at the ground site during OP3 was 1.0% of the mean ambient total organic aerosol loading. Accounting for fragments of the molecular MF ion, this gives a mean MF_{amb} loading of 0.06 µg m^{-3}, or 8% of the organic aerosol. The maximum (95th percentile) MF_{amb} loading was 0.14 µg m^{-3}, and the maximum fractional loading was 15% of the simultaneously measured total organic aerosol.

The mass of particulate SOA due to isoprene oxidation in the ambient will be greater than the mass of MF it produces upon analysis, meaning this approach underestimates the loading of isoprene derived SOA. An estimate of the total amount of organic aerosol due to isoprene oxidation can be made using the 82Fac from the PMF analysis of the HR-AMS unit mass resolution spectrum (see Supplement). It should be noted that the mass spectrum of 82Fac (Fig. 2d) is more complex than the 3MF laboratory mass spectrum (Fig. 2e) implying other organic components also contribute to the 82Fac PMF factor. However, the close correlation of 82Fac with *m/z* 82 ($r^2 = 0.86$) identifies it as being derived from the same organic aerosol as MF, either directly as other components that are also formed on thermal degradation, or indirectly as isoprene SOA species that are produced simultaneously but through a different mechanism.

Note that it is conceivable that isoprene SOA produced at a different rate to the MF-precursor aerosol may also be contributing to other factors (such as OOA2), although we have no evidence to suggest this is the case. It is likely that, if MF is indeed indicative of isoprene SOA, the 82Fac PMF factor provides a good estimate of the amount of isoprene SOA in the region.

6 Global extent of MF

Such a prominent *m/z* 82 signal has not been reported in previously published studies over biogenic sources of VOCs. However, analysis of HR-AMS mass spectra from a study in the Amazon Basin, previously published as part of the Amazonian Aerosol Characterization Experiment (AMAZE-08) (Chen et al., 2009), also shows evidence for $C_5H_6O^+$ during periods dominated by in-Basin sources, though with a lower mean signal comprising 0.5% of the organic mass, compared to the mean $C_5H_6O^+$ signal of 1% measured in Borneo. Table 1 compares *m/z* 82 and $C_5H_6O^+$ signals from projects in various locations around the World showing the fractional contribution of *m/z* 82 to the total organic matter and its comparison with the adjacent peaks, which is an indicator of how distinct the signal is compared to other peaks in that part of the mass spectrum. Though these two metrics are useful for comparing projects, care should be taken in their interpretation as both are vulnerable to conflating circumstances: for example, the *m/z* 82 peak will appear as a low fraction of the total mass if MF yielding aerosol is present in low levels compared to other organic aerosol, and if large amounts of a species that fragment at masses around *m/z* 82 are measured then the *m/z* 82 peak may be a significant fraction of the total mass without being prominent. It should also be noted that it is impossible to assess the contribution of non-MF ions to *m/z* 82 peaks unless high mass resolution data is available.

The *m/z* 82 peak in the rainforest environments is more prominent, implying these measurements are from stable molecular ions, rather than background fragments resultant from the breakup of non-MF-precursor organic aerosol. Higher levels of $C_5H_6O^+$ yielding aerosol have been measured in these two isoprene dominated rainforest environments than in a North American temperate forest of mixed terpene and isoprene influence (BEARPEX campaign, see

Table 1. Comparison of % of organic aerosol signal measured at *m/z* 82 and at $C_5H_6O^+$, the ratio of organic *m/z* 82 to the mean adjacent organic peak heights, and the % of the organic *m/z* 82 peak that is $C_5H_6O^+$, at different locations across the World, and in isoprene oxidation experiments (isoprene:$NO_x > 200:1$) in the Harvard Environmental Chamber. Standard errors calculated from propagation of standard deviations of time series are shown (where appropriate). The Borneo data points are from the OP3 project as reported in this paper. The Amazonia data are from the AMAZE campaign as reported by Chen et al. (2009), in-basin classification. The boreal European data were collected as part of the EUCAARI campaign (Kulmala et al., 2009). The North American temparate data (see Appendix A) were taken as part of the BEARPEX campaign.

	Borneo ensemble	Borneo PMF factor	Chen et al. Amazonia	European boreal	North American temperate	Isoprene SOA in HEC
org82:org	1.24±0.01%	3.82%	0.68±<0.01%	0.48±0.01%	0.40±<0.01%	0.44±<0.01%
$C_5H_6O^+$:org	1.01±0.01%		0.50±0.01%	0.25±0.01%	0.40±<0.01%	0.43±<0.01%
82:avg(81,83)	2.14±0.02	5.84	1.18±0.01	0.66±0.02	0.49±<0.01	3.38±0.05
$C_5H_6O^+$:org82	81.5±0.4%		74.0±0.6%	50±1%	98.2±0.2%	97.2±0.4%

Appendix A), which in turn has higher levels than a terpene dominated environment (Kulmala et al., 2009). This is consistent with the detection of MF being a result of isoprene derived SOA.

HR-AMS data from low NO_x isoprene photo-oxidation experiments (isoprene:$NO_x > 200:1$) in the Harvard Environmental Chamber (King et al., 2010) also show an *m/z* 82 peak distinct from the adjacent peaks. While the *m/z* 82 peak is responsible for less signal than in either of the tropical field studies (0.4% of total organic mass), the prominance of the $C_5H_6O^+$ ion at *m/z* 82 strongly suggests that the same SOA formation mechanism is taking place and could be isolated through further laboratory work. Sulphate levels in Borneo are around four times greater than in the Amazon. Inspection of back trajectories suggests marine and anthropogenic sources of sulphate external to Borneo (Robinson et al., 2011a). A charge balance of sulphate and ammonium ions show excess sulphate over the oceans (Robinson et al., 2011b) compared to the ground site where charge is usually balanced. As acidic sulphate had been shown to play an important role in isoprene SOA fomation in previous studies, its prescence may contribute to the greater significance of MF in Borneo, although chamber studies have not shown sulphate-isoprene SOA mechanisms likely to yield MF (Surratt et al., 2010).

7 Conclusions

AMS and GC × GC measurements of organic aerosol composition in Borneo identified a MF signal at *m/z* 82 and 53, the parent ion and major fragment respectively. This was confirmed by laboratory measurements of a 3MF sample which showed the same *m/z* 82 and 53 peaks. The *m/z* 82 signal was present throughout the boundary layer with the signal increasing throughout the day, associated with the isoprene oxidation products MVK + MACR through correlation of aircraft data and diurnal profiles of ground data. This is consistent with production of SOA from photochemical processing of isoprene. Volatility modelling calculations showed MF to be too volatile to be present in the condensed phase meaning it is likely to be a product of some other molecule, produced upon the vapourisation involved in both the AMS and GC × GC analyses. One such potential condensible MF precursor could be peroxyhemiacetal oligomers, derived from gas-phase isoprene photo-oxidation products such as unsaturated 1,4-hydroxycarbonyls. However, the actual specific MF precursor (or precursors) require laboratory identification. Future work will attempt to detect the *m/z* 82 peak in the laboratory, both from established isoprene SOA and from the compounds suggested here. Comparisons of two metrics, *m/z* 82 fractional organic mass and peak prominence, show that isoprene dominated environments seem to have greater MF loadings than terpene dominated. The *m/z* 82 peak was also observed in isoprene oxidation chamber experiments. PMF analysis of the HR-AMS mass spectral time series yielded a robust factor that was characterised by strong *m/z* 82 and 53 signals.

The ubiquity of the enhanced *m/z* 82 peak at all measurement locations influenced by isoprene suggests that the mechanism forming this SOA is important in all high isoprene/low NO_x (i.e. NO_x limited) environments, which are widespread throughout the unpolluted tropics. Given the lower fractional contribution in the Amazon, it could be speculated that other factors may decide its importance, such as the presence of acids, which have been shown to be important in other SOA studies (Lim and Ziemann, 2009; Surratt et al., 2010).

Although progress is being made, evidence from chamber studies of isoprene photo-oxidation still does not reveal a consistent picture, with greater variation in isoprene SOA yields than for systems such as α-pinene (Carlton et al., 2009). Models estimating the global contribution of isoprene SOA give a wide range of values (Carlton et al., 2009). Better agreement with measurements can be reached with top-down approaches (Capes et al., 2009), however these do not account for any conflating uncertainties in processes and emissions, so are of limited use as predictive tools under future

climates, CO_2 concentrations and land uses. While established isoprene SOA such as IEPOX derived organosulphates may be the precursor aerosol to MF measurements, it is unclear what mechanism could produce MF from these species. It is possible therefore that MF is produced from previously unidentified isoprene product(s). As such, identification of the MF precursor aerosol may provide key insights into missing SOA, and the identification of the relationship of the AMS *m/z* 82 peak to isoprene SOA opens up the opportunity for more high time resolution isoprene SOA measurements in other projects. The PMF analysis suggests that an average of 23% (0.18 µg m^{-3}), and as much as 53% (0.5 µg m^{-3}) of the organic aerosol may be produced from isoprene oxidation in Borneo. The natural balance of isoprene is being affected by deforestation for oil palm agriculture (McMorrow and Talip, 2001) which emits five times as much isoprene as the natural forest (Hewitt et al., 2009), meaning isoprene SOA will only become more important with further similar land use change.

Appendix A

Details of unpublished data from the BEARPEX campaign

The North American temperate HR-AMS measurements presented in Table 1 of the main text, took place during the BEARPEX (Biosphere Effects on AeRosols and Photochemistry EXperiment) campaign at Blodgett Forest Ameriflux site in 2007. The site is a mid-elevation ponderosa pine plantation owned by Sierra Pacific Industries, and located ∼75 km northeast of Sacramento on the western slope of California's mid-elevation Sierra Nevada mountains (38.90° N, 120.63° W, 1315 m elevation). AMS measurements were taken between 19 August and 28 September2007, at the top of an 18 m tower. The site has been previously described in detail Dreyfus et al. (2002). Wind patterns throughout the measurement period were consistent, with westerly to southwesterly wind during the day and northeasterly to easterly winds at night Murphy et al. (2006). This results in a consistent diurnal pattern of VOCs in which a mix of terpenes and other pine-derived biogenic VOCs are observed in the morning followed by isoprene and its oxidation products at mid-day as air is transported over a lower elevation band of oak forest Dreyfus et al. (2002). In the afternoon, a mix of biogenic and anthropogenic VOCs are caused by transport of polluted air from the Sacramento area. The Blodgett forest canopy is dominated by Pinus ponderosa L., planted in 1990 with a mean height of 8 m, with few Douglas fir, white fir and incense cedar. The understory includes mountain whitehorn and manzanita. The data presented have been screened for the influence of biomass burning.

Supplementary material related to this article is available online at: http://www.atmos-chem-phys.net/11/1039/2011/acp-11-1039-2011-supplement.pdf.

Acknowledgements. Thanks to J. Kroll (Massachusetts Institute of Technology) and M. Alfarra (NCAS, University of Manchester) for conversations during the preparation of this manuscript. This work was supported by the UK Natural Environment Research Council through the OP3 (grant NE/D002117/1) and ACES (grant NE/E011179/1) projects. QC and STM thank US NSF ATM-0723582. KSD, DKF, and JLJ thank US NSF ATM-0449815, ATM-0449815, and NOAA NA08OAR4310565. We thank the Malaysian and Sabah Governments for their permission to conduct research in Malaysia; the Malaysian Meteorological Department for access to the measurement site; Yayasan Sabah and the Royal Society's South East Asian Rain Forest Research Programme for logistical support; and the ground staff, engineers, scientists and flight crew of the FAAM aircraft. This is paper number 515 of the Royal Societys South East Asian Rainforest Research Programme.

Edited by: A. B. Guenther

References

Alfarra, M. R., Prevot, A. S. H., Szidat, S., Sandradewi, J., Weimer, S., Lanz, V. A., Schreiber, D., Mohr, M., and Baltensperger, U.: Identification of the Mass Spectral Signature of Organic Aerosols from Wood Burning Emissions, Environ. Sci. Technol., 41, 5770–5777, doi:10.1021/es062289b, 2007.

Atkinson, R., Aschmann, S. M., Tuazon, E. C., Arey, J., and Zielinska, B.: Formation of 3-Methylfuran from the gas-phase reaction of OH radicals with isoprene and the rate constant for its reaction with the OH radical, Int. J. Chem. Kin., 21, 593–604, 1989.

Baker, J., Arey J., and Atkinson, R.: Formation and reaction of hydroxycarbonyls from the reaction of OH radicals with 1, 3-butadiene and isoprene, Environ. Sci. Technol., 39, 4091–4099, 2005.

Barley, M. H. and McFiggans, G.: The critical assessment of vapour pressure estimation methods for use in modelling the formation of atmospheric organic aerosol, Atmos. Chem. Phys., 10, 749–767, doi:10.5194/acp-10-749-2010, 2010.

Barley, M., Topping, D. O., Jenkin, M. E., and McFiggans, G.: Sensitivities of the absorptive partitioning model of secondary organic aerosol formation to the inclusion of water, Atmos. Chem. Phys., 9, 2919–2932, doi:10.5194/acp-9-2919-2009, 2009.

Burness, D. M.: Beta-Keto acetals. II. Synthesis of 3-methyl- and 3-phenyl-furans., J. Org. Chem., 21, 102–104, 1956.

Canagaratna, M. R, Jayne, J. T, Jimenez, J. L., Allan, J. D., Alfarra, M. R., Zhang,Q., Onasch, T. B., Drewnick, F., Coe, H., Middlebrook, A., Delia, Williams, L. R., Trimborn, A. M., Northway, M. J., DeCarlo, P. F., Kolb, C. E., Davidovits, P., and Worsnop, D. R.: Chemical and microphysical characterization of ambient aerosols with the aerodyne aerosol mass spectrometer, Mass Spectrom. Rev., 26, 185–222, 2007.

Capes, G., Johnson, B., McFiggans, G., Williams, P. I., Haywood, J., and Coe, H.: Aging of biomass burning aerosols over West Africa: Aircraft measurements of chemical composition, microphysical properties, and emission ratios, J. Geophys. Res., 113, D00C15, doi:10.1029/2008JD009845, available online at: http://www.agu.org/pubs/crossref/2008/2008JD009845.shtml, 2008.

Capes, G., Murphy, J. G., Reeves, C. E., McQuaid, J. B., Hamilton, J. F., Hopkins, J. R., Crosier, J., Williams, P. I., and Coe, H.: Secondary organic aerosol from biogenic VOCs over West Africa during AMMA, Atmos. Chem. Phys., 9, 3841–3850, doi:10.5194/acp-9-3841-2009, 2009.

Carlton, A. G., Wiedinmyer, C., and Kroll, J. H.: A review of Secondary Organic Aerosol (SOA) formation from isoprene, Atmos. Chem. Phys., 9, 4987–5005, doi:10.5194/acp-9-4987-2009, 2009.

Chan, M. N., Surratt, J. D., Claeys, M., Edgerton, E. S., Tanner, R. L., Shaw, S. L., Zheng, M., Knipping, E. M., Eddingsaas, N. C., Wennberg, P. O., and Seinfeld, J. H.: Characterization and Quantification of Isoprene-Derived Epoxydiols in Ambient Aerosol in the Southeastern United States, Environ. Sci. Technol., 44, 4590–4596, available online at: http://dx.doi.org/10.1021/es100596b, 2010.

Chen, Q., Farmer, D. K., Schneider, J., Zorn, S. R., Heald, C. L., Karl, T. G., Guenther, A., Allan, J. D., Robinson, N., Coe, H., Kimmel, J. R., Pauliquevis, T., Borrmann, S., Poschl, U., Andreae, M. O., Artaxo, P., Jimenez, J. L., and Martin, S. T.: Mass spectral characterization of submicron biogenic organic particles in the Amazon Basin, Geophys. Res. Lett., 36, L20806, doi:10.1029/2009GL039880, 2009.

Claeys, M., Graham, B., Vas, G., Wang, W., Vermeylen, R., Pashynska, V., Cafmeyer, J., Guyon, P., Andreae, M. O., Artaxo, P., and Maenhaut, W.: Formation of Secondary Organic Aerosols Through Photooxidation of Isoprene, Science, 303, 1173–1176, 2004.

DeCarlo, P. F., Kimmel, J. R., Trimborn, A., Northway, M. J., Jayne, J. T., Aiken, A. C., Gonin, M., Fuhrer, K., Horvath, T., Docherty, K. S., Worsnop, D. R., and Jiminez, J. L.: Field-deployable, high-resolution, time-of-flight aerosol mass spectrometer., Anal. Chem., 78, 8281–8289, 2006.

Dibble, T. S.: Cyclization of 1,4-hydroxycarbonyls is not a homogenous gas phase process, Chem. Phys. Lett., 447, 5–9, doi:10.1016/j.cplett.2007.08.088, available online at: http://dx.doi.org/10.1016/j.cplett.2007.08.088, 2007.

Docherty, K. S., Wu, W., Lim, Y. B., and Ziemann, P. J.: Contributions of Organic Peroxides to Secondary Aerosol Formed from Reactions of Monoterpenes with O 3, Environ. Sci. Technol., 39, 4049–4059, doi:10.1021/es050228s, available online at: http://pubs.acs.org/doi/abs/10.1021/es050228s, 2005.

Drewnick, F., Hings, S. S., Decarlo, P., Jayne, J. T., Gonin, M., Fuhrer, K., Weimer, S., Jimenez, J. L., Borrmann, K. L. D. S., and Worsnop, D. R.: A new time-of-flight aerosol mass spectrometer (TOF-AMS) – Instrument description and first field deployment, Aerosol Sci. Technol., 39, 637–658, 2005.

Dreyfus, G. B., Schade, G. W., and Goldstein, A.: Observational constraints on the contribution of isoprene oxidation to ozone production on the western slope of the Sierra Nevada, California, J. Geophys. Res., 107, 4365, doi:10.1029/2001JD001490, 2002.

Foltescu, V. L., Selin, E., and Below, M.: Corrections for particle losses and sizing errors during aircraft aerosol sampling using a rosemounts inlet and the PMS LAS-X, Atmos. Environ., 29, 449–453, 1995.

Froyd, K. D., Murphy, S. M., Murphy, D. M., de Gouw, J. A., Eddingsaas, N. C., Wennberg, P. O.: Contribution of isoprene-derived organosulfates to free tropospheric aerosol mass, P. Natl. Acad. Sci., 107(50), 21360–21365, doi:10.1073/pnas.1012561107, 2010.

Hallquist, M., Wenger, J. C., Baltensperger, U., Rudich, Y., Simpson, D., Claeys, M., Dommen, J., Donahue, N. M., George, C., Goldstein, A. H., Hamilton, J. F., Herrmann, H., Hoffmann, T., Iinuma, Y., Jang, M., Jenkin, M. E., Jimenez, J. L., Kiendler-Scharr, A., Maenhaut, W., McFiggans, G., Mentel, Th. F., Monod, A., Prévôt, A. S. H., Seinfeld, J. H., Surratt, J. D., Szmigielski, R., and Wildt, J.: The formation, properties and impact of secondary organic aerosol: current and emerging issues, Atmos. Chem. Phys., 9, 5155–5236, doi:10.5194/acp-9-5155-2009, 2009.

Hamilton, J. F., Webb, P. J., Lewis, A. C., Hopkins, J. R., Smith, S., and Davy, P.: Partially oxidised organic components in urban aerosol using GCXGC-TOF/MS, Atmos. Chem. Phys., 4, 1279–1290, doi:10.5194/acp-4-1279-2004, 2004.

Heald, C., Jacob, D., Park, R. J., Russell, L. M., Huebert, B. J., Seinfeld, J. H., Liao, H., and Weber, R. J.: A large organic aerosol source in the free troposphere missing from current models, Geophys. Res. Lett., 32, 1–4, 2005.

Henze, D. and Seinfeld, J. H.: Global secondary organic aerosol from isoprene oxidation, Geophys. Res. Lett., 33, L09812, doi:10.1029/2006GL025976, 2006.

Hewitt, C. N., MacKenzie, A. R., Carlo, P. D., Marco, C. F. D., Dorsey, J. R., Evans, M., Fowler, D., Gallagher, M. W., Hopkins, J. R., Jones, C. E., Langford, B., Lee, J. D., Lewis, A. C., Lim, S. F., McQuaide, J., Misztal, P., Moller, S. J., Monks, P. S., Nemitz, E., Oram, D. E., Owen, S. M., Phillips, G. J., Pugh, T. A. M., Pyle, J. A., Reeves, C. E., Ryder, J., Siong, J., Skiba, U., and Stewart, D. J.: Nitrogen management is essential to prevent tropical oil palm plantations from causing ground level ozone pollutio, P. Natl. Acad. Sci. USA, 106, 18447–18451, doi:10.1073/pnas.0907541106, 2009.

Hewitt, C. N., Lee, J. D., MacKenzie, A. R., Barkley, M. P., Carslaw, N., Carver, G. D., Chappell, N. A., Coe, H., Collier, C., Commane, R., Davies, F., Davison, B., DiCarlo, P., Di Marco, C. F., Dorsey, J. R., Edwards, P. M., Evans, M. J., Fowler, D., Furneaux, K. L., Gallagher, M., Guenther, A., Heard, D. E., Helfter, C., Hopkins, J., Ingham, T., Irwin, M., Jones, C., Karunaharan, A., Langford, B., Lewis, A. C., Lim, S. F., MacDonald, S. M., Mahajan, A. S., Malpass, S., McFiggans, G., Mills, G., Misztal, P., Moller, S., Monks, P. S., Nemitz, E., Nicolas-Perea, V., Oetjen, H., Oram, D. E., Palmer, P. I., Phillips, G. J., Pike, R., Plane, J. M. C., Pugh, T., Pyle, J. A., Reeves, C. E., Robinson, N. H., Stewart, D., Stone, D., Whalley, L. K., and Yin, X.: Overview: oxidant and particle photochemical processes above a south-east Asian tropical rainforest (the OP3 project): introduction, rationale, location characteristics and tools, Atmos. Chem. Phys., 10, 169–199, doi:10.5194/acp-10-169-2010, 2010.

Ion, A. C., Vermeylen, R., Kourtchev, I., Cafmeyer, J., Chi, X., Gelencsr, A., Maenhaut, W., and Claeys, M.: Polar organic compounds in rural PM2.5 aerosols from K-puszta, Hungary, during a 2003 summer field campaign: Sources and diel variations, At-

mos. Chem. Phys., 5, 1805–1814, doi:10.5194/acp-5-1805-2005, 2005.

Jenkin, M. E., Boyd, A. A., and Lesclaux, R.: Peroxy radical kinetics resulting from the OH-initiated oxidation of 1, 3-butadiene, 2, 3-dimethyl-1, 3-butadiene and isoprene, J. Atmos. Chem., 29, 267–298, 1998.

Kanakidou, M., Seinfeld, J. H., Pandis, S. N., Barnes, I., Dentener, F. J., Facchini, M. C., Van Dingenen, R., Ervens, B., Nenes, A., Nielsen, C. J., Swietlicki, E., Putaud, J. P., Balkanski, Y., Fuzzi, S., Horth, J., Moortgat, G. K., Winterhalter, R., Myhre, C. E. L., Tsigaridis, K., Vignati, E., Stephanou, E. G., and Wilson, J.: Organic aerosol and global climate modelling: a review, Atmos. Chem. Phys., 5, 1053–1123, doi:10.5194/acp-5-1053-2005, 2005.

King, S. M., Rosenoern, T., Shilling, J. E., Chen, Q., Wang, Z., Biskos, G., McKinney, K. A., Pöschl, U., and Martin, S. T.: Cloud droplet activation of mixed organic-sulfate particles produced by the photooxidation of isoprene, Atmos. Chem. Phys., 10, 3953–3964, doi:10.5194/acp-10-3953-2010, 2010.

Kleindienst, T. E., Lewandowski, M., Offenberg, J. H., Jaoui, M., and Edney, E. O.: The formation of secondary organic aerosol from the isoprene + OH reaction in the absence of NO_x, Atmos. Chem. Phys., 9, 6541–6558, doi:10.5194/acp-9-6541-2009, 2009.

Kourtchev, I., Ruuskanen, T. M., Keronen, P., Sogacheva, L., Dal Maso, M., Reissell, A., Chi, X., Vermeylen, R., Kulmala, M., Maenhaut, W., and Claeys, M.: Determination of isoprene and alpha-/beta-pinene oxidation products in boreal forest aerosols from Hyytiälä, Finland: diel variations and possible link with particle formation events., Plant Biology (Stuttgart, Germany), 10, 138–49, doi:10.1055/s-2007-964945, available online at: http://www.ncbi.nlm.nih.gov/pubmed/18211553, 2008.

Kulmala, M., Asmi, A., Lappalainen, H. K., Carslaw, K. S., Pöschl, U., Baltensperger, U., Hov, Ø., Brenquier, J.-L., Pandis, S. N., Facchini, M. C., Hansson, H.-C., Wiedensohler, A., and O'Dowd, C. D.: Introduction: European Integrated Project on Aerosol Cloud Climate and Air Quality interactions (EUCAARI) – integrating aerosol research from nano to global scales, Atmos. Chem. Phys., 9, 2825–2841, doi:10.5194/acp-9-2825-2009, 2009.

Kwok, E. S. C., Atkinson, R., and Arey, J.: Observation of hydroxycarbonyls from the OH radical-initiated reaction of isoprene, Environ. Sci. Technol., 29, 2467–2469, 1995.

Lane, T. E., Donahue, N. M., and Pandis, S. N.: Effect of NO_x on Secondary Organic Aerosol Concentrations, Environ. Sci. Technol., 42, 6022–6027, doi:10.1021/es703225a, available online at: http://pubs.acs.org/doi/abs/10.1021/es703225a, 2008.

Langford, B., Misztal, P. K., Nemitz, E., Davison, B., Helfter, C., Pugh, T. A. M., MacKenzie, A. R., Lim, S. F., and Hewitt, C. N.: Fluxes and concentrations of volatile organic compounds from a South-East Asian tropical rainforest, Atmos. Chem. Phys., 10, 8391–8412, doi:10.5194/acp-10-8391-2010, 2010.

Lim, Y. B. and Ziemann, P. J.: Kinetics of the heterogeneous conversion of 1,4-hydroxycarbonyls to cyclic hemiacetals and dihydrofurans on organic aerosol particles, Phys. Chem. Chem. Phys., 11, 8029–8039, doi:10.1039/b904333k, available online at: http://www.ncbi.nlm.nih.gov/pubmed/19727510 2009.

Lindinger, W., Hansel, A., and Jordan, A.: Proton-transfer-reaction mass spectrometry (PTR-MS): On-line monitoring of volatile organic compounds at pptv levels, Chem. Soc. Rev., 27, 347–354, 1998.

McLafferty, F. W. and Turecek, F.: Interpretation of Mass Spectra, University Science Books, US, ISBN: 0935702253, 1993.

McMorrow, J. and Talip, M. A.: Decline of forest area in Sabah, Malaysia: Relationship to state policies, land code and land capability, Global Environ. Change, 11, 217–230, doi:10.1016/S0959-3780(00)00059-5, available online at: http://dx.doi.org/10.1016/S0959-3780(00)00059-5 2001.

Montzka, S. A., Trainer, M., Angevine, W. M., and Fehsenfeld, F. C.: Measurements of 3-methylfuran, methyl vinyl ketone, and methacrolein at a rural forested site in the southeastern United States, J. Geophys. Res., 100(11), 11393–11401, http://www.agu.org/journals/jd/v100/iD06/95JD01132/95JD01132.pdf , 1995.

Morgan, W. T., Allan, J. D., Bower, K. N., Highwood, E. J., Liu, D., McMeeking, G. R., Northway, M. J., Williams, P. I., Krejci, R., and Coe, H.: Airborne measurements of the spatial distribution of aerosol chemical composition across Europe and evolution of the organic fraction, Atmos. Chem. Phys., 10, 4065–4083, doi:10.5194/acp-10-4065-2010, 2010.

Murphy, J. G., Day, D. A., Cleary, P. A., Wooldridge, P. J., and Cohen, R. C.: Observations of the diurnal and seasonal trends in nitrogen oxides in the western Sierra Nevada, Atmos. Chem. Phys., 6, 5321–5338, doi:10.5194/acp-6-5321-2006, 2006.

Murphy, J. G., Oram, D. E., and Reeves, C. E.: Measurements of volatile organic compounds over West Africa, Atmos. Chem. Phys., 10, 5281–5294, doi:10.5194/acp-10-5281-2010, 2010.

Nannoolal, Y., Rarey, J., Ramjugernath, D., and Cordes, W.: Estimation of pure component properties: Part 1. Estimation of the normal boiling point of non-electrolyte organic compounds via group contributions and group interactions, Fluid Phase Equilibria, 226, 45–63, doi:10.1016/j.fluid.2004.09.001, http://dx.doi.org/10.1016/j.fluid.2004.09.001, 2004.

Nannoolal, Y., Rarey, J., and Ramjugernath, D.: Estimation of pure component properties: Part 3. Estimation of the vapor pressure of non-electrolyte organic compounds via group contributions and group interactions, Fluid Phase Equilibria, 269, 117–133, doi:10.1016/j.fluid.2008.04.020, http://dx.doi.org/10.1016/j.fluid.2008.04.020, 2008.

Ng, N. L., Canagaratna, M. R., Zhang, Q., Jimenez, J. L., Tian, J., Ulbrich, I. M., Kroll, J. H., Docherty, K. S., Chhabra, P. S., Bahreini, R., Murphy, S. M., Seinfeld, J. H., Hildebrandt, L., Donahue, N. M., DeCarlo, P. F., Lanz, V. A., Prévôt, A. S. H., Dinar, E., Rudich, Y., and Worsnop, D. R.: Organic aerosol components observed in Northern Hemispheric datasets from Aerosol Mass Spectrometry, Atmos. Chem. Phys., 10, 4625–4641, doi:10.5194/acp-10-4625-2010, 2010.

Paulot, F., Crounse, J. D., Kjaergaard, H. G., Kurten, A., St. Clair, J. M., Seinfeld, J. H., and Wennberg, P. O.: Unexpected Epoxide Formation in the Gas-Phase Photooxidation of Isoprene, Science, 325, 730–733, doi:10.1126/science.1172910, 2009.

Phillips, J. B. and Beens, J.: Comprehensive two-dimensional gas chromatography: a hyphenated method with strong coupling between the two dimensions, J. Chromatogr. A, 856, 331–347, doi:10.1016/S0021-9673(99)00815-8, http://www.sciencemag.org/cgi/content/abstract/325/5941/730 1999.

Ruppert, L. and Becker, H. H.: A product study of the OH radical-initiated oxidation of isoprene: formation of C5-unsaturated di-

ols, Atmos. Environ., 34, 1529–1542, 2000.

Paatero, P.: Least squares formulation of robust non-negative factor analysis, Chemometr. Intell. Lab. Syst., 37, 23–35, 1997.

Paatero, P. and Tapper U.: Positive matrix factorization: A non-negative factor model with optimal utilization of error estimates of data values, Environmetrics, 5, 111–126, 1994.

Robinson, N. H., Newton, H., Allan, J. D., Irwin, M., Hamilton, J. F., Chen, Q., Martin, S. T., McFiggans, G., and Coe, H.: Source attribution during the OP3 project using backwards air mass trajectories, in preparation, Atmos. Chem. Phys., 2011a.

Robinson, N. H., Allan, J. D., and Coe, H.: Airborne measurements of aerosol chemical and physical properties over Borneo, in preparation Atmos. Chem. Phys., 2011b.

Sprengnether, M., Demerjian, K. L., Donahue, N. M., and Anderson, J. G.: Product analysis of the OH oxidation of isoprene and 1,3-butadiene in the presence of NO, J. Geophys. Res., 107, 4268, doi:10.1029/2001JD000716, 2002.

Stein, S. E.: "Mass Spectra" in NIST Chemistry WebBook, NIST Standard Reference Database Number 69, http://webbook.nist.gov, 2009.

Surratt, J. D., Murphy, S. M., Kroll, J. H., Ng, N. L., Hildebrandt, L., Sorooshian, A., Szmigielski, R., Vermeylen, R., Maenhaut, W., Claeys, M., Flagan, R. C., and Seinfeld, J. H.: Chemical Composition of Secondary Organic Aerosol Formed from the Photooxidation of Isoprene, J. Phys. Chem. A, 110, 9665–9690, doi.org/10.1021/jp061734m, 2006.

Surratt, J. D., Gomez-Gonzalez, Y., Chan, A. W. H., Vermeylen, R., Shahgholi, M., Kleindienst, T. E., Edney, E. O., Offenberg, J. H., Lewandowski, M., Jaoui, M., Maenhaut, W., Claeys, M., Flagan, R. C., and Seinfeld, J. H.: Organosulfate Formation in Biogenic Secondary Organic Aerosol, J. Phys. Chem. A, 112, 8345–8378, available online at: http://dx.doi.org/10.1021/jp061734m, 2008.

Surratt, J. D., Chan, A. W. H., Eddingsaas, N. C., Chan, M., Loza, C. L., Kwan, A. J., Hersey, S. P., Flagan, R. C., Wennberg, P. O., and Seinfeld, J. H.: Atmospheric Chemistry Special Feature: Reactive intermediates revealed in secondary organic aerosol formation from isoprene, P. Natl. Acad. Sci. USA, 15, 6640–6645, doi:10.1073/pnas.0911114107, 2010.

Tobias, H. J. and Ziemann, P. J.: Thermal Desorption Mass Spectrometric Analysis of Organic Aerosol Formed from Reactions of 1-Tetradecene and O_3 in the Presence of Alcohols and Carboxylic Acids, Environ. Sci. Technol., 34, 2105–2115, doi:10.1021/es9907156, available online at: http://pubs.acs.org/doi/abs/10.1021/es9907156, 2000.

Ulbrich, I. M., Canagaratna, M. R., Zhang, Q., Worsnop, D. R., and Jimenez, J. L.: Interpretation of organic components from Positive Matrix Factorization of aerosol mass spectrometric data, Atmos. Chem. Phys., 9, 2891–2918, doi:10.5194/acp-9-2891-2009, 2009.

Whitehead, J. D., Gallagher, M. W., Dorsey, J. R., Robinson, N., Gabey, A. M., Coe, H., McFiggans, G., Flynn, M. J., Ryder, J., Nemitz, E., and Davies, F.: Aerosol fluxes and dynamics within and above a tropical rainforest in South-East Asia, Atmos. Chem. Phys., 10, 9369–9382, doi:10.5194/acp-10-9369-2010, 2010.

Zhang, Q., Alfarra, M. R., Worsnop, D. R., Allan, J. D., Coe, H., Canagaratna, M. R., and Jimenez, J. L.: Deconvolution and quantification of hydrocarbon-like and oxygenated organic aerosols based on aerosol mass spectrometry, Environ. Sci. Technol., 39, 4938–4952, 2005.

Zhang, Q., Jimenez, J. L., Canagaratna, M. R., Allan, J. D., Coe, H., Ulbrich, I., Alfarra, M. R., Takami, A., Middlebrook, A. M., Sun, Y. L., Dzepina, K., Dunlea, E., Docherty, K., DeCarlo, P. F., Salcedo, D., Onasch, T. B., Jayne, J. T., Miyoshi, T., Shimono, A., Hatakeyama, S., Takegawa, N., Kondo, Y., Schneider, J., Drewnick, F., Borrmann, S., Weimer, S., Demerjian, K., Williams, P., Bower, K. N., Bahreini, R., Cottrell, L., Griffin, R. J., Rautiainen, J., Sun, J. Y., Zhang, Y. M., and Worsnop, D. R.: Ubiquity and dominance of oxygenated species in organic aerosols in anthropogenically-influenced Northern Hemisphere midlatitudes, Geophys. Res. Lett., 34, L13801, doi:10.1029/2007GL029979, available online at: http://www.agu.org/pubs/crossref/2007/2007GL029979.shtml, 2007.

Zhao, J., Zhang, R., Fortner, E. C., and North, S. W.: Quantification of Hydroxycarbonyls from OH-Isoprene Reactions, J. Am. Chem. Soc., 126, 2686–2687, doi:10.1021/ja0386391, available online at: http://dx.doi.org/10.1021/ja0386391, 2004.

4.5 Summary of Other Findings from the OP3 project

Various other publications have shed light on aerosol and gas phase composition since the OP3 project was performed, and the salient results are summarised here. Long term rainfall data from Danum Valley showed that 2008 was an exceptionally wet year with the lowest seasonal variability in the last 23 years (Hewitt et al., 2010). The average yearly rainfall at the site is around 30% higher than the AMAZE-08 project (Martin et al., 2010a). A photograph time series of a typical day is shown in Figure 4.1. During the night fog formed in the boundary layer, which dropped below the level of the measurement site. As the sun rose in the early morning the fog dissipated and a mixed layer started to form. By the early afternoon the well mixed surface layer had grown in depth and was capped by cumulus clouds. Convection was often strong enough to produce thunderstorms by late afternoon. This sequence is confirmed by in-situ Doppler Light Detection and Ranging (LIDAR) measurements performed during OP3-I at a nearby site, which observes fog at night and a growing well mixed layer through the day (Pearson et al., 2010). This is consistent with the aerosol and thermodynamic data presented in Section 4.3.

Gabey et al. (2010) performed measurements of primary biological aerosol particles (PBAP) using a Wide Interest Biological Sampler (WIBS), an ultra violet fluorescence technique. These particles may play and important role in the hydrological cycle as giant CCN or highly efficient IN, and have been shown to be important IN in Amazonia (Prenni et al., 2009). PBAP showed clear diurnal patterns in both the Bukit Atur site, and the below-canopy site which was situated in a nearby valley. Particularly large concentrations (up to $\sim$4000 l^{-1}) were observed in the understory, with the peak occurring in mid-afternoon. Lower concentrations (50–200 l^{-1}) were observed at the above canopy site. The major mode was between 2 and 4 μm at both sites. It was thought to be composed primarily of fungal spores emitted in the rainforest understory due to its fluorescence and relation to ambient relative humidity. This mode may be depleted with land use change as oil palm plantations are less conducive to fungus growth (MacKenzie et al., 2011). There was also a non-fluorescent mode between 0.8 and 1.5 μm which was attributed to transport from without the rainforest.

Further measurements of the understory were reported in Whitehead et al. (2010). Flux measurements show that the above-canopy site and the below-canopy site were decoupled at night as a shallow nocturnal boundary layer formed in the valley. During the day the two sites are coupled by large scale sporadic turbulent events which transported sub-micron aerosol through the forest canopy. This was supported by in-canopy AMS composition measurements[1] (performed by analysis of in canopy bag samples; Figure 4.3) which were comparable to simultaneous measurements performed above canopy. DMPS number/size distributions from the above-canopy site[2] consistently showed a dominant

[1] Robinson performed AMS measurement (in collaboration with co-authors) and analysis, and aided in preparation of the manuscript

[2] Robinson performed DMPS measurements (in collaboration with co-authors) and analysis

Figure 4.1: Time sequence of photographs through a typical day at the ground site. Reproduced from MacKenzie et al. (2011)

.

mode at around 50 nm with a second mode at 150 nm, and a mean total number concentration of $\sim$1300 cc^{-1} (Figure 4.2(a)). This distribution was not affected during periods of upward particle flux from the rainforest understory, implying emissions were insignificant or similar to those above canopy. The volume/size distribution (not reported in Whitehead et al. (2010), but included here for completeness in Figure 4.2(b)) showed one mode around 200-300 nm. There was no relationship apparent between the two sites for super-micron aerosol. There was little net particle flux detected at the above-canopy site with both upward and downwards fluxes occurring during the day. In 80% of the days an upward particle flux was measured between 9 AM and 10 AM local time, which was attributed to the break-up of the nocurnal boundary layer.

The AMS aerosol composition measurements and period classifications (reported in Section 4.2) from the Bukit Atur site were used by Irwin et al. (2011) for the analysis of aerosol sub- and super-saturated hygroscopicity. While CCN concentrations were higher in Borneo than those observed in Amazonia (701 cc^{-1} at a super-saturation of 0.73% cf. 162 cc^{-1} at a super-saturation of 0.82% (Gunthe et al., 2009) respectively), they are still low when compared to most terrestrial environments. Irwin et al. (2011) reiterate the differences in hygroscopicity in the *Marine* and *Terrestrial* clusters (reported in Section 4.2), and the consequent relation to aerosol composition.

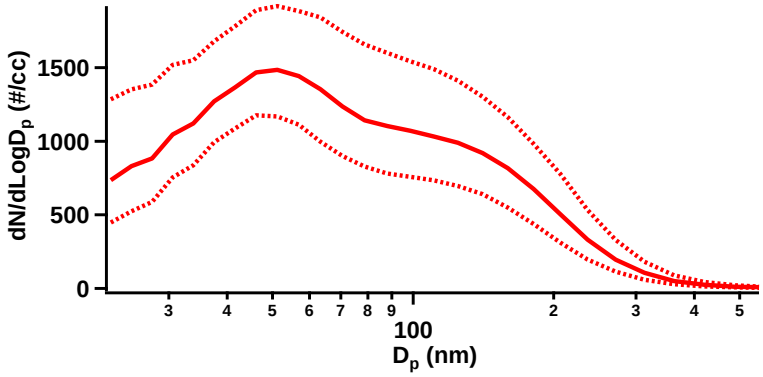

(a)

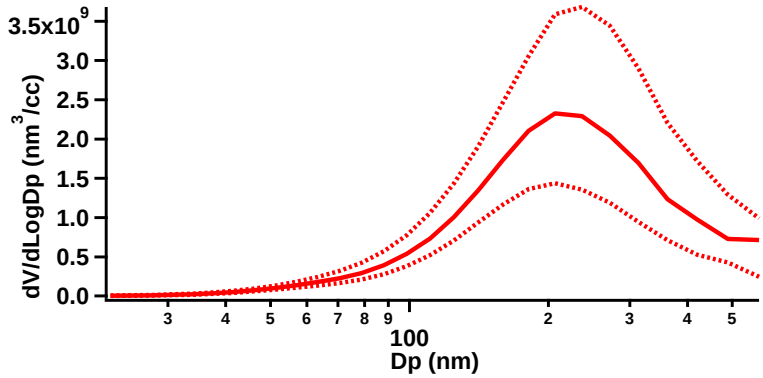

(b)

Figure 4.2: (a) number/size and (b) volume/size log normal distributions, averaged over all DMPS data from the ground site during OP3-III.

Aircraft and ground based measurements from the rainforest and the oil palm plantations were compared to assess the impact of land use conversion (Hewitt et al., 2010; MacKenzie et al., 2011). MacKenzie et al. (2011) contrasted the atmospheric composition above the two land use types.[1] They found that the rainforest was dominated by isoprene but also with significant amounts of monoterpenes present (α-pinene, camphene, limonene and γ-terpinene). It might be expected that the relatively strong VOC source in the rainforest would lead to a depletion of OH, however observed OH levels were much higher than those predicted by models, implying some kind of OH recycling (a similar result to that observed in Surinam; Lelieveld et al., 2008). The oil palm plantations show greater isoprene (Figure 4.4) and NO_x concentrations with the monoterpenes relatively less important. Hewitt et al. (2010) cite the agro-industrialisation of the oil palms as the most likely source of the increased NO_x concentrations, from combustion of fuel but also from the intensive fertilisation of the crops. They warn that if NO_x concentrations were to reach those of North America or Europe with further industrialisation, ozone concentrations would be likely to reach levels harmful to human health. This is a particular issue at the oil palm plantations due to the dominance of isoprene which is conducive to ozone formation in the presence of NO_x. (It should be noted that the VOC:NO_x ratio is greater

[1]Robinson performed AMS data analysis and interpretation, and aided in preparation of the manuscript

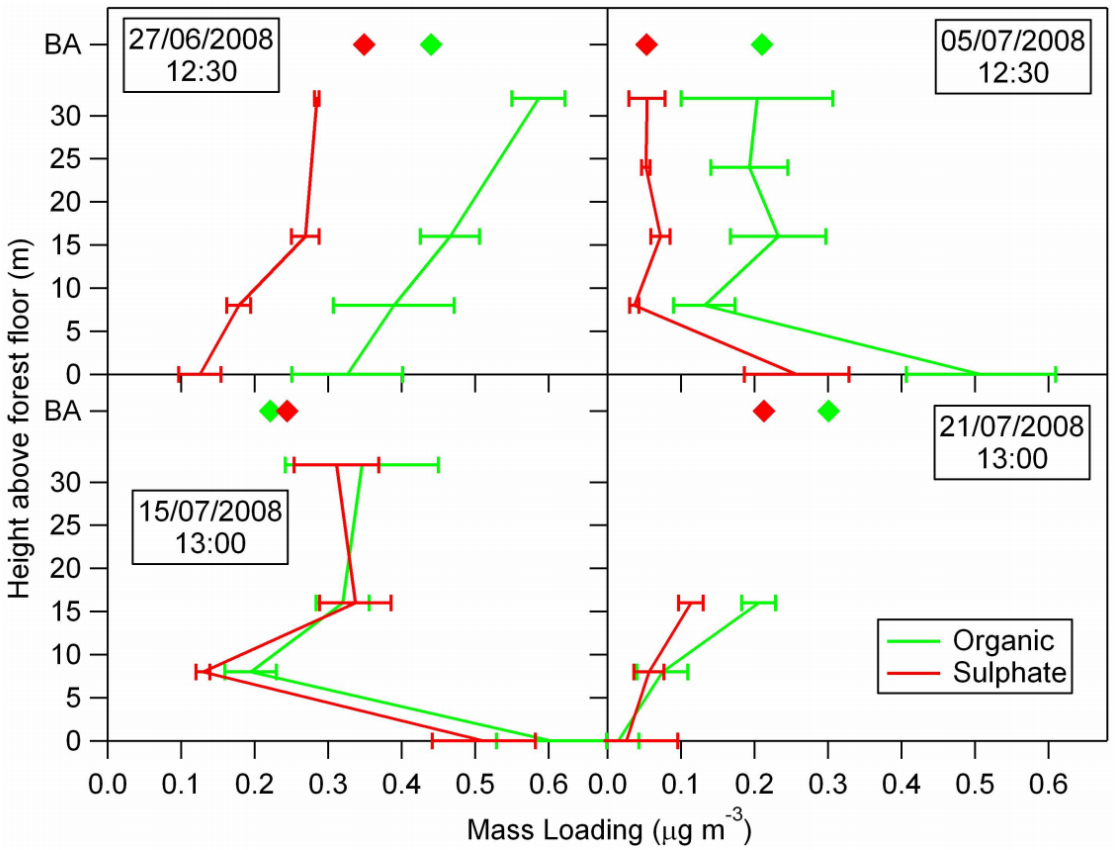

Figure 4.3: Aerosol composition as a function of height above the ground within the rainforest canopy. Air was sampled from different heights into Teflon bags before being sampled with the HR-AMS. The points mark the concurrent loadings measured at the above canopy site. Published in Whitehead et al. (2010) with measurements (in collaboration with other co-authors) and analysis performed by Robinson.

over the oil palm plantations despite the increased NO_x concentrations, and both the rainforest and plantations are NO_x limited.) MacKenzie et al. (2011) also say that the ratio of isoprene to the sum of two first generation isoprene oxidation products, methylvinylketone (MVK) and methacrolein (MACR), was the same at a height of 1 m above the oil palm plantations and a height of 100–150 m about the rainforest. This suggests that the mixing of the boundary layer occurs much faster than the chemical lifetime of isoprene.

MacKenzie et al. (2011) reported that AMS aerosol measurements showed greater organic and sulphate aerosol loadings over the oil palms than the rainforest (17% and 20% respectively) which was stated as a modest difference compared to the large differences in VOC concentrations. Organic aerosol is also more oxidised over the oil palms than the rainforest, with an m/z 44:43 ratio (indicative of the degree of oxidation; see Section 1.4) of 1.35 compared to 1.26 respectively. Organic aerosol and m/z 44:43 ratio were not found to corelate with markers of anthropogenic influence suggesting any anthropogenic organic aerosol source was not dominant. Palm oil processing plants were major local sources of organic aerosol with loadings $>100\mu$g m^{-3} within the chimney plume. The mass spectrum was similar to that observed of biomass burning in other studies. It is not clear, however, to what extent palm oil processing plant emissions are a regional source.

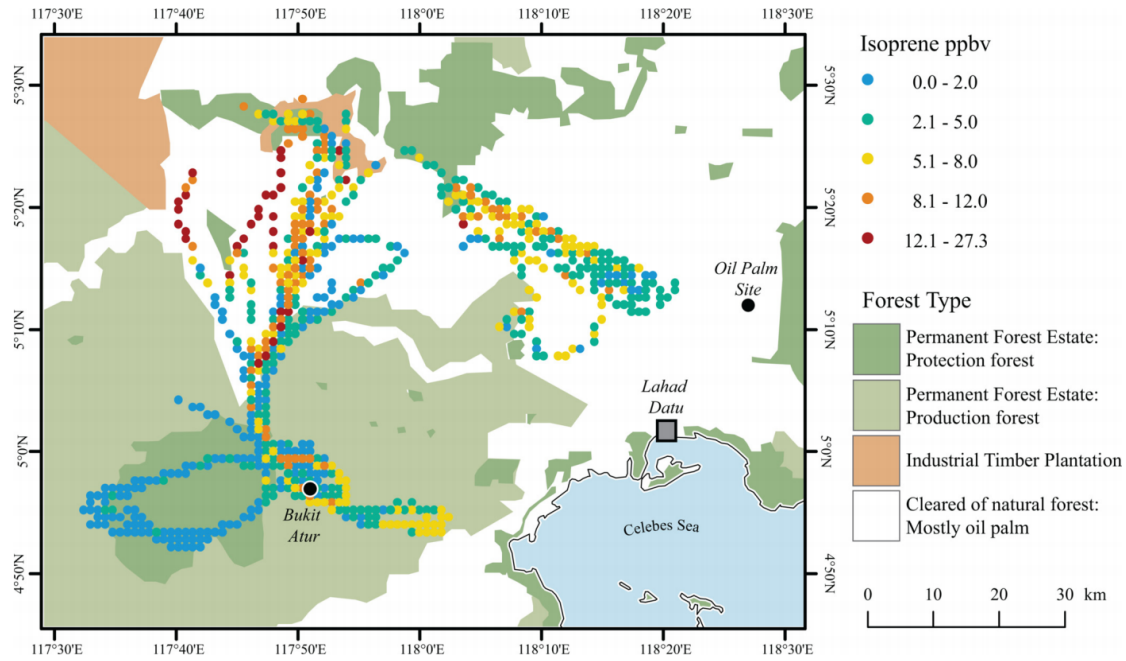

Figure 4.4: Boundary layer isoprene measurements performed on the BAe-146 research aircraft by Hewitt et al. (2009). The map colours indicate the land use, with white areas predominantly oil palm plantations. Isoprene mixing ratios marked with coloured points show that isoprene concentrations are higher to the over the oil palm plantations to the north of the ground site.

Misztal et al. (2010) measured organic gas and aerosol fluxes from a palm oil plantation during OP3 and during the Aerosol Coupling in the Earth's System (ACES) project, a sister project to OP3 which was performed between the OP3-I and OP3-III measurement intensives. PTRMS measurements showed particularly large emissions of estragole (1-ally-4-methoxybenzene) from the plantations, a species which was not previously considered to be of global importance and is not included in the MCM. GC-MS analysis of leaf cuvettes and Teflon flower enclosures showed that the estragole was emitted from the flowers of the oil palms. Estragole has previously been shown to be an attractant for weevils which efficiently pollinate the oil palms. It is thought to be semi-volatile, meaning it is likely that some of its mass was present in the condensed phase. This proportion was estimated by sampling nebulised estragole with an AMS and identifying major peaks (m/z 15, 53, 70, 77, 91, 115, 147) which could then be summed in the ambient mass spectrum. This approach is similar to that presented in Section 4.4 to estimate the amount of methyfuran aerosol, except that all of the major estragole peaks are likely to have had significant contributions from other species, meaning that this is an extreme upper bound estimate. This showed that there is a factor of approximately 1×10^3–1×10^4 more estragole in the gas phase than the condensed phase. Estragole is thought to react readily with OH and O_3, but it is not clear how much aerosol is formed from its oxidation products in the atmosphere. Given the large gas phase loadings, and previous chamber studies which have measured ozoneolysis aerosol mass yields as high as 6% (Lee et al., 2006), estragole and its products could make a significant contribution to the organic aerosol mass

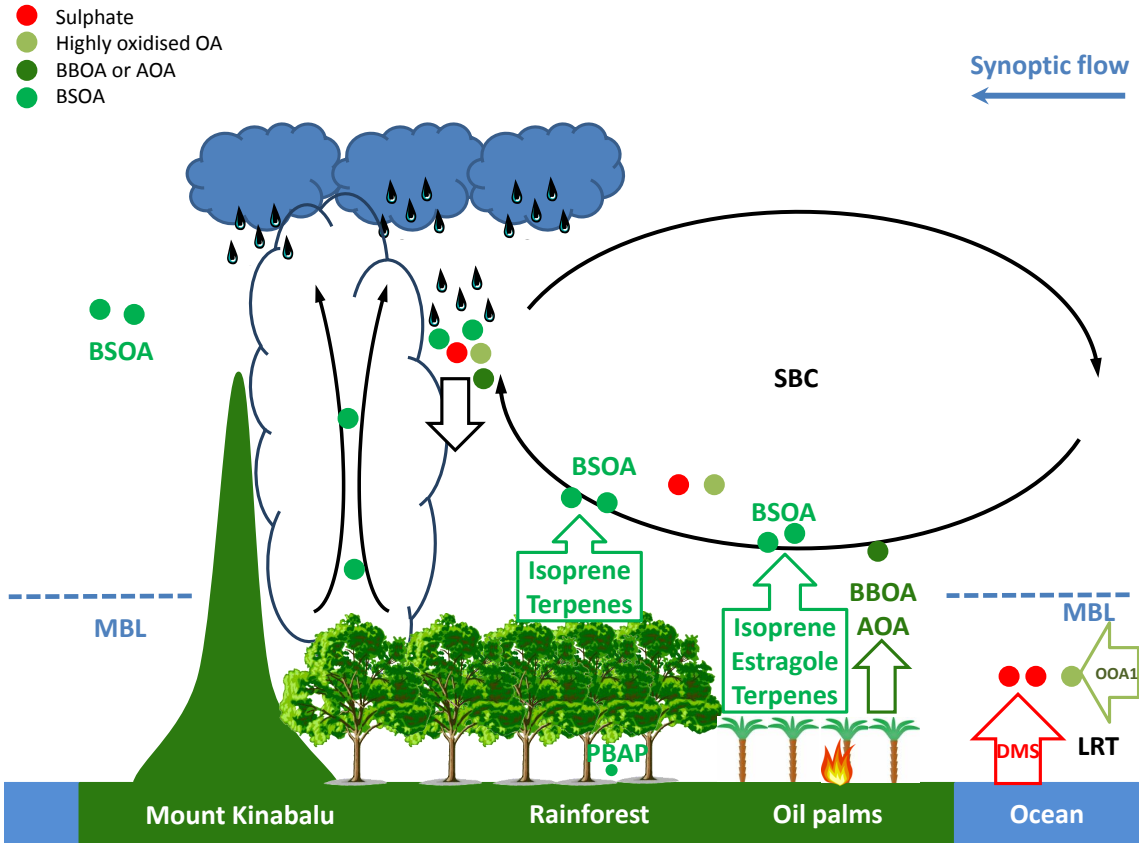

Figure 4.5: A schematic of aerosol processes in Borneo. Sulphate (probably from DMS) and highly oxidised organic aerosol (OOA1) arrive at the east coast via long range transport with the synoptic flow in the marine boundary layer (MBL). These are lifted higher into the atmosphere by sea breeze cells (SBC) and moist convection. The oil palm plantations (and settlements near the coast) are a source of biomass burning aerosol (BBOA) and other anthropogenic organic aerosol (AOA). The oil palms are also a major source of isoprene, estragole, and terpenes, and associated BSOA. The rainforest understory is a source of PBAP, however, the supermicron PBAP are not efficiently transported through the canopy. BSOA is also created from rainforest emissions of terpenes and isoprene. Precipitation, of which there is more inland were the orography increases moist convection, acts to remove aerosol. The inland sources of aerosol, that is BSOA, are replenished en-route, while the regional and coastal aerosol are depleted. The BSOA leaves the island in the lower and mid free troposphere, where its atmospheric lifetime is likely to be longer than the aerosol population upwind, which was confined to the MBL.

in Borneo. The similarity of estragole to the terpenes means it is likely that any estragole SOA detected by the AMS at Bukit Atur would be expressed as part of the OOA2 factor. A cartoon of main aerosol processes in Borneo is shown in Figure 4.5.

CHAPTER

FIVE

CONCLUSIONS

This thesis provides insight into aerosol composition and processes in a previously unstudied region of the World. The tropics experience a higher top of the atmosphere solar flux than any other region meaning that aerosol effects have proportionally more influence on global climate. South-East Asia represents a significant and previously unexplored portion of the tropics. The measurements show important differences to previously studied environments, both in the northern mid-latitudes and in Amazonia. It is likely that the data reported in this thesis are more representative of South-East Asia as a whole than any existing data sets. The organic aerosol measurements have already been used (as part of a larger collection of AMS datasets) to inform a global model which estimates the magnitude of SOA climate effects (Spracklen et al., 2011). South-East Asia is also experiencing rapid land use change, with rainforest being logged to make way for oil palm agriculture. This thesis can aid future studies of the effects of regional land use change, both by acting as a benchmark to compare further changes against, and through the identification of possible production of isoprene SOA from oil palm emissions.

5.1 Summary of Findings

Sub-micron NR aerosol composition at the surface was, on average, approximately half organic and half ammonium sulphate with the remaining inorganics making up less than 3%. Factor analysis of the organic mass spectra yielded four factors. Some of the factors were similar to those regularly observed in other studies: OOA1 and OOA2 representing respectively more and less oxidised OA were observed. One factor had some similarities to biomass burning emissions measured in previous studies, although it was present in low amounts suggesting relatively little influence of local biomass burning emissions on the measurement site. (This does not proscribe an influence from long range transport of aged biomass burning emissions that could be included in the OOA1 factor.) A PMF factor was associated with isoprene SOA for the first time.

Two methods using analysis of back trajectories showed sulphate loadings tended to be greater in air masses that did not travel across the interior of the island. Aircraft mea-

surements also directly detected sulphate upwind to the east of Borneo. In contrast, the air masses that travelled over the interior of Borneo from the south-west tended to show lower sulphate loadings (although they were still high when compared to Amazonia). Aircraft measurements from the downwind (west) coast of Borneo showed lower sulphate than measurements upwind on the east of Borneo. Taken together this implies an off-island source, and an inland sink of sulphate aerosol. It is likely that aerosol is being removed through precipitation as it travels across the island. This is corroborated by ECMWF reanalysis which shows greater levels of precipitation inland, particularly over the mountainous interior, as well as greater rainfall and cloud cover measured at the rainforest site compared to the oil palm site (MacKenzie et al., 2011). When taken as a whole this provides convincing evidence for a sulphate source external to the island.

It is likely that a significant proportion of this sulphate is from processing of marine DMS emissions from phytoplankton. This is a well established sulphate source in marine environments, and its influence may be expected to be prevalent on an island such as Borneo. It is also possible that volcanic emissions are responsible for some of the regional sulphate, however sulphate rich air masses showed no association with volcanic events reported during the project. There seems to intermittently be some degree of correlation between sulphate and organic aerosol. The highly oxidised factor is associated with air masses that originate externally to the island, and it is likely to be from long range transport of organic aerosol. This aerosol could be from primary or secondary and biogenic or anthropogenic sources. The correlation could be indicative of long range transport of simultaneous anthropogenic emissions of sulphate and organics, such as that from fossil fuel combustion. However, there is no particular association of air masses with any large conurbations. It may also be internally mixed marine biogenic sulphate and organic aerosol. It is not known what fraction of the OOA1 was from aged regional biomass burning emissions. However inspection of seven day trajectories showed the site to be influenced by air mass from regions of comparatively low biomass burning activity suggesting this to be a minor contribution.

The remainder of the organic aerosol is associated with air masses that travel across the island. Aircraft altitude profiles over the island show production of SOA from photochemical processing of precursors as the day progresses. Aircraft mass spectra tended to show similarities to the 82Fac and OOA2 factors, which are both associated with BSOA. Back trajectory analyses show isoprene SOA may be particularly associated with the oil palm plantations, which have been reported to emit five times as much isoprene as the rainforest (Hewitt et al., 2009). The OOA2 shows contrasting sources to 82Fac which suggests it signifies a different source of fresh organic aerosol such as terpene SOA.

Transport of air mass across the island lofts aerosol higher into the troposphere, compared to the upwind region where aerosol is confined to a shallow marine boundary layer. This is likely to be caused by the interaction of synoptic flow with marine sea breeze circulations and moist convection over the island. There also appears to be a depletion in

regional sulphate (and organic) aerosol and an enhancement of BSOA from processing of terrestrial on-island VOC emissions.

Emissions from biomass burning were observed at the beginning of the campaign, although not to the same extent as has been observed in biomass burning dominated periods in West Africa (Capes et al., 2008) and Amazonia (Artaxo et al., 2002). This period was also associated with an increase in loadings of aerosol not typically associated with biomass burning. This may be explained if fire emissions increased regional oxidant levels, increasing the amount of secondary aerosol production. It could also be due to a suppression of regional precipitation by biomass burning aerosol emissions, which has previously been reported in Borneo (Rosenfeld, 1999).

5.2 Implications

The current picture of tropical aerosol composition

Total sub-micron NR aerosol loadings in Borneo (1.6 μg m^{-3}) are lower than in previous studies of remote rural sites in the northern mid-latitudes (an average of 5.9 μg m^{-3} for "remote/rural" sites in Zhang et al. (2007)). Some of the remote coastal sites (i.e. Chabogue Point, Duke Forest and Mace Head) show the most similarity to Borneo, with approximately equal amounts of organic and ammonium/sulphate aerosol. However, they all have around twice the total aerosol loading observed in Borneo.

Sulphate aerosol loadings (0.61 μg m^{-3}) were much greater than in the only other AMS study performed in a rainforest environment, namely Amazonia (0.15 μg m^{-3}; Chen et al. (2009)). Organic aerosol levels in Borneo (0.74 μg m^{-3}), while lower than the average remote rural loading in the northern mid-latitudes (2.8 μg m^{-3} using same data as above), were comparable to the concentrations of organic aerosol observed in Amazonia (0.67 μg m^{-3}; Chen et al. (2009)). The average m/z 44:43 ratio (which signifies organic aerosol ageing) was observed to be 2.2 in Borneo compared to 1 for in-basin and 1.3–2 for out-of-basin sources in Amazonia (Chen et al., 2009). This shows organic aerosol in Borneo to be more aged than in Amazonia on average, which may be expected given the greater role far field organic sources would play in Borneo, as the major near field sources are constrained to the island.

The AMMA campaign in West Africa did detect relatively high concentrations of sulphate aerosol although these were not the primary foci of publications. These AMS measurements were performed over a large spatial scale and in a variety of conditions ranging from intense biomass burning to remote biogenic background. This makes it difficult to establish what data would be suitable for a direct comparison to the OP3 project. However, in Section 4.2 a comparison is drawn by averaging only data classified as being of low altitude and biogenic influence. This average appears to show fairly similar aerosol composition to Borneo, with organic and sulphate concentrations of 1.01 and 0.82 μg m^{-3} respectively. It is possible that the sulphate in West Africa was due to emissions from the

Atlantic Ocean. It is also possible that the screening applied to remove biomass burning and anthropogenic influence (both potential sulphate aerosol sources) could not account for regional background signals, which could have been high.

It is clear that aerosol composition in Borneo during OP3 is different to most northern mid-latitude environments previously studied using AMS techniques. There may be some similarities to aerosol composition in West Africa but this dataset is complicated by strong regional sources and may not be directly comparable as it is measured from an airborne platform. While there are still very few datasets from tropical rainforest environments, aerosol composition in Borneo appears to be strikingly different to the Amazon, with much higher concentrations of sulphate aerosol.

Global models predict there to be between 0–3 μg m^{-3} of organic aerosol in North Borneo (Chung and Seinfeld, 2002; Lack et al., 2004; Tsigaridis and Kanakidou, 2003). The measured organic aerosol concentrations are consistent with this range however the models are highly uncertain. Capes et al. (2009) found that, while their organic aerosol loadings were in agreement with these same models, this was likely to be due to conflating errors, with calculations based on detected VOC levels underestimating organic mass by an order of magnitude. By using more up-to-date yields they were able to improve the accuracy of the modelled loadings, but they were still imprecise. More recently, Chen et al. (2009) used the GEOS-Chem model to predict organic aerosol concentrations in Amazonia during the period of the AMAZE-08 project, and found an under-prediction of only 35%, although they state that the modelled value is highly uncertain.

Concentrations of SOA formed in Borneo can be estimated to be at least OOA2 and 82Fac (0.26 μg m^{-3}) and at most all of the organic aerosol (0.74 μg m^{-3}). Similarly, POA concentrations can be estimated to be at most 91Fac and OOA1 (0.31 μg m^{-3}). It should be noted that this POA estimate is an upper bound as almost all of the OOA1 is likely to be secondary. Henze and Seinfeld (2006) and Tsigaridis and Kanakidou (2007) predict around 0.5 μg m^{-3} of SOA to be present in Borneo, with the latter stating that virtually all SOA was biogenic. It should be noted that the region where OP3 was performed in North Borneo was predicted to have lower SOA loadings than reported above. However, this is likely to be caused by the relevant model pixel containing regions of both land and sea, so loadings predicted for the nearest inland pixel were used instead. More recently Utembe et al. (2011) predicted 0.5–1 μg m^{-3} of organic aerosol in Borneo with 0.1–0.5 μg m^{-3} of that SOA. These values are consistent with the ranges stated above.

The concentration of PBAP (probably fungal spores) detected in the understory of the rainforest by Gabey et al. (2010) is likely to be significant in terms of total aerosol mass given the dominance of a supermicron mode. However Whitehead et al. (2010) show it is unlikely that these aerosols are efficiently transported out of the rainforest understory where they are produced. The WIBS technique does not resolve sub-micron particles well and it may be possible that PBAP contribute in this regime, however inspection of AMS mass spectrum peaks associated with model PBAP (unpublished data by J. Schneider, as

in Chen et al. (2009)) show that, if present, they do not contribute a significant amount of mass. PBAP are insignificant in terms of aerosol number, with only 4 cc^{-1} measured compared to the DMPS total sub-micron number of 1300 cc^{-1}. It may be possible that low concentrations of PBAP are important as ice nuclei in the region, as was the case in Amazonia (Prenni et al., 2009), however there is no evidence to suggest this. It seems, then, that the sub-micron particles are likely to be the most significant on a regional scale.

The AMS data did not allow effective resolution of composition resolved size distributions due to the low aerosol concentrations and relatively low signal-to-noise ratio of the HR-AMS (when compared to previous models such as the C-AMS, see Section 2.1). However sub-micron size distributions were measured and reported in Whitehead et al. (2010), showing a number/size distribution with two modes (at $\sim$50 nm and $\sim$150 nm), and a volume/size distribution with only one mode ($\sim$250 nm). The mono-modal volume/size distribution suggests that the aerosol detected using the AMS are likely to be largely internally mixed, with fresher aerosol tending to condense onto pre-existing aerosol. The number/size distribution showed similar modes to aerosol in Amazonia, which had modes at 68 nm and 151 nm (Zhou et al., 2002). However, number concentrations in Borneo ($\sim$1300 cc^{-1}) were higher than Amazonia, which had a mean concentration of 450 cc^{-1} (Zhou et al., 2002).

MacKenzie et al. (2011) reported that different aerosol composition was measured over different land use types on the FAAM aircraft. They also comment that this difference is slight when compared to the differences observed in gas phase species. Section 4.2 showed that a significant amount of regional aerosol is transported onto the island, particularly in conditions dominated by south-westerly air flow, as was the case during the flying campaign. Section 4.3 then showed that these regional aerosol are depleted (probably through wet deposition) as they travel across the island, and on-island sources of aerosol become more important. More rainfall was observed at the rainforest site than the oil palm plantation site (MacKenzie et al., 2011) which would act to deplete aerosol concentrations leading to a greater amount of freshly produced aerosol, which could be replenished en-route. This would explain the higher concentrations of aged organic aerosol and sulphate (both thought to be typical of the regional background) nearer the coast, and the less aged depleted aerosol concentrations further downwind (inland). The greater differences observed in gas phase composition than particulate composition over the two regions is likely to be because aerosol tend to have a longer atmospheric lifetime than VOCs. This would allow transport of aerosol between the oil palm and rainforest regions, reducing any differences due to surface emissions. This also means that island emissions dominate the VOC population, as opposed to the aerosol population which has a significant off-island component. The local VOC population is, therefore, more sensitive to changes in surface emissions. The relatively modest difference in aerosol population between rainforest and oil palms should not be treated as evidence that land use conversion is of little consequence for aerosol composition, as it is hard to say to what extent aerosol

measured in and above the rainforest are currently influenced by oil palm emissions (and vice versa).

Global organic aerosol models appear to predict concentrations in Borneo better than in other regions, particularly the northern mid-latitudes (Volkamer et al., 2006). However there has been evidence from previous studies that this may be due to conflating errors (Capes et al., 2009). Although modelled organic aerosol concentrations are consistent with measured concentrations in Borneo, bespoke SOA bottom-up calculations should be performed with contemporaneously measured VOC data in future work. Doing this will test the accuracy of the model and its mechanisms, and by using more up-to-date models it may be possible to improve the precision.

Aerosol hygroscopicity was found to be related to composition, specifically the organic:inorganic (i.e. organic:sulphate) ratio (Irwin et al., 2011). While CCN concentrations were found to be higher than in Amazonia, they are still low when compared to most continental sites reinforcing the "green ocean" analogy which observes that pristine rainforest conditions are similar to those found in the remote marine environment (Roberts et al., 2001). That aerosol hygroscopicity was observed to vary depending on composition highlights the influence aerosol emissions in South East Asia can have on climate through indirect aerosol effects.

Isoprene SOA

Isoprene SOA has been the focus of much debate and research in recent years. Until recently it was considered to have too low an SOA yield to generate significant amounts of aerosol, however this picture has changed and it is now thought to be a large global source (Carlton et al., 2009; Henze and Seinfeld, 2006). The work presented in Section 4.4 identifies substantial amounts of isoprene SOA in Borneo. An AMS peak which is, so far, unique to isoprene SOA was identified. This in itself is an important result as it allows for the identification of isoprene SOA in other studies which use AMS techniques, of which there are many. In addition there is only one other reported instance of isoprene SOA being measured with a high time resolution instrument (i.e. not filter measurements; Froyd et al., 2010). Enabling the AMS identification of isoprene SOA allows for more comparison of concentrations to contemporaneous high time resolution measurements of precursors and photochemical parameters.

Slowik et al. (2011) reported a similar factor from combined PMF analysis of two sets of simultaneous AMS measurements, both from rural sites around 70 km apart in south western Ontario. In general, this factor is only a minor contributor to the total organic mass. However, for a period of a few days it is a substantial factor, especially at one of the sites where it is the dominant factor, present in concentrations of around 8 μg m^{-3}. This period was associated with high isoprene and sulphate concentrations. Slowik et al. (2011) attribute the m/z 82 yielding factor to isoprene SOA on the back of the work presented in Section 4.4. Similarly, they also suggest the presence of sulphate could be a

controlling factor in the formation of this isoprene SOA.

Using PMF analysis, isoprene SOA was estimated to make up 23% (0.18 μg m^{-3}) of the organic aerosol population on average in Borneo — a substantial amount of the organic aerosol present. The compound that directly yields the novel signal (methylfuran) makes up 8% of the organic aerosol alone. It is not clear how any established isoprene SOA could be yielding the exact signal detected by the AMS. This may be due to a lack of understanding of the precise way the isoprene SOA is processed in the instrument during detection. However, it may also be indicative of a novel type of isoprene SOA. If this is the case, then identification of the novel formation mechanism is likely to improve modelling of isoprene SOA and therefore SOA in general.

It appears that isoprene SOA was considered to be zero for the global organic aerosol models that predicted the correct range of values for Borneo (discussed above; Chung and Seinfeld, 2002; Lack et al., 2004; Tsigaridis and Kanakidou, 2003). This supports the assertion made by Capes et al. (2009) that these models may serendipitously predict the correct organic aerosol loadings, as the work presented here shows isoprene to be a significant SOA source. After the revelation that isoprene could be a very important source of SOA despite the low yields by Henze and Seinfeld (2006), models seem to more precisely predict concentrations in Borneo. Henze and Seinfeld (2006) and Tsigaridis and Kanakidou (2007) both predicted around 0.15 μg m^{-3} (30% of total SOA) of isoprene SOA in Borneo. These values are in-line with the observations reported here.

While the isoprene SOA signal has now been reported in other studies, the large quantities present in Borneo are, so far, unique. It is possible that production of methylfuran yielding aerosol in Borneo is facilitated by atmospheric chemistry that is different to the other studies. Three properties of Borneo that have been shown to affect isoprene SOA chemistry in previous studies, and may therefore control the formation of methylfuran yielding isoprene SOA are:

1. High isoprene concentrations, particularly due to oil palm emissions but also from the rainforest.

2. A low NO_x:VOC ratio due to the relatively small local anthropogenic influence.

3. High concentrations of sulphate which, while neutralised by the time of arrival at the ground site, was found to be acidic nearer the coast. Additionally, the coast is also where isoprene rich oil palms tend to be situated.

These qualities would be expected to be common to much of the “maritime continent” meaning that methylfuran yielding isoprene SOA, and isoprene SOA in general, may be of particularly great importance throughout this large unstudied region of the tropics. As such one recommendation of this thesis is further study of the regional importance of these aerosol and the mechanisms by which they are formed. This may be achieved by searching for notably large concentrations of methylfuran yielding aerosol in further projects in other regions of the “maritime continent”. While methylfuran yielding aerosol

was observed in chamber isoprene oxidation as part of the work reported here, it was at low concentrations compared to those observed in Borneo. Further work should be performed in oxidation chambers to probe aerosol formation in conditions representative of the Bornean atmosphere.

Effects of Island Dynamics on Regional Aerosol

Convection and orography in Borneo appear to act as mechanisms that loft aerosol into the lower and mid free troposphere. This will have implications downwind, as the aerosol would be expected to be above a greater amount of regional precipitation resulting in less wet deposition and a longer atmospheric lifetime. The extension in aerosol lifetime, and the change in altitude relative to cloud cover will affect the direct, indirect and semi-direct aerosol effects in the region. Similar processes are likely to occur along the whole island chain from continental South East Asia to Australia and hence may provide a substantial source of tropical terrestrial aerosol to the free troposphere. Future regional transport modelling should attempt to incorporate the average increased altitude of aerosol downwind of the island. They should also attempt to accurately emulate the increase of terrestrial organic aerosol and the decrease in regional aerosol as air mass travels across the island. Aerosol may be being recirculated in the downwind sea breeze, causing it to accumulate throughout the day. If this is the case then it may be expected that the aerosol would be released when the sea breeze circulation is at its weakest (approximately sunrise and sunset) and the synoptic flow can carry the aerosol away. Future studies of the region should be vigilant for pulses of elevated aerosol concentrations approximately 12 hours apart downwind of Borneo, or other tropical islands.

Aerosol in Borneo Under Future Land Use Change

Borneo, and the tropics in general, are likely to undergo profound land use changes in the future. The VOC emissions of oil palms were shown to be different to the rainforest, with much higher isoprene (Hewitt et al., 2010; MacKenzie et al., 2011) and estragole (Misztal et al., 2010) emissions than the rainforest. This work shows BSOA from the oxidation of isoprene is a major contributor to the total organic aerosol mass in Borneo. Hence it is likely that the regional isoprene SOA burden will increase in the future. At present it is unclear what proportion of the organic aerosol measured in Borneo was BSOA from estragole, either from partitioning of estragole itself, or its oxidation products. However, it may be a significant fraction given the yields observed in chamber experiments. The estragole organic aerosol burden should be the focus of future studies, as this also would be expected to increase in the future. The local anthropogenic aerosol burden in Borneo does not appear to be as large as the biogenic but this may change in the future. One of the least predictable atmospheric effects of future development is the potential for a latent source of anthropogenically controlled BSOA which could be realised

as anthropogenic pollution increases across the region. Hoyle et al. (2011) report that several studies suggest as much as 50% of the detected organic mass was anthropogenically controlled SOA, with Spracklen et al. (2011) placing this figure at 90%. Assuming the value of Hoyle et al. (2011) to be typical, the implication is this effect could more than double aerosol loadings from biogenic precursors if anthropogenic pollution increases.

5.3 Recommendations and Outstanding Questions

The work presented here is an important contribution to the global set of detailed in-situ aerosol measurements. However, there is still a lack of measurements in the tropics, particularly in South East Asia. It is recommended that further similar studies are performed to assess to what extent these data are representative of the wider region. Similarly it is not clear how representative the period of study was, for instance, while the influence of local biomass burning was relatively low during OP3, it may be much more significant during the biomass burning season in March/April (Dwyer et al., 2000).

These results provide important insight into organic aerosol processes in Borneo, and elsewhere. Two unexpected and potentially very significant sources of BSOA in Borneo were identified: estragole (Misztal et al., 2010) and isoprene. Comparison of the AMS isoprene signal to data from other locations indicate Borneo has unusually large isoprene SOA concentrations. While it is clear that the detection of methylfuran signifies isoprene SOA, it is not clear how this molecule could be produced by degradation of any established isoprene SOA upon analysis. More work should be done to investigate the atmospheric composition of MF-yielding isoprene SOA. This should proceed by attempting to identify MF-yielding isoprene SOA in chamber studies. The particular abundance of this isoprene SOA in Borneo combined with the particularly high sulphate loadings suggest that sulphate may be affecting the isoprene chemistry. As such, chamber oxidation experiments attempting to identify MF-yielding SOA should further investigate the effect of the presence of sulphate aerosol, particularly at the NO_x limited, high relative humidity conditions representative of Borneo. Similarly, more work should be done investigating the oxidation products of estragole to try and constrain the amount of SOA that may be produced given the emissions in Borneo. Modelling of organic aerosol concentrations, whilst consistent with the measurements, are imprecise. Work should be done to allow explicit models of organic aerosol to include accurate descriptions of isoprene and estragole SOA in Borneo.

The discovery of anthropogenically controlled BSOA has cast much doubt on the predictive ability of organic aerosol models under future land use change scenarios. It is potentially a large source of tropical aerosol in the future given increased regional urbanisation, which appears inevitable. More studies should attempt to further constrain its production in future chamber studies and field work.

5.4 Closing Remarks

This work presents the first characterisation of aerosol composition in a climatologically important region of the World which is under-represented in the literature. These measurements have already been applied to the issue of climate change, on the microphysical scale through comparison with measurements of aerosol cloud forming potential (Irwin et al., 2011), and in a model that estimates the global climate effects of secondary organic aerosol (Spracklen et al., 2011). The significant concentration of sulphate aerosol, which is likely to be due to the proximity of marine sources, makes aerosol composition different from other studies in rainforest environments. Important questions have been raised about the processing of VOC emissions, in particular isoprene. This work suggests that there is still progress to be made uncovering the way isoprene SOA is formed in the atmosphere. Even when considering the OP3 results, the region still remains under-studied. However, in the absence of further studies, this work stands as a valuable representation of the region. The OP3 project provided an important opportunity to study a once pristine region that is in the early stages of anthropogenic development, and it provides a benchmark that future, more extreme, perturbations to the regional biosphere can be measured against. Increased urbanisation in the region could unlock a latent source of organic aerosol, with pollution acting to more efficiently convert the plentiful BVOCs to SOA. This could have implications not only for climate, but for the health of the new settlers. Given the increase in global demand for palm oil and the aspiration for developing countries such as Malaysia to achieve a first world standard of living, it seems that further destruction of the rainforest ecosystems and conversion to palm oil plantations is inevitable.

APPENDIX

A

LIST OF OTHER PAPERS AND CONFERENCE PROCEEDINGS

Other papers

1. Whitehead, J. D., M. W. Gallagher, J. R. Dorsey, N. Robinson, A. M. Gabey, H. Coe, G. McFiggans, et al. 2010. Aerosol fluxes and dynamics within and above a tropical rainforest in South-East Asia. Atmospheric Chemistry and Physics 10, no. 19 (October): 9369-9382. doi:10.5194/acp-10-9369-2010. http://www.atmos-chem-phys.net/10/9369/2010/.

   Robinson performed (in collaboration with co-authors) AMS and DMPS measurements, performed the associated analysis, assisted with interpretation and helped with the preparation of the manuscript.

2. Irwin, M, N H Robinson, J. D. Allan, P. I. Williams, J R Dorsey, H. Coe, and G. B. McFiggans. 2010. Marine and secondary organic aerosol influences on cloud forming potential as measured above a South-East Asian Rainforest during OP3., in prep. Atmos. Chem. Phys. Discuss.

   Robinson performed (in collaboration with co-authors) AMS measurements, performed AMS analysis and assisted with the preparation of the manuscript.

3. Chen, Q., D. K. Farmer, J. Schneider, S. R. Zorn, C. L. Heald, T. G. Karl, A. Guenther, et al. 2009. Mass spectral characterization of submicron biogenic organic particles in the Amazon Basin. Geophysical Research Letters 36, no. 20. doi:10.1029/2009GL039880.

   Robinson assisted with AMS measurements.

4. Hewitt, C.N., J Lee, M P Barkley, N Carslaw, N A Chappell, Hugh Coe, C Collier, et al. 2010. Oxidant and particle photochemical processes above a south-east Asian tropical rain forest (the OP3 project): introduction, rationale, location characteristics and tools. Atmospheric Chemistry and Physics, no. 163: 18899-18963. http://www.atmos-chem-phys.net/10/169/2010/acp-10-169-2010.pdf.

Robinson supplied back trajectory analysis and figures, AMS data and interpretation, and assisted with the preparation of the manuscript.

5. MacKenzie, A. R., B. Langford, T.A.M. Pugh, N. Robinson, P. K. Misztal, D. E. Heard, J. D. Lee, et al. 2011. The atmospheric chemistry of trace gases and particulate matter emitted by different land uses in Borneo (in press). Philosophical transactions of the Royal Society of London. Series B, Biological sciences.

   Robinson supplied AMS data and interpretation and assisted with the preparation of the manuscript.

Conference proceedings

1. Robinson, N.H., Coe, H., Allan, J.D., McFiggans, G., Hamilton, J.F., Chen, Q., Martin, S.T. Analysis of Chemical Composition of Atmospheric Aerosols Above a South East Asian Rainforest. American Geophysical Union, San Francisco, Dec. 2008.

2. Robinson, N.H., Coe, H., Allan, J.D., McFiggans, G., Williams, P.I., Hamilton, J.F., Chen, Q., Martin, S.T. Chemical Composition of Atmospheric Aerosols Above a S.E. Asian Rainforest. European Geoscience Union, Vienna, Apr. 2009.

3. Robinson, N.H., Coe, H., Allan, J.D., McFiggans, G., Williams, P.I., Hamilton, J.F., Chen, Q., Martin, S.T. Chemical Composition of Atmospheric Aerosols Above a S.E. Asian Rainforest. Association for Atmospheric Aerosol Research, Minneapolis, Oct. 2009.

APPENDIX

B

SUPPORTING MATERIAL FOR PAPER I

The following Appendix is a reproduction of the supporting material for Paper I, itself reproduced in Section 4.2. It details air mass classifications for use in the analysis of other OP3 datasets, as well as supplementary figures.

Manuscript prepared for Atmos. Chem. Phys.
with version 3.2 of the LaTeX class copernicus.cls.
Date: 2 December 2010

Source attribution during the OP3 project using backwards air mass trajectories: Supplementary Material

Robinson et al
Correspondence to: H. Coe
(hugh.coe@manchester.ac.uk)

This supporting material includes any figures that could not be included in the principal text but may be relevant for the interested reader. Figure S1 shows a scatter plot of organic vs sulphate aerosol, similar to the Figure 14 in Section 3.5 of the principal text. It is coloured by level of organic m/z 44:43 (a proxy for oxidation). Points at line A show a range of oxidation levels, points a line B show generally high levels of oxidation and points at line C show generally low levels of oxidation. This supports the assertion from the main text that the points at different lines are related to different sources:

- points at line A are from periods dominated by natural sulphate emissions that are not necessarily related to organic emissions (for example from marine dimethyl sulphide production or volcanic emissions) meaning a range of oxidation levels is sampled
- points at line B are representative of long range transport of organic aerosol which is highly oxidised. This is associated with sulphate which is either emitted simultaneously or coats the organic aerosol during transit.
- and points at line C which are from periods of inland air that is dominated by comparatively local biogenic aerosol and biomass burning meaning the aerosol are less oxidised and less related to sulphate.

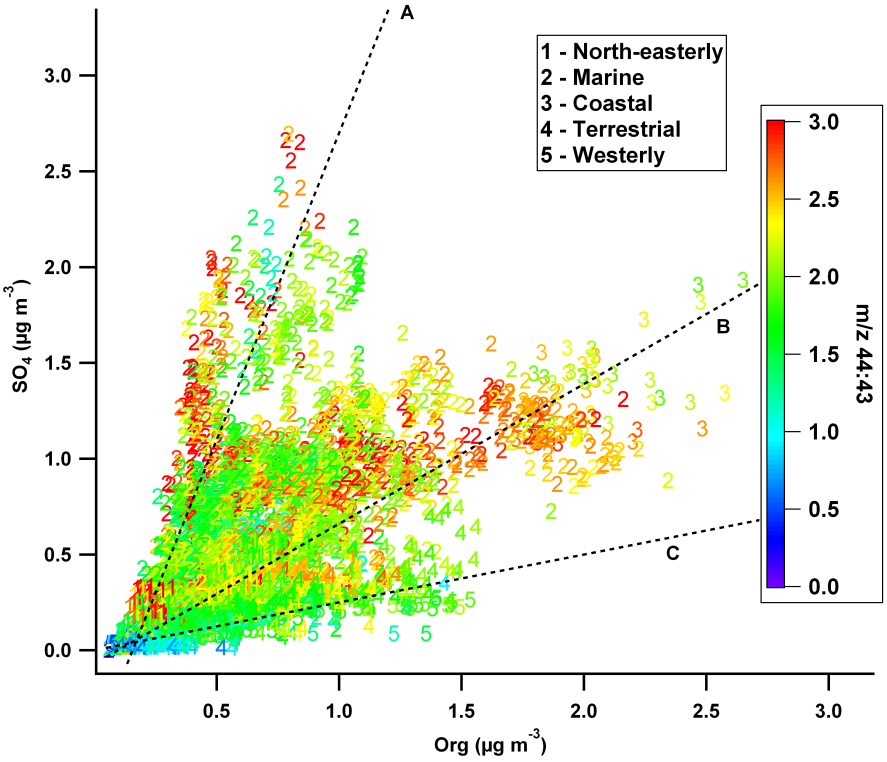

Fig. 1. SO_4 loading vs organic matter loading numbered by cluster. Point colour signifies m/z 44:43 magnitude, a proxy for oxidation. Lines, labelled with letters, indicate different proposed dependencies. Lines represent modes of the SO_4:org ratio histogram of values.

Tables 1 and 2 detail the precise times of the cluster analysis period classifications of OP3-I and OP3-III respectively, and are included here for reference.

OP3-I	
04/04/2008 08:00	1
04/04/2008 20:00	1
05/04/2008 08:00	1
05/04/2008 20:00	1
06/04/2008 08:00	1
06/04/2008 20:00	1
07/04/2008 08:00	1
07/04/2008 20:00	0
08/04/2008 08:00	2
08/04/2008 20:00	1
09/04/2008 08:00	1
09/04/2008 20:00	1
10/04/2008 08:00	1
10/04/2008 20:00	0
11/04/2008 08:00	0
11/04/2008 20:00	2
12/04/2008 08:00	2
12/04/2008 20:00	2
13/04/2008 08:00	2
13/04/2008 20:00	0
14/04/2008 08:00	4
14/04/2008 20:00	4
15/04/2008 08:00	4
15/04/2008 20:00	4
16/04/2008 08:00	4
16/04/2008 20:00	4
17/04/2008 08:00	4
17/04/2008 20:00	2
18/04/2008 08:00	2
18/04/2008 20:00	2
19/04/2008 08:00	2
19/04/2008 20:00	2
20/04/2008 08:00	2
20/04/2008 20:00	2
21/04/2008 08:00	0
21/04/2008 20:00	1
22/04/2008 08:00	1
22/04/2008 20:00	1
23/04/2008 08:00	1
23/04/2008 20:00	0
24/04/2008 08:00	2
24/04/2008 20:00	2
25/04/2008 08:00	2
25/04/2008 20:00	0
26/04/2008 08:00	3
26/04/2008 20:00	3
27/04/2008 08:00	0
27/04/2008 20:00	4
28/04/2008 08:00	4
28/04/2008 20:00	4
29/04/2008 08:00	4
29/04/2008 20:00	4
30/04/2008 08:00	4
30/04/2008 20:00	4
01/05/2008 08:00	4
01/05/2008 20:00	4
02/05/2008 08:00	4
02/05/2008 20:00	4
03/05/2008 08:00	0
03/05/2008 20:00	0
03/05/2008 20:00	0
03/05/2008 20:00	0
03/05/2008 20:00	0
03/05/2008 20:00	0
03/05/2008 20:00	0
03/05/2008 20:00	0

Table 1. Cluster analysis period classifications for OP3-I. Times are start times of six hour periods in local time (UTC+8) where: 0 is unclassified; 1 is *Easterly*; 2 is *North-Easterly*; 3 is *Westerly*; and 4 is *Terrestrial* and defined in Section 2.2.2 of the principal text.

OP3-III	
20/06/2008 20:00	5
21/06/2008 08:00	5
21/06/2008 20:00	0
22/06/2008 08:00	2
22/06/2008 20:00	2
23/06/2008 08:00	2
23/06/2008 20:00	2
24/06/2008 08:00	2
24/06/2008 20:00	0
25/06/2008 08:00	0
25/06/2008 20:00	3
26/06/2008 08:00	3
26/06/2008 20:00	3
27/06/2008 08:00	3
27/06/2008 20:00	3
28/06/2008 08:00	3
28/06/2008 20:00	3
29/06/2008 08:00	3
29/06/2008 20:00	3
30/06/2008 08:00	3
30/06/2008 20:00	3
01/07/2008 08:00	3
01/07/2008 20:00	3
02/07/2008 08:00	0
02/07/2008 20:00	1
03/07/2008 08:00	1
03/07/2008 20:00	1
04/07/2008 08:00	5
04/07/2008 20:00	5
05/07/2008 08:00	5
05/07/2008 20:00	5
06/07/2008 08:00	5
06/07/2008 20:00	5
07/07/2008 08:00	0
07/07/2008 20:00	3
08/07/2008 08:00	3
08/07/2008 20:00	3
09/07/2008 08:00	3
09/07/2008 20:00	3
10/07/2008 08:00	3
10/07/2008 20:00	3
11/07/2008 08:00	3
11/07/2008 20:00	3
12/07/2008 08:00	3
12/07/2008 20:00	3
13/07/2008 08:00	3
13/07/2008 20:00	3
14/07/2008 08:00	3
14/07/2008 20:00	3
15/07/2008 08:00	3
15/07/2008 20:00	3
16/07/2008 08:00	0
16/07/2008 20:00	0
17/07/2008 08:00	0
17/07/2008 20:00	0
18/07/2008 08:00	3
18/07/2008 20:00	3
19/07/2008 08:00	3
19/07/2008 20:00	0
20/07/2008 08:00	4
20/07/2008 20:00	4
21/07/2008 08:00	0
21/07/2008 20:00	0
22/07/2008 08:00	0
22/07/2008 20:00	5
23/07/2008 08:00	5
23/07/2008 20:00	0

Table 2. Cluster analysis period classifications for OP3-III. Times are start times of six hour periods in local time (UTC+8) where: 0 is unclassified; 1 is *North-Easterly*, 2 is *Coastal*; 3 is *Marine*; 4 is *Westerly*; and 5 is *Terrestrial* as described in Section 2.2.2 of the principal text.

APPENDIX

C

SUPPORTING MATERIAL FOR PAPER II

The following Appendix is a reproduction of the supporting material for Paper II, itself reproduced in Section 4.2. It details aircraft profiles used in averages but not included in the main paper.

Manuscript prepared for J. Name
with version 3.2 of the LaTeX class copernicus.cls.
Date: 11 March 2011

Suppliment for The effect of a tropical island on regional transport of aerosol

immediate
Correspondence to: H. Coe
(hugh.coe@manchester.ac.uk)

1 Introduction

This supplement details aircraft altitude profiles that were not included in the main text. Profiles that were not performed over a small constrained area (usually due to flight control restrictions) were rejected. It should be noted that some profiles were recorded on a lower time resolution (30 s rather than the usual 10 s) due to restrictions switching instrument modes. All times are middle points of profiles in local time (UTC+8).

2 Upwind profiles

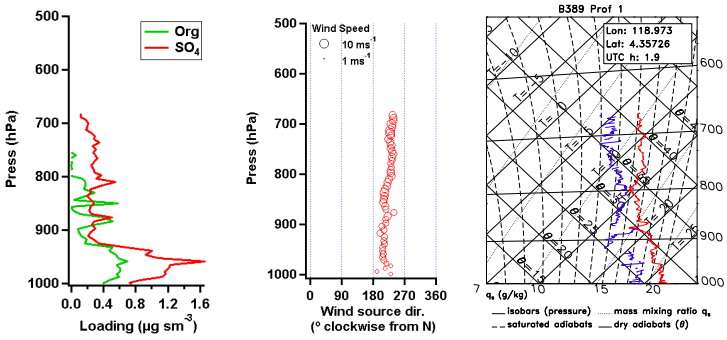

(a) (b) (c)

Fig. 1. Upwind marine profile. Flight B389a, 17/07/2008 09:55:15.

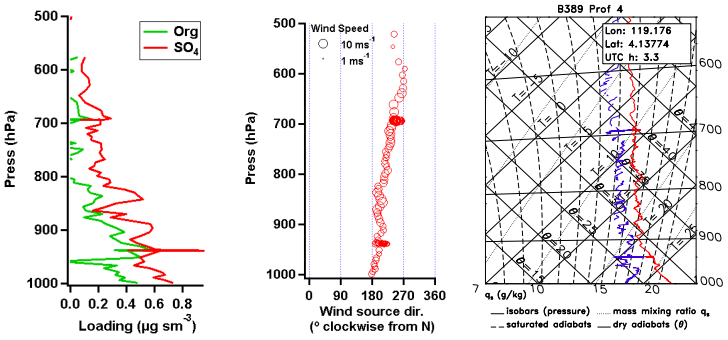

(a) (b) (c)

Fig. 2. Upwind marine profile. Flight B389a, 17/07/2008 11:19:39. Precipitation observed in the boundary layer which may have depleted aerosol concentrations.

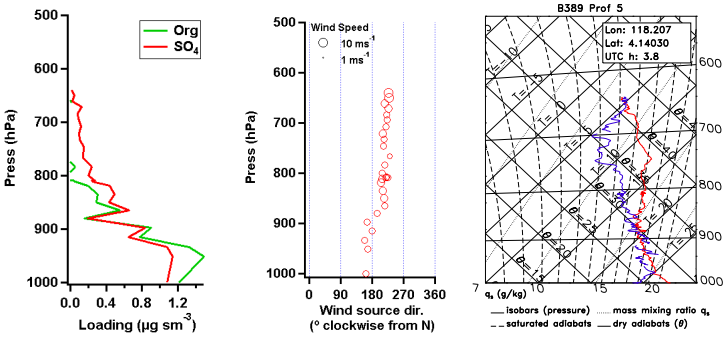

(a) (b) (c)

Fig. 3. Upwind marine profile. Flight B389a, 17/07/2008 11:52:03.

3 East Sabah Profiles

3.1 Morning

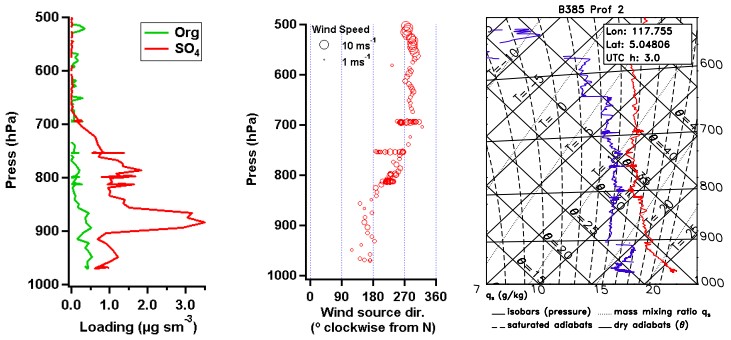

(a) (b) (c)

Fig. 4. East Sabah morning profile. Flight B385a, 11/07/2008 11:01:30.

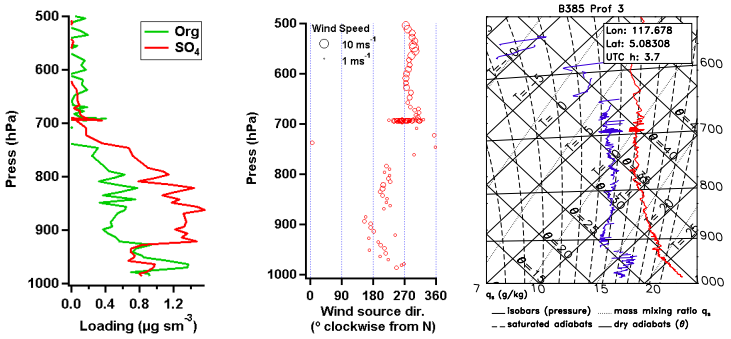

(a) (b) (c)

Fig. 5. East Sabah morning profile. Flight B385a, 11/07/2008 11:46:15.

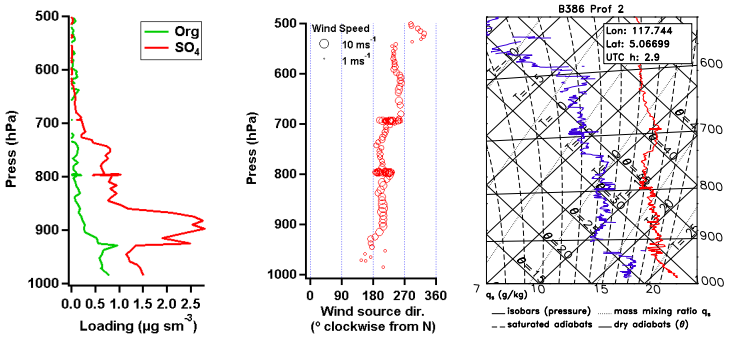

(a) (b) (c)

Fig. 6. East Sabah morning profile. Flight B386a, 13/07/2008 10:54:27.

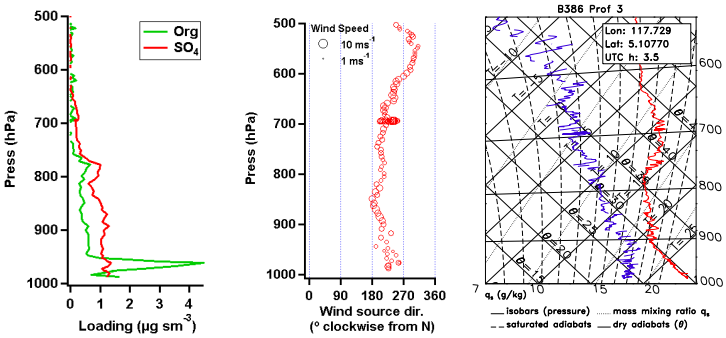

(a) (b) (c)

Fig. 7. East Sabah morning profile. Flight B386a 13/07/2008 11:35:38.

3.2 Afternoon

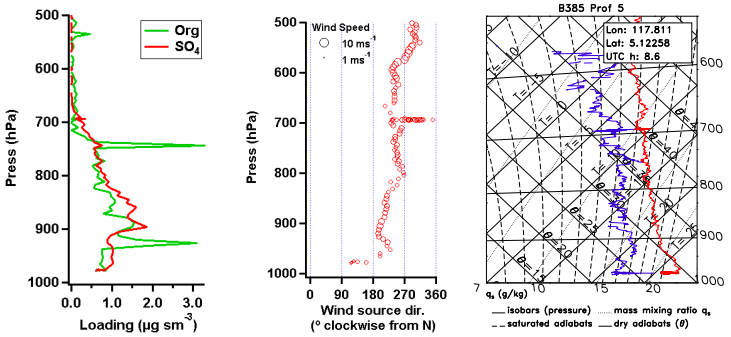

(a) (b) (c)

Fig. 8. East Sabah afternoon profile. Flight B385b, 11/07/2008 16:37:00.

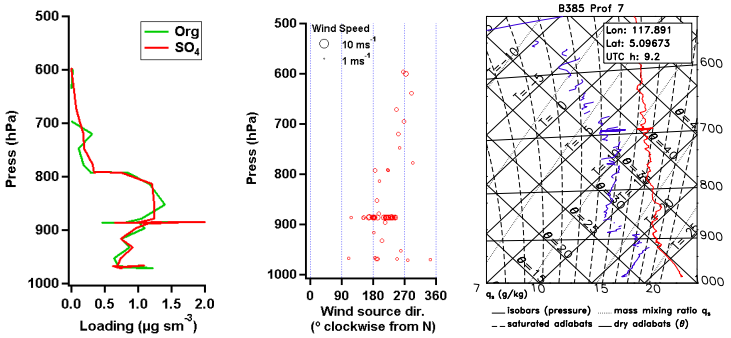

(a) (b) (c)

Fig. 9. East Sabah afternoon profile. Flight B385b, 11/07/2008 17:11:50.

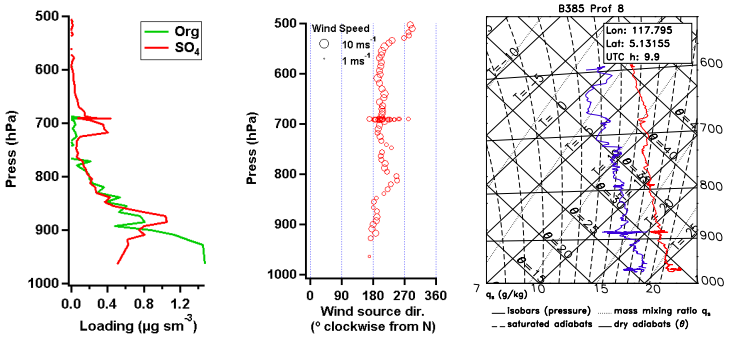

(a) (b) (c)

Fig. 10. East Sabah afternoon profile. Flight B385b, 11/07/2008 17:58:06.

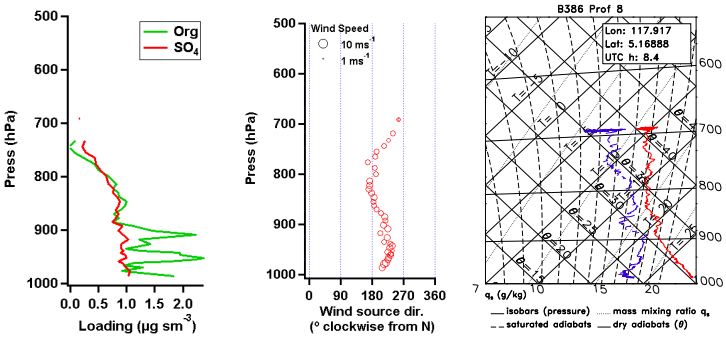

(a) (b) (c)

Fig. 11. East Sabah afternoon profile. Flight B386a, 13/07/2008 16:32:06. Performed during a period of cumulonimbus activity.

4 Kota Kinabalu Profiles

4.1 Morning

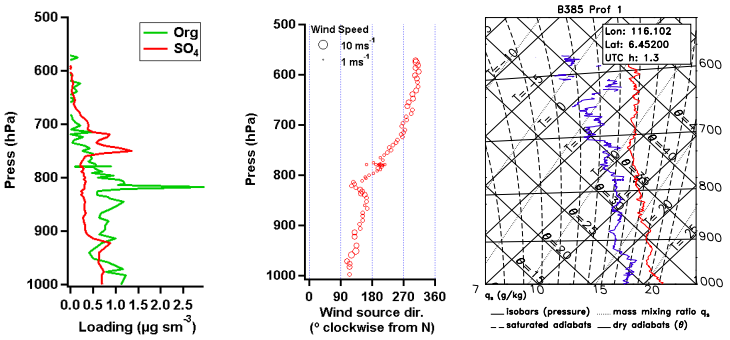

(a) (b) (c)

Fig. 12. East Sabah afternoon profile. B385a, 11/07/2008 09:17:07.

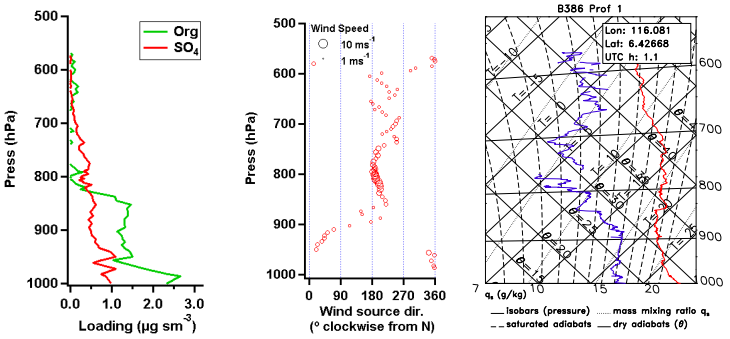

(a) (b) (c)

Fig. 13. Kota Kinabalu morning profile. B386a, 13/07/2008 09:10:07.

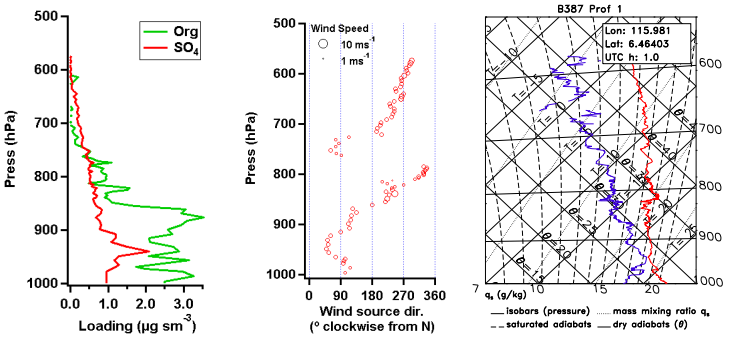

(a) (b) (c)

Fig. 14. Kota Kinabalu morning profile. B387a, 14/07/2008 09:03:18.

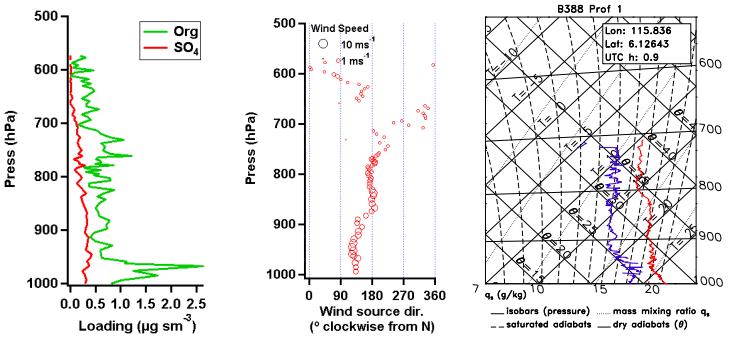

(a) (b) (c)

Fig. 15. Kota Kinabalu morning profile. B388a, 16/07/2008 08:52:21.

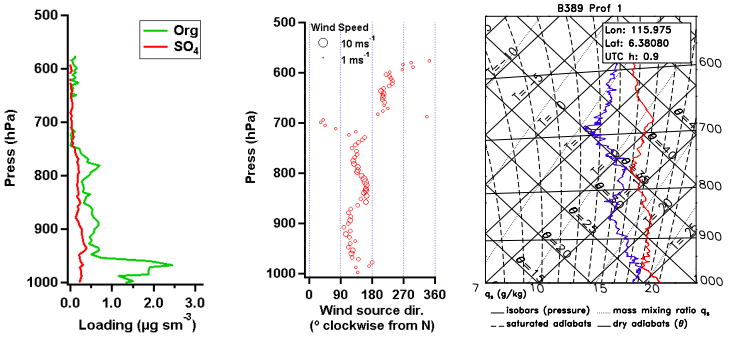

(a) (b) (c)

Fig. 16. Kota Kinabalu morning profile. B389a, 17/07/2008 08:56:07.

4.2 Around Midday

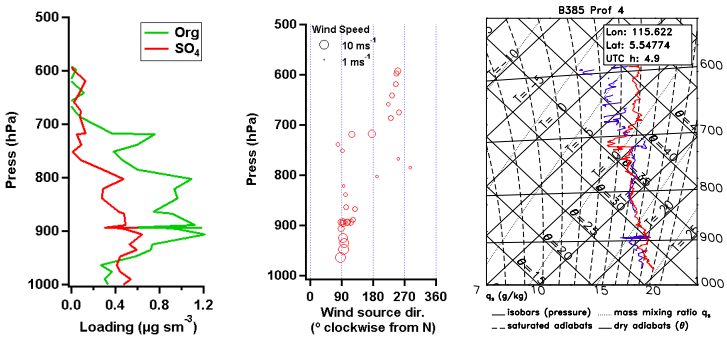

(a) (b) (c)

Fig. 17. Kota Kinabalu around midday profile. B385a, 11/07/2008 12:56:35.

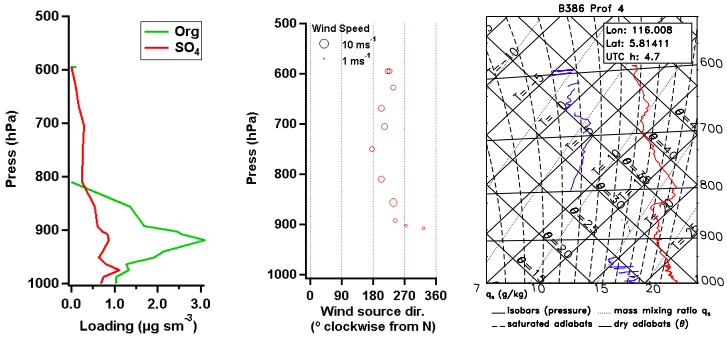

(a) (b) (c)

Fig. 18. Kota Kinabalu around midday profile. B386a, 13/07/2008 12:44:04.

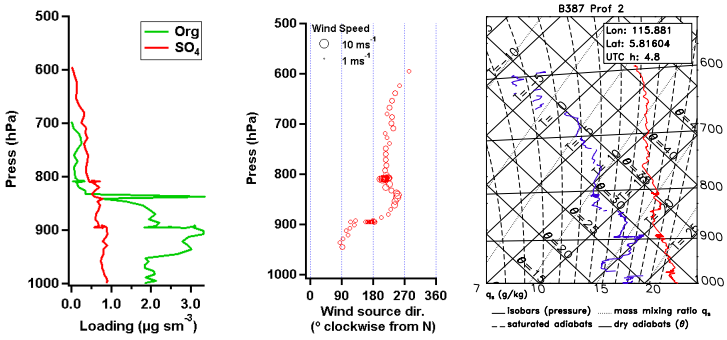

(a) (b) (c)

Fig. 19. Kota Kinabalu around midday profile. B387a, 14/07/2008 12:53:37.

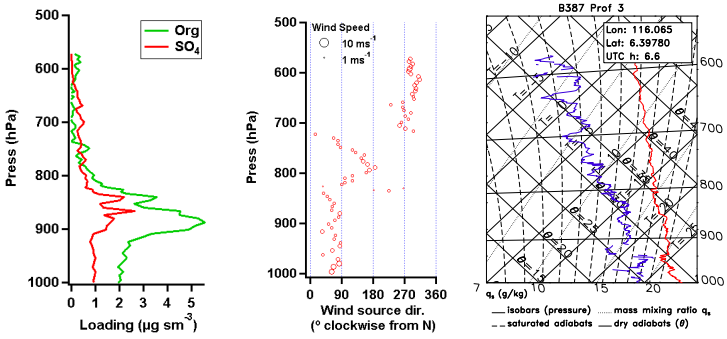

(a) (b) (c)

Fig. 20. Kota Kinabalu around midday profile. B387b, 14/07/2008 14:37:08.

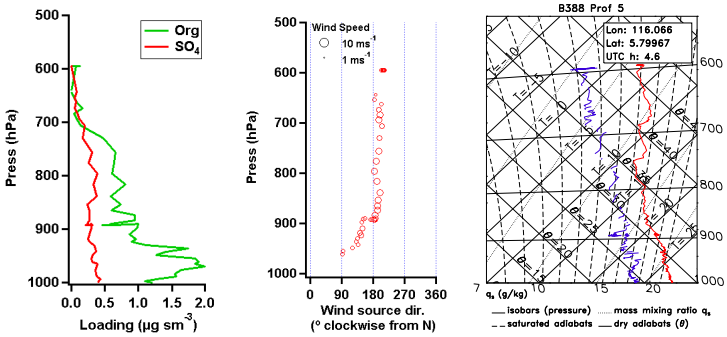

(a) (b) (c)

Fig. 21. Kota Kinabalu around midday profile. B388a, 16/07/2008 12:38:19.

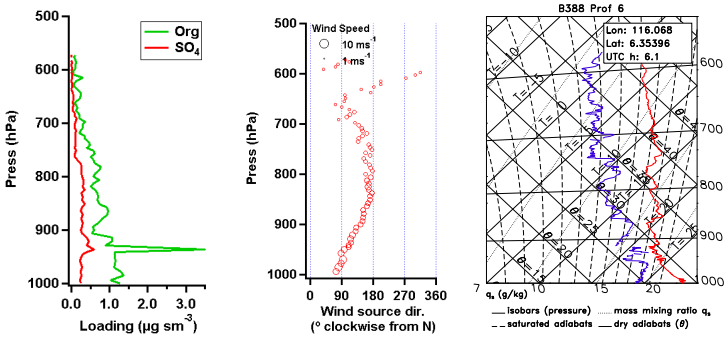

(a) (b) (c)

Fig. 22. Kota Kinabalu around midday profile. B388b, 16/07/2008 14:07:05.

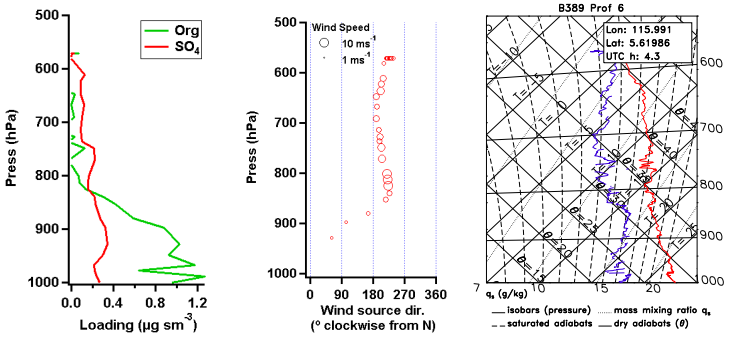

(a) (b) (c)

Fig. 23. Kota Kinabalu around midday profile. B389a, 17/07/2008 12:23:36.

4.3 Late Afternoon

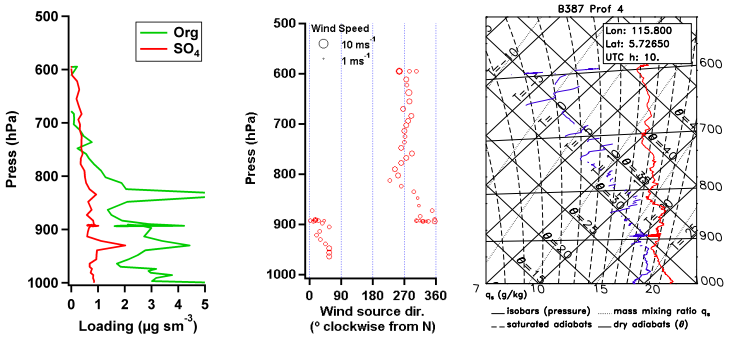

(a) (b) (c)

Fig. 24. Kota Kinabalu late afternoon profile. B387b, 14/07/2008 18:02:31.

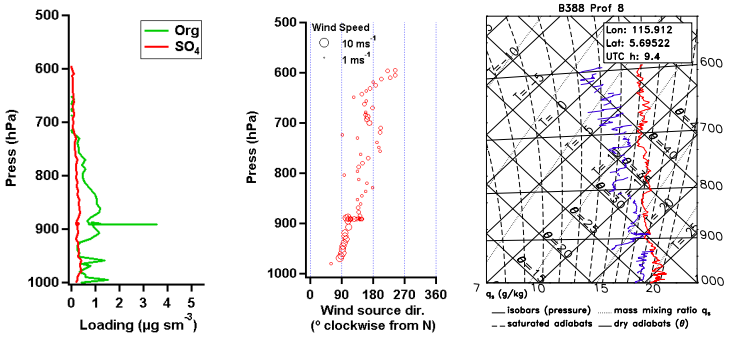

(a) (b) (c)

Fig. 25. Kota Kinabalu late aftenoon profile. B388b, 16/07/2008 17:26:37.

APPENDIX

D

SUPPORTING MATERIAL FOR PAPER III

The following Appendix is a reproduction of the supporting material for Paper III, itself reproduced in Section 4.4. It outlines the positive matrix factorisation analysis of the organic mass spectra.

Evidence for a Significant Proportion of Secondary Organic Aerosol from Isoprene Above a Maritime Tropical Forest: Supplementary Material

Robinson, N. H., et al. Atmos. Chem. Phys. Discuss.

Scope

This purpose of this document is to describe the methods used to generate the PMF factor outputs used in the main article. This includes how the data was handled, the outputs generated and the methods used to choose the most appropriate solution set. No attempt is made to interpret chemically the outputs of the analysis beyond assigning names for the factors based on marker peaks or comparisons with previously published material. The analysis was handled in a similar manner to Allan et al. (2010), in that solutions (according to number of factors, fpeak value and starting seed) were assessed according to uniqueness, numerical stability and whether the derived factors had realistic mass spectral profiles.

Data pretreatment and PMF operation

A matrix of organic mass spectral data was generated using the 'fragmentation table' technique (Allan et al., 2004) and errors generated using the error model described by Allan et al. (2003), with an additional arbitrary 'electronic noise' parameter included (equivalent to a standard error of 32 digitiser bits per data capture), which served to prevent unrealistically small error estimates being generated for low-signal channels. In order to prevent excessive weighting of the m/z=44 variable, the signals of m/z<20 were removed (these were added back in before further analysis). In addition, the signals of m/z>120 were found to hamper convergence. Given their low signal-to-noise ratios (<3, reducing to <1 after around m/z=250) and the fact they contributed little to the derived spectra, they were deemed 'weak' and removed (Paatero and Hopke, 2003).

The PMF Evaluation Toolkit (PET), as introduced by Ulbrich et al. (2009), was used to process the data, which acted as a front-end for the PMF2 version 4.2 executable (Paatero, 1997). The default conversion criteria were used. An initial run was performed and 'bad' runs were removed from the time series, based on the overall Q/Q_{exp} for the row being greater than 20. The rows removed were mainly in the form of spikes in the time series, either from local contamination or logging software malfunction. The analysis was then rerun with the filtered data.

Choice of number of factors

The analysis was performed with various numbers of factors and it was found that 5 or more yielded unsatisfactory results. This is illustrated by the 5-factor (fpeak=0) case below:

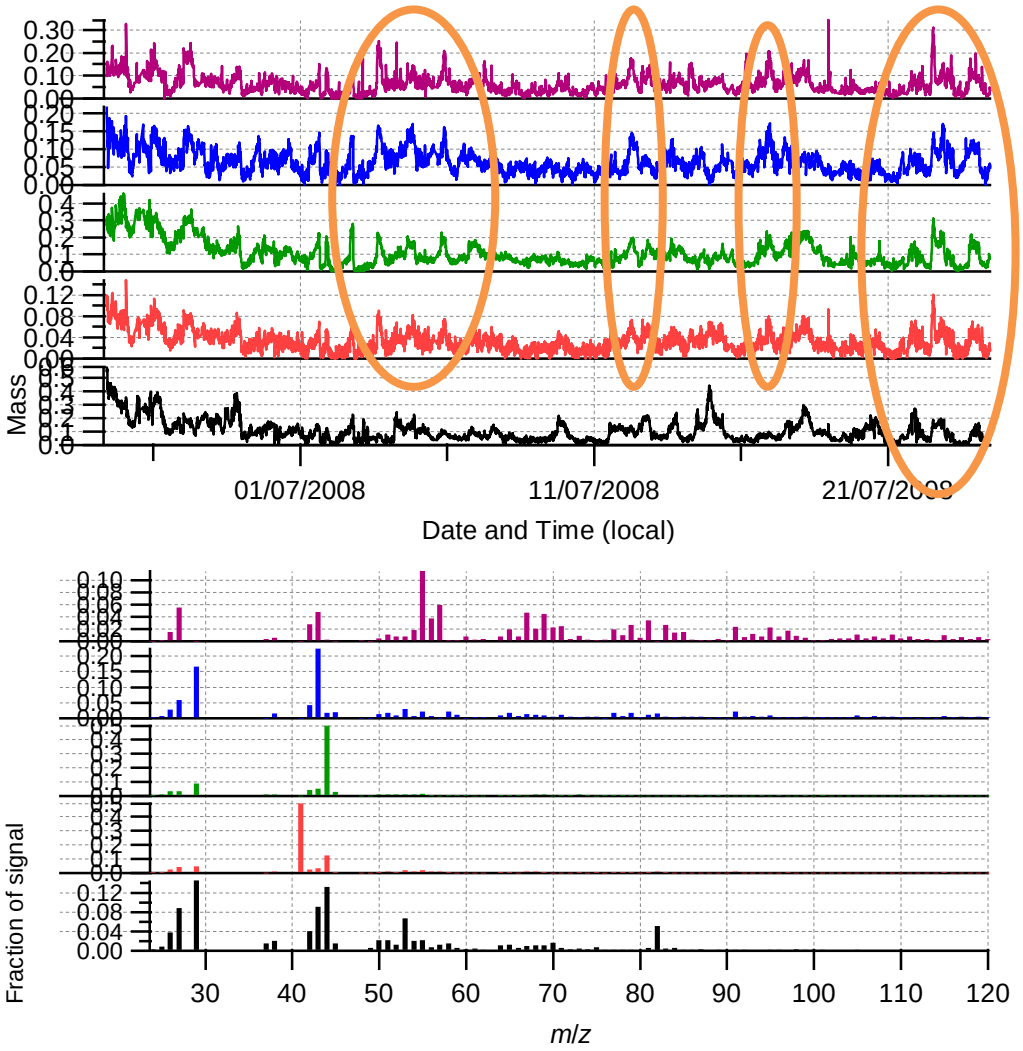

This solution was deemed unacceptable for two reasons; firstly, there were many common features, in particular in the time series of the top four time series (as plotted). Certain features are circled for clarity, but there were few features in the respective time series that were unique to a single factors. This was taken as indicative of 'mixing' taking place (Ulbrich et al., 2009). Secondly, a number of the mass spectral profiles (specifically the middle three) consisted of one or two peaks with little other signal at other *m/z* channels. Given that AMS mass spectra (in common with other EI mass spectrometers) typically consist of numerous fragment ions, it was thought that these were unlikely to be physically meaningful. In principle, it may have been possible to eliminate these behaviours by adjusting the pfeak parameter, however it was found that different values caused the algorithm to fail to converge.

Choice of pfeak

Within the 4 factor solution set, the fpeak=0 solution was found to have similar mixing and physicality issues as the 5 factor solution:

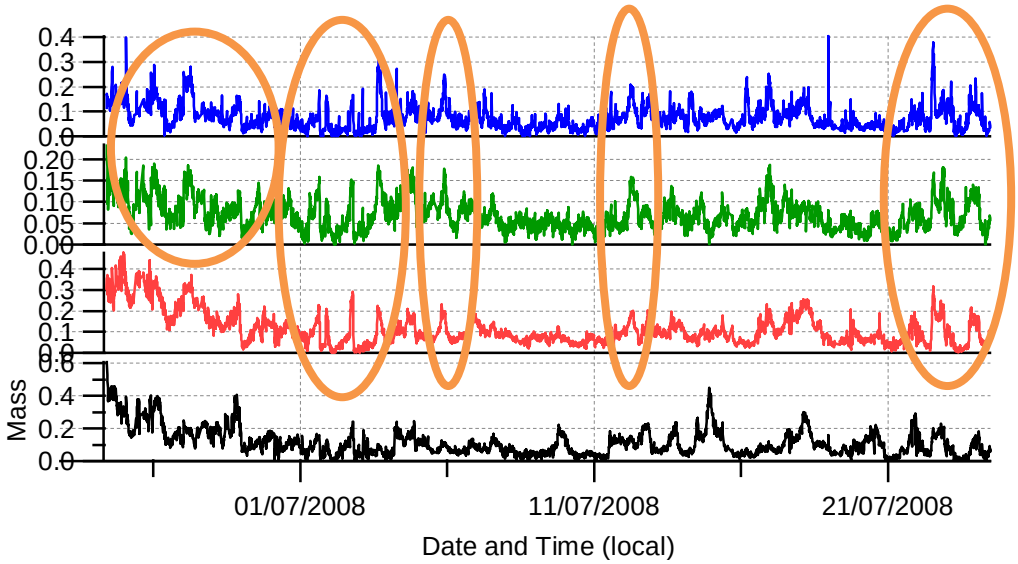

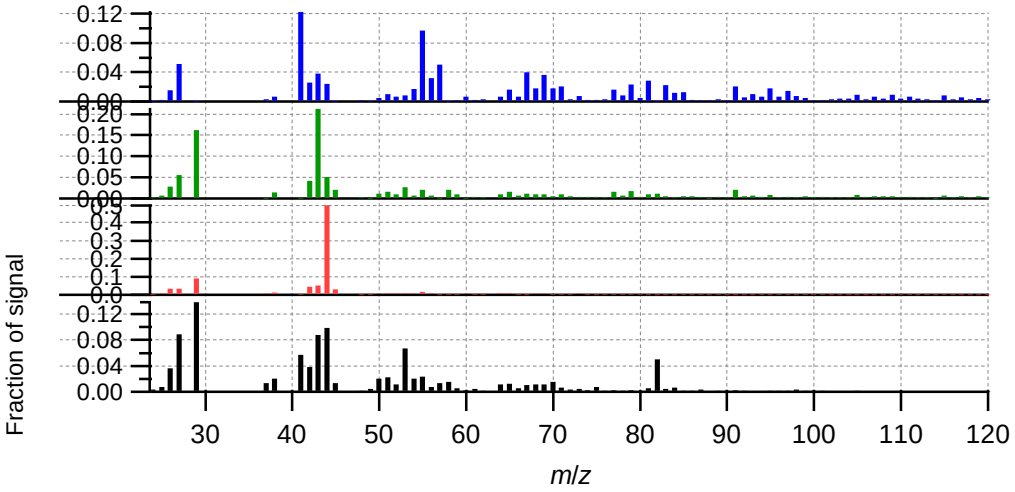

Note that there are many common features in the top three factors' time series and that the middle two profiles feature similar one- or two-peak spectra as the 5 factor solution. However, with the 4 factor case, other values of fpeak down to -1 were found to converge and the fpeak=-1 was deemed to be much more acceptable for a modest overall increase in Q/Q_{exp} (3.30 instead of 3.29):

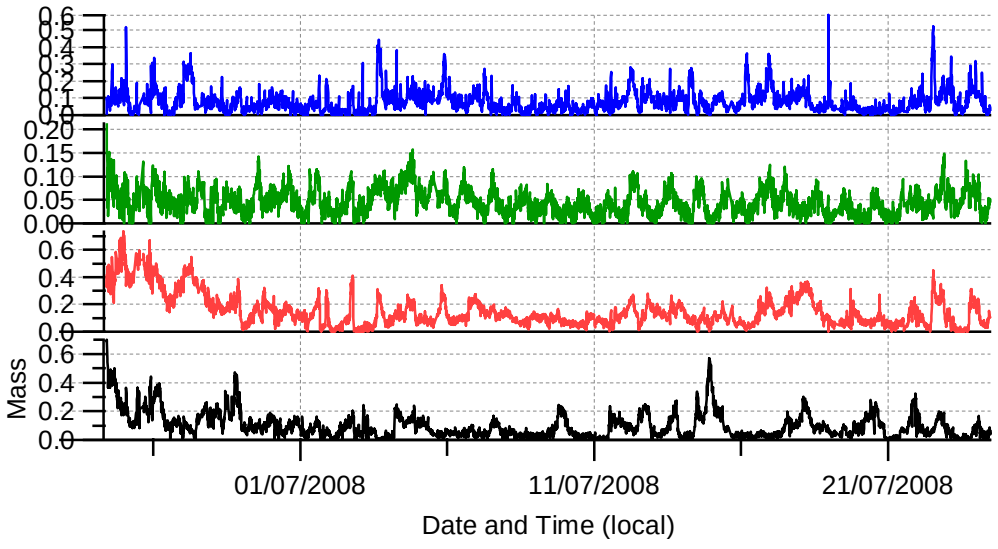

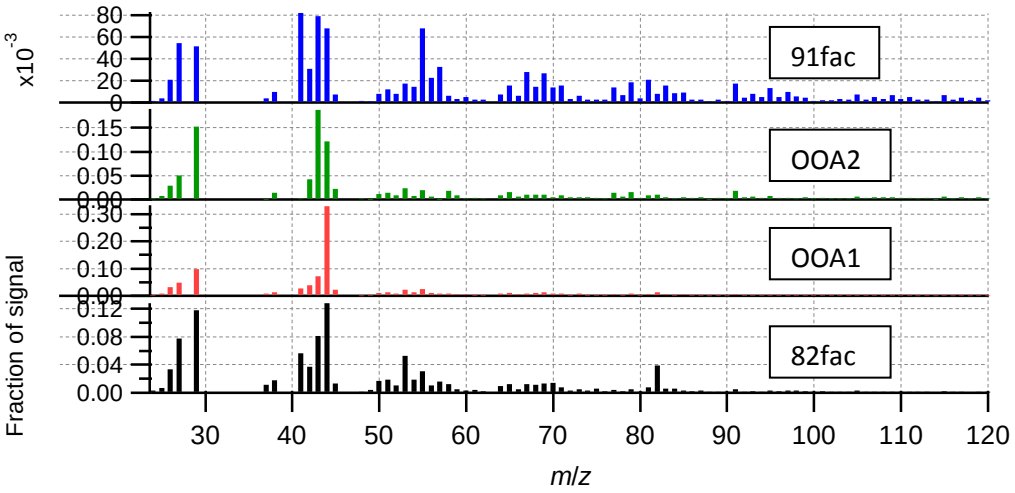

Note that the time series show many more unique features. Additionally, the mass spectra bear more of a resemblance to those previously published. The middle two spectra have been labelled 'OOA1' and 'OOA2' based on their similarity to previously published spectra (Lanz et al., 2007; Ulbrich et al., 2009). These have been linked to low volatility (LV) and semivolatile (SV) oxygenated organic aerosol (Jimenez et al., 2009), but without a direct measure of volatility, it is difficult to draw this conclusion with this data. The top factor bears a resemblance in some of its profile to biomass burning aerosols (Alfarra et al., 2007; Allan et al., 2010), although it does not possess the strong signals at *m*/*z* 60 and 73 often associated with levoglucosan, which could be expected (Jordan et al., 2006). It is possible that this particular chemical marker is not present in sufficient quantities, due to burn conditions or plume age, but it is difficult to tell with this data taken in isolation. Therefore, this factor is simply labelled as '91fac' for now. The remaining factor, is labelled '82fac', based on its most prominent marker peak. This is not a feature that has been widely reported in previous AMS datasets.

Stability of the '82fac' factor

The solution above (4 factors, peak=-1) was deemed to be the most satisfactory, however it was generally found that the 82fac factor, which is the subject of the main article, was remarkably stable across different solutions. For instance, while it represented 26% of the mass in the chosen solution (before correction for the missing mass below *m*/*z* 20), this figure only changed to 30% for the corresponding fpeak=0 solution and 28% for the 5 factor solution. When the numerical stability was checked by varying the starting seed, it was found that there was negligible differences between the solutions that converged. In all of the cases so far described, the mass spectrum was largely unaffected with key peaks at *m*/*z* 43, 44, 53 and 82. Also note that the peak at *m*/*z*=82 was mostly absent from the other factors. This shows that not only is the 82fac factor very stable and unambiguous, it has a very strong association with the 82 peak in isolation. While it may be possible to generate different solutions through further modification of the data treatment or algorithm function, we believe that any changes to this factor would be relatively small. Note that this does not apply to any other factors derived.

References

Alfarra, M. R., Prevot, A. S. H., Szidat, S., Sandradewi, J., Weimer, S., Lanz, V. A., Schreiber, D., Mohr, M., and Baltensperger, U.: Identification of the mass spectral signature of organic aerosols from wood burning emissions, Environ. Sci. Technol., 41, 5770-5777, Doi 10.1021/Es062289b, 2007.

Allan, J. D., Jimenez, J. L., Williams, P. I., Alfarra, M. R., Bower, K. N., Jayne, J. T., Coe, H., and Worsnop, D. R.: Quantitative sampling using an aerodyne aerosol mass spectrometer - 1. Techniques of data interpretation and error analysis, J. Geophys. Res.-Atmos., 108, 4090, doi:10.1029/2002JD002358, 2003.
Allan, J. D., Coe, H., Bower, K. N., Alfarra, M. R., Delia, A. E., Jimenez, J. L., Middlebrook, A. M., Drewnick, F., Onasch, T. B., Canagaratna, M. R., Jayne, J. T., and Worsnop, D. R.: A generalised method for the extraction of chemically resolved mass spectra from aerodyne aerosol mass spectrometer data, J. Aerosol. Sci., 35, 909-922, 2004.
Allan, J. D., Williams, P. I., Morgan, W. T., Martin, C. L., Flynn, M. J., Lee, J., Nemitz, E., Phillips, G. J., Gallagher, M. W., and Coe, H.: Contributions from transport, solid fuel burning and cooking to primary organic aerosols in two uk cities, Atmos. Chem. Phys., 10, 647-668, 2010.
Jimenez, J. L., Canagaratna, M. R., Donahue, N. M., Prevot, A. S. H., Zhang, Q., Kroll, J. H., DeCarlo, P. F., Allan, J. D., Coe, H., Ng, N. L., Aiken, A. C., Docherty, K. S., Ulbrich, I. M., Grieshop, A. P., Robinson, A. L., Duplissy, J., Smith, J. D., Wilson, K. R., Lanz, V. A., Hueglin, C., Sun, Y. L., Tian, J., Laaksonen, A., Raatikainen, T., Rautiainen, J., Vaattovaara, P., Ehn, M., Kulmala, M., Tomlinson, J. M., Collins, D. R., Cubison, M. J., E, Dunlea, J., Huffman, J. A., Onasch, T. B., Alfarra, M. R., Williams, P. I., Bower, K., Kondo, Y., Schneider, J., Drewnick, F., Borrmann, S., Weimer, S., Demerjian, K., Salcedo, D., Cottrell, L., Griffin, R., Takami, A., Miyoshi, T., Hatakeyama, S., Shimono, A., Sun, J. Y., Zhang, Y. M., Dzepina, K., Kimmel, J. R., Sueper, D., Jayne, J. T., Herndon, S. C., Trimborn, A. M., Williams, L. R., Wood, E. C., Middlebrook, A. M., Kolb, C. E., Baltensperger, U., and Worsnop, D. R.: Evolution of organic aerosols in the atmosphere, Science, 326, 1525-1529, 10.1126/science.1180353, 2009.
Jordan, T. B., Seen, A. J., and Jacobsen, G. E.: Levoglucosan as an atmospheric tracer for woodsmoke, Atmos. Environ., 40, 5316-5321, DOI 10.1016/j.atmosenv.2006.03.023, 2006.
Lanz, V. A., Alfarra, M. R., Baltensperger, U., Buchmann, B., Hueglin, C., and Prevot, A. S. H.: Source apportionment of submicron organic aerosols at an urban site by factor analytical modelling of aerosol mass spectra, Atmos. Chem. Phys., 7, 1503-1522, 2007.
Paatero, P.: Least squares formulation of robust non-negative factor analysis, Chemometr Intell Lab, 37, 23-35, 1997.
Paatero, P., and Hopke, P. K.: Discarding or downweighting high-noise variables in factor analytic models, Anal Chim Acta, 490, 277-289, Doi 10.1016/S0003-2670(02)01643-4, 2003.
Ulbrich, I. M., Canagaratna, M. R., Zhang, Q., Worsnop, D. R., and Jimenez, J. L.: Interpretation of organic components from positive matrix factorization of aerosol mass spectrometric data, Atmos. Chem. Phys., 9, 2891-2918, 2009.

BIBLIOGRAPHY

F. Achard, H. D. Eva, H.-J. Stibig, P. Mayaux, J. Gallego, T. Richards, and J.-P. Malingreau. Determination of deforestation rates of the world's humid tropical forests. *Science (New York, N.Y.)*, 297(5583):999–1002, Aug. 2002. ISSN 1095-9203. doi: 10.1126/science.1070656. URL http://www.sciencemag.org/content/297/5583/999.abstract.

A. S. Ackerman, O. B. Toon, D. E. Stevens, A. J. Heymsfield, V. Ramanathan, and E. J. Welton. Reduction of tropical cloudiness by soot. *Science*, 288(5468):1042–1047, 2000a. ISSN 00368075. doi: 10.1126/science.288.5468.1042. URL http://www.ncbi.nlm.nih.gov/pubmed/10807573.

A. S. Ackerman, O. B. Toon, J. P. Taylor, D. W. Johnson, P. V. Hobbs, and R. J. Ferek. Effects of Aerosols on Cloud Albedo : Evaluation of Twomey's Parameterization of Cloud Susceptibility Using Measurements of Ship Tracks. *Physics*, 57(1995):2684–2695, 2000b. ISSN 15200469. doi: 10.1175/1520-0469(2000)057<2684:EOAOCA>2.0.CO;2.

A. C. Aiken, P. F. DeCarlo, and J. L. Jimenez. Elemental analysis of organic species with electron ionization high-resolution mass spectrometry. *Analytical chemistry*, 79 (21):8350–8, Nov. 2007. ISSN 0003-2700. doi: 10.1021/ac071150w. URL http://www.ncbi.nlm.nih.gov/pubmed/17914892.

A. C. Aiken, P. F. DeCarlo, J. H. Kroll, D. R. Worsnop, J. A. Huffman, K. S. Docherty, I. M. Ulbrich, C. Mohr, J. R. Kimmel, D. Sueper, Y. Sun, Q. Zhang, A. Trimborn, M. J. Northway, P. J. Ziemann, M. R. Canagaratna, T. B. Onasch, M. R. Alfarra, A. S. H. Prevot, J. Dommen, J. Duplissy, A. Metzger, U. Baltensperger, and J. L. Jimenez. O/C and OM/OC Ratios of Primary, Secondary, and Ambient Organic Aerosols with High-Resolution Time-of-Flight Aerosol Mass Spectrometry. *Environmental Science & Technology*, 42(12):4478–4485, 2008. ISSN 0013-936X. doi: 10.1021/es703009q. URL http://pubs.acs.org/doi/abs/10.1021/es703009q.

M. R. Alfarra. *Insights into atmospheric organic aerosols using an aerosol mass spectrometer*. Phd, The University of Manchester, 2004.

M. R. Alfarra, H. Coe, J. Allan, K. N. Bower, H. Boudries, M. R. Canagaratna, J. L. Jimenez, J. T. Jayne, A. Garforth, and S. Li. Characterization of urban and rural organic particulate in the Lower Fraser Valley using two Aerodyne Aerosol Mass Spectrometers. *Atmospheric Environment*, 38(34):5745–5758, 2004. ISSN 13522310. doi: 10.1016/j.atmosenv.2004.01.054. URL http://linkinghub.elsevier.com/retrieve/pii/S1352231004005977.

J. D. Allan, M. R. Alfarra, K. N. Bower, P. I. Williams, M. W. Gallagher, J. L. Jimenez, A. G. McDonald, E. Nemitz, M. R. Canagaratna, J. T. Jayne, H. Coe, and D. R. Worsnop. Quantitative sampling using an Aerodyne aerosol mass spectrometer 2. Measurements of fine particulate chemical composition in two U.K. cities. *Journal of Geophysical Research*, 108(D3), 2003. ISSN 0148-0227. doi: 10.1029/2002JD002359. URL http://www.agu.org/pubs/crossref/2003/2002JD002359.shtml.

J. D. Allan, H. Coe, K. N. Bower, M. R. Alfarra, A. E. Delia, J. L. Jimenez, A. M. Middlebrook, F. Drewnick, T. B. Onasch, M. R. Canagaratna, J. T. Jayne, and D. R. Worsnop. A generalised method for the extraction of chemically resolved mass spectra from Aerodyne aerosol mass spectrometer data. *Journal of aerosol science*, 35(7):909–922, 2004. ISSN 0021-8502.

J. D. Allan, M. R. Alfarra, K. N. Bower, H. Coe, J. T. Jayne, D. R. Worsnop, P. P. Aalto, M. Kulmala, F. Cavalli, and A. Laaksonen. Size and composition measurements of background aerosol and new particle growth in a Finnish forest during QUEST 2 using an Aerodyne Aerosol Mass Spectrometer. *Atmospheric Chemistry and Physics*, 6(2):315–327, 2006. URL http://www.atmos-chem-phys.net/6/315/2006/acp-6-315-2006.pdf.

A. G. Allen, M. F. Oppenheimer, P. J. Baxter, L. A. Horrocks, B. Galle, A. J. S. McGonigle, and H. J. Duffell. Primary sulfate aerosol and associated emissions from Masaya Volcano, Nicaragua. *Journal of Geophysical Research*, 107(D23), 2002. ISSN 0148-0227. doi: 10.1029/2002JD002120. URL http://www.agu.org/pubs/crossref/2002/2002JD002120.shtml.

M. O. Andreae. Aerosols before pollution. *Science (New York, N.Y.)*, 315(5808):50–1, Jan. 2007. ISSN 1095-9203. doi: 10.1126/science.1136529. URL http://www.ncbi.nlm.nih.gov/pubmed/17204632.

M. O. Andreae and H. Raemdonck. Dimethyl sulfide in the surface ocean and the marine atmosphere: a global view. *Science (New York, N.Y.)*, 221(4612):744–7, Aug. 1983. ISSN 0036-8075. doi: 10.1126/science.221.4612.744. URL http://www.ncbi.nlm.nih.gov/pubmed/17829533.

M. O. Andreae, R. J. Ferek, F. Bermond, K. P. Byrd, R. T. Engstrom, S. Hardin, P. D. Houmere, F. LeMarrec, H. Raemdonck, and R. B. Chatfield. Dimethyl Sulfide in the Marine Atmosphere. *Journal of Geophysical Research*, 90(D7):12891–12900, 1985. ISSN 0148-0227. doi: 10.1029/JD090iD07p12891. URL http://www.agu.org/pubs/crossref/1985/JD090iD07p12891.shtml.

M. O. Andreae, D. Rosenfeld, P. Artaxo, A. Costa, G. Frank, K. Longo, and M. Silva-Dias. Smoking rain clouds over the Amazon. *Science*, 303(5662):1337, 2004. URL http://www.sciencemag.org/cgi/content/abstract/303/5662/1337.

P. Artaxo, J. V. Martins, M. A. Yamasoe, A. S. Procopio, T. M. Pauliquevis, M. O. Andreae, P. Guyon, L. V. Gatti, and A. Maria Cordova Leal. Physical and chemical properties of aerosols in the wet and dry seasons in Rondônia, Amazonia. *Journal of Geophysical Research*, 107(D20), 2002. ISSN 0148-0227. doi: 10.1029/2001JD000666. URL http://www.agu.org/pubs/crossref/2002/2001JD000666.shtml.

P. W. Atkins and J. de Paula. *Atkins' Physical Chemistry, 7th Ed.* Oxford University Press, 2002. ISBN 0198792859. URL http://www.amazon.co.uk/Atkins-Physical-Chemistry-7th-Ed/dp/0198792859.

R. Avissar, P. Silva Dias, M. Silva Dias, and C. A. Nobre. The Large-Scale Biosphere-Atmosphere Experiment in Amazonia (LBA): Insights and future research needs. *Journal of Geophysical Research*, 107(D20), 2002. ISSN 0148-0227. doi: 10.1029/2002JD002704. URL http://www.agu.org/pubs/crossref/2002/2002JD002704.shtml.

R. Bahreini, J. L. Jimenez, J. Wang, R. C. Flagan, J. H. Seinfeld, J. T. Jayne, and D. R. Worsnop. Aircraft-based aerosol size and composition measurements during ACE-Asia using an Aerodyne aerosol mass spectrometer. *Journal of Geophysical Research-Atmospheres*, 108 (D23)(D23):8645, Aug. 2003a. ISSN 0148-0227. doi: 10.1029/2002JD003226.

R. Bahreini, J. L. Jimenez, J. Wang, R. C. Flagan, J. H. Seinfeld, J. T. Jayne, and D. R. Worsnopya. Aircraft-based aerosol size and composition measurements during ACE-Asia using an Aerodyne aerosol mass spectrometer. *Journal of Geophysical Research*, 108(D23):1–22, 2003b. ISSN 0148-0227. doi: 10.1029/2002JD003226. URL http://www.agu.org/pubs/crossref/2003/2002JD003226.shtml.

T. S. Bates, B. K. Lamb, A. Guenther, J. Dignon, and R. E. Stoiber. Sulfur emissions to the atmosphere from natural sources. *Journal of Atmospheric Chemistry*, 14(1-4):315–337, Apr. 1992. ISSN 0167-7764. doi: 10.1007/BF00115242. URL http://www.springerlink.com/index/10.1007/BF00115242.

K. Biswas and A. Dennis. Formation of a Rain Shower by Salt Seeding. *Journal of Applied Meteorology*, 10:780–784, 1971. ISSN 0894-8763. URL http://adsabs.harvard.edu/abs/1971JApMe..10..780B.

W. Bley. Quantitative measurements with quadrupole mass spectrometers: important specifications for reliable measurements. *Vacuum*, 38(2):103–109, 1988. ISSN 0042207X. doi: 10.1016/0042-207X(88)90606-9. URL http://linkinghub.elsevier.com/retrieve/pii/0042207X88906069.

T. C. Bond, D. G. Streets, K. F. Yarber, S. M. Nelson, J.-H. Woo, and Z. Klimont. A technology-based global inventory of black and organic carbon emissions from combustion. *Journal of Geophysical Research*, 109(D14), 2004. ISSN 0148-0227. doi: 10.1029/2003JD003697. URL http://www.agu.org/pubs/crossref/2004/2003JD003697.shtml.

A. M. Booth, M. H. Barley, D. O. Topping, G. McFiggans, A. Garforth, and C. J. Percival. Solid state and sub-cooled liquid vapour pressures of substituted dicarboxylic acids using Knudsen Effusion Mass Spectrometry (KEMS) and Differential Scanning Calorimetry. *Atmospheric Chemistry and Physics*, 10(10):4879–4892, May 2010. ISSN 1680-7324. doi: 10.5194/acp-10-4879-2010. URL http://www.atmos-chem-phys.net/10/4879/2010/.

P. Brohan, J. J. Kennedy, I. Harris, S. F. B. Tett, and P. D. Jones. Uncertainty estimates in regional and global observed temperature changes: A new data set from 1850. *Journal of Geophysical Research*, 111(D12), 2006. ISSN 0148-0227. doi: 10.1029/2005JD006548. URL http://www.agu.org/pubs/crossref/2006/2005JD006548.shtml.

M. R. Canagaratna, J. T. Jayne, J. L. Jimenez, J. D. Allan, M. R. Alfarra, Q. Zhang, T. B. Onasch, F. Drewnick, H. Coe, A. Middlebrook, A. Delia, L. R. Williams, A. M. Trimborn, M. J. Northway, P. F. DeCarlo, C. E. Kolb, P. Davidovits, and D. R. Worsnop. Chemical and microphysical characterization of ambient aerosols with the aerodyne aerosol mass spectrometer. *Mass spectrometry reviews*, 26(2):185–222, 2007. ISSN 0277-7037. doi: 10.1002/mas.20115. URL http://www.ncbi.nlm.nih.gov/pubmed/17230437.

G. Capes, B. Johnson, G. McFiggans, P. I. Williams, J. Haywood, and H. Coe. Aging of biomass burning aerosols over West Africa: Aircraft measurements of chemical composition, microphysical properties, and emission ratios. *Journal of Geophysical Research*, 113, 2008. ISSN 0148-0227. doi: 10.1029/2008JD009845. URL http://www.agu.org/pubs/crossref/2008/2008JD009845.shtml.

G. Capes, J. G. Murphy, C. E. Reeves, J. B. McQuaid, J. F. Hamilton, J. R. Hopkins, J. Crosier, P. I. Williams, and H. Coe. Secondary organic aerosol from biogenic VOCs

over West Africa during AMMA. *Atmospheric Chemistry and Physics*, 9(12):3841–3850, June 2009. ISSN 1680-7324. doi: 10.5194/acp-9-3841-2009. URL http://www.atmos-chem-phys.net/9/3841/2009/.

A. Carlton, C. Wiedinmyer, and J. Kroll. A review of Secondary Organic Aerosol (SOA) formation from isoprene. *Atmos. Chem. Phys*, 2009. URL http://www.atmos-chem-phys.net/9/4987/2009/acp-9-4987-2009.pdf.

C. Carter, W. Finley, J. Fry, D. Jackson, and L. Willis. Palm oil markets and future supply. *European Journal of Lipid Science and Technology*, 109(4):307–314, Apr. 2007. ISSN 14387697. doi: 10.1002/ejlt.200600256. URL http://doi.wiley.com/10.1002/ejlt.200600256.

M. N. Chan, J. D. Surratt, M. Claeys, E. S. Edgerton, R. L. Tanner, S. L. Shaw, M. Zheng, E. M. Knipping, N. C. Eddingsaas, P. O. Wennberg, and J. H. Seinfeld. Characterization and Quantification of Isoprene-Derived Epoxydiols in Ambient Aerosol in the Southeastern United States. *Environmental Science & Technology*, 44(12):4590–4596, May 2010. URL http://dx.doi.org/10.1021/es100596b.

R. J. Charlson, S. E. Schwartz, J. M. Hales, R. D. Cess, J. A. Coakley, J. E. Hansen, and D. J. Hofmann. Climate forcing by anthropogenic aerosols. *Science (New York, N.Y.)*, 255(5043):423–30, Jan. 1992. ISSN 0036-8075. doi: 10.1126/science.255.5043.423. URL http://www.ncbi.nlm.nih.gov/pubmed/17842894.

Q. Chen, D. K. Farmer, J. Schneider, S. R. Zorn, C. L. Heald, T. G. Karl, A. Guenther, J. D. Allan, N. Robinson, H. Coe, J. R. Kimmel, T. Pauliquevis, S. Borrmann, U. Pöschl, M. O. Andreae, P. Artaxo, J. L. Jimenez, and S. T. Martin. Mass spectral characterization of submicron biogenic organic particles in the Amazon Basin. *Geophysical Research Letters*, 36(20), Oct. 2009. ISSN 0094-8276. doi: 10.1029/2009GL039880. URL http://www.agu.org/pubs/crossref/2009/2009GL039880.shtml.

C. E. Chung and V. Ramanathan. Weakening of North Indian SST Gradients and the Monsoon Rainfall in India and the Sahel. *Journal of Climate*, 19(10):2036–2045, 2006. ISSN 08948755. doi: 10.1175/JCLI3820.1. URL http://journals.ametsoc.org/doi/abs/10.1175/JCLI3820.1.

S. Chung and J. Seinfeld. Global distribution and climate forcing of carbonaceous aerosols. *J. Geophys. Res.*, 107(19):4407, 2002. URL http://www.earthjustice.org/our_work/issues/international/black-carbon/documents/chung-and-sienfeld-2002.pdf.

M. Claeys, B. Graham, G. Vas, W. Wang, R. Vermeylen, V. Pashynska, J. Cafmeyer, P. Guyon, M. O. Andreae, P. Artaxo, and W. Maenhaut. Formation of secondary organic

aerosols through photooxidation of isoprene., 2004. ISSN 1095-9203. URL http://www.ncbi.nlm.nih.gov/pubmed/14976309.

E. Cross, J. Slowik, P. Davidovits, J. Allan, D. Worsnop, J. Jayne, D. Lewis, M. Canagaratna, and T. Onasch. Laboratory and Ambient Particle Density Determinations using Light Scattering in Conjunction with Aerosol Mass Spectrometry. *Aerosol Science and Technology*, 41(4):343–359, 2007. ISSN 0278-6826. doi: 10.1080/02786820701199736. URL http://www.informaworld.com/openurl?genre=article&issn=0278-6826&volume=41&issue=4&spage=343.

J. A. de Gouw, A. M. Middlebrook, C. Warneke, P. D. Goldan, W. C. Kuster, J. M. Roberts, F. C. Fehsenfeld, D. R. Worsnop, M. R. Canagaratna, A. A. P. Pszenny, W. C. Keene, M. Archewka, S. B. Bertman, Bates, and T. S. Budget of organic carbon in a polluted atmosphere: Results from the New England Air Quality Study in 2002. *Journal of Geophysical Research*, 110(D16), 2005. ISSN 0148-0227. doi: 10.1029/2004JD005623. URL http://www.agu.org/pubs/crossref/2005/2004JD005623.shtml.

J. A. de Gouw, A. M. Middlebrook, C. Warneke, R. Ahmadov, E. L. Atlas, R. Bahreini, D. R. Blake, C. A. Brock, J. Brioude, D. W. Fahey, F. C. Fehsenfeld, J. S. Holloway, M. Le Henaff, R. A. Lueb, S. A. McKeen, J. F. Meagher, D. M. Murphy, C. Paris, D. D. Parrish, A. E. Perring, I. B. Pollack, A. R. Ravishankara, A. L. Robinson, T. B. Ryerson, J. P. Schwarz, J. R. Spackman, A. Srinivasan, and L. A. Watts. Organic Aerosol Formation Downwind from the Deepwater Horizon Oil Spill. *Science*, 331 (6022):1295–1299, Mar. 2011. ISSN 0036-8075. doi: 10.1126/science.1200320. URL http://www.sciencemag.org/cgi/doi/10.1126/science.1200320.

P. F. DeCarlo, J. Slowik, D. Worsnop, P. Davidovits, and J. L. Jimenez. Particle Morphology and Density Characterization by Combined Mobility and Aerodynamic Diameter Measurements. Part 1: Theory. *Aerosol Science & Technology*, 38(12):1185–1205, 2004. ISSN 0278-6826. doi: 10.1080/027868290903907. URL http://www.informaworld.com/openurl?genre=article&doi=10.1080/027868290903907&magic=crossref||D404A21C5BB053405B1A640AFFD44AE3.

P. F. DeCarlo, J. R. Kimmel, A. Trimborn, M. J. Northway, J. T. Jayne, A. C. Aiken, M. Gonin, K. Fuhrer, T. Horvath, K. S. Docherty, D. R. Worsnop, and J. L. Jimenez. Field-deployable, high-resolution, time-of-flight aerosol mass spectrometer. *Analytical chemistry*, 78(24):8281–9, Dec. 2006. ISSN 0003-2700. doi: 10.1021/ac061249n. URL http://www.ncbi.nlm.nih.gov/pubmed/17165817.

P. F. DeCarlo, E. J. Dunlea, J. R. Kimmel, A. C. Aiken, D. Sueper, J. Crounse, P. O. Wennberg, L. Emmons, Y. Shinozuka, A. Clarke, J. Zhou, J. Tomlinson, D. R. Collins,

D. Knapp, A. J. Weinheimer, D. D. Montzka, T. Campos, and J. L. Jimenez. Fast airborne aerosol size and chemistry measurements above Mexico City and Central Mexico during the MILAGRO campaign. *Atmospheric Chemistry and Physics*, 8 (14):4027–4048, July 2008. ISSN 1680-7324. doi: 10.5194/acp-8-4027-2008. URL http://www.atmos-chem-phys.net/8/4027/2008/.

K. Denman, G. Brasseur, A. Chidthaisong, P. Ciais, P. Cox, R. Dickinson, D. Hauglustaine, C. Heinze, E. Holland, D. Jacob, U. Lohmann, S. Ramachandran, P. D. S. Dias, S. Wofsy, and X. Zhang. Couplings Between Changes in the Climate System and Biogeochemistry. In S. Solomon, D.Qin, M. Manning, Z. Chen, M. Marquis, K. Averyt, M. Tignor, and H. Miller, editors, *Climate Change 2007: The Physical Science Basis. Contribution of Working Group I to the Fourth Assessment Report of the Intergovernmental Panel on Climate Change*, chapter Couplings. Cambridge University Press, Cambridge, United Kingdom and New York, NY, USA, 2007.

N. Donahue, A. Robinson, and S. Pandis. Atmospheric organic particulate matter: From smoke to secondary organic aerosol. *Atmospheric Environment*, 43(1):94–106, Jan. 2009. ISSN 13522310. doi: 10.1016/j.atmosenv.2008.09.055. URL http://dx.doi.org/10.1016/j.atmosenv.2008.09.055.

N. M. Donahue, A. L. Robinson, C. O. Stanier, and S. N. Pandis. Coupled partitioning, dilution, and chemical aging of semivolatile organics. *Environmental science & technology*, 40(8):2635–43, Apr. 2006. ISSN 0013-936X. URL http://www.ncbi.nlm.nih.gov/pubmed/16683603.

F. Drewnick, S. S. Hings, P. Decarlo, J. T. Jayne, M. Gonin, K. Fuhrer, S. Weimer, J. L. Jimenez, K. L. D. S. Borrmann, and D. R. Worsnop. A new time-of-flight aerosol mass spectrometer TOF-AMS - Instrument description and first field deployment. *Aerosol Science & Technology*, 39(7):637–658, 2005. ISSN 0278-6826.

E. Dwyer, S. Pinnock, J. M. Gregoire, and J. M. C. Pereira. Global spatial and temporal distribution of vegetation fire as determined from satellite observations. *International Journal of Remote Sensing*, 21(6):1289–1302, 2000. ISSN 0143-1161. doi: 10.1080/014311600210182. URL http://www.informaworld.com/openurl?genre=article&doi=10.1080/014311600210182&magic=crossref||D404A21C5BB053405B1A640AFFD44AE3.

Encycopaedia Britannica. Heterogeneous reaction, 2011. URL http://www.britannica.com/EBchecked/topic/264278/heterogeneous-reaction.

R. J. Ferek, T. Garrett, P. V. Hobbs, S. Strader, D. Johnson, J. P. Taylor, K. Nielsen, A. S. Ackerman, Y. Kogan, Q. Liu, B. A. Albrecht, and D. Babb. Drizzle

Suppression in Ship Tracks. *Journal of the Atmospheric Sciences*, 57(16):2707–2728, 2000. ISSN 15200469. doi: 10.1175/1520-0469(2000)057<2707:DSIST>2.0.CO;2. URL http://journals.allenpress.com/jrnlserv/?request=get-abstract&issn=1520-0469&volume=57&page=2707.

G. Fisch, J. Tota, L. A. T. Machado, M. Dias, R. F. D. Lyra, C. A. Nobre, A. J. Dolman, and J. H. C. Gash. The convective boundary layer over pasture and forest in Amazonia. *Theoretical and Applied Climatology*, (78):47—-59, 2004.

Food and Agriculture Organisation. *Global Forest Resources Assessment 2010: Main Report*. Bernan Assoc, Rome, 2010. ISBN 925106654X. URL http://books.google.com/books?id=vEcJTwEACAAJ&pgis=1.

P. Forster, V. Ramaswamy, P. Artaxo, T. Berntsen, R. Betts, D. W. Fahey, J. Haywood, J. Lean, D. C. Lowe, G. Myhre, J. Nganga, R. Prinn, G. Raga, M. Schulz, R. van Dorland, G. Bodeker, O. Boucher, W. D. Collins, T. J. Conway, E. Dlugokencky, J. W. Elkins, D. Etheridge, P. Foukal, P. Fraser, M. Geller, F. Joos, C. D. Keeling, S. Kinne, K. Lassey, U. Lohmann, A. C. Manning, S. Montzka, D. Oram, K. O'Shaughnessy, S. Piper, G.-K. Plattner, M. Ponater, N. Ramankutty, G. Reid, D. Rind, K. Rosenlof, R. Sausen, D. Schwarzkopf, S. K. Solanki, G. Stenchikov, N. Stuber, T. Takemura, C. Textor, R. Wang, R. Weiss, and T. Whorf. Contribution of Working Group I to the Fourth Assessment Report of the Intergovernmental Panel on Climate Change. In S. Solomon, D. Qin, M. Manning, Z. Chen, M. Marquis, K. Averyt, M.Tignor, and H. Miller, editors, *Climate Change 2007: The Physical Science Basis*, chapter 2, pages 129–234. Cambridge University Press, Cambridge, United Kingdom and New York, NY, USA, Oct. 2007. URL http://elib.dlr.de/51416/.

K. D. Froyd, S. M. Murphy, D. M. Murphy, J. A. de Gouw, N. C. Eddingsaas, and P. O. Wennberg. Contribution of isoprene-derived organosulfates to free tropospheric aerosol mass. *Proceedings of the National Academy of Sciences of the United States of America*, 107(50):21360–21365, Nov. 2010. ISSN 1091-6490. doi: 10.1073/pnas.1012561107. URL http://www.ncbi.nlm.nih.gov/pubmed/21098310.

A. M. Gabey, M. W. Gallagher, J. Whitehead, J. R. Dorsey, P. H. Kaye, and W. R. Stanley. Measurements and comparison of primary biological aerosol above and below a tropical forest canopy using a dual channel fluorescence spectrometer. *Atmospheric Chemistry and Physics*, 10(10):4453–4466, May 2010. ISSN 1680-7324. doi: 10.5194/acp-10-4453-2010. URL http://www.atmos-chem-phys.net/10/4453/2010/.

S. Gao, D. A. Hegg, P. V. Hobbs, T. W. Kirchstetter, B. I. Magi, and M. Sadilek. Water-soluble organic components in aerosols associated with savanna fires in southern Africa: Identification, evolution, and distribution. *Journal of Geophysical Research*,

108(D13), 2003. ISSN 0148-0227. doi: 10.1029/2002JD002324. URL http://www.agu.org/pubs/crossref/2003/2002JD002324.shtml.

A. Goldstein and I. Galbally. Known and unexplored organic constituents in the earth's atmosphere. *Environmental Science & Technology*, 41(5):1514–1521, 2007. URL http://pubs.acs.org/doi/abs/10.1021/es072476p.

A. H. Goldstein, M. McKay, M. R. Kurpius, G. W. Schade, A. Lee, R. Holzinger, and R. A. Rasmussen. Forest thinning experiment confirms ozone deposition to forest canopy is dominated by reaction with biogenic VOCs. *Geophysical Research Letters*, 31(22):2–5, 2004. ISSN 0094-8276. doi: 10.1029/2004GL021259. URL http://www.agu.org/pubs/crossref/2004/2004GL021259.shtml.

H.-F. Graf, J. Feichter, and B. Langmann. Volcanic sulfur emissions: Estimates of source strength and its contribution to the global sulfate distribution. *Journal of Geophysical Research*, 102(D9):10727–10738, 1997. ISSN 0148-0227. doi: 10.1029/96JD03265. URL http://www.agu.org/pubs/crossref/1997/96JD03265.shtml.

C. Grossi and C. Brimblecombe. The effect of atmospheric pollution on building materials. *Journal de Physique. IV*, 12(10), 2002. doi: 35400010558048.0140. URL http://d.wanfangdata.com.cn/NSTLQK_NSTL_QK6191951.aspx.

A. Guenther, C. Hewitt, D. Erickson, R. Fall, C. Geron, T. Graedel, P. Harley, L. Klinger, M. Lerdau, W. McKay, T. Pierce, B. Scholes, R. Steinbrecher, R. Tallmaraju, J. Taylor, and P. Zimmerman. A global model of natural volatile organic compound emissions. *Journal of Geophysical Research-Atmospheres*, 100(D5):8873–8892, 1995. URL http://www.agu.org/pubs/crossref/1995/94JD02950.shtml.

S. Gunthe, S. King, D. Rose, Q. Chen, P. Roldin, D. Farmer, J. Jimenez, P. Artaxo, and M. Aneae. Cloud condensation nuclei in pristine tropical rainforest air of Amazonia: size-resolved measurements and modeling of atmospheric aerosol composition and CCN activity. *Atmospheric Chemistry and Physics*, 9:7551–7575, 2009.

M. Gysel, J. Crosier, D. O. Topping, J. D. Whitehead, K. N. Bower, M. J. Cubison, P. I. Williams, M. J. Flynn, G. B. McFiggans, and H. Coe. Closure study between chemical composition and hygroscopic growth of aerosol particles during TORCH2. *Atmospheric Chemistry and Physics*, 7(24):6131–6144, Dec. 2007. ISSN 1680-7324. doi: 10.5194/acp-7-6131-2007. URL http://www.atmos-chem-phys.net/7/6131/2007/.

M. Hallquist, J. C. Wenger, U. Baltensperger, Y. Rudich, D. Simpson, M. Claeys, J. Dommen, N. M. Donahue, C. George, A. Goldstein, J. F. Hamilton, H. Herrmann, L. E. Hudson, Y. Iinuma, M. Jang, M. E. Jenkin, J. L. Jimenez, A. Kiendler-Scharr, W. Maenhaut, G. McFiggans, T. F. Mentel, A. Monod, A. S. H. Prévôt, J. H.

Seinfeld, J. D. Surratt, R. Szmigielski, and J. Wildt. The formation, properties and impact of secondary organic aerosol: current and emerging issues. *Atmospheric Chemistry and Physics*, 9(14):5155–5235, 2009. ISSN 1680-7316. URL http://www.atmos-chem-phys.net/9/5155/2009/.

J. Hansen, M. Sato, and R. Ruedy. Radiative forcing and climate response. *Journal of Geophysical Research*, 102(D6):6831–6864, 1997. ISSN 0148-0227. doi: 10.1029/96JD03436. URL http://www.agu.org/pubs/crossref/1997/96JD03436.shtml.

J. Haywood and O. Boucher. Estimates of the direct and indirect radiative forcing due to tropospheric aerosols: A review. *Reviews of Geophysics*, 38(4):513, 2000. ISSN 8755-1209. doi: 10.1029/1999RG000078. URL http://www.agu.org/pubs/crossref/2000/1999RG000078.shtml.

C. L. Heald, D. J. Jacob, R. J. Park, L. M. Russell, B. J. Huebert, J. H. Seinfeld, H. Liao, and R. J. Weber. A large organic aerosol source in the free troposphere missing from current models. *Geophysical research letters*, 32(18):1–4, 2005. ISSN 0094-8276. doi: 10.1029/2005GL02383.

C. L. Heald, D. K. Henze, L. W. Horowitz, J. Feddema, J.-F. Lamarque, A. Guenther, P. G. Hess, F. Vitt, J. H. Seinfeld, A. H. Goldstein, and I. Fung. Predicted change in global secondary organic aerosol concentrations in response to future climate, emissions, and land use change. *Journal of Geophysical Research*, 113(D5):—-, Mar. 2008. ISSN 0148-0227. doi: 10.1029/2007JD009092. URL http://www.agu.org/pubs/crossref/2008/2007JD009092.shtml.

C. L. Heald, J. H. Kroll, J. L. Jimenez, K. S. Docherty, P. F. DeCarlo, A. C. Aiken, Q. Chen, S. T. Martin, D. K. Farmer, and P. Artaxo. A simplified description of the evolution of organic aerosol composition in the atmosphere. *Geophysical Research Letters*, 37(8), Apr. 2010. ISSN 0094-8276. doi: 10.1029/2010GL042737. URL http://www.agu.org/pubs/crossref/2010/2010GL042737.shtml.

D. Henze and J. Seinfeld. Global secondary organic aerosol from isoprene oxidation. *Geophysical research letters*, 33(9):101029/, 2006. URL http://acmg.seas.harvard.edu/publications/henze2006a.pdf.

D. K. Henze, J. H. Seinfeld, N. L. Ng, J. H. Kroll, T.-M. Fu, D. J. Jacob, and C. L. Heald. Global modeling of secondary organic aerosol formation from aromatic hydrocarbons: high- vs. low-yield pathways. *Atmospheric Chemistry and Physics*, 8(9):2405–2420, May 2008. ISSN 1680-7324. doi: 10.5194/acp-8-2405-2008. URL http://www.atmos-chem-phys.net/8/2405/2008/.

C. Hewitt, J. Lee, M. P. Barkley, N. Carslaw, N. A. Chappell, H. Coe, C. Collier, R. Commane, F. Davies, P. Di Carlo, C. F. D. Marco, P. M. Edwards, M. J. Evans,

D. Fowler, K. L. Furneaux, M. W. Gallagher, A. Guenther, D. E. Heard, C. Helfter, J. Hopkins, T. Ingham, M. Irwin, C. Jones, A. Karunaharan, B. Langford, A. C. Lewis, S. F. Lim, S. M. Macdonald, A. R. Mackenzie, A. S. Mahajan, S. Malpass, G. Mcfiggans, G. Mills, P. Misztal, S. Moller, P. S. Monks, E. Nemitz, H. Oetjen, D. Oram, P. I. Palmer, G. J. Phillips, J. M. C. Plane, T. Pugh, J. A. Pyle, C. E. Reeves, N. H. Robinson, D. Stewart, D. Stone, and L. K. Whalley. Oxidant and particle photochemical processes above a south-east Asian tropical rain forest (the OP3 project): introduction, rationale, location characteristics and tools. *Atmospheric Chemistry and Physics*, 163:18899–18963, 2010. URL http://www.atmos-chem-phys.net/10/169/2010/acp-10-169-2010.pdf.

C. N. Hewitt, A. R. MacKenzie, P. Di Carlo, C. F. Di Marco, J. R. Dorsey, M. Evans, D. Fowler, M. W. Gallagher, J. R. Hopkins, C. E. Jones, B. Langford, J. D. Lee, A. C. Lewis, S. F. Lim, J. McQuaid, P. Misztal, S. J. Moller, P. S. Monks, E. Nemitz, D. E. Oram, S. M. Owen, G. J. Phillips, T. A. M. Pugh, J. A. Pyle, C. E. Reeves, J. Ryder, J. Siong, U. Skiba, and D. J. Stewart. Nitrogen management is essential to prevent tropical oil palm plantations from causing ground-level ozone pollution. *Proceedings of the National Academy of Sciences of the United States of America*, 106(44):18447–51, Nov. 2009. ISSN 1091-6490. doi: 10.1073/pnas.0907541106. URL http://www.ncbi.nlm.nih.gov/pubmed/19841269.

W. C. Hinds. *Aerosol Technology: Properties, Behaviour and Measurement of Airborne Particles (Wiley-Interscience)*. WileyBlackwell, 1999. ISBN 0471194107. URL http://www.amazon.co.uk/Aerosol-Technology-Properties-Measurement-Wiley-Interscience/dp/0471194107.

C. R. Hoyle, M. Boy, N. M. Donahue, J. L. Fry, M. Glasius, a. Guenther, a. G. Hallar, K. Huff Hartz, M. D. Petters, T. Petäjä, T. Rosenoern, and a. P. Sullivan. A review of the anthropogenic influence on biogenic secondary organic aerosol. *Atmospheric Chemistry and Physics*, 11(1):321–343, Jan. 2011. ISSN 1680-7324. doi: 10.5194/acp-11-321-2011. URL http://www.atmos-chem-phys.net/11/321/2011/.

International Fuel Quality Center. International Desil Rankings - Top 100 Sulphur, 2009. URL http://www.ifqc.org/UserFiles/file/Misc/DieselRankings0909(1).pdf.

J. Irwin and M. Williams. Acid rain: Chemistry and transport. *Environmental Pollution*, 50(1-2):29–59, 1988. ISSN 02697491. doi: 10.1016/0269-7491(88)90184-4. URL http://linkinghub.elsevier.com/retrieve/pii/0269749188901844.

M. Irwin, N. Robinson, J. D. Allan, H. Coe, and G. McFiggans. Size-resolved aerosol water uptake and cloud condensation nuclei measurements as measured above a Southeast Asian rainforest during OP3. *Atmospheric Chemistry and Physics Discussions*, 11(1): 3117–3159, Jan. 2011. ISSN 1680-7375. doi: 10.5194/acpd-11-3117-2011. URL http://www.atmos-chem-phys-discuss.net/11/3117/2011/.

M. Jacobson, R. J. Charlson, H. Rodhe, and G. H. Orians. *Earth System Science: From Biogeochemical Cycles to Global Changes (International Geophysics)*. Academic Press, 2000. ISBN 012379370X. URL http://www.amazon.co.uk/Earth-System-Science-Biogeochemical-International/dp/012379370X.

J. T. Jayne, D. C. Leard, X. Zhang, P. Davidovits, K. A. Smith, C. E. Kolb, and D. R. Worsnop. Development of an Aerosol Mass Spectrometer for Size and Composition Analysis of Submicron Particles. *Aerosol Science & Technology*, 33(1-2):49–70, July 2000. ISSN 0278-6826. doi: 10.1080/027868200410840. URL http://www.informaworld.com/openurl?genre=article&doi=10.1080/027868200410840&magic=crossref||D404A21C5BB053405B1A640AFFD44AE3.

J. L. Jimenez, J. T. Jayne, Q. Shi, C. E. Kolb, D. R. Worsnop, I. Yourshaw, J. H. Seinfeld, R. C. Flagan, X. Zhang, K. A. Smith, J. W. Morris, and P. Davidovits. Ambient aerosol sampling using the Aerodyne Aerosol Mass Spectrometer. *Journal of Geophysical Research*, 108(D7), 2003. ISSN 0148-0227. doi: 10.1029/2001JD001213. URL http://www.agu.org/pubs/crossref/2003/2001JD001213.shtml.

J. L. Jimenez, M. R. Canagaratna, N. M. Donahue, A. S. H. Prevot, Q. Zhang, J. H. Kroll, P. F. DeCarlo, J. D. Allan, H. Coe, N. L. Ng, A. C. Aiken, K. S. Docherty, I. M. Ulbrich, A. P. Grieshop, A. L. Robinson, J. Duplissy, J. D. Smith, K. R. Wilson, V. A. Lanz, C. Hueglin, Y. L. Sun, J. Tian, A. Laaksonen, T. Raatikainen, J. Rautiainen, P. Vaattovaara, M. Ehn, M. Kulmala, J. M. Tomlinson, D. R. Collins, M. J. Cubison, E. J. Dunlea, J. A. Huffman, T. B. Onasch, M. R. Alfarra, P. I. Williams, K. N. Bower, Y. Kondo, J. Schneider, F. Drewnick, S. Borrmann, S. Weimer, K. Demerjian, D. Salcedo, L. Cottrell, R. Griffin, A. Takami, T. Miyoshi, S. Hatakeyama, A. Shimono, J. Y. Sun, Y. M. Zhang, K. Dzepina, J. R. Kimmel, D. Sueper, J. T. Jayne, S. C. Herndon, A. M. Trimborn, L. R. Williams, E. C. Wood, A. M. Middlebrook, C. E. Kolb, U. Baltensperger, and D. R. Worsnop. Evolution of organic aerosols in the atmosphere. *Science*, 326(5959):1525–9, 2009. ISSN 1095-9203. doi: 10.1126/science.1180353. URL http://www.ncbi.nlm.nih.gov/pubmed/20007897.

D. Johnson, S. R. Utembe, M. E. Jenkin, R. G. Derwent, G. D. Hayman, M. R. Alfarra, H. Coe, and G. McFiggans. Simulating regional scale secondary organic aerosol formation during the TORCH 2003 campaign in the southern UK. *Atmospheric*

Chemistry and Physics, 6(2):403–418, Feb. 2006. ISSN 1680-7324. doi: 10.5194/acp-6-403-2006. URL http://www.atmos-chem-phys.net/6/403/2006/.

M. Kanakidou, J. Seinfeld, S. N. Pandis, I. Barnes, F. Dentener, M. Facchini, R. Van Dingenen, B. Ervens, A. Nenes, and C. Nielsen. Organic aerosol and global climate modelling: a review. *Atmospheric Chemistry and Physics*, 5(4):1053–1123, 2005. URL http://authors.library.caltech.edu/620/1/KANacp05.pdf.

Y. J. Kaufman and R. S. Fraser. The Effect of Smoke Particles on Clouds and Climate Forcing. *Science*, 277(5332):1636–1639, Sept. 1997. ISSN 00368075. doi: 10.1126/science.277.5332.1636. URL http://www.sciencemag.org/cgi/doi/10.1126/science.277.5332.1636.

J. Kesselmeier, P. Ciccioli, U. Kuhn, P. Tefani, T. Biesenthal, S. Rottenberger, A. Wolf, M. Vitullo, R. Valentini, A. Nobre, P. Kabat, and M. O. Andreae. Volatile organic compound emissions in relation to plant carbon fixation and the terrestrial carbon budget. *Global Biogeochemical Cycles*, 16(4), 2002. ISSN 0886-6236. doi: 10.1029/2001GB001813. URL http://www.agu.org/pubs/crossref/2002/2001GB001813.shtml.

T. E. Kleindienst, M. Lewandowski, J. H. Offenberg, M. Jaoui, and E. O. Edney. The formation of secondary organic aerosol from the isoprene+ OH reaction in the absence on NOx. *Atmos. Chem. Phys.*, 9:6541–6558, 2009. URL http://www.atmos-chem-phys.org/9/6541/2009/acp-9-6541-2009.pdf.

E. Knutson and K. Whitby. Aerosol classification by electric mobility: apparatus, theory, and applications. *Journal of Aerosol Science*, 6(6):443–451, Nov. 1975. ISSN 00218502. doi: 10.1016/0021-8502(75)90060-9. URL http://linkinghub.elsevier.com/retrieve/pii/0021850275900609.

I. Koren, Y. J. Kaufman, L. a. Remer, and J. V. Martins. Measurement of the effect of Amazon smoke on inhibition of cloud formation. *Science*, 303(5662):1342–5, Feb. 2004. ISSN 1095-9203. doi: 10.1126/science.1089424. URL http://www.ncbi.nlm.nih.gov/pubmed/14988557.

R. Krejci, M. D. Reus, J. Williams, H. Fischer, and M. O. Andreae. Spatial and temporal distribution of atmospheric aerosols in the lowermost troposphere over the Amazonian tropical rainforest. *Atmospheric Chemistry and Physics*, 1985:1527–1543, 2005a. URL http://hal.archives-ouvertes.fr/docs/00/30/13/22/PDF/acpd-4-3565-2004.pdf.

R. Krejci, J. Strom, M. de Reus, and W. Sahle. Single particle analysis of the accumulation mode aerosol over the northeast Amazonian tropical rain forest, Surinam,

South Americ. *Atmos. Chem. Phys.*, (5):3331–3344, 2005b. URL http://www.atmos-chem-phys.org/5/3331/2005/acp-5-3331-2005.pdf.

J. H. Kroll and J. H. Seinfeld. Chemistry of secondary organic aerosol: Formation and evolution of low-volatility organics in the atmosphere. *Atmospheric Environment*, 42(16):3593–3624, May 2008. ISSN 13522310. doi: 10.1016/j.atmosenv.2008.01.003. URL http://linkinghub.elsevier.com/retrieve/pii/S1352231008000253.

J. H. Kroll, N. M. Donahue, J. L. Jimenez, S. H. Kessler, M. R. Canagaratna, K. R. Wilson, K. E. Altieri, L. R. Mazzoleni, A. S. Wozniak, H. Bluhm, E. R. Mysak, J. D. Smith, C. E. Kolb, and D. R. Worsnop. Carbon oxidation state as a metric for describing the chemistry of atmospheric organic aerosol. *Nature Chemistry*, Jan. 2011. ISSN 1755-4330. doi: 10.1038/nchem.948. URL http://www.nature.com/doifinder/10.1038/nchem.948.

M. Kulmala. Atmospheric science. How particles nucleate and grow. *Science*, 302(5647):1000–1, 2003. ISSN 1095-9203. doi: 10.1126/science.1090848. URL http://www.ncbi.nlm.nih.gov/pubmed/14605359.

M. Kulmala, V.-M. Kerminen, T. Anttila, A. Laaksonen, OâĂŹDowd, and C. D. Organic aerosol formation via sulphate cluster activation. *Journal of Geophysical Research*, 109(D4), 2004. ISSN 0148-0227. doi: 10.1029/2003JD003961. URL http://www.agu.org/pubs/crossref/2004/2003JD003961.shtml.

A. Laaksonen, M. Kulmala, C. D. O'Dowd, J. Joutsensaari, P. Vaattovaara, S. Mikkonen, K. E. J. Lehtinen, L. Sogacheva, M. Dal Maso, P. Aalto, T. Petäjä, A. Sogachev, Y. J. Yoon, H. Lihavainen, D. Nilsson, M. C. Facchini, F. Cavalli, S. Fuzzi, T. Hoffmann, F. Arnold, M. Hanke, K. Sellegri, B. Umann, W. Junkermann, H. Coe, J. D. Allan, M. R. Alfarra, D. R. Worsnop, M. L. Riekkola, T. Hyötyläinen, and Y. Viisanen. The role of VOC oxidation products in continental new particle formation. *Atmospheric Chemistry and Physics*, 8(10):2657–2665, May 2008. ISSN 1680-7324. doi: 10.5194/acp-8-2657-2008. URL http://www.atmos-chem-phys.net/8/2657/2008/.

D. A. Lack, X. X. Tie, N. D. Bofinger, A. N. Wiegand, and S. Madronich. Seasonal variability of secondary organic aerosol: A global modeling study. *Journal of Geophysical Research*, 109(D3), 2004. ISSN 0148-0227. doi: 10.1029/2003JD003418. URL http://www.agu.org/pubs/crossref/2004/2003JD003418.shtml.

T. E. Lane, N. M. Donahue, and S. N. Pandis. Simulating secondary organic aerosol formation using the volatility basis-set approach in a chemical transport model. *Atmospheric Environment*, 42(32):7439–7451, 2008. ISSN 13522310. doi:

10.1016/j.atmosenv.2008.06.026. URL http://linkinghub.elsevier.com/retrieve/pii/S1352231008005840.

V. A. Lanz, M. R. Alfarra, U. Baltensperger, B. Buchmann, C. Hueglin, and A. S. H. Prevot. Source apportionment of submicron organic aerosols at an urban site by factor analytical modelling of aerosol mass spectra. *Atmospheric chemistry and physics*, 7(6): 1503–1522, 2007.

J. Latham and M. H. Smith. Effect on global warming of wind-dependent aerosol generation at the ocean surface. *Nature*, 347(6291):372–373, Sept. 1990. ISSN 0028-0836. doi: 10.1038/347372a0. URL http://www.nature.com/doifinder/10.1038/347372a0.

H. Le Treut, R. Somerville, U. Cubasch, Y. Ding, C. Mauritzen, A. Mokssit, T. Peterson, M. Prather, D. Qin, M. Manning, Z. Chen, M. Marquis, K. B. Averyt, and M. Tignor. Historical Overview of Climate Change Science. In S. Solomon, D. Qin, M. Manning, Z. Chen, M. Marquis, K. Averyt, M. Tignor, and H. Miller, editors, *Climate Change 2007: The Physical Science Basis*, chapter 1, pages 94–127. Cambridge University Press, Cambridge, United Kingdom and New York, NY, USA, 2007. URL http://www.ipcc.ch/pdf/assessment-report/ar4/wg1/ar4-wg1-chapter1.pdf.

T. Lebel, D. J. Parker, C. Flamant, B. Bourlès, B. Marticorena, E. Mougin, C. Peugeot, A. Diedhiou, J. M. Haywood, J. B. Ngamini, J. Polcher, J.-L. Redelsperger, and C. D. Thorncroft. The AMMA field campaigns: multiscale and multidisciplinary observations in the West African region. *Quarterly Journal of the Royal Meteorological Society*, 136(S1):8–33, Jan. 2010. ISSN 00359009. doi: 10.1002/qj.486. URL http://doi.wiley.com/10.1002/qj.486.

A. Lee, A. H. Goldstein, M. D. Keywood, S. Gao, V. Varutbangkul, R. Bahreini, N. L. Ng, R. C. Flagan, and J. H. Seinfeld. Gas-phase products and secondary aerosol yields from the ozonolysis of ten different terpenes. *Journal of Geophysical Research*, 111 (D7), 2006. ISSN 0148-0227. doi: 10.1029/2005JD006437. URL http://www.agu.org/pubs/crossref/2006/2005JD006437.shtml.

J. Lelieveld, T. M. Butler, J. N. Crowley, T. J. Dillon, H. Fischer, and Others. Atmospheric oxidation capacity sustained by a tropical forest. *Nature*, 452(7188):737–740, 2008. ISSN 0028-0836.

Z. Levin and W. R. Cotton. Aerosol pollution impact on precipitation: A scientific revie. In Z. Levin and W. R. Cotton, editors, *Report from the WMO/ IUGG International Aerosol Precipitation Science, Assessment Group (IAPSAG)*, page 482. World Meteorological Organization, Geneva, Switzerland, 2008. ISBN 9781402086892.

doi: 10.1007/978-1-4020-8690-8. URL http://www.springerlink.com/index/10.1007/978-1-4020-8690-8.

S. L. Lewis, P. M. Brando, O. L. Phillips, G. M. F. van der Heijden, and D. Nepstad. The 2010 Amazon Drought. *Science*, 331(6017):554–554, Feb. 2011. ISSN 0036-8075. doi: 10.1126/science.1200807. URL http://www.sciencemag.org/cgi/doi/10.1126/science.1200807.

A. R. MacKenzie, B. Langford, T. Pugh, N. Robinson, P. K. Misztal, D. E. Heard, J. D. Lee, A. C. Lewis, C. E. Jones, J. R. Hopkins, G. Phillips, P. S. Monks, A. Karunaharan, K. E. Hornsby, V. Nicolas-Perea, H. Coe, A. M. Gabey, M. W. Gallagher, L. Whalley, P. M. Edwards, M. J. Evans, D. Stone, T. Ingham, R. Commane, K. L. Furneaux, J. B. McQuaid, E. Nemitz, Y. K. Seng, D. Fowler, J. A. Pyle, and C. Hewitt. The atmospheric chemistry of trace gases and particulate matter emitted by different land uses in Borneo (in press). *Philosophical transactions of the Royal Society of London. Series B, Biological sciences*, 2011.

S. T. Martin, M. O. Andreae, D. Althausen, P. Artaxo, H. Baars, S. Borrmann, Q. Chen, D. K. Farmer, a. Guenther, S. S. Gunthe, J. L. Jimenez, T. Karl, K. Longo, a. Manzi, T. Müller, T. Pauliquevis, M. D. Petters, a. J. Prenni, U. Pöschl, L. V. Rizzo, J. Schneider, J. N. Smith, E. Swietlicki, J. Tota, J. Wang, a. Wiedensohler, and S. R. Zorn. An overview of the Amazonian Aerosol Characterization Experiment 2008 (AMAZE-08). *Atmospheric Chemistry and Physics*, 10(23):11415–11438, Dec. 2010a. ISSN 1680-7324. doi: 10.5194/acp-10-11415-2010. URL http://www.atmos-chem-phys.net/10/11415/2010/.

S. T. Martin, M. O. Andreae, P. Artaxo, D. Baumgardner, Q. Chen, A. H. Goldstein, A. Guenther, C. L. Heald, O. L. Mayol-Bracero, P. H. McMurry, T. Pauliquevis, U. Pöschl, K. A. Prather, G. C. Roberts, S. R. Saleska, M. A. Silva Dias, D. V. Spracklen, E. Swietlicki, and I. Trebs. Sources and properties of Amazonian aerosol particles. *Reviews of Geophysics*, 48(2), Apr. 2010b. ISSN 8755-1209. doi: 10.1029/2008RG000280. URL http://www.agu.org/pubs/crossref/2010/2008RG000280.shtml.

G. K. Mather. Coalescence Enhancement in large Multicell Storms Caused by the Emissions from a Kraft Paper Mill. *Journal of Applied Meteorology*, 30(8):1134–1146, Aug. 1991. ISSN 0894-8763. doi: 10.1175/1520-0450(1991)030<1134:CEILMS>2.0.CO;2. URL http://journals.ametsoc.org/doi/abs/10.1175/1520-0450(1991)030<1134:CEILMS>2.0.CO;2.

B. Matthew, A. Middlebrook, and T. Onasch. Collection Efficiencies in an Aerodyne Aerosol Mass Spectrometer as a Function of Particle Phase for Laboratory Generated

Aerosols. *Aerosol Science and Technology*, 42(11):884–898, Sept. 2008. ISSN 0278-6826. doi: 10.1080/02786820802356797. URL http://www.informaworld.com/smpp/content~db=all~content=a902918478.

S. Matthias-Maser and R. Jaenicke. The size distribution of primary biological aerosol particles with radii > 0.2 μm in an urban/rural influenced region. *Atmospheric Research*, 39(4):279–286, Dec. 1995. ISSN 01698095. doi: 10.1016/0169-8095(95)00017-8. URL http://linkinghub.elsevier.com/retrieve/pii/0169809595000178.

J. L. Mauderly and J. C. Chow. Health effects of organic aerosols. *Inhalation toxicology*, 20(3):257–88, 2008. ISSN 1091-7691. doi: 10.1080/08958370701866008. URL http://www.ncbi.nlm.nih.gov/pubmed/18300047.

M. P. McCormick, L. W. Thomason, and C. R. Trepte. Atmospheric effects of the Mt Pinatubo eruption. *Nature*, 373(6513):399–404, 1995. ISSN 00280836. doi: 10.1038/373399a0. URL http://jack.pixe.lth.se/kfgu/KOO090_FKF075/Artiklar/P05.pdf.

I. G. McKendry, J. P. Hacker, R. Stull, S. Sakiyama, D. Mignacca, and K. Reid. Long-range transport of Asian dust to the Lower Fraser Valley, British Columbia, Canada. *Journal of Geophysical Research Atmospheres*, 106(D16):18361–18370, 2001. ISSN 07477309.

F. McLafferty and F. Turecek. *Interpretation of Mass Spectra*. University Science Books,U.S., 1993. ISBN 0935702253. URL http://www.amazon.co.uk/Interpretation-Mass-Spectra-F-W-McLafferty/dp/0935702253.

J. McMorrow and M. A. Talip. Decline of forest area in Sabah, Malaysia: Relationship to state policies, land code and land capability. *Global Environmental Change*, 11(3):217–230, Oct. 2001. ISSN 09593780. doi: 10.1016/S0959-3780(00)00059-5. URL http://linkinghub.elsevier.com/retrieve/pii/S0959378000000595.

P. K. Misztal, S. M. Owen, A. B. Guenther, R. Rasmussen, C. Geron, P. Harley, G. J. Phillips, A. Ryan, D. P. Edwards, C. N. Hewitt, E. Nemitz, J. Siong, M. R. Heal, and J. N. Cape. Large estragole fluxes from oil palms in Borneo. *Atmospheric Chemistry and Physics*, 10(9):4343–4358, May 2010. ISSN 1680-7324. doi: 10.5194/acp-10-4343-2010. URL http://www.atmos-chem-phys.net/10/4343/2010/.

W. T. Morgan, J. D. Allan, K. N. Bower, E. J. Highwood, D. Liu, G. R. McMeeking, M. J. Northway, P. I. Williams, R. Krejci, and H. Coe. Airborne measurements of the spatial distribution of aerosol chemical composition across Europe and evolution of the organic fraction. *Atmospheric Chemistry and Physics*, 10(8):4065–

4083, Apr. 2010. ISSN 1680-7324. doi: 10.5194/acp-10-4065-2010. URL http://www.atmos-chem-phys.net/10/4065/2010/.

N. L. Ng, M. R. Canagaratna, Q. Zhang, J. L. Jimenez, J. Tian, I. M. Ulbrich, J. H. Kroll, K. S. Docherty, P. S. Chhabra, R. Bahreini, S. M. Murphy, J. H. Seinfeld, L. Hildebrandt, N. M. Donahue, P. F. DeCarlo, V. A. Lanz, A. S. H. Prévôt, E. Dinar, Y. Rudich, and D. R. Worsnop. Organic aerosol components observed in Northern Hemispheric datasets from Aerosol Mass Spectrometry. *Atmospheric Chemistry and Physics*, 10(10):4625–4641, May 2010. ISSN 1680-7324. doi: 10.5194/acp-10-4625-2010. URL http://www.atmos-chem-phys.net/10/4625/2010/.

C. O'Dowd, G. McFiggans, D. J. Creasey, L. Pirjola, C. Hoell, M. H. Smith, B. J. Allan, J. M. C. Plane, D. E. Heard, J. D. Lee, M. J. Pilling, and M. Kulmala. On the photochemical production of new particles in the coastal boundary layer. *Geophysical Research Letters*, 26(12):1707, 1999. ISSN 0094-8276. doi: 10.1029/1999GL900335. URL http://www.agu.org/pubs/crossref/1999/1999GL900335.shtml.

Oxford English Dictionary. *"free radical, n."*. Oxford University Press, Oxford, 3rd online edition, 2010a. URL http://www.oed.com/view/Entry/270231?redirectedFrom=freeradical#.

Oxford English Dictionary. *"organic, adj. and n."*. Oxford University Press, Oxford, 3rd online edition, 2010b. URL http://www.oed.com/view/Entry/132431?redirectedFrom=organic.

Oxford English Dictionary. *"partial pressure, n."*. Oxford University Press, Oxford, 3rd online edition, 2010c. URL http://www.oed.com/view/Entry/138227?redirectedFrom=partialpressure#eid31567355.

Oxford English Dictionary. *"hygroscopic, adj."*. Oxford University Press, Oxford, 3rd online edition, 2010d. URL http://www.oed.com/view/Entry/90159?rskey=r5vhsm&result=2&isAdvanced=false#.

P. Paatero. Least squares formulation of robust non-negative factor analysis. *Chemometrics and Intelligent Laboratory Systems*, 37(1):23–35, May 1997. ISSN 01697439. doi: 10.1016/S0169-7439(96)00044-5. URL http://linkinghub.elsevier.com/retrieve/pii/S0169743996000445.

P. Paatero and U. Tapper. Positive matrix factorization: A non-negative factor model with optimal utilization of error estimates of data values. *Environmetrics*, 5(2):111–126, June 1994. ISSN 11804009. doi: 10.1002/env.3170050203. URL http://doi.wiley.com/10.1002/env.3170050203.

S. Pandis, S. Paulson, J. Seindeld, and R. Flagan. Aerosol formation in the photooxidation of isoprene and β-pinene. *Atmospheric Environment. Part A. General Topics*, 25(5-6): 997–1008, 1991. ISSN 09601686. doi: 10.1016/0960-1686(91)90141-S. URL http://linkinghub.elsevier.com/retrieve/pii/096016869190141S.

R. J. Park, D. J. Jacob, M. Chin, and R. V. Martin. Sources of carbonaceous aerosols over the United States and implications for natural visibility. *Journal of Geophysical Research*, 108(D12), 2003. ISSN 0148-0227. doi: 10.1029/2002JD003190. URL http://www.agu.org/pubs/crossref/2003/2002JD003190.shtml.

M. Parry, O. Canziani, J. Palutikof, P. van der Linden, and C. Hanson. Contribution of Working Group II to the Fourth Assessment Report of the Intergovernmental Panel on Climate Change. In *Climate Change 2007: Impacts, Adaptation and Vulnerability*. Cambridge University Press, 2007. URL http://www.ipcc-wg2.gov.

B. Parthasarathy, A. A. Munot, and D. R. Kothawale. All-India monthly and seasonal rainfall series: 1871–1993. *Theoretical and Applied Climatology*, 49(4):217–224, 1994. URL http://www.springerlink.com/index/GR005N1U7X1U5H12.pdf.

P. K. Patra, S. K. Behera, J. R. Herman, S. Maksyutov, H. Akimoto, and Y. Yamagata. The Indian summer monsoon rainfall: interplay of coupled dynamics, radiation and cloud microphysics. *Atmospheric Chemistry and Physics*, 5(8):2181–2188, Aug. 2005. ISSN 1680-7324. doi: 10.5194/acp-5-2181-2005. URL http://www.atmos-chem-phys.net/5/2181/2005/.

F. Paulot, J. D. Crounse, H. G. Kjaergaard, A. Kürten, J. M. St Clair, J. H. Seinfeld, and P. O. Wennberg. Unexpected epoxide formation in the gas-phase photooxidation of isoprene. *Science*, 325(5941):730–3, 2009. ISSN 1095-9203. doi: 10.1126/science.1172910. URL http://www.ncbi.nlm.nih.gov/pubmed/19661425.

G. Pearson, F. Davies, and C. Collier. Remote sensing of the tropical rain forest boundary layer using pulsed Doppler lidar. *Atmospheric Chemistry and Physics*, 10(13):5891–5901, July 2010. ISSN 1680-7324. doi: 10.5194/acp-10-5891-2010. URL http://www.atmos-chem-phys.net/10/5891/2010/.

L. Pirjola, A. Laaksonen, P. Aalto, and M. Kulmala. Sulfate aerosol formation in the Arctic boundary layer. *Journal of Geophysical Research*, 103(D7):8309–8321, 1998. ISSN 0148-0227. doi: 10.1029/97JD03079. URL http://www.agu.org/pubs/crossref/1998/97JD03079.shtml.

U. Poschl, S. T. Martin, B. Sinha, Q. Chen, S. S. Gunthe, J. A. Huffman, S. Borrmann, D. K. Farmer, R. M. Garland, G. Helas, J. L. Jimenez, S. M. King, A. Manzi, E. Mikhailov, T. Pauliquevis, M. D. Petters, A. J. Prenni, P. Roldin, D. Rose,

J. Schneider, H. Su, S. R. Zorn, P. Artaxo, and M. O. Andreae. Rainforest Aerosols as Biogenic Nuclei of Clouds and Precipitation in the Amazon. *Science*, 329(5998): 1513–1516, Sept. 2010. ISSN 0036-8075. doi: 10.1126/science.1191056. URL http://www.sciencemag.org/cgi/content/abstract/329/5998/1513.

A. J. Prenni, M. D. Petters, S. M. Kreidenweis, C. L. Heald, S. T. Martin, P. Artaxo, R. M. Garland, A. G. Wollny, and U. Pöschl. Relative roles of biogenic emissions and Saharan dust as ice nuclei in the Amazon basin. *Nature Geoscience*, 2(6):402–405, May 2009. ISSN 1752-0894. doi: 10.1038/ngeo517. URL http://www.nature.com/doifinder/10.1038/ngeo517.

R. G. Prinn. Evidence for variability of atmospheric hydroxyl radicals over the past quarter century. *Geophysical Research Letters*, 32(7):2—-5, 2005. ISSN 0094-8276. doi: 10.1029/2004GL022228. URL http://www.agu.org/pubs/crossref/2005/2004GL022228.shtml.

G. C. Roberts, M. O. Andreae, J. Zhou, and P. Artaxo. Cloud condensation nuclei in the Amazon Basin: âĂIJmarineâĂİ conditions over a continent? *Geophysical Research Letters*, 28(14):2807, 2001. ISSN 0094-8276. doi: 10.1029/2000GL012585. URL http://www.agu.org/pubs/crossref/2001/2000GL012585.shtml.

A. L. Robinson, N. M. Donahue, M. K. Shrivastava, E. a. Weitkamp, A. M. Sage, A. P. Grieshop, T. E. Lane, J. R. Pierce, and S. N. Pandis. Rethinking organic aerosols: semivolatile emissions and photochemical aging. *Science*, 315(5816):1259–62, 2007. ISSN 1095-9203. doi: 10.1126/science.1133061. URL http://www.ncbi.nlm.nih.gov/pubmed/17332409.

J. Rockström, W. Steffen, K. Noone, A. Persson, F. S. Chapin, E. F. Lambin, T. M. Lenton, M. Scheffer, C. Folke, H. J. Schellnhuber, B. Nykvist, C. A. de Wit, T. Hughes, S. van der Leeuw, H. Rodhe, S. Sörlin, P. K. Snyder, R. Costanza, U. Svedin, M. Falkenmark, L. Karlberg, R. W. Corell, V. J. Fabry, J. Hansen, B. Walker, D. Liverman, K. Richardson, P. Crutzen, and J. A. Foley. A safe operating space for humanity. *Nature*, 461(7263):472–5, Sept. 2009. ISSN 1476-4687. doi: 10.1038/461472a. URL http://www.ncbi.nlm.nih.gov/pubmed/19779433.

D. Rosenfeld. TRMM observed first direct evidence of smoke from forest fires inhibiting rainfall. *October*, 26(20):3105–3108, 1999. URL http://dx.doi.org/10.1029/1999GL006066.

D. Rosenfeld, U. Lohmann, G. B. Raga, C. D. O'Dowd, M. Kulmala, S. Fuzzi, A. Reissell, and M. O. Andreae. Flood or drought: how do aerosols affect precipitation? *Science (New York, N.Y.)*, 321(5894):1309–13, Sept. 2008. ISSN 1095-9203. doi: 10.1126/science.1160606. URL http://www.ncbi.nlm.nih.gov/pubmed/18772428.

D. Salcedo, T. B. Onasch, M. R. Canagaratna, K. Dzepina, J. A. Huffman, J. T. Jayne, D. R. Worsnop, C. E. Kolb, S. Weimer, F. Drewnick, J. D. Allan, A. E. Delia, and J. L. Jimenez. Technical Note: Use of a beam width probe in an Aerosol Mass Spectrometer to monitor particle collection efficiency in the field. *Atmospheric Chemistry and Physics*, 7(2):549–556, 2007. ISSN 1680-7316. URL http://www.atmos-chem-phys.net/7/549/2007/.

J. H. Seinfeld and S. N. Pandis. *Atmospheric Chemistry and Physics: From Air Pollution to Climate Change*. WileyBlackwell, 2006. ISBN 0471720186. URL http://www.amazon.co.uk/Atmospheric-Chemistry-Physics-Pollution-Climate/dp/0471720186.

J. E. Shilling, Q. Chen, S. M. King, T. Rosenoern, J. H. Kroll, D. R. Worsnop, P. F. DeCarlo, A. C. Aiken, D. Sueper, J. L. Jimenez, and S. T. Martin. Loading-dependent elemental composition of {alpha}-pinene SOA particles. *Atmospheric Chemistry and Physics*, 9(3):771–782, 2009. ISSN 1680-7316. URL http://www.atmos-chem-phys.net/9/771/2009/.

M. K. Shrivastava, E. M. Lipsky, C. O. Stanier, and A. L. Robinson. Modeling semivolatile organic aerosol mass emissions from combustion systems. *Environmental science & technology*, 40(8):2671–7, Apr. 2006. ISSN 0013-936X. URL http://www.ncbi.nlm.nih.gov/pubmed/16683607.

J. G. Slowik, J. Brook, R. Y.-W. Chang, G. J. Evans, K. Hayden, C.-H. Jeong, S.-M. Li, J. Liggio, P. S. K. Liu, M. McGuire, C. Mihele, S. Sjostedt, A. Vlasenko, and J. P. D. Abbatt. Photochemical processing of organic aerosol at nearby continental sites: contrast between urban plumes and regional aerosol. *Atmospheric Chemistry and Physics*, 11(6):2991–3006, Mar. 2011. ISSN 1680-7324. doi: 10.5194/acp-11-2991-2011. URL http://www.atmos-chem-phys.net/11/2991/2011/.

D. V. Spracklen, J. L. Jimenez, K. S. Carslaw, D. R. Worsnop, M. J. Evans, G. W. Mann, Q. Zhang, M. R. Canagaratna, J. Allan, H. Coe, G. McFiggans, A. Rap, and P. Forster. Aerosol mass spectrometer constraint on the global secondary organic aerosol budget. *Atmos. Chem. Phys. Discuss.*, 11:5699—-5755, 2011. doi: 10.5194/acpd-11-5699-2011. URL www.atmos-chem-phys-discuss.net/11/5699/2011/.

L. L. Stowe, R. M. Carey, and P. P. Pellegrino. Monitoring the Mt. Pinatubo aerosol layer with NOAA/11 AVHRR data. *Geophysical Research Letters*, 19(2):159, 1992. ISSN 0094-8276. doi: 10.1029/91GL02958. URL http://www.agu.org/pubs/crossref/1992/91GL02958.shtml.

J. D. Surratt, S. M. Murphy, J. H. Kroll, N. L. Ng, L. Hildebrandt, A. Sorooshian, R. Szmigielski, R. Vermeylen, W. Maenhaut, M. Claeys, R. C. Flagan, and J. H. Seinfeld. Chemical Composition of Secondary Organic Aerosol Formed from the Photooxidation of Isoprene. *The Journal of Physical Chemistry A*, 110(31):9665–9690, Aug. 2006. ISSN 1089-5639. URL http://dx.doi.org/10.1021/jp061734m.

J. D. Surratt, Y. Gomez-Gonzalez, A. W. H. Chan, R. Vermeylen, M. Shahgholi, T. E. Kleindienst, E. O. Edney, J. H. Offenberg, M. Lewandowski, M. Jaoui, W. Maenhaut, M. Claeys, R. C. Flagan, and J. H. Seinfeld. Organosulfate Formation in Biogenic Secondary Organic Aerosol. *The Journal of Physical Chemistry A*, 112(36):8345–8378, 2008. doi: 10.1021/jp802310p. URL http://pubs.acs.org/doi/abs/10.1021/jp802310p.

J. D. Surratt, A. W. H. Chan, N. C. Eddingsaas, M. Chan, C. L. Loza, A. J. Kwan, S. P. Hersey, R. C. Flagan, P. O. Wennberg, and J. H. Seinfeld. Atmospheric Chemistry Special Feature: Reactive intermediates revealed in secondary organic aerosol formation from isoprene. *Proceedings of the National Academy of Sciences of the United States of America*, 15(107):6640–6645, 2010. ISSN 1091-6490. doi: 10.1073/pnas.0911114107. URL http://www.ncbi.nlm.nih.gov/pubmed/20080572.

S. Szreter and G. Mooney. Urbanization, Mortality, and the Standard of Living Debate: New Estimates of the Expectation of Life at Birth in Nineteenth-Century British Cities. *The Economic History Review*, 51(1):84–112, 1998. URL http://www.jstor.org/stable/2599693.

C. Textor, M. Schulz, S. Guibert, S. Kinne, Y. Balkanski, S. Bauer, T. Berntsen, T. Berglen, O. Boucher, M. Chin, F. Dentener, T. Diehl, R. Easter, H. Feichter, D. Fillmore, S. Ghan, P. Ginoux, S. Gong, A. Grini, J. Hendricks, L. Horowitz, P. Huang, I. Isaksen, I. Iversen, S. Kloster, D. Koch, A. Kirkevå g, J. E. Kristjansson, M. Krol, A. Lauer, J. F. Lamarque, X. Liu, V. Montanaro, G. Myhre, J. Penner, G. Pitari, S. Reddy, O. Seland, P. Stier, T. Takemura, and X. Tie. Analysis and quantification of the diversities of aerosol life cycles within AeroCom. *Atmospheric Chemistry and Physics*, 6(7):1777–1813, 2006. ISSN 16807324. doi: 10.5194/acp-6-1777-2006. URL http://www.atmos-chem-phys.net/6/1777/2006/.

K. Tsigaridis and M. Kanakidou. Global modelling of secondary organic aerosol in the troposphere: a sensitivity analysis. *Atmospheric Chemistry and Physics*, 3(5):1849–1869, Oct. 2003. ISSN 1680-7324. doi: 10.5194/acp-3-1849-2003. URL http://www.atmos-chem-phys.net/3/1849/2003/.

K. Tsigaridis and M. Kanakidou. Secondary organic aerosol importance in the future atmosphere. *Atmospheric Environment*, 41(22):4682–4692, 2007. ISSN 13522310.

doi: 10.1016/j.atmosenv.2007.03.045. URL http://linkinghub.elsevier.com/retrieve/pii/S1352231007002865.

S. Twomey. The influence of pollution on the shortwave albedo of clouds. *Journal of the Atmospheric Sciences*, 34(7):1149–1152, 1977a. ISSN 15200469. doi: 10.1175/1520-0469(1977)034<1149:TIOPOT>2.0.CO;2.

S. Twomey. *Atmospheric Aerosols (Developments in atmospheric science)*. Elsevier Science Ltd, 1977b. ISBN 0444415270. URL http://www.amazon.co.uk/Atmospheric-Aerosols-Developments-atmospheric-science/dp/0444415270.

I. M. Ulbrich, M. R. Canagaratna, Q. Zhang, D. R. Worsnop, and J. L. Jimenez. Interpretation of organic components from Positive Matrix Factorization of aerosol mass spectrometric data. *Atmospheric Chemistry and Physics*, 9:2891–2918, 2009.

US Central Intellegence Agency. India, 2011. URL https://www.cia.gov/library/publications/the-world-factbook/geos/in.html.

S. Utembe, M. Cooke, A. Archibald, D. Shallcross, R. Derwent, and M. Jenkin. Simulating secondary organic aerosol in a 3-D Lagrangian chemistry transport model using the reduced Common Representative Intermediates mechanism (CRI v2-R5). *Atmospheric Environment*, 45(8):1604–1614, Mar. 2011. ISSN 13522310. doi: 10.1016/j.atmosenv.2010.11.046. URL http://linkinghub.elsevier.com/retrieve/pii/S1352231010010149.

D. W. Van Krevelen. Graphical-Statistical method for the study of structure and reaction processes of coal. *Fuel*, 29:269–284, 1950.

R. Volkamer, J. L. Jimenez, F. San Martini, K. Dzepina, Q. Zhang, D. Salcedo, L. T. Molina, D. R. Worsnop, and M. J. Molina. Secondary organic aerosol formation from anthropogenic air pollution: Rapid and higher than expected. *Geophysical Research Letters*, 33(17):101029/, 2006. ISSN 0094-8276. doi: 10.1029/2006GL026899. URL http://www.agu.org/pubs/crossref/2006/2006GL026899.shtml.

F. J. Wentz, L. Ricciardulli, K. Hilburn, and C. Mears. How much more rain will global warming bring? *Science*, 317(5835):233–235, 2007. URL http://www.ncbi.nlm.nih.gov/pubmed/17540863.

J. D. Whitehead, M. W. Gallagher, J. R. Dorsey, N. Robinson, A. M. Gabey, H. Coe, G. McFiggans, M. J. Flynn, J. Ryder, E. Nemitz, and F. Davies. Aerosol fluxes and dynamics within and above a tropical rainforest in South-East Asia. *Atmospheric Chemistry and Physics*, 10(19):9369–9382, Oct. 2010. ISSN 1680-7324. doi: 10.5194/acp-10-9369-2010. URL http://www.atmos-chem-phys.net/10/9369/2010/.

Q. Zhang, M. R. Alfarra, D. R. Worsnop, J. D. Allan, H. Coe, M. R. Canagaratna, and J. L. Jimenez. Deconvolution and quantification of hydrocarbon-like and oxygenated organic aerosols based on aerosol mass spectrometry. *Environmental Science & Technology*, 39(13):4938–4952, 2005.

Q. Zhang, J. L. Jimenez, M. R. Canagaratna, J. D. Allan, H. Coe, I. Ulbrich, M. R. Alfarra, A. Takami, A. M. Middlebrook, Y. L. Sun, K. Dzepina, E. Dunlea, K. Docherty, P. F. DeCarlo, D. Salcedo, T. B. Onasch, J. T. Jayne, T. Miyoshi, A. Shimono, S. Hatakeyama, N. Takegawa, Y. Kondo, J. Schneider, F. Drewnick, S. Borrmann, S. Weimer, K. Demerjian, P. Williams, K. N. Bower, R. Bahreini, L. Cottrell, R. J. Griffin, J. Rautiainen, J. Y. Sun, Y. M. Zhang, and D. R. Worsnop. Ubiquity and dominance of oxygenated species in organic aerosols in anthropogenically-influenced Northern Hemisphere midlatitudes. *Geophysical Research Letters*, 34(13):101029/, 2007. ISSN 0094-8276. doi: 10.1029/2007GL029979. URL `http://www.agu.org/pubs/crossref/2007/2007GL029979.shtml`.

X. Zhang, K. A. Smith, D. R. Worsnop, J. L. Jimenez, J. T. Jayne, C. E. Kolb, J. Morris, and P. Davidovits. A numerical characterization of particle beam collimation by an aerodynamic lens-nozzle system: Part I. An individual lens or nozzle. *Aerosol Science & Technology*, 36(5):617–631, 2002.

M. Zhao and S. W. Running. Drought-Induced Reduction in Global Terrestrial Net Primary Production from 2000 Through 2009. *Science*, 329(5994):940–943, Aug. 2010. ISSN 0036-8075. doi: 10.1126/science.1192666. URL `http://www.sciencemag.org/cgi/doi/10.1126/science.1192666`.

J. Zhou, E. Swietlicki, H. C. Hansson, and P. Artaxo. Submicrometer aerosol particle size distribution and hygroscopic growth measured in the Amazon rain forest during the wet season. *Journal of geophysical research*, 107(20):XCXIII—-XCXIV, 2002. ISSN 0148-0227.

If science teaches us anything, it is to accept our failures, as well as our successes, with quiet dignity and grace.

Dr. Frederick Frankenstein, Young Frankenstein 1974